

This document was produced
by scanning the original publication.

Ce document est le produit d'une
numérisation par balayage
de la publication originale.



**GEOLOGICAL SURVEY OF CANADA
COMMISSION GÉOLOGIQUE DU CANADA**

**CURRENT RESEARCH 1995-D
EASTERN CANADA AND NATIONAL AND
GENERAL PROGRAMS**

**RECHERCHES EN COURS 1995-D
EST DU CANADA ET PROGRAMMES
NATIONAUX ET GÉNÉRAUX**



1995



Natural Resources
Canada

Ressources naturelles
Canada

Canada

NOTICE TO LIBRARIANS AND INDEXERS

The Geological Survey's Current Research series contains many reports comparable in scope and subject matter to those appearing in scientific journals and other serials. Most contributions to Current Research include an abstract and bibliographic citation. It is hoped that these will assist you in cataloguing and indexing these reports and that this will result in a still wider dissemination of the results of the Geological Survey's research activities.

AVIS AUX BIBLIOTHÉCAIRES ET PRÉPARATEURS D'INDEX

La série Recherches en cours de la Commission géologique contient plusieurs rapports dont la portée et la nature sont comparables à ceux qui paraissent dans les revues scientifiques et autres périodiques. La plupart des articles publiés dans Recherches en cours sont accompagnés d'un résumé et d'une bibliographie, ce qui vous permettra, on l'espère, de cataloguer et d'indexer ces rapports, d'où une meilleure diffusion des résultats de recherche de la Commission géologique.

**GEOLOGICAL SURVEY OF CANADA
COMMISSION GÉOLOGIQUE DU CANADA**

**CURRENT RESEARCH 1995-D
EASTERN CANADA AND
NATIONAL AND GENERAL PROGRAMS**

**RECHERCHES EN COURS 1995-D
EST DU CANADA ET
PROGRAMMES NATIONAUX ET GÉNÉRAUX**

1995

© Minister of Energy, Mines and Resources Canada 1995

Available in Canada through
authorized bookstore agents and other bookstores or by mail from

Canada Communication Group - Publishing
Ottawa, Canada K1A 0S9

and from

Geological Survey of Canada offices:

601 Booth Street
Ottawa, Canada K1A 0E8

3303-33rd Street N.W.,
Calgary, Alberta T2L 2A7

100 West Pender Street
Vancouver, B.C. V6B 1R8

A deposit copy of this publication is also available for reference
in public libraries across Canada

Cat. No. M44-1995/4E
ISBN 0-660-15811-6

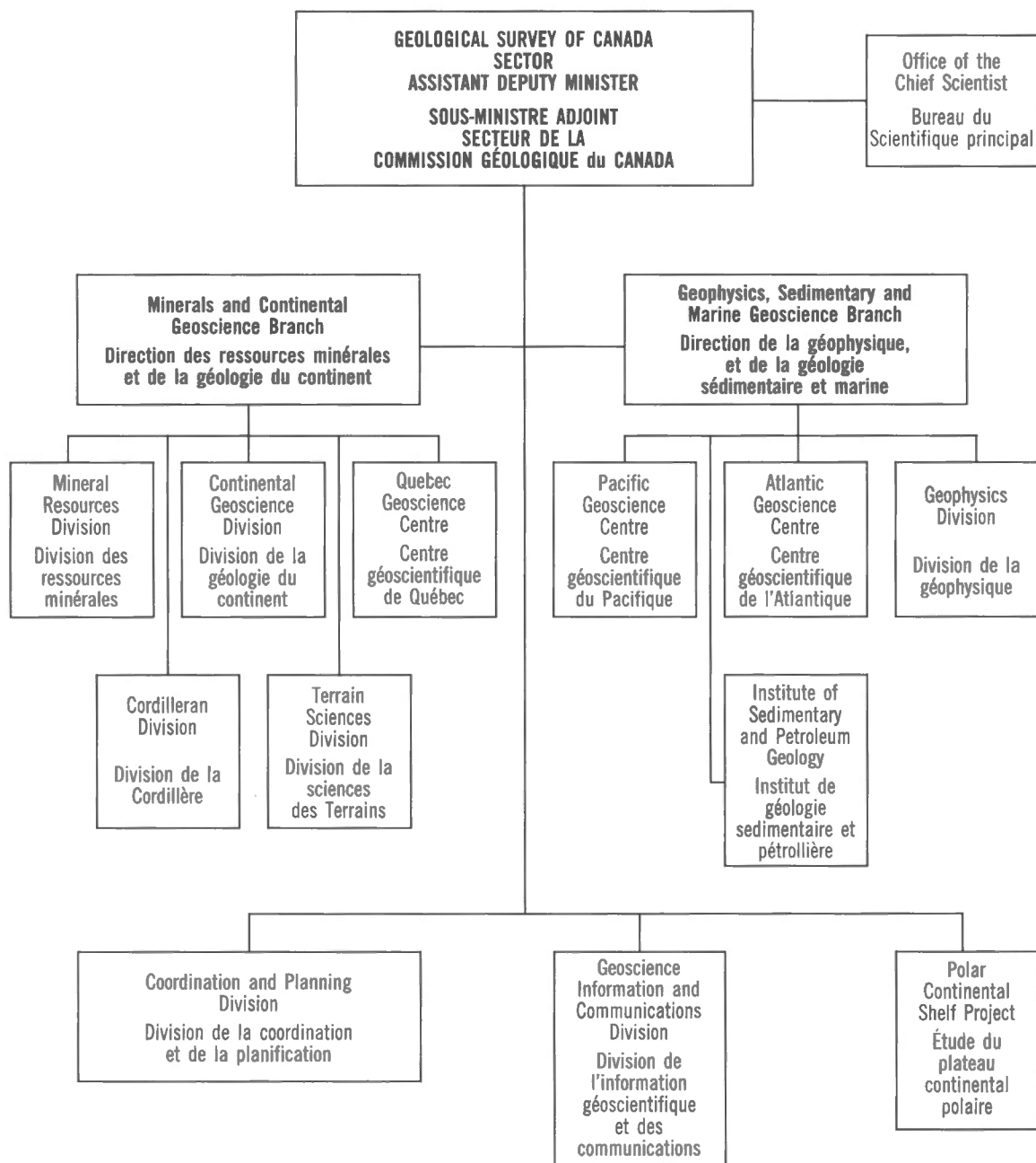
Price subject to change without notice

Cover description

Wave-cut bench at Saint-Maurice-de-l'Échouerie, on the northern
coast of Gaspésie. (Photo by J.J. Veillette; GSC 1994-787).

Description de la photo couverture

Terrasse marine à Saint-Maurice-de-l'Échouerie, sur la côte nord
de la Gaspésie. (Photo prise par J.J. Veillette; GSC 1994-787).



Separates

A limited number of separates of the papers that appear in this volume are available by direct request to the individual authors. The addresses of the Geological Survey of Canada offices follow:

601 Booth Street
OTTAWA, Ontario
K1A 0E8
(FAX: 613-996-9990)

Institute of Sedimentary and Petroleum Geology
3303-33rd Street N.W.
CALGARY, Alberta
T2L 2A7
(FAX: 403-292-5377)

Cordilleran Division
100 West Pender Street
VANCOUVER, B.C.
V6B 1R8
(FAX: 604-666-1124)

Pacific Geoscience Centre
P.O. Box 6000
9860 Saanich Road
SIDNEY, B.C.
V8L 4B2
(Fax: 604-363-6565)

Atlantic Geoscience Centre
Bedford Institute of Oceanography
P.O. Box 1006
DARTMOUTH, N.S.
B2Y 4A2
(FAX: 902-426-2256)

Québec Geoscience Centre
2700, rue Einstein
C.P. 7500
Ste-Foy (Québec)
G1V 4C7
(FAX: 418-654-2615)

When no location accompanies an author's name in the title of a paper, the Ottawa address should be used.

Tirés à part

On peut obtenir un nombre limité de «tirés à part» des articles qui paraissent dans cette publication en s'adressant directement à chaque auteur. Les adresses des différents bureaux de la Commission géologique du Canada sont les suivantes:

601, rue Booth
OTTAWA, Ontario
K1A 0E8
(facsimilé : 613-996-9990)

Institut de géologie sédimentaire et pétrolière
3303-33rd St. N.W.,
CALGARY, Alberta
T2L 2A7
(facsimilé : 403-292-5377)

Division de la Cordillère
100 West Pender Street
VANCOUVER, British Columbia
V6B 1R8
(facsimilé : 604-666-1124)

Centre géoscientifique du Pacifique
P.O. Box 6000
9860 Saanich Road
SIDNEY, British Columbia
V8L 4B2
(facsimilé : 604-363-6565)

Centre géoscientifique de l'Atlantique
Institut océanographique Bedford
B.P. 1006
DARTMOUTH, Nova Scotia
B2Y 4A2
(facsimilé : 902-426-2256)

Centre géoscientifique de Québec
2700, rue Einstein
C.P. 7500
Ste-Foy (Québec)
G1V 4C7
(facsimilé : 418-654-2615)

Lorsque l'adresse de l'auteur ne figure pas sous le titre d'un document, on doit alors utiliser l'adresse d'Ottawa.

CONTENTS

Origins and timing of basal Windsor carbonate breccias, Nova Scotia Denis Lavoie and D.F. Sangster	1
Geology of the central part of St. Mary's Basin, Nova Scotia J. Brendan Murphy, Randolph J. Rice, Timothy R. Stokes, and D. Fraser Keppie	11
Structural investigations in the Stellarton pull-apart basin, Nova Scotia John W.F. Waldron K.S. Gillis, R.D.Naylor , and F.W. Chandler	19
Field evidence for the character of the Precambrian rocks south of the Rockland Brook fault, Bass River block, Cobequid Highlands, Nova Scotia Georgia Pe-Piper, David J.W. Piper, and Ioannis Koukouvelas	27
The role of granites in the evolution of the Folly Lake diorite, Cobequid Highlands, Nova Scotia I. Koukouvelas and Georgia Pe-Piper	33
Halokinetic controls on the sedimentary architecture of the Inverness Formation, western Cape Breton Island, Nova Scotia J.P.Brown	39
Preliminary results from reprocessing of seismic reflection data in the Cumberland Basin, Nova Scotia F. Marillier and P. Durling	45
A preliminary microthermometric study of the Sugar Camp, Yankee Line, and MacPhails Brook Pb-Zn showings, Cape Breton Island, Nova Scotia Guoxiang Chi and Martine M. Savard	53
A further note on the occurrence of beryl associated with southern Nova Scotia plutons K.L. Currie and J.B.Whalen	59
Improving measurement accuracy of formation resistivity factor measurements for tight shales from the Scotian Shelf T.J. Katsube, N. Scromeda, and M. Williamson	65
A tale of shale - stratigraphic problems in the Gander River map area, Newfoundland K.L. Currie	73

✓	The Plage-Charron, Quebec, landslide of August 5, 1994 J.M. Aylsworth, D.E. Lawrence, and J.A. Traynor	81
✓	Particle size analysis of fine grained Champlain Sea sediments from a borehole near Ottawa, Ontario J.A. Traynor	87
	Northeastern North American earthquake potential – new challenges for seismic hazard mapping John Adams, Peter W. Basham, and Stephen Halchuk	91
	Aeromagnetic survey program of the Geological Survey of Canada, 1994-1995 R. Dumont, F. Kiss, P.E. Stone, K. Anderson, D.J. Teskey, R.A. Gibb, and G. Palacky	101
	National gravity survey program of the Geological Survey of Canada, 1994-1995 D.B. Hearty and R.A. Gibb	105

Origins and timing of basal Windsor carbonate breccias, Nova Scotia¹

Denis Lavoie and D.F. Sangster²
Quebec Geoscience Centre, Sainte-Foy

Lavoie, D. and Sangster, D.F., 1995: Origins and timing of basal Windsor carbonate breccias, Nova Scotia; in Current Research 1995-D; Geological Survey of Canada, p. 1-10.

Abstract: Carbonate breccias occur at the base of the Windsor Group and are commonly associated with Pb-Zn mineralization. Three types of breccias are recognized; one synsedimentary and two late (post-burial) ones. The latter comprise tectonic and karstic breccias. The synsedimentary breccia occurs in the Macumber Formation and in the so-called Pembroke siderite (Walton area); sedimentological and diagenetic elements point to an early rotational slide formation on a deep-water slope. The late tectonic breccia occurs at the very top of the Macumber and was formed through hydraulic fracturing following significant burial and hydrocarbon migration. Finally, the informal Pembroke (*sensu stricto*) designation is restricted to an irregularly distributed late karstic breccia. Because the synsedimentary and tectonic breccias are pre-ore and could have played a role in localizing mineral deposition whereas the karstic breccia is post-ore, criteria for distinguishing the breccias should be helpful for metallogenic studies of the Carboniferous Magdalen Basin.

Résumé : Des brèches carbonatées sont présentes à la base du Groupe de Windsor et sont fréquemment associées à des intervalles minéralisés en Pb-Zn. Trois types de brèches sont reconnues: une brèche synsédimentaire et deux brèches tardives (postérieures à l'enfouissement). Ces dernières sont d'origine soit tectonique ou karstique. La brèche synsédimentaire est présente dans la Formation de Macumber et dans la sidérite de Pembroke (région de Walton); les éléments sédimentologiques et diagénétiques suggèrent une formation précoce par glissement rotationnel sur une pente en eau profonde. La brèche tectonique tardive est présente au sommet de la Formation de Macumber et a été formée par fracturation hydraulique après l'enfouissement et la migration d'hydrocarbures dans le bassin. Enfin, la désignation informelle de Pembroke (*sensu stricto*) est donnée à une brèche karstique tardive à distribution très irrégulière dans le bassin. Puisque les brèches synsédimentaires et tectoniques sont antérieures à la minéralisation et qu'elles auraient donc pu y contribuer et que la brèche karstique lui est postérieure, les critères pour distinguer les différentes brèches devraient être utiles pour les études métallogéniques du bassin carbonifère de Madeleine.

¹ Contribution to the Magdalen Basin NATMAP Project.

² Mineral Resources Division, Ottawa

INTRODUCTION

The Viséan Macumber (Weeks, 1948) and the locally overlying Pembroke (Weeks, 1948) formations of the Windsor Group, with the laterally equivalent Gays River Formation, represent the first carbonate units in the post-Acadian successor Magdalen Basin of Nova Scotia (Fig. 1). These units constitute the base of the first transgressive-regressive cycle of the Windsor Group (Giles, 1981). A study of sedimentary paleoenvironments of basal Windsor carbonates is critical for the reconstruction of initial marine infilling of the basin; moreover, the presence of base metal occurrences further adds to the interest in studying these units.

Of critical metallogenic importance for the lower part of the Windsor Group is the presence of fairly abundant carbonate breccias. Although some of these breccias differ significantly in many aspects, over the years, they have all been included in the Pembroke Formation. Moreover, the term "Pembroke" is also used to designate, in drill cores from the Walton area, a mound-shaped massive and mottled sideritized unit overlying the sideritized laminated material of the Macumber Formation. All of the above gave rise to astonishing confusion not only in the description of

the Pembroke Formation, and hence its local occurrence and distribution, but also in the proposed genetic model for these breccias. As a consequence, almost all early sedimentary (Weeks, 1948; Sage, 1954; Stevenson, 1958; Schenk, 1967) to late diagenetic (Clifton, 1967; Geldsetzer, 1977; Smith and Collins, 1979) and tectonic (Lynch and Giles, 1993; Lynch and Brisson, 1994; Giles and Lynch, 1994; Fallara et al., 1994) mechanisms able to generate a breccia have been put forward (and strongly debated) in the literature dealing with basal Windsor breccias. On the other hand, only a few reports have discussed a likely multiple origin (early and late) of breccias incorporated in the Pembroke (Hein et al., 1993; Lavoie, 1994). However, because the latter studies were not specifically directed at understanding the origin of the Pembroke, they were incomplete. Therefore, a clear understanding of the Pembroke is both lacking and urgently needed.

This study is, to some extent, a follow-up of last year's research by the senior author which partly addressed the origin of the Pembroke Formation (Lavoie, 1994). During the 1994 field season, more than 80 drill cores (mostly centred around the Walton area) intersecting the Macumber and "Pembroke" formations were described and sampled. Moreover, a dozen basal Windsor carbonate field sections, distributed all over mainland Nova Scotia, were measured and

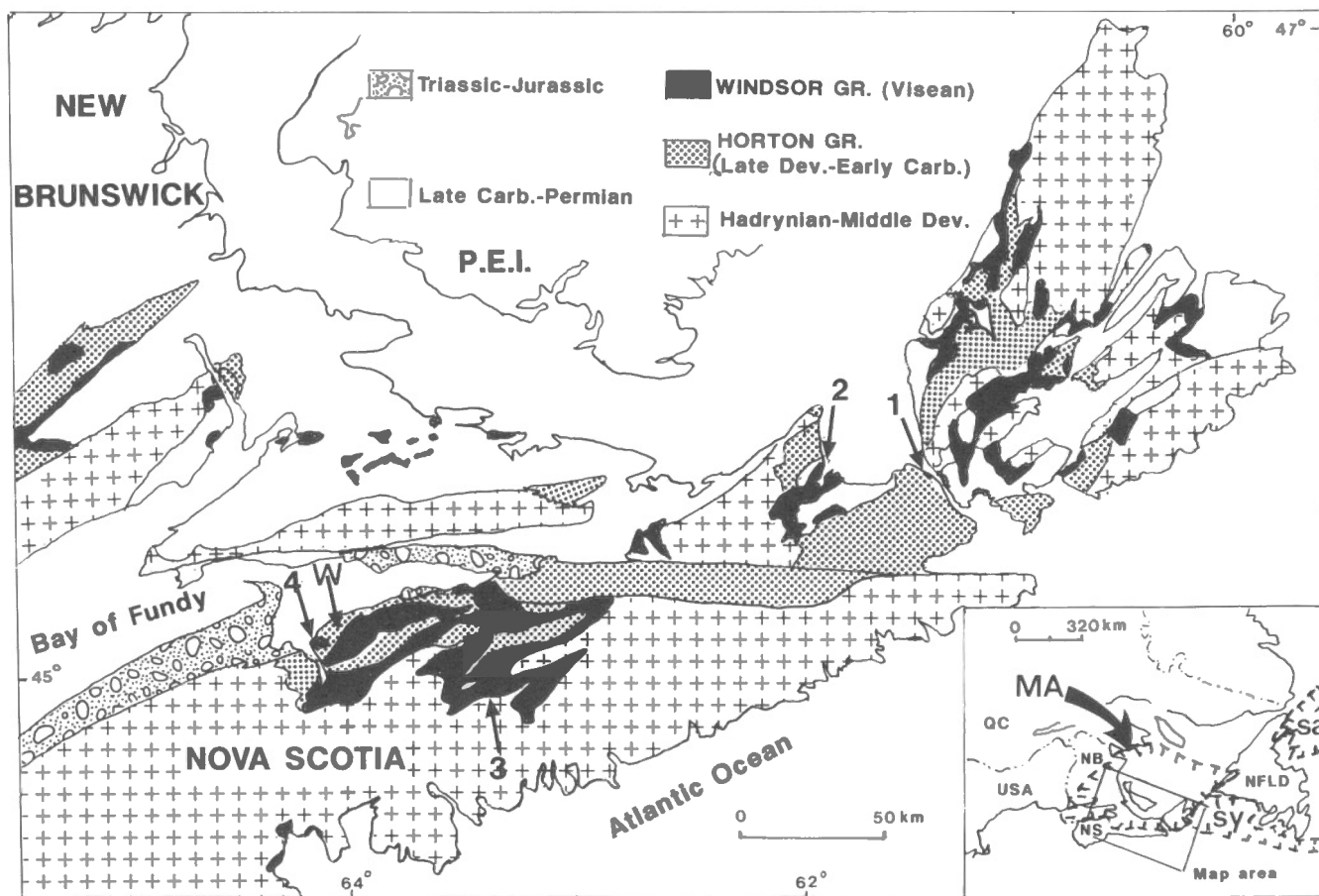


Figure 1. Simplified geological and location map of studied sections and cores of basal Windsor carbonates. Sections are: (1) Aulds Cove, (2) Crystal Cliff, (3) Far Brook, and (4) Cheverie. W: Walton area. Inset locates the Magdalen Basin (MA); sa Saint-Anthony Basin; and sy Sydney Basin. Modified from Boehner et al. (1989).

sampled. This contribution presents megascopic observations and preliminary interpretations relating to the breccia problem. Detailed petrographic and isotopic studies of the breccias are currently in progress. It is proposed that basal Windsor carbonate breccias are multiple in origin and timing, some being syndimentary while others are either karstic or tectonic in origin. Criteria for distinguishing between the various types are presented and, hopefully, will assist in our understanding of the breccias and their relation to base metal mineralization in basal Windsor carbonates. The term *Pembroke*, based on the original description of Weeks (1948), is restricted to a late, irregularly distributed, solution-collapse breccia and, following the recommendation of Clifton (1967), is now considered an informal unit.

GEOLOGICAL AND STRATIGRAPHIC SETTINGS

The Lower Carboniferous Windsor Group outcrops in many structural subbasins forming part of the Magdalen Basin (Fig. 1). This successor basin was initiated by the extensional collapse of the Acadian Orogen in the Late Devonian (Lynch and Giles, 1993). A thick Hadrynian-Middle Devonian succession constitutes the basement of the successor basin. The Windsor Group overlies conformably to paraconformably the Upper Devonian-lowermost Carboniferous Horton Group or unconformably the Cambrian-Ordovician Meguma Group (Fig. 2). The Windsor Group is in turn conformably to unconformably overlain by a thick succession of Carboniferous to Jurassic siliciclastics (Fig. 2). The Windsor Group is made up of five transgressive-regressive cycles (Fig. 2) and contains almost exclusively the only marine record of the Magdalen

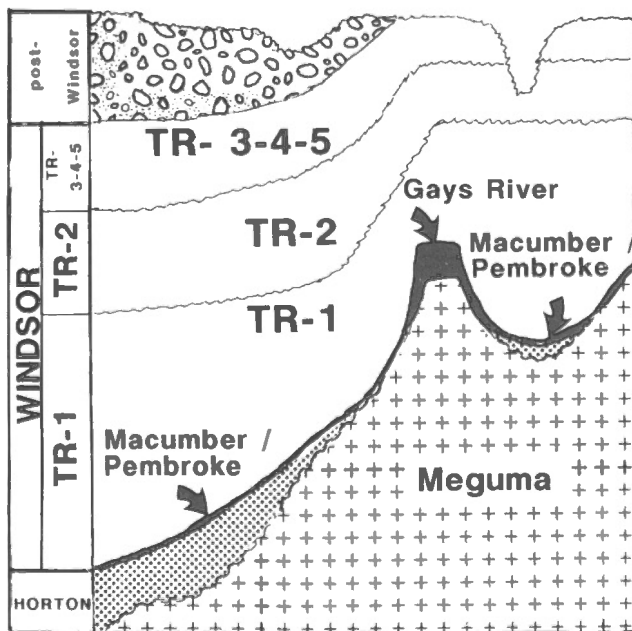


Figure 2. Major transgressive-regressive (T-R) cycles in the Windsor Group and stratigraphic position of the Macumber-Pembroke succession. Modified from Giles (1981).

Basin (Giles, 1981). Its stratigraphy is strongly dominated by siliciclastic sediments and evaporite deposits; carbonates are only a minor part of it (Giles, 1981).

The Macumber Formation occurs basin-wide at the bottom of the Windsor Group (Fig. 2). It overlies the Horton Group, a dominantly continental siliciclastic unit deposited in post-orogenic distensive fault-bounded basins (Hamblin and Rust, 1989). The laterally equivalent Gays River reefoid mounds unconformably overlie metawackes of the Meguma Group. It is noteworthy, however, that the so-called "transition beds" between typical Macumber and Gays River lithofacies are dominated by Macumber-like lithologies (e.g. deep-water microbial laminites, slump breccias) and unconformably overlie Meguma lithologies in section 3 (Fig. 1).

BASAL WINDSOR CARBONATE BRECCIAS

Anyone addressing the problem of the *Pembroke* has to deal with the origin of the enigmatic Macumber Formation, because some of the breccias assigned to the *Pembroke* (e.g. Walton area) are also found embedded within the Macumber (see below). Over the years, major divergences have arisen concerning the proposed paleoenvironmental significance of the Macumber Formation. The upper two-thirds of the Macumber Formation is typified by a subcentimetric planar fabric developed in limestones. The environmental interpretation of these planar limestones is controversial since they have been regarded as intertidal algal mats (Schenk, 1967), as deep-water algal laminites deposited after rapid and major flooding of the basin (Giles, 1981; Hein et al., 1993), as deep-water methane-vent related laminar bioaccumulations (von Bitter et al., 1992), or even as a lacustrine deposit (Schenk et al., 1992). More recently, however, a late tectonic origin (calc-mylonite) has been put forward (Lynch and Giles, 1993; Giles and Lynch, 1994; Lavoie, 1994; Lynch and Brisson, 1994). However, following last year's field report (Lavoie, 1994), the senior author examined nearly 100 thin sections of the Macumber; the platy lithofacies is a primary, below storm-wave base, bioturbated microbial laminite facies upon which indisputable evidence for tectonics is overprinted only very locally. Therefore, in most cases, the tectonic interpretation of interbedded breccias is now seen as equivocal.

MACUMBER BRECCIAS

Although the Macumber Formation reaches a maximum thickness of about 15 m, in many localities the measured thickness is less than a couple of metres (Giles, 1981). The Macumber can be divided into two major lithostromes (Lavoie, 1994). The lower one is a nonplaty limestone unit devoid of breccias. It consists of various lime mudstone and wackestone/packstone beds, the latter characterized by restricted fauna (mostly ostracodes), burrowers (*Planolites*-like), abundant peloids, grapestones, and oolites (Fig. 3a). The coarser-grained lithofacies display abundant sedimentary structures indicative of high-energy pulses in a dominantly low-energy, below fair-weather wave base setting

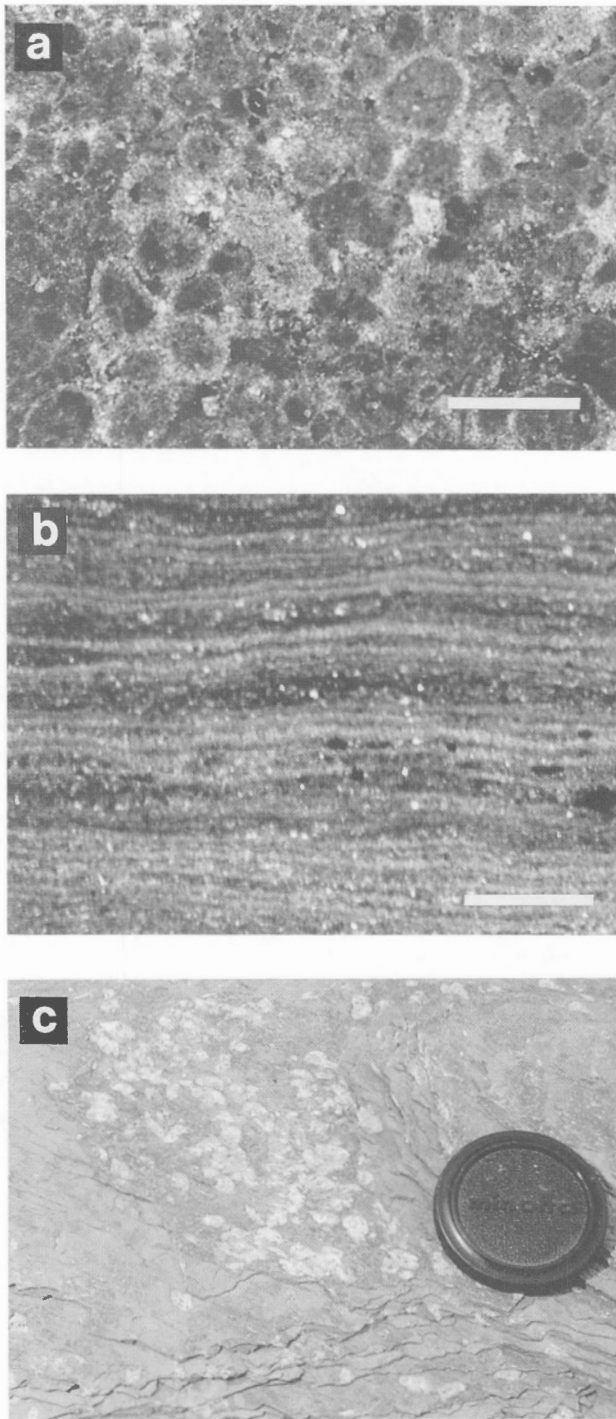


Figure 3. Macumber Formation. *a)* Photomicrograph of the lower lithostrome of the Macumber showing poorly sorted sediment with abundant peloids, small intraclasts, and proto-oolites. Plane-polarized light. Scale bar is 1 mm. *b)* Photomicrograph of the upper lithostrome of the Macumber showing deep-water laminites. Note recrystallization with some locally preserved peloidal material of microbial origin. The laminites are here interbedded with quartz-rich wackestone. Plane-polarized light. Scale bar is 1 mm. *c)* Plane-bedding view of abundant nodules of former evaporites (now calcite) growing in the deep-water laminite lithostrome. Section 1.

(Lavoie, 1994). The upper lithostrome consists of the typical platy limestone lithofacies in which detailed petrographic examination clearly suggests deep-water biosedimentation resulting in microbial mats. Even if some recrystallization affected the lithofacies, plane-bedded aligned peloidal mats with poorly preserved calcimicrobes typify the lithofacies (Fig. 3b). At the bottom of the lithostrome, microbial mats are interbedded with the coarser grained lithofacies. Moreover, burrows cutting through the mats are filled with peloidal wackestone/packstone suggesting that microbial-dominated sedimentation occurred downslope from the coarse-grained carbonates. Therefore, the microbial mats are most likely indicative of a below storm-wave base setting. It is also noteworthy that no evidence (e.g. desiccation or teepee structures, early meteoric diagenesis) exists for subaerial exposure of the mats. The uppermost part of the Macumber platy lithostrome is characterized by interbedded (on a macro- and micro-scale) microbial mats and sulphate pseudomorphs (laminae and nodules; Fig. 3c). These features suggest increased hypersaline conditions in a deep-water setting leading to sulphate precipitation, a relationship also reported for other rock successions (Kendall, 1984). Early and late breccias in the Macumber are restricted to the upper part of the second lithostrome.

Synsedimentary slump breccia

This type of breccia, occurring in centimetre- to decametre-thick intervals, has been observed in both the Macumber Formation (Fig. 4a) and the "transition beds" (Fig. 4b) and constitutes one of the dominant rock types in the so-called Pembroke mound-shaped siderite unit of the Walton area. Therefore, the Pembroke problem is directly linked to the Macumber. Lavoie (1994) described this Macumber breccia as the lower breccia and interpreted it as a tectonic breccia related to the Ainslie Detachment (Lynch and Giles, 1993). However, detailed core examination and re-examination of field sections seriously weaken that hypothesis. Although tectonic breccias are present in the uppermost metres of the Macumber, they differ in many aspects (see below).

As seen in most drill cores (Macumber Formation and Pembroke siderite) and some field sections (Macumber Formation and transition beds), the breccia occurs in a predictive cyclic rock pattern. This succession forms decametre to metre-thick intervals of initial well bedded and undeformed microbial mats passing upward into a zone of crenulated and contorted mats with centimetre-thick slump folds, grading into the breccia with the latter overlain by either the contorted facies or the undeformed mats (Fig. 5). From the limited view available in drill cores, the contacts between these zones are fairly conformable; however, outcrops show that the breccia cuts through the underlying zones (Fig. 4a and 4b).

The breccia is clast supported with fragments commonly making up an average of more than 80 per cent volume. The fragments are chaotically piled up with no granulometric trend (Fig. 6a). The clasts consist solely of microbial mat fragments; less commonly some of these show soft sediment deformation structures transected at the clast margins. The fragments are usually small, ranging in size from less than

1 mm to a maximum of 10 cm (average 2 cm). Owing to the nature of the brecciated lithofacies, they are elongated although no clear or subtle imbrication was noted. Of critical importance to the genesis of this breccia is the presence of some rounded to subrounded clast margins (Fig. 6b) suggesting transport or remobilization. The breccia matrix is usually made up of fine-grained carbonate material composed of a mixture of minute fragments identical to the larger clasts and of lime mud (Fig. 6c). Locally, the matrix is annealed into coarse-grained pseudospar. For the Pembroke siderite of the Walton area, it seems that brecciation predated sideritization of carbonates and abundant barite cements fill voids between clasts.

Some diagenetic elements found in the breccia are also significant with respect to its origin. One is stylolites, which were seen at the contacts between clasts. None were cut by fragment margins suggesting that the breccia was formed prior to significant burial. The other is the presence of a small secondary dissolution porosity with individual centimetre-sized pores cutting both clast and matrix. The walls of the

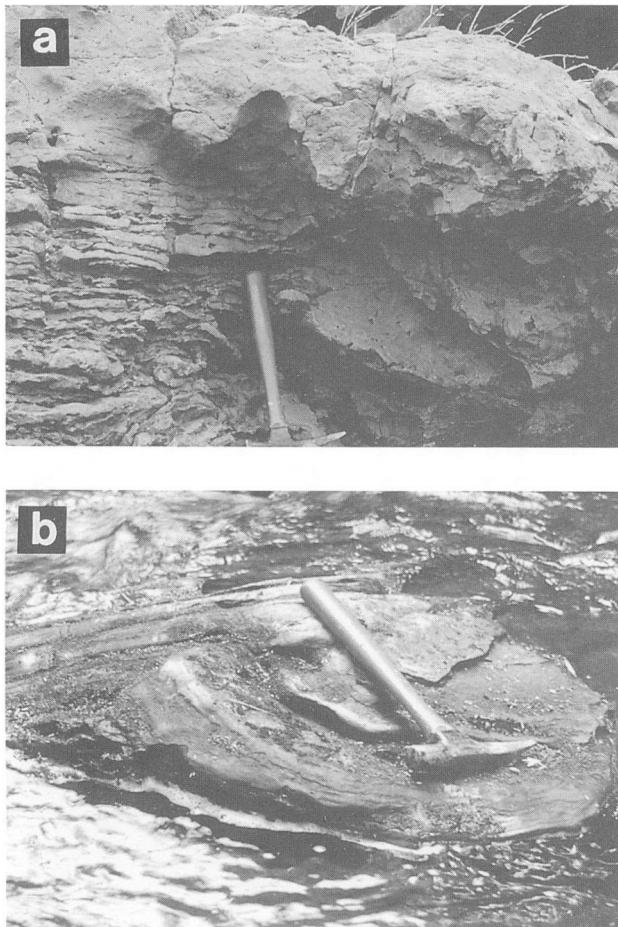


Figure 4. a) Synsedimentary slump breccia within the Macumber Formation. Note the concave shear failure plane cutting through underlying beds. Section 4. b) Synsedimentary slump breccia within the "transition beds". The shear failure plane cuts through deep-water laminites. Section 3.

voids are lined with isopachous fringes of calcite cement and the remaining space is filled with solid bitumen (Fig. 6d). This suggests that the breccia was formed not only prior to some significant burial but also prior to hydrocarbon migration.

The combined sedimentological and diagenetic evidence is seen as a strong advocate for synsedimentary formation of the breccia. The latter is regarded as a dismembered rotational slide resulting from extreme soft sediment deformation (slumping) occurring on a slope below wave base. This interpretation is based on: 1) the presence of discrete concave shear failure planes, 2) the lack of wave- or current-induced sedimentary structures, 3) the presence of a fine-grained matrix in part derived from background suspension sedimentation, 4) the rounding of some clast margins reflecting remobilization from gravity-driven movement of disrupted beds, 5) the nature of the cyclic succession hosting the breccia showing variable degrees of internal deformation and, 6) the preferred association to the Macumber platy lithofacies, i.e. deep-water microbial mats. All the previous evidence, besides the Macumber interpretation, are commonly reported for modern and ancient slope breccias (see Cook and Mullins, 1983). It is also noteworthy that this breccia occurs in the upper part of the Macumber, where interbedding with deep-water evaporites starts. It is possible, as reported for other rock successions (Kendall, 1984), that the presence of these evaporites was instrumental in inducing synsedimentary movement along depositional slopes, although this assumption has yet to be documented for the study succession.

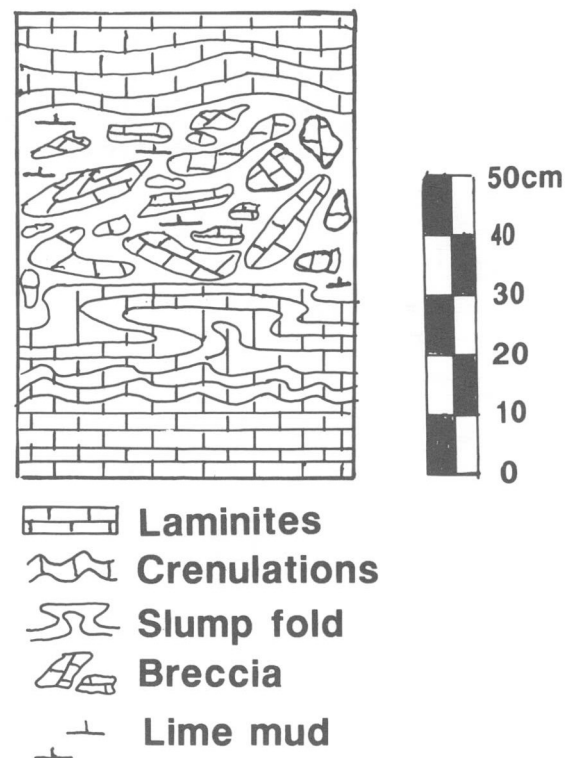


Figure 5. Schematic illustration of the repetitive rock succession that hosts the synsedimentary breccia for both the Macumber Formation and the "Pembroke siderite".

Late tectonic breccia

Some breccias in the uppermost part of the Macumber Formation are considered to be related to post-Windsor Group extensional tectonism that affected the Maritimes Basin. Recognition of this event is supported mainly by stratigraphic omission of the middle and upper parts of the Windsor Group along a plane parallel to bedding. This led to the proposed positioning of the Ainslie Detachment at the Macumber/first evaporite (Carrolls Corner) interface (Lynch and Giles, 1993; Giles and Lynch, 1994). Consequently tectonic origin for the breccias occurring at this position has been proposed (Giles and Lynch, 1994; Lavoie, 1994; Fallara et al., 1994). Although we believe that most of the breccias close to the Macumber/Carrolls Corner are of the syndepositional type, we have also recognized tectonic breccias.

This late tectonic breccia is observed in drill cores and in outcrops of the Macumber Formation. Its best field exposure is at Aulds Cove (Fig. 1) where nearly 15 m of Macumber Formation are abruptly overlain by the Upper Viséan-Namurian Mabou Group, which from regional stratigraphic considerations, signifies that close to 1500 m of Windsor Group strata are missing (Giles and Lynch, 1994). Immediately underlying the Mabou, 30 cm of highly brecciated Macumber material is observed (Fig. 7). It could be tempting to relate this breccia to either a lag deposit overlying a major unconformity or a solution collapse breccia; however, this breccia lacks the polymictic nature of clasts that typifies the latter (see below) and the sedimentary characteristics that one should expect from the former. Breccias that are somewhat

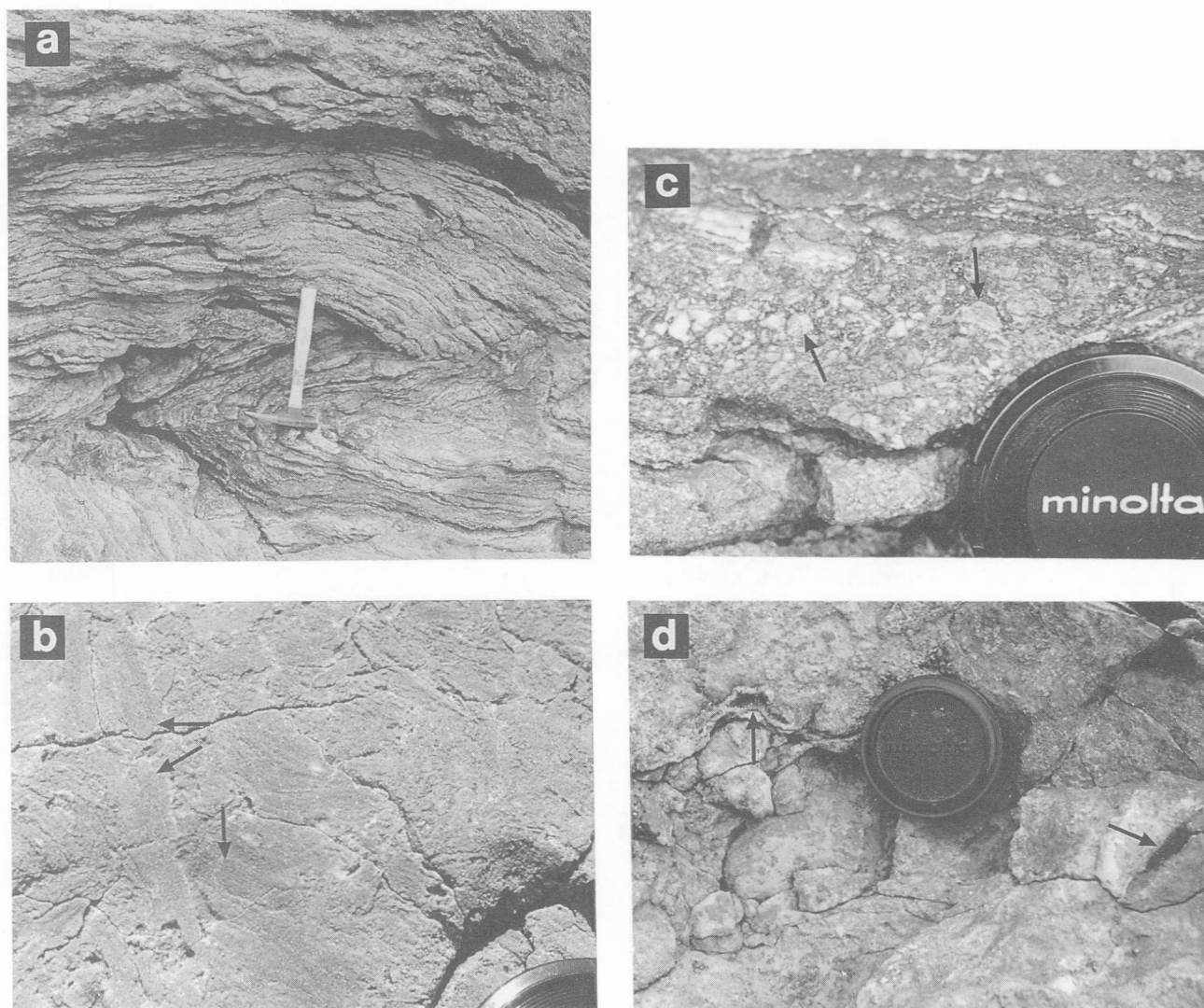


Figure 6. Macumber Formation. **a)** Slump fold associated with syndepositional slump breccia (underlying the fold). The Pembroke karst breccia irregularly overlies the structure. Section 2. **b)** Small fragments with rounded margins (arrows) within the syndepositional breccia. Note major annealing of both the matrix and clasts. Section 4. **c)** Sedimentary filling between fragments of the syndepositional breccia, consisting of small rounded fragments of laminites and lime mud. Section 2. **d)** Dissolution pores (arrows) cutting through both clasts and matrix of the syndepositional breccia. The void is filled with initial calcite cement and late solid bitumen. Section 4.



Figure 7. Tectonic breccia occurring at the top of the Macumber Formation at Aulds Cove. Immediately overlying the cement-supported breccia is the Mabou Group. Section 1.

similar in their constituents and general aspect are also observed in some drill cores from the Walton area where they are overlain by the usual Windsor rock package.

The breccia is cement-supported to locally clast-supported with the amount of clasts reaching about 40 to 75 per cent. The clasts are chaotically piled up and no sedimentary structures are visible. The fragments are composed of the typical platy lithofacies of the Macumber, are elongated in shape, and show angular margins. At a few localities, fragments have a definitive puzzle-like texture with edge-matching adjacent clasts, suggesting no significant displacement. Contrary to the previously described breccia, this one does not form part of a cyclic rock pattern. The breccia fragments are cemented by sparite with some barite in the Walton area. In some cases, an isopachous cement fabric is clearly visible suggesting that this peculiar cement is not a recrystallized product. Similar breccias are described at the Jubilee deposit (Cap Breton Island), they are cemented by coarse fibrous calcite of relatively high temperature ($\approx 70^{\circ}\text{C}$) and salinity (25 wt% equivalent NaCl) (Chi et al., in prep.). Close examination of the clasts showed some fragments with voids filled with the previously described calcite-bitumen cement succession and, in one case, a secondary void is clearly cut by the clast margin. Unfortunately, no ubiquitous stylolites were visible at a megascopic scale.

From the above description, it seems obvious that this type of breccia is quite different from the syndimentary one. It offers good evidence for a late origin (following hydrocarbon migration) and is best explained by hydraulic-forced fracturing and rapid cementation of fragments. Its presence immediately under the Mabou Group at Aulds Cove is seen as a supporting argument for tectonic activity at this locality. Moreover, the Macumber Formation at Port Hasting (6 km to the southeast) is the only section from which thin sections (available to the senior author) show clear and indisputable evidence of tectonic overprints (sigmoidal

calcite fibres associated with stretched peloids). On the other hand, similar tectonic breccias observed in drill cores from the Walton area are overlain by a thick succession of evaporites and in the vicinity, middle Windsor stratigraphy is preserved (R. Moore, pers. comm., 1994). Therefore, there is a complete stratigraphy of the middle part of the Windsor Group in this area, and these tectonic breccias could be related to another tectonic event (Allegheny Orogeny?).

PEMBROKE UNIT

The term Pembroke Formation was introduced by Weeks (1948) to designate an assemblage of limestone breccias and red calcareous siliciclastics overlying the Macumber Formation. Clifton (1967) proposed to abandon the name Pembroke Formation since it had already been used for a Silurian volcano-sedimentary unit in Maine (Bastin and Williams, 1914). Therefore, the term Pembroke is herein used informally. Over the years, the lithostratigraphic meaning of the Pembroke has been seriously altered, as described in the introduction. Because considerable confusion exists regarding the meaning of the Pembroke, we suggest restricting its use to the late karstic breccia (see below) as originally proposed by Weeks (1948). Therefore, the breccias previously described (i.e., the syndimentary and tectonic breccias) should be designated as Macumber breccias.

Late karstic breccia

From outcrops and drill cores, the late karstic breccia has an erratic distribution. Where present, it overlies either the two previously described breccias or the nonbrecciated Macumber microbial mats.

The Pembroke breccia ranges in thickness from less than a few centimetres (drill cores from the Walton area) up to about 3 m (drill cores and field outcrops). It is usually clast-supported but matrix-supported intervals are commonly present. Fining- and muddying-upward as well as coarsening- and graining-upward trends are locally developed over metric intervals although these trends are not correlatable between even closely spaced drill holes. In outcrop, the clasts can reach 50 cm (Fig. 8a) although the average size is usually centimetric. Of critical importance for the recognition of this peculiar breccia is the polymictic nature of the fragments. The largest and dominant are clasts of the typical Macumber platy lithostrome (Fig. 8a). They are very irregular in shape and show angular margins suggesting a very local origin. Many of these clasts are typified by oxidized (reddish) rims whereas others show clear surface evidence of dissolution. Also found in the Pembroke breccia are angular fragments of the syndimentary breccia (Fig. 8b) and, in the Walton area, of pre-ore sideritized carbonates, all supporting a late origin for the Pembroke breccia. The sideritized carbonate fragments also demonstrate the post-ore timing of brecciation. Besides carbonate fragments, up to 25 per cent red mudstone clasts are distributed throughout the breccia. They are small (less than 4 cm), elongated to equigranular, and have rounded margins suggesting some significant remobilization. Finally, a few small evaporite clasts are observed in drill cores from the

Walton area. The greyish to reddish matrix of the breccia consists of millimetre-sized limestone fragments with subordinate lime mud. In some voids, this matrix is graded. Moreover, centimetre- to metre-sized pockets of cross-stratified and locally graded, reddish calcareous siltstones and fine-grained sandstones (Fig. 8a and 8c) are found in the breccia. Isopachous calcite crusts sometimes line cavity walls and either precede or postdate internal sediments (Fig. 8d). These locally gravitational cement crusts (Fig. 8d) are associated with either the siliciclastic infill (Fig. 8c) or the usual fine-grained carbonate matrix (Fig. 8d).

From the above, it is obvious that the aspect and composition of the Pembroke breccia is quite different from those of the two previously described breccias. The Pembroke breccia is interpreted to be a collapse breccia based on the following evidence: 1) dissolution features are visible on the surface of many limestones clasts; 2) oxidized rims typify

many carbonate fragments; 3) variable sedimentary trends (coarsening- and fining-upward) are commonly observed in karst porosity; 4) the common reddish colour of the carbonate matrix; 5) the difference in rounding of fragments suggesting local derivation of angular carbonate fragments from the host succession and remobilization of siliciclastic fragments originating most likely higher in the Windsor stratigraphy; 6) the red siliciclastic infills in some pores; and 7) the likely meteoric origin of the isopachous and gravitational calcite cement associated with the sedimentary infills (M. Savard, pers. comm., 1993). The late origin of the karstic breccia is supported by 1) the presence of fragments of the synsedimentary breccia of the Macumber Formation; 2) the presence of siliciclastic and evaporite fragments that could only originate from higher up in the Windsor stratigraphy; 3) the presence in some carbonate fragments of the burial-related calcite-solid bitumen cement succession observed for the Macumber Formation; and

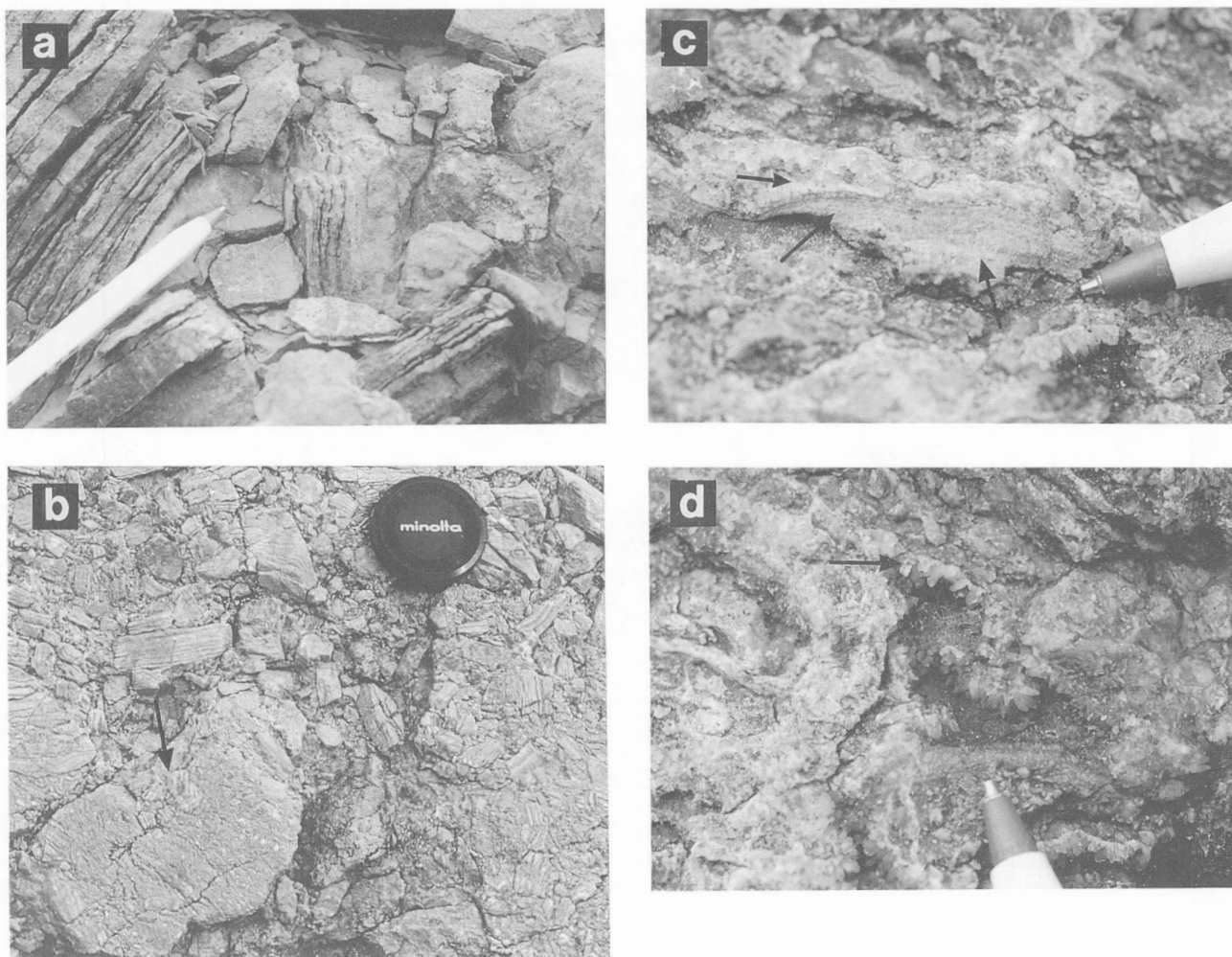


Figure 8. Pembroke breccia. **a**) Angular fragments of laminites in a matrix-supported framework. The pen points to red siltstone infill between clasts. Section 4. **b**) Clast-supported framework consisting of angular laminites fragments and subrounded clasts of synsedimentary breccias (arrow). Section 2. **c**) Isopachous crusts of calcite cement (small arrow) overlying graded red siliciclastic infill (arrows). Section 4. **d**) Gravitational dog-tooth-like calcite cement (arrow) roofing an open cavity; note the fine-grained carbonate material flooring the void (pen tip). Section 4.

Table 1. Main characteristics of basal Windsor carbonate breccias.

BRECCIAS			
	EARLY	LATE	
	Synsedimentary	Tectonic	Karstic
% clasts	60-95%	40-75%	40-90%
Nature	Laminite	Laminite	Laminite, breccia, red mudstone (+siderite: Walton)
Rounding	Some	None	Some for mudstone
Size	(1mm to 10cm)	(1mm to 5cm)	1mm to 50cm
Matrix/cement	Crushed fragments and lime mud	Crushed fragments and calcite cement	Carbonate fragments, red siltstone, calcite cement
Sedimentary structures	Soft-sediment deformation, concave-up shear failure planes, predictive rock pattern	Puzzle-like texture	Coarsening- and fining-upward, graded matrix
Diagenetic elements	Pre-stylolites, prior secondary dissolution	Post-secondary dissolution	Dissolution surfaces on grain, oxidized rims and matrix, post-stylolites (post-siderite: Walton) and post-sulphides
Timing of formation	Prior burial and hydrocarbon migration	Post-burial and hydrocarbon migration (locally)	Post-burial and other breccias
Unit	MACUMBER (Pembroke siderite: Walton)	MACUMBER	PEMBROKE (<i>sensu stricto</i>)

4) the presence of sideritized carbonate fragments in the Walton area. The age of this subaerial exposure is poorly constrained but is considered to be likely Westphalian or younger (G. Lynch, pers. comm., 1993).

The karstic collapse interpretation for the Pembroke breccia has been previously reported in the literature (Clifton, 1967; Geldsetzer, 1977), but, in many cases, this interpretation was applied for the entire brecciated interval of lower Windsor carbonates. Our study shows that karstic collapse of basal Windsor carbonates did take place, but the event post-dated synsedimentary brecciation of the Macumber and subsequent burial. We were unable to unequivocally temporally link the karst breccia with the tectonic breccia although it would seem reasonable to suppose that the karst event post-dated the tectonic one.

CONCLUSIONS

The carbonate units forming the lower part of the Windsor Group (Macumber-Pembroke-Gays River) have, over the years, been the subject of major divergences in the interpretation of their depositional history. Moreover, the fairly abundant and diversified breccias were all simplistically assigned to the Pembroke, thereby profoundly altering the original description of that unit. This led to considerable confusion regarding the correct meaning of the Pembroke and its local occurrence. This has important metallogenic significance since Pb-Zn and Ba-Cu mineralization in lower Windsor carbonates is spatially closely associated with brecciated intervals, especially the synsedimentary and karstic breccias. The metallogenic significance of distinguishing between breccia types lies in the fact that the synsedimentary breccia is pre-ore, and therefore could have played a role in ore control, whereas the karst breccia is post-ore. The karst breccia has, in fact, removed large portions of the

Walton, Gays River, and Smithfield deposits. Moreover, this poorly consolidated material has resulted in serious mining problems at both the Walton and Gays River mines.

From preliminary field and drill core information, breccias in the lower Windsor carbonate succession are of three types. Table 1 summarizes the main characteristics that have been used 1) to distinguish between these breccias and 2) to propose possible formation mechanisms. The synsedimentary and late tectonic breccias are now considered to belong to the Macumber Formation, whereas the informal Pembroke designation is applied to a late karstic breccia.

ACKNOWLEDGMENTS

The authors wish to express their deepest gratitude to the staff of the Nova Scotia Ministry of Natural Resources Core Library in Stellarton. Our thanks are extended to M. Savard from her fine suggestions on the original manuscript.

REFERENCES

- Bastin, E.S. and Williams, H.S.**
1914: Description of the Eastport quadrangle, Maine; United States Geological Survey, Geological Atlas, Eastport Folio 192, 15 p.
- Boehner, R.C., Giles, P.S., Murray, D.A., and Ryan, R.J.**
1989: Carbonate buildups of the Gays River Formation, Lower Carboniferous Windsor Group, Nova Scotia; in Reefs, Canada and adjacent areas, (ed.) H.H.J. Geldsetzer, N.P. James, and G.E. Tebbutt; Canadian Society of Petroleum Geologists, Memoir 13, p. 609-621.
- Clifton, H.E.**
1967: Solution-collapse and cavity filling in the Windsor Group, Nova Scotia, Canada; Bulletin of the Geological Society of America, v. 78, p. 819-832.

Cook, H.E. and Mullins, H.T.

1983: Basin Margin; in Carbonate depositional environments, (ed.) P.A. Scholle, D.G. Bebout, and C.H. Moore, American Association of Petroleum Geologists, Memoir 33, p. 539-617.

Fallara, F., Savard, M.M., Lynch, G., and Paradis, S.

1994: Preliminary geological and geochemical results characterizing the mineralization processes in the Jubilee Pb-Zn deposit, Cape Breton Island, Nova Scotia; in Current Research 1994-D, Geological Survey of Canada, p. 63-71.

Geldsetzer, H.H.J.

1977: The Windsor Group of Cape Breton Island, Nova Scotia; in Report of Activities, Part A; Geological Survey of Canada, Paper 77-1A, p. 425-428.

Giles, P.S.

1981: Major transgressive-regressive cycles in Middle to Late Viséan rocks of Nova Scotia; Nova Scotia Department of Mines and Energy, Paper 81-2.

Giles, P.S. and Lynch, G.

1994: Stratigraphic omission across the Ainslie Detachment in east-central Nova Scotia; in Current Research 1994-D, Geological Survey of Canada, p. 89-94.

Hamblin, A.P. and Rust, B.R.

1989: Tectono-sedimentary analysis of alternate-polarity half-graben basin-fill successions: Late Devonian-Early Devonian Carboniferous Horton Group, Cape Breton Island, Nova Scotia; Basin Research, v. 2, p. 239-255.

Hein, F.J., Graves, M.C., and Ruffman, A.

1993: The Jubilee Zn-Pb deposit, Nova Scotia: the role of synsedimentary faults; in Mineral Deposit Studies in Nova Scotia, v. 2, (ed.) A.L. Sangster; Geological Survey of Canada, Paper 91-9, p. 49-69.

Kendall, A.C.

1984: Evaporites; in Facies Models, 2nd edition, (ed.) R.G. Walker; Geoscience Canada, Reprint Series 1, p. 259-296.

Lavoie, D.

1994: Lithology and preliminary paleoenvironmental interpretation of the Macumber and Pembroke formations (Windsor Group, Early Carboniferous), Nova Scotia; in Current Research 1994-D; Geological Survey of Canada, p. 79-88.

Lynch, G. and Brisson, H.

1994: Ainslie Detachment in the Carboniferous River Denys basin of Cape Breton Island, Nova Scotia, with regional implications for Pb-Zn mineralization; in Current Research 1994-D; Geological Survey of Canada, p. 57-62.

Lynch, G. and Giles, P.S.

1993: Extensional tectonics and evolution of the Upper Devonian-Carboniferous Maritimes Basin, Nova Scotia; Geological Association of Canada-Mineralogical Association of Canada, 1993 Joint Annual Meeting, Edmonton; Program with abstracts, p. A-62.

Sage, N.M.

1954: The stratigraphy of the Windsor Group in the Antigonish quadrangles and Mahone Bay-St. Margarets Bay area, Nova Scotia; Nova Scotia Department of Mines, Memoir 3.

Schenk, P.E.

1967: The Macumber Formation of the Maritimes Provinces - a Mississippian analogue to Recent strand-line carbonates of the Persian Gulf; Journal of Sedimentary Petrology, v. 37, p. 365-376.

Schenk, P.E., von Bitter, P.H., and Matsumoto, R.

1992: A lacustrine origin for the Basal Windsor/Codroy Groups (Carboniferous) of Atlantic Canada - Introducing Loch Macumber!; Geological Association of Canada-Mineralogical Association of Canada, 1992 Joint Annual Meeting, Wolfville. Program with abstracts, p. A-99.

Smith, L. and Collins, J.A.

1979: Unconformities, sedimentary copper mineralization, and thrust faulting in the Horton and Windsor groups, Cape Breton Island and central Nova Scotia; Neuvième congrès international de stratigraphie et de géologie du Carbonifère, Washington and Champaign-Urbana, v. 3, Southern Illinois University Press, p. 105-116.

Stevenson, I.M.

1958: Truro map-area, Colchester and Hants counties, Nova Scotia; Geological Survey of Canada, Memoir 297, 124 p.

von Bitter, P.H., Scott, S.D., and Schenk, P.E.

1992: Chemosynthesis: An alternate hypothesis for Carboniferous biotas in bryozoan/microbial mounds, Newfoundland, Canada; Palaios, v. 7, p. 466-484.

Weeks, L.J.

1948: Londonderry and Bass River map-areas, Colchester and Hants Counties, Nova Scotia; Geological Survey of Canada, Memoir 245.

Geological Survey of Canada Project 920004 BS

Geology of the central part of St. Mary's Basin, Nova Scotia¹

J. Brendan Murphy², Randolph J. Rice², Timothy R. Stokes³,
and D. Fraser Keppie²

Continental Geoscience Division

Murphy, J.B., Rice, R.J., Stokes, T.R., and Keppie, D.F., 1995: Geology of the central part of St. Mary's Basin, Nova Scotia; in Current Research 1995-D; Geological Survey of Canada, p. 11-18.

Abstract: The central portion of the St. Mary's Basin, Nova Scotia, straddles the Avalon-Meguma boundary and is underlain by Tournaisian fluvial to lacustrine clastic rocks of the Horton Group. These rocks overlie Meguma basement and generally strike northeast to east-northeast, face southeast, coarsen upward, thicken towards the southeastern margin of the basin and contain clasts of Meguma derivation. In the western portion of the study area, clastic rocks have a mixed provenance. Strike-slip motion between the Avalon and Meguma terranes resulted in heterogeneous deformation prior to the deposition of the Windsor Group characterized by a variety of dextral kinematic indicators. The zone of greatest deformation occurs in lithologically incompetent units and transects the basin in a northeast-southwest direction where it is characterized by a relatively intense, narrow (ca. 2 km) region of small-scale and regional tight to isoclinal folds, associated faults in the hinges of these folds and locally developed mylonitic fabrics.

Résumé : La partie centrale du bassin St. Mary's, en Nouvelle-Écosse, chevauche la frontière Avalon-Meguma et repose sur des roches clastiques, tournaisiennes, fluviales à lacustres, du Groupe de Horton. Ces roches reposent sur le socle de Meguma et leur direction générale est nord-est à est-nord-est; elles sont orientées au sud-ouest, présentent un granoclassement inverse, s'épaississent vers la marge sud-est du bassin et contiennent des clastes issus du socle de Meguma. Dans la partie occidentale de la région étudiée, les roches clastiques ont une provenance diverse. Un mouvement de décrochement entre les terranes d'Avalon et de Meguma a donné lieu à une déformation hétérogène préalablement au dépôt du Groupe de Windsor, caractérisé par une variété d'indicateurs cinématiques dextres. La zone de plus grande déformation se trouve dans des unités incompétentes par leur lithologie et traverse transversalement le bassin selon une direction nord-estsud-ouest où elle produit une zone étroite (environ 2 km) d'intensité relative caractérisée par des plis serrés à isoclinaux de petite échelle et régionaux, des failles associées dans les charnières de ces plis ainsi que des fabriques mylonitiques locales.

¹ Contribution to Canada-Nova Scotia Cooperation Agreement on Mineral Development (1992-1995), a subsidiary agreement under the Canada-Nova Scotia Economic and Regional Development Agreement.

² Department of Geology, P.O. Box 5000, St. Francis Xavier University, Antigonish, Nova Scotia B2G 2W5

³ Terra Firma Geological Services, 246 Pine St., Nanaimo, British Columbia V9R 2B6

INTRODUCTION

The St. Mary's Basin of central mainland Nova Scotia is generally considered to be one of several post-Acadian successor basins (e.g., Williams, 1978) which lie along the southern flank of the composite late Paleozoic Maritimes Basin (Fig. 1). It differs from other components of the Maritimes Basin in that it straddles the Avalon-Meguma terrane boundary.

The St. Mary's Basin averages 15 km in width and extends for about 130 km, from Chedabucto Bay in the east, to the Bay of Fundy in the west (Fig. 2). On the basis of previous (e.g., Benson, 1974; Utting and Hamblin, 1991) and current palynological studies (G. Dolby, written communication, 1994), basin-fill strata are assigned to the Late Devonian(?)–Early Carboniferous (Tournaisian) Horton Group. The basin is separated from the Avalon Composite Terrane to the north by the Cobequid-Chedabucto Fault. The contact with the Meguma Terrane to the south is (typically) unconformable, although (locally) fault contacts are seen. In the southwestern part of the basin, the Horton Group is overlain, presumably unconformably, by the Windsor Group. Although the Windsor Group is concordant to strata in the Horton Group, paleontological evidence indicates a significant hiatus (Utting, 1989; Utting et al., 1989).

PREVIOUS WORK

Fletcher and Faribault (1887) prepared the first geological maps of the area as part of a regional survey of northeastern mainland Nova Scotia. Stevenson (1956) mapped part of the basin near Truro (Map 1058A, 1958, 1:63 360). Benson (1967, 1974) mapped the majority of the basin (parts of map sheets 11E/7 and 8) and referred to the area as the St. Mary's Graben. Murphy et al., (1994) argued that this was misleading and referred to the area as the St. Mary's Basin. Benson (1974) divided the group into the Craignish, Strathlorne and Ainslie formations on the basis of lithological and stratigraphic similarities with the type areas of these formations in Cape Breton Island as described by Murray (1960) and Kelley (1967). Murphy et al. (1994) indicated that direct correlation with the Horton Group in Cape Breton Island may not be appropriate because the St. Mary's Basin is dominated by clastic rocks derived locally from the Meguma Terrane, in contrast to the predominantly Avalonian derivation of strata in Cape Breton Island. At present, detailed correlations with the Horton Group in its type area have not been established, hence, for present purposes, the group is divided into numbered map units as presented in Murphy et al. (1994, Fig. 2).

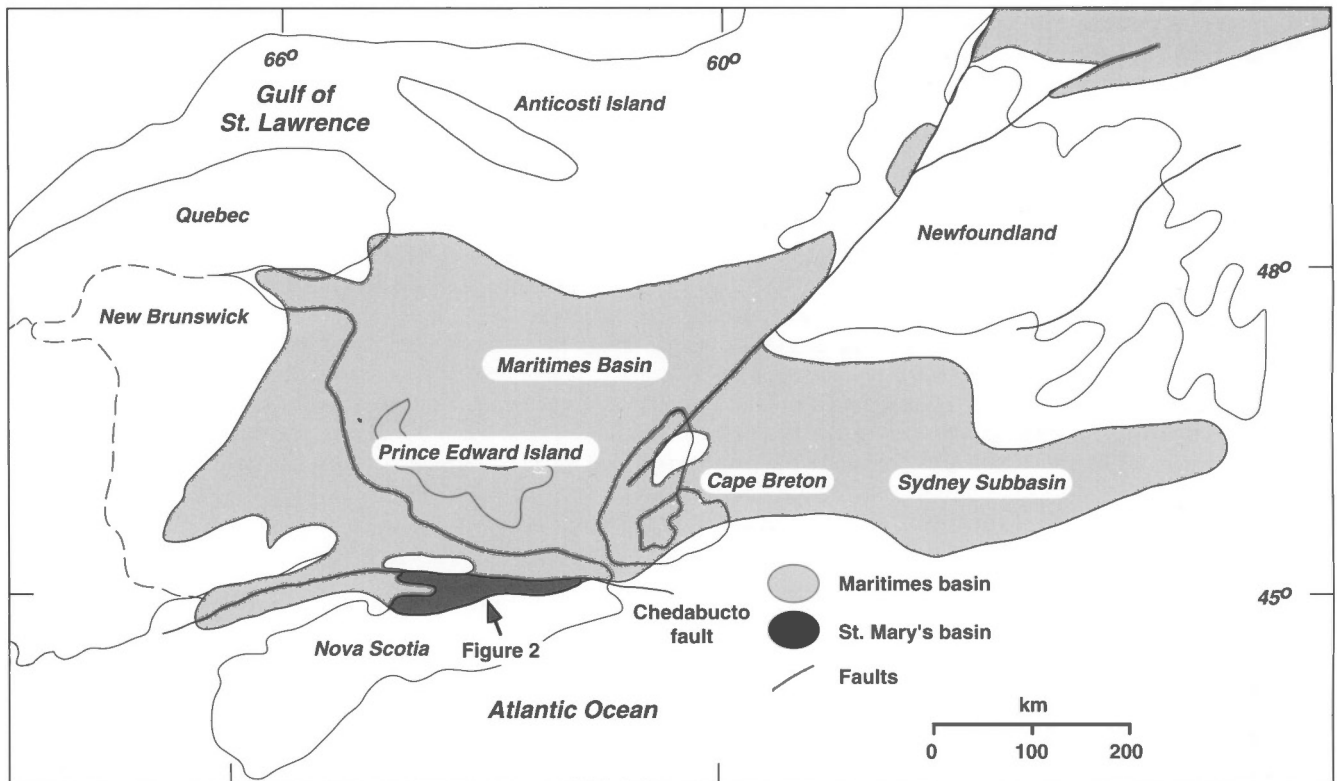


Figure 1. Location of St. Mary's Basin within the Maritimes Basin (Williams, 1978), Canadian Appalachians. Diagram modified after Martel (1987).

SUMMARY OF THE GEOLOGY OF THE EASTERN ST. MARY'S BASIN

Mapping in the eastern St. Mary's Basin (Murphy et al., 1994) showed that this region is dominated by intra-continental fluvial and lacustrine rocks of the Horton Group that coarsen upwards and face towards the southeast part of the basin where they are seen to unconformably overlie rocks of the Meguma Terrane. The clastic rocks were derived from the Meguma Terrane with no definitive evidence of a detrital contribution from the Avalon Terrane. Deposition along the southern flank of the basin (units 3 and 4) occurred as alluvial fan stream flows and debris flows derived from the flanks of the basin. Alluvial fan deposition may have been associated with coeval tectonic activity along active faults (Murphy et al., 1994). Rocks in the central part of the basin (units 2a, 2b) predominantly consisting of fine- to coarse-grained quartz-rich clastic rocks underlie units 3 and 4. These may have been deposited by longitudinal transport along the axis of the basin. The northwest part of the map area is dominated by dark shales and siltstones (unit 1) whose relationship to other units is unclear.

The intensity of deformation differs markedly from south to north. Near the southern margin, units 3 and 4 dip gently to the south and their deposition is thought to have accompanied basin subsidence along northerly dipping listric normal faults. The central part of the area is dominated by upright, open, shallowly east-northeast to northeasterly plunging folds, whose orientation is consistent with dextral shear along the bounding faults. Deformation in the northern part of the area is intense adjacent to the Chedabucto Fault, along the entire length of which the beds steepen and have been rotated clockwise, consistent with dextral shear.

CURRENT WORK

Geological mapping and data collection in the St. Mary's Basin forms part of the 1992-95 Canada-Nova Scotia Co-operation agreement on Mineral Development. During the summer of 1994, the central St. Mary's basin was mapped between latitudes 45°24' and 45°15'N and longitudes 62°17' and 63°10'W and sampled for paleontological, petrographic, and geochemical studies as well as radiometric dating. Palynological samples are currently being examined by Graham Dolby of the Institute of Sedimentary and Petroleum Geology, Calgary.

With the exception of unit 2b, all units in the eastern basin can be mapped across the central basin although in some places the thickness changes significantly.

The stratigraphic position of unit 1 is problematic in the eastern basin (Murphy et al., 1994). In the central part of the basin this unit conformably underlies unit 2a. This interpretation differs from that of Benson (1974) who argued that the oldest rocks occur in the central part of the basin and are overlain by younger rocks to the north and south.

An additional map unit, unit 5, is introduced for red- and grey-weathering siliciclastic strata in the western part of the area. This unit has, as yet, unresolved structural and stratigraphic complexities and will be the focus of next year's mapping. Preliminary work indicates that it may be possible to divide unit 5 into a number of map units. Although its genetic relationship to the other units is indicated by the presence of characteristic lithologies, their stratigraphic relationships are unclear, in particular the relative age of unit 5 to unit 1. Abundant red clastic rocks in unit 5 contain the first record of a mixed Avalonian-Meguma provenance within the Horton Group.

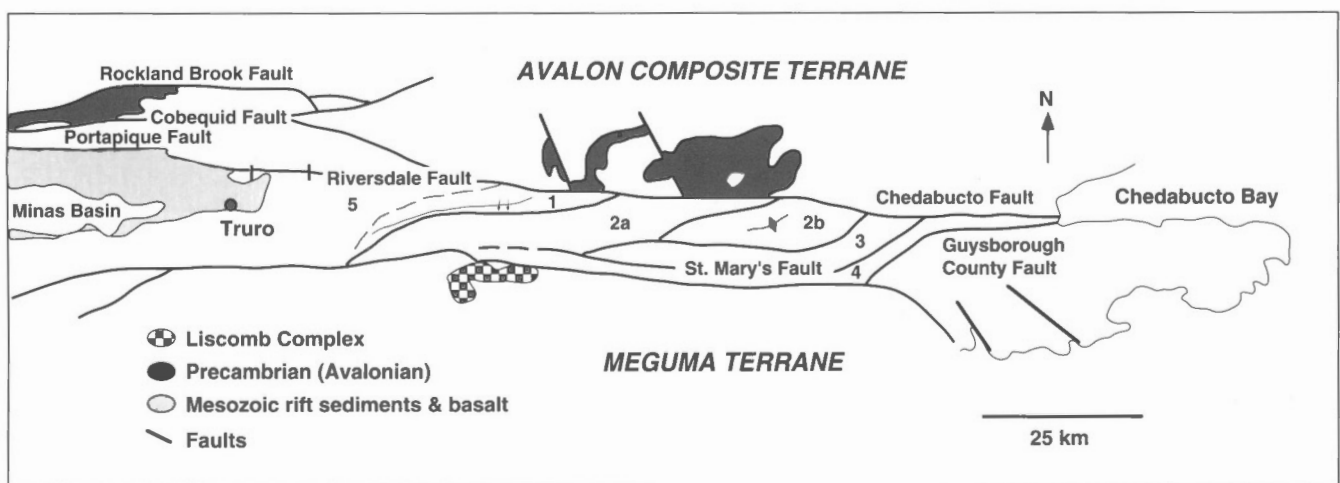


Figure 2. Current regional map units (1-5), Horton Group, St. Mary's Basin.

Murphy et al. (1994) noted that the intensity of deformation in the eastern basin increased from south to north, implying a direct relationship with motion along the Chedabucto Fault. Mapping in the central basin suggests more complex relations. As this zone of deformation is traced farther west, it transects the basin in a northeast-southwest direction, to produce a narrow (ca. 2 km) zone characterized by small-scale and regional tight to isoclinal folds. Associated faults are present in the hinges of these folds as are locally developed mylonitic fabrics. In general deformation is concentrated in the relatively incompetent finer grained lithologies of unit 1. The orientation of these structures and the clockwise rotation of the zone of deformation into the Chedabucto Fault provides additional evidence of the importance of dextral strike-slip along this fault in controlling the style of deformation in the basin. It also suggests that the deformation is not merely concentrated along the northern margin of the basin. To the northwest of this zone the intensity of deformation diminishes and rocks adjacent to the Chedabucto Fault are not as strongly deformed.

STRATIGRAPHY

Five mappable units occur in the central St. Mary's Basin (Fig. 2). Four of these units (1, 2a, 3, 4) are conformable and gradational with interstratification of characteristic lithologies. This, together with the paleontological data of Benson (1967) and G. Dolby (pers. comm., 1994), suggests that the units are broadly coeval and may be related by facies variations. On a regional scale, the sequence of these four units faces from northwest to southeast. As noted above, the relationship of unit 5 to these units is not yet fully understood.

Unit 1 strikes from southwest to northeast across the map area and is well exposed along road and river sections in the vicinity of Highway 289 (Fig. 2). It consists of interstratified red-grey to dark grey, locally organic-rich, fissile mudstone, siltstone, and sandstone. At some localities sandstones display



Figure 3. Soft-sediment deformation, possibly induced by seismic activity, in sandstone near the top of unit 1, Stewiacke River. Facing is toward top of photograph.

soft-sediment deformation features suggestive of fabric collapse possibly induced by seismic disturbance (Fig. 3). Coarsening- and thickening-upward cycles, approximately 2-25 m thick, are recognizable in roadcut exposures. Individual beds range in thickness from about 2 mm to 15 cm and at some localities are bioturbated. The unit appears to have been the focus of heterogeneous deformation in the area. As a consequence, bedding is commonly discontinuous and may be locally transposed along cleavage planes. Mylonitic fabrics are developed locally. The map pattern of unit 1 broadly corresponds with Benson's (1967, 1974) Strathlorne Formation. However, the inferred stratigraphic position of unit 1 contrasts with the interpretation of Benson (1974) who considered these rocks to overlie strata here assigned to unit 2a (see below). This apparent inversion of stratigraphic position, relative to unit 2a implies that Benson's correlation of unit 1 with clastic strata along the southern flank of the basin (here called units 3 and 4) is no longer valid. Although estimates of thickness are complicated by structural complexities, it appears unit 1 may be at least 1000 m thick.

The base of the overlying **unit 2a** is well exposed along the Stewiacke River and is positioned where sand- to granule-size quartz-rich clastic sediment starts to predominate. The contact is transitional over ca. 1 m. It is easily recognized along Stewiacke River by the abrupt occurrence of thin (10-20 cm) lenses of pebbly sandstone and/or quartz-pebble conglomerate in the first few metres of unit 2a. Unit 2a ranges in thickness from ca. 500 m in the eastern basin to ca. 2000 m in the west-central part of the basin and apparently thins westward. It is best exposed along the Stewiacke River where it is ca. 1960 m thick and is conformably overlain (contact not exposed) by unit 3. Unit 2a consists of moderately feldspathic to compositionally mature sandstone and granule to small pebble conglomerate, interlayered with less abundant mudstone and siltstone and minor quartz-pebble conglomerate. The sandstones and granule to small pebble conglomerates (Fig. 4) are grey- to buff-weathering, indurated, fine- to coarse-grained and poorly to moderately sorted with a subangular to



Figure 4. Resistant, grey, coarse grained sandstone and granule to small pebble conglomerate in unit 2a, Stewiacke River. Facing to right.

subrounded framework. Feldspars are generally intensely altered to kaolin. Variably well-defined fining-upward cycles range from 2 to 10 m thick. Ripple cross-lamination and trough cross-stratification (4-20 cm) are common. Contacts between coarser- and finer-grained beds are sharp to gradational. Siltstone and mudstone beds are fissile and weather predominantly dark grey. Organic debris occurs locally. The finer grained beds weather recessively and, in road sections, are poorly exposed relative to the sandstones. In the eastern St. Mary's Basin, unit 2a is laterally continuous with unit 2b.

Unit 3 consists dominantly of green-weathering sandstone with minor interlayered conglomerate, siltstone, and mudstone. Unit 3 is exposed in river sections near the southern flank of the basin. It is significantly thinner than in the eastern portion of the basin. Sandstone units range in thickness from 0.5 to 2 m and are characteristically fine- to coarse-grained, occasionally with minor granule-size detritus. Trough cross-stratification in sets up to 1 m thick and ripple cross-lamination are characteristic. The sandstone and conglomerate contain clasts typical of Meguma Terrane lithologies including schist, metagreywacke, slate, micaceous granite, vein quartz, and muscovite. Other rock types represented include carbonaceous shale, siltstone, other types of sandstone and carbonate. The contact between unit 3 and unit 2a is gradational and occurs where grey- to buff-weathering sandstone and granule to small pebble conglomerate become less abundant than green-weathering sandstone.

Unit 4, composed of poorly sorted pebble to boulder conglomerate (<1 cm to 1 m) and interstratified sandstone, is not exposed in the axial part of the St. Mary's Basin but extends along most of the basin's southern margin (Fig. 2). It appears to thicken markedly eastwards, ranging in thickness from about 100 to 600 m. In some localities, unit 4 oversteps the St. Mary's Fault and rests with local angular unconformity on rocks of the Meguma Terrane (Fig. 2). The conglomerates locally vary from poorly sorted and matrix-supported to moderately sorted and framework-supported. Normal and reverse graded bedding are common and clasts are typical of the

Meguma Terrane. Sandstones that intertongue with the conglomerates are indistinguishable from those of unit 3 and, in the eastern basin, paleocurrents in the conglomerate indicate a northward paleoflow. This suggests a facies relation between units 3 and 4.

Unit 5 (Fig. 2) occurs only in the northwest portion of the current project area and is well exposed along the Pembroke and Salmon rivers. The relationship of this unit to the units described above is unclear and its detailed stratigraphy and structure are the subject of ongoing study. In general, this unit is characterized by red- and grey-weathering clastic sedimentary rocks, the former ranging from conglomerate (Fig. 5) to mudstone and the latter dominantly sandstone (Fig. 6) with minor conglomerate. Lithologies typical of units 1 and 2a also occur. Clasts in the red and grey sandstones and conglomerates indicate a mixed provenance. In addition to Meguma Terrane lithologies they contain mafic and felsic volcanic detritus typical of the Avalon Terrane to the north of the Chedabucto Fault. Red sandstones contain scour surfaces, trough cross-stratification, root casts, and rip-up clasts and occur in thinner fining-upward cycles. Grey sandstones occur in thicker, amalgamated, frequently cross-stratified intervals with occasional thin conglomerate bases. Near the faulted contact with the younger Riversdale Group on the Salmon River compositionally mature sandstone and marl and dolomite occur.

ENVIRONMENTS OF DEPOSITION AND PROVENANCE – PRELIMINARY INTERPRETATION

The rocks of the central St. Mary's Basin were deposited in a fluvial to lacustrine environment characteristic of the Horton Group in mainland Nova Scotia. Units along the southern flank of the basin (units 3 and 4) are interpreted to be locally derived from the adjacent Meguma Terrane and are



Figure 5. Intraformational conglomerate in interstratified red sandstone and siltstone, unit 5, Salmon River. Matrix is white calcareous mud. Conglomerate may represent an arid climate debris flow. Facing toward top of photograph.



Figure 6. Upper parallel-laminated portion of 5 m grey sandstone, unit 5, Salmon River. Facing toward top of photograph.

considered to represent a northward-fining sequence of alluvial fan/fan-delta deposits associated with syn-depositional tectonic instability along the southern basin margin. The gentle dip of these units towards the basin marginal fault is consistent with syn-depositional subsidence along a northward dipping listric normal fault.

The grey- to buff-weathering sandstones and granule to small pebble conglomerates of unit 2a may represent braided stream deposits. Clast lithologies are typical of the Meguma Terrane, but preliminary paleocurrent data appear to be indicating longitudinal flow along the axis of the basin. The predominance of quartz and feldspar clasts in unit 2a suggests a granitic source, although some of the coarser quartz clasts may represent vein material.

The organic-rich, bioturbated shales and siltstones of unit 1 are compatible with a lacustrine setting. Where coarsening- and thickening-upward cycles of mudstone, siltstone, and sandstone occur, a lacustrine-deltaic environment is likely.

The grey and red siliciclastics that dominate unit 5 are thought to represent either overbank and principal channel deposits of a single, higher sinuosity, fluvial system or interfingering of two fluvial systems. The compositionally mature sandstone, marl, and dolomite occurring in proximity to the faulted contact with the Riversdale Group on the Salmon River may represent upper shoreface to paralic deposition. The occurrence of abundant volcanic detritus in unit 5 indicates the presence of Avalonian rocks in the source area. However, neither the character of these rocks, nor those of the other units adjacent to the northern margin of the basin vary with proximity to the Chedabucto Fault. Hence, this fault does not constitute the original basin margin and an unknown portion of the original basin and its basement have been tectonically removed. Consequently, there is no reason to suppose that rocks of the Meguma Terrane cannot be found north of the Chedabucto Fault (Murphy et al., 1994).

STRUCTURE

The intensity of deformation varies markedly from south to north across the central St. Mary's Basin. The most intense deformation occurs in a narrow (2 km wide) northeasterly trending zone (Fig. 2). This zone is a regional anticlinal structure slightly overturned to the northwest (Fig. 2). The deformation is especially intense in unit 1 which in this zone is characterized by small and meso-scale folds (Fig. 7), locally developed penetrative cleavage and mylonitic fabrics. Small-scale antiformal and synformal structures have contrasting styles. The antiformal hinge zones are tight to isoclinal with a relatively well developed axial planar cleavage. Flexure in the hinges of these structures is commonly accommodated by minor offsets along fractures and by local faulting (Fig. 8). In contrast, small-scale synformal structures are broad to open, have greater half-wavelengths, and are rarely cleaved or offset by local fractures. This contrast suggests the presence of a subjacent northeasterly-trending thrust, with the antiformal hinges representing minor faults emanating from near the tip of the thrust. The relative intensity of the deformation in unit 1 is attributed to the predominance of relatively incompetent

finer-grained sedimentary rocks relative to units 2a and 5. At the northeastern end of this structure fabrics steepen markedly and are rotated clockwise into parallelism with the Chedabucto Fault, consistent with dextral shear (Fig.2).

MULTIFACETED RESOURCE POTENTIAL

The economic potential of the St. Mary's Basin is multifaceted and has never been properly documented. Horton Group strata contain evidence of liquid hydrocarbon generation and movement as well as paleoplacer gold and base metal mineralization.

Recent studies of source rock potential and thermal maturation indicate the sediments are intermediate between the oil and gas windows (Utting and Hamblin, 1991) and include major potential source rocks (Type II and II-III kerogens) which have generated mature bitumen suitable for liquid



Figure 7. Folding of interstratified grey sandstone and siltstone, unit 1, Fall Brook. Flow from right to left.



Figure 8. Fault in interstratified grey sandstone and siltstone, unit 1, Big Stewiacke River.

hydrocarbon reservoirs (Mukhopadhyay, 1991). Solid bitumen is known in the Horton Group and a probable instance in coarse sandstone and granule to small pebble conglomerate of unit 2a, Stewiacke River, was noted this field season. This location is above potential source rocks of unit 1 and within the zone of relatively intense dextral movement discussed above. It creates the possibility of several types of structural traps, e.g., fault propagation folds, hanging wall antiforms.

The Horton-Windsor contact constitutes base-metal potential for the Horton Group as mineralizing fluids that emplaced Pb-Zn-Ba mineralization in the Gays River Formation carbonates, and facies equivalents, might have mineralized Horton Group siliciclastics. Sulphide mineralization in Horton sediments near this contact has been mentioned in industry assessment reports. Disseminated and/or nodular sulphide (py) mineralization in mudstones and siltstones of unit 1 was noted this field season, in particular along Highway 289 and on the Stewiacke River, both within the zone of relatively intense dextral movement trending southwest-northeast across the basin. This emphasizes the need for a careful assessment of the relationship between mineralization and basin marginal and internal fault movement in the half graben. It also suggests that Horton strata should be investigated to help determine if the fluids that mineralized the basal Windsor Group derived their metal from the Horton Group or from basement rocks.

The St. Mary's Basin has the potential for new deposits of paleoplacer gold. Historically, the unconformable Horton-Meguma contact has been explored for paleoplacer gold. Gold showings from unit 4 conglomerate along this contact in the eastern part of the basin are reported in Hill (1991). The past-producing Gays River Gold Mine was a paleoplacer deposit on the Horton-Meguma contact in the Shubenacadie Basin. From 1873 to 1881, 1878 ounces of gold were produced from Coldstream Formation conglomerate. Provincial government analyses in 1946 of old workings returned an average of 0.36 gm/ton Au (1.38 gm/ton max.). Also, 1988 industry assessment work reports an auriferous quartz pebble conglomerate reef ca. 9 m thick and traceable for 10 km of strike length ca. 15 km north of the Horton-Meguma contact, Brookfield area, Colchester County. In 1891 the provincial government declared this area a gold district (Waverley Gold District) and mill tests on a four ton sample returned 0.03-0.22 oz/ton Au. Little subsequent exploration has occurred in this area. In 1986 the provincial government sampled the matrix of the conglomerate which assayed 0.04 oz/ton Au. These auriferous conglomerates likely represent proximal to distal fan-delta deposits along the basin margin, not dissimilar to our unit 4 conglomerate, and as such would represent point sources. If so, it is not unreasonable to anticipate that additional point sources of Meguma-derived conglomerate might be auriferous.

SUMMARY AND DISCUSSION

The St. Mary's Basin is a Late Devonian-Early Carboniferous basin-fill sequence that straddles the Avalon-Meguma Terrane boundary, for which there is abundant evidence of late

Paleozoic dextral strike-slip motion (e.g., Keppie, 1982, 1993). It is one of several depocentres within the larger Maritimes Basin.

In general, most of the units defined in the eastern part of the basin (Murphy et al., 1994) can be identified in the central part of the basin. Their regional strike is northeast to east-northeast, oblique to the margins of the basin. As a consequence, they transect the entire (present) width of the basin. The stratigraphic position of the mudstone-siltstone dominated unit 1 of Murphy et al. (1994) is resolved. It underlies the relatively coarser grained arenaceous unit 2a. This interpretation differs with that of Benson (1967, 1974) who considered the oldest rocks to form a regional anticline in the centre of the basin. The different stratigraphic interpretation proposed here suggests that unit 1 lies at the base of a regional-scale, coarsening-upward, southeasterly facing sequence that spans the entire width of the basin.

The geology of the western portion of the study area is complex and will be the focus of future work. Although the details remain unresolved, a genetic relationship with other units of the basin-fill sequence is indicated by the presence of lithologies characteristic of units 1 and 2a. It also contains red siliciclastics that have volcanic detritus interpreted to be derived from an Avalonian source, in addition to clasts typical of the Meguma Terrane. Thus, these rocks display a mixed Avalonian-Meguma provenance confirming the status of the Horton Group as an overstep sequence.

As in the eastern portion of the basin, the character of the sedimentary rocks in units that occur along the northern flank of the basin does not change with proximity to the Chedabucto Fault. This provides additional evidence (see Murphy et al., 1994) that the Chedabucto Fault does not constitute the original basin margin, implying that an unknown portion of the basin, and its basement, may have been tectonically removed and may be found north of the fault. This contrasts with facies relationships along the southern flank of the basin which suggests deposition close to a basin margin.

The exact nature of the basement to the St. Mary's Basin rocks remains unclear. The unconformable relationships between basin-fill rocks and the Meguma Terrane preserved along much of southern flank of the basin implies that at least some of the basin is underlain by Meguma basement. On the other hand, the identification of the proximity of Avalonian rocks suggest the possibility that a portion of the basin may also be underlain by Avalonian crust. If so, the Avalonian-Meguma suture may lie beneath the basin, underscoring the need for geophysical surveys to resolve the basement structure.

A narrow (ca. 2 km) zone of relatively intense deformation, characterized by isoclinal folds and associated faults, transects the central portion of the basin and trends northeast to east-northeast. The deformation is heterogeneous and is concentrated in relatively incompetent finer grained lithologies of unit 1. This zone of relatively intense deformation has been rotated in a clockwise manner into parallelism with the Chedabucto Fault where it can be traced across the eastern basin. Thus, the inference of Murphy et al. (1994) that the deformation intensity decreases from north to south across the basin is incorrect. Kinematic indicators within this narrow

deformation zone, the orientation of the structures relative to the margins of the basin, and the manner of rotation of the structures into parallelism with the Chedabucto Fault are all consistent with deformation associated with dextral shear. This is in agreement with regional tectonic interpretations (e.g., Keppie 1982, 1993) that imply dextral motion between the Avalon and Meguma terranes during the late Paleozoic.

ACKNOWLEDGMENTS

We thank Fred Chandler for organizational support. Fred Chandler, Quentin Gall, John Waldron, Bob Ryan, Tony Hamblin, Peter Giles, Duncan Keppie, Damian Nance, Wes Gibbons and Sandra Barr are thanked for informative discussion. Darrel Long and Damian Nance are thanked for reviewing the manuscript.

REFERENCES

- Benson, D.G.**
 1967: Geology of the Hopewell map area, Nova Scotia; Geological Survey of Canada, Memoir 343, 58p.
 1974: Geology of the Antigonish Highlands, Nova Scotia; Geological Survey of Canada, Memoir 376, 92p.
- Fletcher, H. and Faribault, E.R.,**
 1887: Geological surveys and explorations in the counties of Guysborough, Antigonish, Pictou, Colchester and Halifax, Nova Scotia from 1882-1886; Geological Survey of Canada Annual Report, v. II, 1886, pt. P, p. 5-128.
- Hill, J.D.**
 1991: Petrology, tectonic setting, and economic potential of Devonian peraluminous granitoid plutons in the Canso and Forest Hill areas, eastern Meguma terrane, Nova Scotia; Geological Survey of Canada, Bulletin 383, 96 pp.
- Kelley, D.G.**
 1967: Some aspects of Carboniferous stratigraphy and depositional history in the Atlantic Provinces; in *Collected Papers on Geology of the Atlantic Region*, (ed.) E.R.W. Neale and H. Williams; Geological Association of Canada, Special Paper 4, p. 213-228.
- Keppie, J.D.**
 1982: The Minas Geofracture; Major Structural Zones and Faults in the Canadian Appalachians, (ed.) P. St. Julien, and J. Beland; Geological Association of Canada, Special Paper 24, p. 263-280.
 1993: Synthesis of Paleozoic deformational events and terrane accretion in the Canadian Appalachians; *Geologische Rundschau*, v. 82, p. 381-431.
- Martel, A.T.**
 1990: Stratigraphy, fluviolacustrine sedimentology and cyclicity of the late Devonian/early Carboniferous Horton Bluff Formation, Nova Scotia, Canada; PhD. thesis, Dalhousie University, Halifax, Nova Scotia, Canada, 297 p.
- Mukhopadhyay, P.K.**
 1991: Source rock potential and maturation of Paleozoic sediments (Devonian-Permian) from onshore Nova Scotia; Global Geoenergy Research Ltd. report submitted to the Petroleum Section, Nova Scotia Department of Mines and Energy, Halifax, Nova Scotia.
- Murphy, J.B., Stokes, T.R., Meagher C., and Mosher, S.J.**
 1994: Geology of the Eastern St. Mary's Basin, Nova Scotia; in *Current Research 1994-A*; Geological Survey of Canada, p. 95-102.
- Murray, B.C.**
 1960: Stratigraphy of the Horton Group in parts of Nova Scotia; Nova Scotia Research Foundation Publication.
- Stevenson, I.M.**
 1956: Shubenacadie and Kennetcook map areas, Colchester, Hants and Halifax counties, N.S.; Geological Survey of Canada, Memoir 302, 87 p.
 1958: Truro, Nova Scotia; Geological Survey of Canada, Map 1058A, scale 1:63 360.
- Utting, J.**
 1989: Palynological analysis of 43 samples from Tennycape, Walton and Harding Brook sections of Nova Scotia, submitted by T. Martel, Dalhousie University, (NTS 21H); Geological Survey of Canada, Paleontological Report 3-JU-89, 11 p.
- Utting, J. and Hamblin, A.P.**
 1991: Thermal maturity of the Lower Carboniferous Horton Group, Nova Scotia; *International Journal of Coal Geology*, v. 19, p. 439-456.
- Utting, J., Keppie, J.D., and Giles, P.S.**
 1989: Palynology and stratigraphy of the Lower Carboniferous Horton Group, Nova Scotia; in *Contributions to Canadian Paleontology*; Geological Survey of Canada, Bulletin 396, p. 117-143.
- Williams, H.**
 1978: Tectonic lithofacies map of the Appalachians; Memorial University Map 1, Department of Geology, Memorial University of Newfoundland, Canada, Scale 1:1 000 000.

Geological Survey of Canada Project 760027 CF

Structural investigations in the Stellarton pull-apart basin, Nova Scotia¹

John W.F. Waldron² K.S. Gillis³, R.D.Naylor⁴ , and F.W. Chandler⁵
Atlantic Geoscience Centre

Waldron, J.W.F., Gillis, K.S., Naylor, R.D., and Chandler, F.W., 1995: Structural investigations in the Stellarton pull-apart basin, Nova Scotia; in Current Research, 1995-D; Geological Survey of Canada, p. 19-25.

Abstract: The Stellarton basin is a pull-apart basin located at a releasing bend on the Cobequid-Hollow fault system in Nova Scotia. The basin fill accumulated during Westphalian time. At the base, redbeds occupy fault bounded basins at the western and eastern extremities of the area. The overlying Stellarton Formation includes shale, sandstone, minor conglomerate, coal, and oil shale. Within the basin, map-scale extensional normal and oblique faults strike northwest-southeast and are listric in profile. Motion on these faults has produced map-scale 'rollover' fault-bend folds. At the northeast margin of the basin, older rocks are uplifted along reverse faults and folds to form a positive flower structure. Outcrop-scale structures within the basin show a history of extension followed by shortening. Early normal faults, formed while sediment was not fully lithified, are overprinted by thrust faults and asymmetric folds indicating eastward transport of stratigraphically higher units.

Résumé : Le bassin de Stellarton en est un d'extension se trouvant à une courbe de relâchement sur le réseau de failles de Cobequid-Hollow, en Nouvelle-Écosse. Le bassin s'est rempli de sédiments au cours du Westphalien. À la base, des couches rouges occupent des bassins limités par des failles aux extrémités est et ouest de la région. La Formation de Stellarton sus-jacente comprend du schiste, du grès, un peu de conglomérat, de charbon et de schiste bitumineux. Au sein du bassin, des failles d'extension, normales et obliques, d'échelle cartographique ont une direction nord-ouest-sud-est et présentent un profil listrique. Le mouvement de ces failles a produit des plis «de compensation» de courbe de faille d'échelle cartographique. À la marge nord-est du bassin, des roches plus anciennes sont soulevées le long de failles inverses et de plis pour former une structure positive en forme de fleur. Les structures de l'échelle des affleurements au sein du bassin évoquent un passé d'extension suivi d'un raccourcissement. Les failles normales précoces, qui se sont formées lorsque les sédiments n'étaient pas complètement lithifiés, sont surimprimées par des failles de chevauchement et des plis asymétriques, ce qui indique un transport vers l'est d'unités stratigraphiquement plus élevées.

¹ Contribution to Canada-Nova Scotia Cooperation Agreement on Mineral Development (1992-1995), a subsidiary agreement under the Canada-Nova Scotia Economic and Regional Development Agreement.

² Geology Department, Saint Mary's University, Halifax, Nova Scotia B3H 3C3

³ Nova Scotia Department of Natural Resources, 32 Bridge Avenue, Stellarton, Nova Scotia, B0K 1S0

⁴ Nova Scotia Department of Natural Resources, P.O. Box 698, 1701 Hollis St., Halifax Nova Scotia B3J 2T9

⁵ Continental Geoscience Division, Ottawa

INTRODUCTION

The Stellarton basin is a lozenge-shaped basin located on the Cobequid-Hollow fault system in Pictou County, Nova Scotia. The basin is occupied by 2-3 km of mainly lacustrine sedimentary rocks mostly of Westphalian C age, substantially thicker than equivalent successions of this age elsewhere in Nova Scotia (Ryan et al., 1991). The Pictou coalfield, with a history of coal extraction extending back to the early 19th century (Bell, 1940) is located entirely within the basin. Ten major coal seams have been exploited historically (Gillis, 1991). Numerous oil shale horizons within the basin assist in correlation. Recent attention has been focussed on the potential resources of coalbed methane (Hughes and MacNeil, 1992).

Yeo and Gao (1987) argued convincingly that the basin formed as a pull-apart at a releasing bend in the dextral Cobequid-Hollow fault system. Formation of the basin was thus probably associated with some of the last Paleozoic dextral movement between the Avalon and Meguma terranes of the Nova Scotia Appalachians. Minor structures located on both the Hollow Fault along the southern margin of the basin, and on the Cobequid Fault along the northern margin, are consistent with a history of dextral strike-slip motion (Eisbacher, 1969; Gao, 1987).

In this study structural slices at the basin margins have been re-mapped with the assistance of new palynological data. Within the basin, existing maps (Poole, 1904; Bell, 1940; Naylor et al., 1986; Yeo, 1987; Smith et al., 1989; Gillis, 1991) are being compiled, together with selected borehole records and mine plans (Gillis, 1991). Correlation within the basin is assisted by approximately 35 coal seams and about 60 oil shale horizons, although correlation becomes difficult in redbeds and conglomerates located at the base of the succession and along the basin margins. Structures within the less deformed central parts of the basin have been systematically examined; a new 400 m strike section exposed in the 'Wimpey Pit' (locality J, Fig. 1) is particularly informative.

STRATIGRAPHY

The basement of the Stellarton basin is formed by deformed clastic sedimentary rocks mainly assigned to the Canso Group of Bell (1940), equivalent to the Mabou Group of Ryan et al. (1991). Locally, around both the northern and southern basin margins, red siltstones, sandstones, conglomerates, and rare limestones of the Windsor Group are in fault contact with the basin fill; the basin fill may locally have overlain Windsor Group rocks but no clear stratigraphic contact is preserved. Both the Mabou Group and Windsor Group rocks are well indurated, and are significantly more deformed than the overlying basin fill. For example in Brown Brook at the southwest margin of the basin (locality A, Fig. 1), poorly indurated conglomerates and siltstones of the Middle River Formation dip 20 to 35° northeast; approximately 100 m to the southwest are subvertical, well indurated, rippled sandstones, siltstones, and shales of the Mabou Group. The relationships imply a profound angular unconformity at the boundary. Farther east,

on East River (locality B, Fig. 1), the angular unconformity is exposed; poorly indurated conglomerates and sandstones of the Stellarton Formation dip gently north, overlying more steeply dipping red siltstones of the Mabou Group.

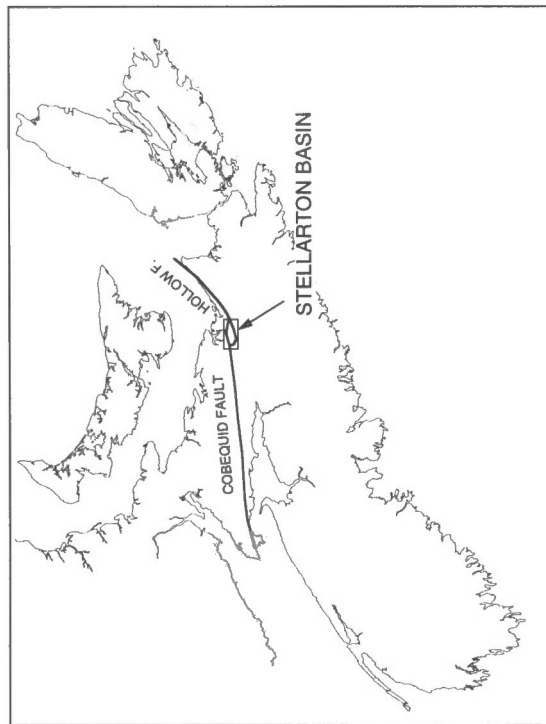
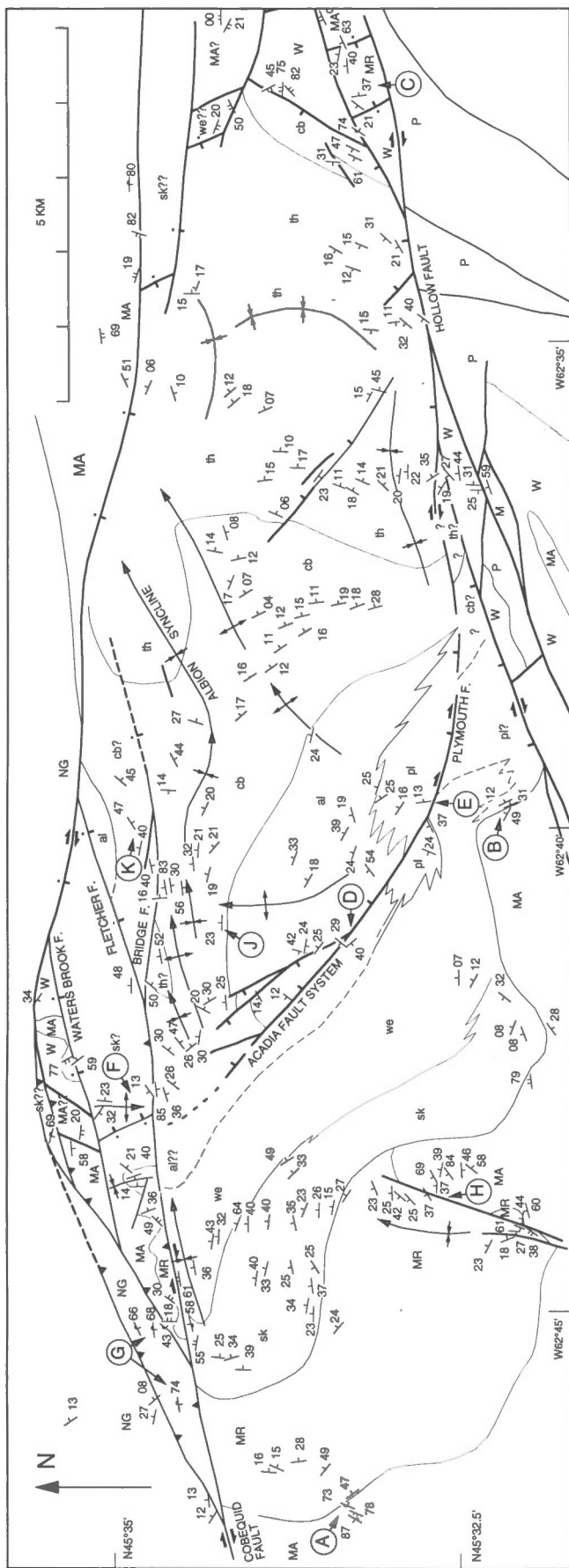
Structurally, the lowest part of the basin fill is formed by the redbeds of Westphalian A age, assigned to the Middle River Formation of Yeo (1987), comprising angular to well rounded, red organized conglomerates, distinctive red pebbly siltstones (disorganized conglomerates), laminated cross-stratified sandstones, and red (locally grey-green) mottled siltstones. The Middle River Formation appears to be restricted to two sub-basins, one at the present southwest margin of the Stellarton basin, and one to the east, in the Maclean Brook area (locality C, Fig. 1). Other strata to the north of the Stellarton basin, previously included in the Middle River Formation by Yeo et al. (1987), are here separated as New Glasgow Formation.

The bulk of the fill of the Stellarton basin consists of lacustrine and associated deltaic and alluvial fan facies, assigned to the Stellarton Formation (Stellarton Series of Bell, 1940). The formation is subdivided into six members as shown in Figure 1. The contact between the lowest (Skinner Brook) Member and the underlying Middle River Formation appears to be gradational, and shows no evidence of discordance; the boundary is placed arbitrarily at the point where mottled red siltstones, characteristic of the Skinner Brook Member, become predominant (Bell, 1940).

Three intervals within the Stellarton Formation carry multiple economic coal seams. The lowest coal-bearing package, together with an overlying section of sandstones and shales, is assigned to the Westville Member. Towards the edges of the basin it interdigitates with redbeds of the Skinner Brook Member. The highest (Acadia) coal seam in the Westville Member can be traced most extensively toward the edges of the basin and provides a useful marker horizon.

The overlying middle coal-bearing package defines the Albion Member. In outcrop, the base of the coal-bearing package is marked by the Norah seam and its top is at the top of the thick (up to 18 m) Foord seam. However, subsurface borehole records in the north of the basin show that several coal seams are present beneath the Norah coal. To the southeast, the Albion Member interdigitates with redbeds assigned to the Plymouth Member (Fig. 1). At the top of the Albion member, the Foord seam can be traced most extensively along strike to the southeast toward the basin margin, and (like its counterpart the Acadia seam in the Westville Member) records a maximum areal extent of coal deposition. However to the west the Foord seam is cut off by a system of faults, the largest of which is inferred on the basis of borehole records to have a throw to the northeast of at least 350 m (Bell, 1940).

The Albion Member is overlain by a succession dominated by oil shales, the Coal Brook Member. The third, highest, coal-bearing succession is preserved toward the eastern end of the basin (and probably locally in synclines along the north margin). It is assigned to the Thorburn Member. The highest strata of the Thorburn Member occur at the centre of a complex synclinal area toward the east-end of the basin; no younger rocks are preserved.



FILL OF STELLARTON BASIN

th	Thorburn Member
cb	Coal Brook Member
al	Albion Member
pi	Plymouth Member
we	Westville Member
sk	Skinner Brook Member
MR	MIDDLE RIVER FORMATION (WESTPHALIAN A)

STELLARTON FORMATION (WESTPHALIAN B?-D)

NEW GLASGOW FORMATION (WESTPHALIAN A - B?)

CANSO GROUP (NAMURIAN)

WINDSOR GROUP (VISEAN)

MCARAS BROOK FORMATION (DEVONIAN)

PRE-DEVONIAN ROCKS

OTHER UNITS

NG

MA

W

M

P

Bedding Orientation

- Upright (observed or inferred)
- Overtumed (observed or inferred)
- Way up unknown

Faults

- Normal separation (tick marks hangingwall)
- Reverse separation (tooth marks hangingwall)
- Dip unknown (tick marks downthrow, dot marks upthrow)

Folds

- Syncline
- Anticline

Locality mentioned in text

Figure 1. Geological map of the Stellarton basin showing localities mentioned in the text. Data are from new mapping and compilation from Poole (1904). Belle (1940), Naylor et al. (1986). Yeo (1987). Giles (1982), Smith et al. (1989), and Gillis (1991).

Available palynological data indicate a Westphalian A age for the Middle River Formation. Low parts of the Stellarton Formation are poorly dated (further sampling may rectify this problem) but the Coal Brook and Thorburn members are of Westphalian C age; early Westphalian D ages have been reported from the upper Thorburn Member.

The succession within the basin contrasts with that to the north, in the Trenton Syncline, where a thick, gently dipping Mabou Group is overlain without conspicuous angular discordance by a Cumberland Group succession (New Glasgow Formation) of Westphalian age that initially coarsens up from predominant sandstone into conglomerate. The conglomerates are abruptly overlain by thin lacustrine limestones at the base of a fluvial succession (Malagash Formation) contemporary with the bulk of the predominantly lacustrine Stellarton Formation to the south (Chandler et al., 1994).

STRUCTURE

Previous work within the basin has shown that the basin fill is tilted broadly northeast but that the structure is complicated by folds and faults. Yeo and Gao (1987) and Gillis (1991) showed that the overall pattern of folds and faults is consistent with an environment of dextral strike-slip motion, with en echelon folds trending northeast-southwest oblique to the basin margins, and extensional structures (mainly normal faults) striking northwest-southeast.

Faults within the basin

The largest of the extensional structures is a major fault system that strikes northwest-southeast across the basin west of the worked area of Albion Member coals (Fig. 1). Deformed rocks seen in outcrop (locality D, Fig. 1) indicate the presence of one fault in this zone; the existence of other strands is inferred on the basis of borehole records, which suggest that the westernmost fault in the zone (the Acadia Fault of Bell, 1940) dips to the northeast and has a stratigraphic throw of at least 350 m. An apparent 'rollover' of coal seams toward this structure, and the change in strike across the fault, indicate that the fault is listric, flattening at depth. Gillis (1991) inferred that this fault zone can be connected with an exposed structure on East River at Plymouth (the Plymouth fault; locality E, Fig. 1) where Gao (1987) recorded minor structures indicative of oblique (dextral and normal) motion.

Other mapped faults within the basin involve smaller offsets. Gillis (1991) mapped numerous faults in the New Glasgow area on the basis of mine plan data and limited surface exposure. The majority of these faults strike northwest-southeast or north-south and indicate significant extension in a direction slightly oblique to the basin margin, consistent with an overall dextral motion. Farther east in the basin there are fewer faults, but a predominance of northwest-southeast strikes is again observed.

Folds

Map-scale folding of the basin fill increases in intensity toward the northern margin (Figure 1), where the combination of folding and faulting, together with rapid facies changes, has hindered stratigraphic correlation. Several large folds can be traced both from patterns of bedding orientation in scattered outcrop and from subsurface mine plan information (Gillis, 1991). Fold axes trend predominantly north-northeast, with the exception of an area in the vicinity of New Glasgow where the Albion syncline and other folds follow an arcuate pattern suggesting that the basin margin may have been indented, perhaps by an irregularity in the basin margin fault system. West of this area, correlation of surface and subsurface folds suggests that fold axial surfaces dip north, consistent with an inferred flower structure developed at the northwest basin margin (see below).

Farther east in the basin, a complex fold pattern in the Thorburn area involves two structural basins linked by a syncline. The individual basins may be related to northwest-southeast shortening but the overall structure appears to mirror the shape of the eastern basin margin, suggesting that the synclinal structure may result from dip-slip movement on non-planar basin-bounding faults.

Basin margin structures

Several fault-bounded slices occur at the basin margins. In the northwest (locality F, Fig. 1), gently dipping redbeds, provisionally assigned to the Skinner Brook Member, are upthrown along the Fletcher Fault against Coal Brook Member and/or Thorburn Member rocks to the south. To the west, an inferred fault separates these strata


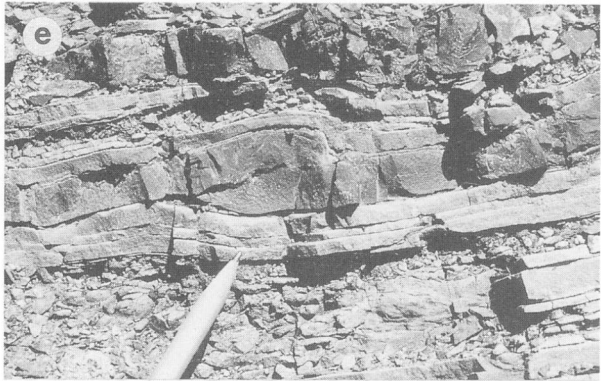
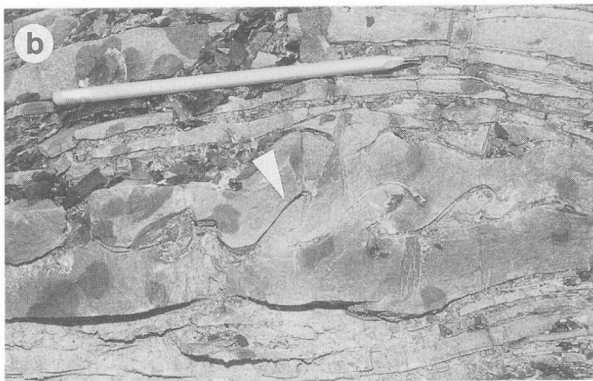
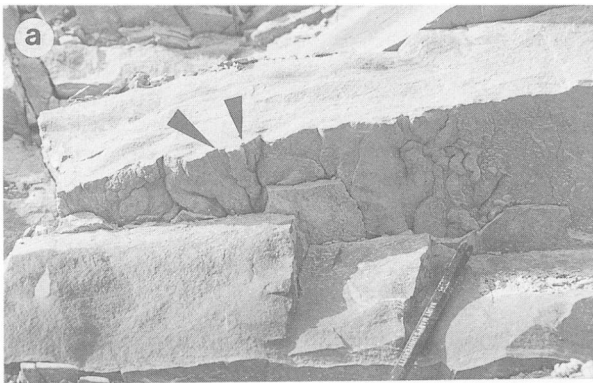
- 
- a) *Conjugate normal faults (arrows) and associated load structures visible on bed basal surface formed by extension of unlithified or poorly lithified sandstone. Pencil for scale at lower right.*
 - b) *East-vergent folds in thin shale layer within a group of sandstone beds, interpreted as products of syndimentary slumping. Pencil for scale.*
 - c) *Small-scale normal faults (arrows), downthrow to east. Pencil for scale.*
 - d) *Normal faults (arrows) and associated rollover fold in shales and sandstones of lower Coal Brook Member. Dark rocks in lower foreground are coal of uppermost Albion Member. Scale bar 10 m approx.*
 - e) *Thrust fault within sideritic siltstone bed. Pencil for scale.*
 - f) *East-vergent folds affecting sandstones and shales of basal Coal Brook Member. Scale bar 10 cm.*

Figure 2. Structures exposed in Wimpey Pit (locality J, Fig. 1). All photographs are taken facing north.

from a block characterized by conglomerates, provisionally assigned to the Middle River Formation, overlying deformed siltstones mapped as Mabou Group (Canso Group of Bell, 1940). To the north, a second fault (Waters Brook Fault, Fig. 1) bounds a slice containing unfossiliferous indurated siltstones (Mabou Group or older?) and localized grey, laminated limestones; historical records of gypsum exposures in this area (Poole, 1904) confirm the existence of Windsor Group rocks in this slice. At the north edge of this slice, poorly indurated siltstones of uncertain affinities young to the north but dip steeply south.

In the Alma area (localities G, Fig. 1), rocks outside the basin (New Glasgow Conglomerate) stand near-vertical to overturned, and young to the north. Exposure is poor in the region between the overturned strata and the gently dipping conglomerates and sandstones to the north; the structure is tentatively interpreted as a faulted fold.

The overall structure at the northwest edge of the basin is marked by fault slices which are uplifted relative to the units both north and south. Along the edges of the zone of uplift, strata are near-vertical to overturned, and face outward, away from the structure. This margin of the basin is interpreted as a positive flower structure.



Map-scale structures at the other margins of the basin are less clear. Rocks in fault-bounded slices at the northeastern basin margin were regarded as correlative with the Skinner Brook and Westville members by Bell (1940) and are shown as such in figure 1, but this correlation is based on lithological similarities only. There is no indication of overturning in the Stellarton Formation strata, and the map pattern is consistent with a system of faults with southward downthrow. At the southeastern basin margin, Gao (1987) mapped minor structures in Stellarton Formation rocks at MacLellan's Brook that are consistent with dextral strike slip motion.

Along the southwest basin margin, a variety of Stellarton and Middle River strata are found in contact with both Canso and Windsor groups. Mapping of members within the basin seems to require that the strata observed unconformably overlying the Mabou Group at East River are substantially higher in the succession than the older parts of the basin fill on Skinner Brook. The basin fill is therefore inferred to onlap the basin margin, with higher parts of the fill transgressing farther over the adjacent upland formed by deformed Mabou and Windsor rocks. In the area of Hazel Glen (locality H, Fig. 1), Middle River conglomerates dip relatively steeply away from Mabou strata, but show few other signs of deformation. This boundary is shown as a fault by Yeo (1987), yet the fault, if it exists, does not appear to cut the mined section of the Westville Member only 3 km to the north. It is possible that this boundary represents a fault that was active during or after deposition of the Middle River Formation and which then became completely inactive; however, the observations are equally consistent with an unconformity marked by onlap of Middle River Formation against a highland of Mabou Group, and modified by relatively minor later faulting and differential compaction.

Outcrop-scale structures

Outcrop scale structures are well exposed in the 'Wimpey' pit on the Foord coal seam in the northwest central part of the basin (locality J, Fig. 1). Deformation becomes less intense to the southeast, and only rare faults and open folds are observed in brooks in the central parts of the basin. More intensely deformed rocks may be seen close to the northern boundary at the Highland Mall (locality K, Fig. 1) and elsewhere in the New Glasgow area, and along the southern basin margin close to the Hollow Fault, where they were described by Gao (1987). Discussion here is focussed on the Wimpey Pit outcrop (locality J, Fig. 1), typical of the moderately deformed central basin fill.

The earliest abundant structures seen in the well exposed sandstones and shales that overlie the Foord coal seam are small normal faults that dip both east and west and that extend bedding (Fig. 2a). Stratigraphic throws on individual faults range from 1 to 5 mm. These faults are associated with linear load structures found on the under-surfaces of sand beds, and are inferred to have formed soon after deposition. Rarer early west-vergent asymmetric folds are characterized by extreme variations in sandstone bed-thickness (Fig. 2b); these are also inferred to have formed before significant lithification, possibly as a result of synsedimentary slumping.

More substantial throws are found on consistently east-dipping normal faults that strike northwest to northeast. Most offset bedding in cross-section by between 5 mm and 20 cm (Fig. 2c), but several major faults display stratigraphic offsets of a few metres. Rollover anticlines in the hangingwalls of these faults indicate that they are listric in profile (Fig. 2d). This is confirmed by the observation that these faults do not cut the underlying Foord seam. Despite their consistent orientation and sense of motion, these faults show neither brecciation nor veining, except in a very few instances where they are cut (and possibly reactivated) by later structures.

Small thrust structures are common in red-brown weathering siderite-cemented siltstone beds (Fig. 2e). These structures shorten bedding in an east-west direction, as indicated by carbonate mineral fibres in veined fault surfaces. Measurements of numerous such faults exposed in a single bed indicate shortening of 8 to 9 per cent. Shortening clearly took place after lithification of the sideritic siltstones, but the failure of adjacent shales and sandstones to show the shortening indicates that these lithologies were less lithified.

Folds and thrust structures that affect all lithologies are observed at several points in the quarry face (Fig. 2f); the majority trend northwest to northeast and have consistent Z-sense asymmetry indicating west over east motion. Several zones of movement can be traced through the cliff. In one instance, the small thrust structures in sideritic siltstone are refolded by west-vergent asymmetric folds. In contrast to the earlier folds of inferred soft-sediment origin, these structures typically show approximate parallel-fold geometry in sandstones, with intervening shales showing thickened hinges and thinned limbs. These structures are typical of folds formed in at least moderately lithified successions.

DISCUSSION

There is a general agreement in orientation and character between the outcrop scale and map scale structures. At map scale, the basin shows a geometry and style of fill that is typical of pull-apart basins formed in extensional settings at releasing bends on strike-slip fault systems. The relative thickness of the succession in the basin compared with other successions of similar age confirms that a distinct tectonic control is necessary to explain the origin of the basin. At outcrop scale, extensional structures – mainly normal faults – also characterize the early suite of structures. The geometry of listric normal faults observed in outcrop closely mirrors the map-scale geometry of the Acadia fault system that lies only a few hundred metres to the west.

Structures produced by shortening of the basin fill are overprinted on the northwest margin of the basin, where a positive flower structure is present at map scale. Within the northwestern part of the basin there is also an abundance of shortening structures, and these consistently post-date the extensional normal faults. Shortening directions deduced from outcrop-scale structures are close to the direction of the earlier extension. However at map scale there is a distinct contrast between northeast-southwest directed extension and northwest-southeast compression.

CONCLUSION

Structures within the Stellarton basin, and along its margins, are broadly consistent in their style and orientation with an environment of dextral strike-slip motion. The basin originated as a pull-apart at a releasing bend on the Cobequid-Hollow fault system. However, a consistent overprinting of shortening on extensional structures suggests a change from transtensional to transpressional deformation. The listric form of faults at both outcrop and map scale is responsible for part of the folding of the basin fill. Further work will investigate the causes of this change and its relationship to the regional tectonics of the Stellarton Gap area.

ACKNOWLEDGMENTS

We acknowledge discussions and helpful comments from Brendan Murphy and Peter Giles. Graham Dolby provided preliminary palynological determination, through the Magdalen Basin NATMAP.

REFERENCES

- Bell, W.A.**
1940: The Pictou Coalfield, Nova Scotia; Geological Survey of Canada, Memoir 225.
- Chandler, F.W., Gall, Q., Gillis, K., Naylor, R., and Waldron, J.**
1994: A progress report on the geology of the Stellarton Gap, Nova Scotia, including the Stellarton Coal Basin; in *Current Research 1994-D*; Geological Survey of Canada, p. 113-122.
- Eisbacher, G.H.**
1969: Displacement and stress field along part of the Cobequid Fault, Nova Scotia; *Canadian Journal of Earth Sciences*, v. 6, p. 1095-1104.
1970: Deformation mechanisms of mylonitic rocks and fractured granites in the Cobequid Mountains, Nova Scotia, Canada; *Geological Society of America Bulletin*, v. 81, p. 2009-2020.
- Hughes, J.D. and MacNeil, D.J.**
1992: Characterization of the coal and coalbed methane resource potential of Nova Scotia. Nova Scotia Department of Natural Resources, Mines and Energy Branches, Report 92-4, p. 3.
- Gao R.**
1987: Deformation Characteristics of the Eastern Cobequid and Hollow Fault Zones and Stellarton Basin, Nova Scotia; M.Sc. Thesis, University of New Brunswick, Fredericton, New Brunswick.
- Giles, P.S.**
1982: Geological map of the Eureka area, central Nova Scotia, scale 1:50 000; Nova Scotia Department of Mines and Energy.
- Gillis, K.S.**
1991: Report on the structural setting and coal resources of the Stellarton Graben, Pictou County, Nova Scotia; Nova Scotia Department of Mines and Energy, Open File Report 91-014.
- Naylor, R.D., Prime, G.A., and Smith, W.D.**
1986: Geological map of the Stellarton Basin (east half); Nova Scotia Department of Mines and Energy, Open File Map 86-047, scale 1:5000.
- Poole, H.S.**
1904: Report on the Pictou Coal Field; Geological Survey of Canada, Annual Report XIV, Part M, p. 1-38.
- Ryan, R.J., Bohner, R.C., and Calder, J.H.**
1991: Lithostratigraphic revisions of the Upper Carboniferous to Lower Permian strata in the Cumberland Basin, Nova Scotia, and the regional implications for the Maritimes Basin in Canada; *Bulletin of Canadian Petroleum Geology*, v. 39, p. 289-314.
- Smith, W.D., Gillis, K.S., and Montgomery, S.A.**
1989: Geological map of the Stellarton Basin (west half); Nova Scotia Department of Mines and Energy, Open File Map 89-017, scale 1:5000.
- Yeo, G.M.**
1987: Geological Map of the New Glasgow - Toney River area (NTS 11E/10 and 11E/15S); Geological Survey of Canada, Open File 1656, scale 1:50 000.
- Yeo, G. and Gao, R.-X.**
1987: Stellarton graben: an upper Carboniferous pull-apart basin in northern Nova Scotia; *Canadian Society of Petroleum Geologists, Memoir 12*, p. 299-309.

Geological Survey of Canada Project 760027 CG

Field evidence for the character of the Precambrian rocks south of the Rockland Brook fault, Bass River block, Cobequid Highlands, Nova Scotia¹

Georgia Pe-Piper², David J.W. Piper, and Ioannis Koukouvelas³
Atlantic Geoscience Centre, Dartmouth

Pe-Piper, G., Piper, D.J.W., and Koukouvelas, I., 1995: Field evidence for the character of the Precambrian rocks south of the Rockland Brook fault, Bass River block, Cobequid Highlands, Nova Scotia; in Current Research 1995-D; Geological Survey of Canada, p. 27-31.

Abstract: Field and petrographic studies, confirmed by published geochronology, show that the southern part of the "Great Village River gneiss" consists of deformed Gamble Brook Formation and Neoproterozoic plutonic rocks and the northern part comprises mylonitized earliest Carboniferous plutonic rocks. The gneiss does not represent an arc root, but rather high-level plutons deformed in a Neoproterozoic shear zone. The sequence of plutonic rocks in the Bass River block is similar to that in southern Cape Breton Island and the Caledonia Highlands.

Résumé : Des études pétrographiques sur le terrain, confirmées par des données géochronologiques publiées, révèlent que la partie sud du «gneiss de Great Village River» consiste en plutonites déformées de la Formation de Gamble Brook et du Néoprotérozoïque, et que la partie nord comprend des plutonites mylonitisées du Carbonifère initial. Le gneiss ne représente pas une racine d'arc, mais plutôt des plutons de niveau élevé déformés dans une zone de cisaillement du Néoprotérozoïque. La séquence de plutonites dans le bloc de Bass River est semblable à celle qui repose dans le sud de l'île du Cap-Breton et les hautes terres de Caledonia.

¹ Contribution to the Canada-Nova Scotia Cooperation Agreement on Mineral Development (1992-1995), a subsidiary agreement under the Canada - Nova Scotia Economic and Regional Development Agreement.

² Department of Geology, Saint Mary's University, Halifax, Nova Scotia B3H 3C3

³ Department of Geology, University of Patras, Patras, 26110 Greece

INTRODUCTION

The Neoproterozoic of the Cobequid Highlands occurs in two major tectonic blocks (Murphy et al., 1988, 1992), separated by the Rockland Brook fault, which was reactivated as recently as the early Carboniferous (Miller et al., 1989). North of the Rockland Brook fault are large diorite and granite plutons of latest Devonian-earliest Carboniferous age (Piper et al., 1993). The Bass River block includes platformal metasediment (Gamble Brook Formation) and metabasalt and pelagic sediments of the Folly River Formation. These were deformed prior to intrusion by a series of plutonic rocks, including diorite, granodiorite, and granite, that have been dated as latest Precambrian by ^{39}Ar - ^{40}Ar (hornblende) and U-Pb (zircon) methods (Keppie et al., 1990; Doig et al., 1991).

Previous workers (Donohoe and Wallace, 1982, 1985; Cullen, 1984; Nance and Murphy, 1990) identified a supposedly older gneissose unit, the Great Village River gneiss, within the Bass River block immediately south of the Rockland Brook fault. More recently, Doig et al. (1991) showed that much of the gneiss was of the same age as the Neoproterozoic plutons and suggested that these rocks were intruded into the roots of a magmatic arc, the upper parts of which were represented by the high-level Neoproterozoic plutons. We have carried out detailed field investigations of the "Great Village River gneiss" that lead us to question both the traditional interpretation of this unit as "basement" to the Avalonian rocks of the Bass River block and the interpretation of an "arc root".

NEOPROTEROZOIC ROCKS OF THE BASS RIVER BLOCK

Nance and Murphy (1990) described the Great Village River gneiss as comprising granitoid orthogneiss, amphibolite, and minor psammitic paragneiss, with a mylonitic ductile shear

zone separating the unit from the Gamble Brook Formation. Doig et al. (1991) obtained moderately concordant U-Pb zircon ages from various lithologies within the Great Village River gneiss of 605 ± 5 , 589 ± 5 , and 580 ± 5 Ma. In the Economy River section, zircons from orthogneiss yielded a concordant U-Pb age of 734 ± 2 Ma (Doig et al., 1993).

The Gamble Brook Formation comprises variably deformed quartzite, metapsammite and metapelitic schist. The Folly River Formation structurally overlies the Gamble Brook Formation and consists of mafic metavolcanic rocks with minor chert and argillite, cut by numerous mafic dykes. Murphy et al. (1988) interpreted the Folly River Formation as unconformable on the Gamble Brook Formation, principally because a dyke geochemically similar to the Folly River Formation cuts deformed Gamble Brook Formation. We are unconvinced by this evidence and on the basis of geochemical character interpret many dykes that cut the Folly River Formation as early Carboniferous.

In their 1:50 000 mapping, Donohoe and Wallace (1982) distinguished some thirteen different plutons south of the Rockland Brook fault that we interpret as late Precambrian (or possibly Cambrian). The boundaries of these plutons are principally tectonic. Similar plutonic rocks also occur in large areas mapped as Great Village River gneiss. Petrographically and geochemically, three major assemblages of plutonic rocks are distinguishable in the Bass River block. We name these from type sections using the pluton nomenclature of Donohoe and Wallace. The Frog Lake diorite, defined in a type section in quarries south of Frog Lake, is similar to rocks that outcrop from the western limit of the Bass River block (in the Economy River) to Mount Thom in the east (Fig. 1). The Debert River granodiorite is defined in a type section on the Debert River (Fig. 2A); similar granodiorite is widespread in the southern parts of the McCallum Settlement and Salmon River plutons of Donohoe and Wallace (1982) extending west of the type section to near Mount Thom. The Frog Lake diorite appears older than the Debert River granodiorite and the one age determination (622 ± 3 Ma) is significantly older than

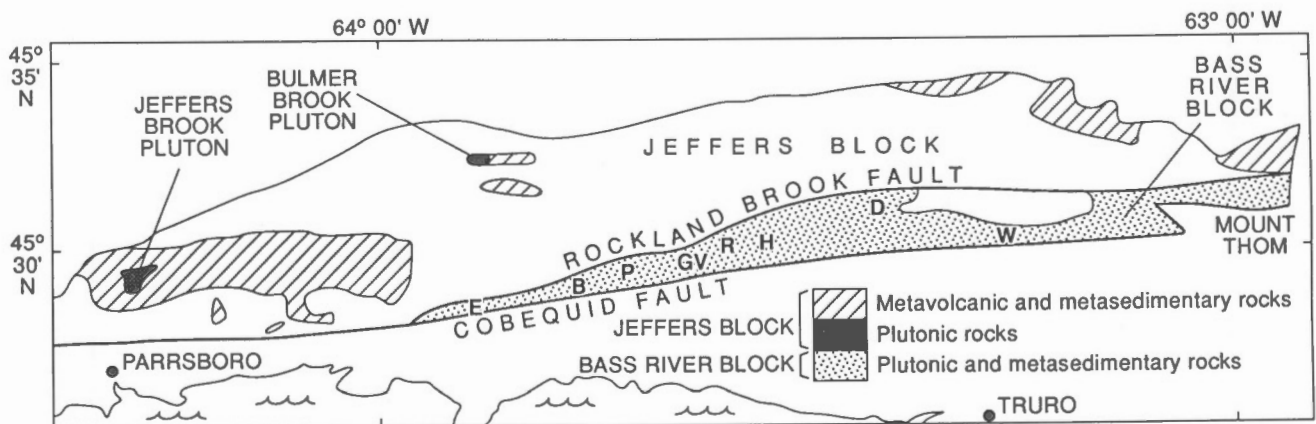


Figure 1. General map of the central and eastern Cobequid Highlands showing Jeffers and Bass River blocks and Neoproterozoic-Cambrian plutons. Sections through Bass River block: E – Economy River; B – Bass River; P – Portapique River; GV – Great Village River; R – Rockland Brook; H – Higgins Mountain - Folly Mountain road; D – Debert River; W – West Branch North River.

determinations from the Debert River and Jeffers Brook granodiorites, whose concordant U-Pb and ^{39}Ar - ^{40}Ar ages range from 609 to 605 Ma. Both the Frog Lake diorite and the Debert River granodiorite appear to have been intruded as thin sheets into the Gamble Brook Formation (Fig. 2A), with many preserved igneous contacts with deformed quartzite and abundant evidence of syn-magmatic deformation. The Frog Lake diorite, in particular, appears to have been emplaced at a high magmatic level, with abundant volatile-rich marginal phases and roof pendants. The Debert River granodiorite was emplaced at a higher level than the geochemically similar Jeffers Brook pluton (Pe-Piper, 1988), which has abundant mafic enclaves, lacks roof pendants, and contains higher-pressure hornblendes. The Jeffers Brook pluton intrudes greenschist facies metavolcanic and metasedimentary rocks.

The McCallum Settlement granite makes up only the northern part of the McCallum Settlement pluton of Donohoe and Wallace (1982), but petrographically and geochemically similar granites outcrop in the East Branch Chiganois River (eastern part of the Debert River pluton of Donohoe and Wallace, 1982), in Shatter Brook, and in parts of the area mapped as Salmon River pluton by Donohoe and Wallace, notably in North River. Doig et al. (1991) obtained discordant U-Pb ages on zircons, the youngest of which was similar to a Rb-Sr age of 575 ± 22 Ma by Gaudette et al. (1984). Thus no reliable geochronological data are available for the McCallum Settlement granite, but its style suggests that it is post-tectonic with respect to deformation of the older plutons.

The Economy River granodiorite described by Doig et al. (1993) represents an older plutonic rock type preserved in the Bass River block. Although texturally and geochemically a typical calc-alkaline granodiorite, it differs from the Debert River granodiorite not only in being about 130 Ma older, but also in its geochemistry. The Economy River granodiorite is significantly richer in MgO, Cr and Ni and contains less Y and Zr than the Debert River granodiorite.

OBSERVATIONS ON SECTIONS THROUGH THE "GREAT VILLAGE RIVER GNEISS"

We have re-examined in the field sections through the rocks mapped by Donohoe and Wallace (1982) as Great Village River gneiss in some eight sections: Economy River, Bass River, Portapique River (Fig. 2C), Rockland Brook, Great Village River and the adjacent two road sections (Fig. 2B) and along the road from Higgins Mountain to Folly Mountain. We have also mapped the rocks immediately south of the Rockland Brook fault in the Debert River (Fig. 2A), east of the West Branch North River and in the Mount Thom area.

Most of these sections show a similar structural style. The northern part of the Great Village River gneiss consists of mylonitic granite and less deformed diorite that show a gradual transition into little-deformed rocks of the late Paleozoic plutons (Koukouvelas and Pe-Piper, 1995). These rocks show progressively more intense deformation and steeper mylonitic



Figure 2. Schematic cross-section of the Neoproterozoic rocks south of the Rockland Brook fault. (A) along the Debert River (D in Fig. 1); (B) north of Londonderry on the Higgins Mountain road (GV in Fig. 1); (C) Portapique River (P in Fig. 1).

foliation southward, culminating in a zone 50 to 200 m wide (Fig. 2B, C) characterized by sheath folds on a centimetre to decimetre scale.

South of the zone in which the highest ductile strain is localized, a complex assemblage of deformed lithologies outcrop that are found elsewhere in the Neoproterozoic of the Bass River block. Deformation ranges from protomylonitic to ultramylonitic. The lithologies include diorite ("amphibolite" of previous authors) and granodiorite ("granitic orthogneiss") with a range of textures and mineralogy in hand specimen similar to that found in the Frog Lake and Debert River plutons. These alternate with metasedimentary rocks ("psammitic paragneiss"), similar to those of the Gamble Brook Formation. As in less deformed areas south of the "gneiss", plutonic rocks show igneous contacts with deformed metasedimentary rocks. There is not just a single ductile shear zone separating the Great Village River gneiss from the Gamble Brook Formation as implied by Doig et al. (1991): rather, the frequency and intensity of ductile shear zones progressively increase northward.

DISCUSSION

Mapping of the "Great Village River gneiss" after mapping less deformed rocks north and south of the Rockland Brook fault indicates that the gneiss unit is a lithologically complex assemblage of rocks deformed in a major ductile shear zone. All the lithologies present can be found in a less-deformed state either to the north or to the south of the gneiss unit. In this respect, it resembles the "Bateman Brook Metamorphic Suite" of Cape Breton Island recently re-interpreted by McMullin et al. (1993). Three U-Pb zircon geochronological determinations (Doig et al. 1991) confirm that pink granite within the area mapped as Great Village River gneiss is of latest Devonian age and therefore correlative with the main phase of late Paleozoic plutonic activity.

In the Bass River block to the south of the gneiss unit, the Frog Lake diorites and Debert River granodiorites were intruded as small bodies, probably originally sheet-like. The rapid lateral variability in igneous phases is typical of that found in shear zones. North-northwest- and north-northeast-trending mylonitic zones between the Debert River pluton and the Folly River Formation were also active syn-magmatically. These patterns of intrusion can be traced northward into the area mapped as Great Village River gneiss, with the intensity of deformation of Precambrian plutonic rocks increasing toward the Rockland Brook fault. The Rockland Brook fault may have been a late Precambrian strike-slip fault, which juxtaposed the Economy River granodiorite with the younger plutonic rocks. The fault appears to have been reactivated in the late Devonian - early Carboniferous (Miller et al., 1989), when movement was lubricated by granitic magmas (Koukouvelas and Pe-Piper, 1995).

Structural observations of synmagmatic and solid state deformation in Precambrian plutons suggest that during this period the Bass River block was deformed in a strike-slip regime. However, much of the strike-slip deformation of this zone took place during the Carboniferous at about 340 Ma

(Miller et al. 1989; Koukouvelas and Pe-Piper, 1995). During this period, many older tectonic features were obscured and/or rotated to be subparallel to the Rockland Brook, Londonderry, and Cobequid faults. Local conditions also played a crucial role. For example, in the Londonderry section (Fig. 2B) where the Rockland Brook fault is close to the Londonderry fault, the flattening is increased dramatically, in contrast with areas such as Debert River Pluton (Fig. 2A) where the two faults are 5 km apart and the deformation is more partitioned.

The progressive increase in deformation from the high-level Debert River and Frog Lake plutons to the ductilely deformed similar plutonic rocks in the Great Village River gneiss, and the occurrence of the plutonic rocks intimately interleaved with Gamble Brook Formation both in the "gneiss" and to the south suggests that it is improbable that the Great Village River gneiss represents the root of an arc, as proposed by Doig et al. (1991). Field studies show no evidence for a change in metamorphic grade, only the intensity of deformation, between the gneiss unit and the less deformed Neoproterozoic plutons. The igneous assemblage is not similar to that described from better documented arc roots, such as the Chortiatas assemblage in Greece (Mussalim and Jung, 1986), the Kohistan arc of the Himalayas (Khan et al., 1989) and the Skolai arc of Alaska (Beard and Barker, 1989).

The sequence of plutonic rocks in the Bass River block is similar to that in southern Cape Breton (Barr, 1993) and the Caledonia Highlands of southern New Brunswick (Barr et al. 1994). The Frog Lake diorite and Debert River granodiorite are geochemically and geochronologically similar to plutons in the eastern Caledonia Highlands and the Coxheath-Sporting Mountain belts of southern Cape Breton. The McCallum Settlement granite is geochemically similar to the plutons of the Coastal belt of southern Cape Breton and felsic plutons of the western Caledonia Highlands, that have been dated at 575-550 Ma.

REFERENCES

- Barr, S.M.**
1993: Geochemistry and tectonic setting of late Precambrian volcanic and plutonic rocks in southeastern Cape Breton Island, Nova Scotia; *Canadian Journal of Earth Sciences*, v. 30, p. 1147-1154.
- Barr, S.M., Bevier, M.L., White, C.E., and Doig, R.**
1994: Magmatic history of the Avalon Terrane of southern New Brunswick, Canada, based on U-Pb (zircon) geochronology; *Journal of Geology*, v. 102, p. 399-409.
- Beard, J.S. and Barker, F.**
1989: Petrology and tectonic significance of gabbros, tonalites, shoshonites, and anorthosites in a late Paleozoic arc-root complex in the Wrangellia terrane, southern Alaska; *Journal of Geology*, v. 97, p. 667-683.
- Cullen, M.P.**
1984: Geology of the Bass River complex, Cobequid Highlands, Nova Scotia; M.Sc. thesis, Dalhousie University, Halifax, Nova Scotia, 183 p.
- Doig, R., Murphy, J.B., and Nance, R.D.**
1991: U-Pb geochronology of Late Proterozoic rocks of the eastern Cobequid Highlands, Avalon Composite Terrane, Nova Scotia; *Canadian Journal of Earth Sciences*, v. 28, p. 504-511.

- Doig, R., Murphy, J.B., and Nance, R.D. (cont.)**
 1993: Tectonic significance of the Late Proterozoic Economy River gneiss, Cobequid Highlands, Avalon Composite Terrane, Nova Scotia; *Canadian Journal of Earth Sciences*, v. 30, p. 474-479.
- Donohoe, H.V. and Wallace, P.I.**
 1982: Geological map of the Cobequid Highlands, Nova Scotia; Nova Scotia Department of Mines and Energy, scale 1:50 000.
 1985: Repeated orogeny, faulting and stratigraphy of the Cobequid Highlands, Avalon Terrane of northern Nova Scotia; Geological Association of Canada - Mineralogical Association of Canada Joint Annual Meeting, Fredericton, New Brunswick, guidebook 3, 77 p.
- Gaudette, H.E., Olszewski, W.J. Jr., and Donohoe, H.V. Jr.**
 1984: Rb/Sr isochrons of Precambrian age from plutonic rocks in the Cobequid Highlands, Nova Scotia; Nova Scotia Department of Mines and Energy, Report 84-1A, p. 285-292.
- Keppie, J.D., Dallmeyer, R.D., and Murphy, J.B.**
 1990: Tectonic implications of $^{40}\text{Ar}/^{39}\text{Ar}$ hornblende ages from late Proterozoic-Cambrian plutons in the Avalon composite terrane, Nova Scotia, Canada; *Geological Society of America Bulletin*, v. 102, p. 516-528.
- Khan, M.A., Jan, M.Q., Windley, B.F., Tarney, J., and Thirlwall, M.F.**
 1989: The Chilas mafic-ultramafic igneous complex: the root of the Kohistan island arc in the Himalaya of northern Pakistan; in *Tectonics of the Western Himalaya*, (ed.) L.L. Malinconico and R.J. Lillie; Geological Society of America, Boulder, Colorado, p. 75-94.
- Koukouvelas, I. and Pe-Piper, G.**
 1995: The role of granites in the evolution of the Folly Lake diorite, Cobequid Highlands, Nova Scotia; in *Current Research 1995-D*; Geological Survey of Canada.
- McMullin, D.W.A., Barr, S.M., and Raeside, R.P.**
 1993: A re-interpretation of the "Bateman Brook metamorphic suite", Cape Breton Highlands, Nova Scotia, as sheared, fault-bounded blocks of other units; *Atlantic Geology*, v. 29, p. 43-50.
- Miller, B.V., Nance, R.D., and Murphy, J.B.**
 1989: Preliminary kinematic analysis of the Rockland Brook Fault, Cobequid Highlands, Nova Scotia; in *Current Research, Part B*; Geological Survey of Canada, Paper 89-1B, p. 7-14.
- Murphy, J.B., Pe-Piper, G., Nance, R.D., and Turner, D.S.**
 1988: Geology of the eastern Cobequid Highlands: a preliminary report; in *Current Research, Part B*; Geological Survey of Canada, Paper 88-1B, p. 99-107.
- Murphy, J.B., Pe-Piper, G., Keppie, J.D., and Piper, D.J.W.**
 1992: Correlation of Neoproterozoic III sequence in the Avalon Composite Terrane of mainland Nova Scotia: tectonic implications; *Atlantic Geology*, v. 28, p. 143-151.
- Mussalam, K. and Jung, D.**
 1986: Petrology and geotectonic significance of salic rocks preceding ophiolites in the eastern Vardar Zone, Greece; *Tschermaks Mineralogische und Petrographische Mitteilungen*, v. 35, p. 217-242.
- Nance, R. D. and Murphy, J. B.**
 1990: Kinematic history of the Bass River Complex, Nova Scotia: Cadomian tectonostratigraphic relations in the Avalon terrane of the Canadian Appalachians; *Geological Society of America, Special Paper 51*, p. 395-406.
- Pe-Piper, G.**
 1988: Calcic amphiboles of mafic rocks of the Jeffers Brook plutonic complex, Nova Scotia, Canada; *American Mineralogist*, v. 73, p. 993-1006.
- Piper, D.J.W., Pe-Piper, G., and Loncarevic, B.D.**
 1993: Devonian - Carboniferous deformation and igneous intrusion in the Cobequid Highlands; *Atlantic Geology*, v. 29, p. 219-232.

Geological Survey of Canada Project 920062

The role of granites in the evolution of the Folly Lake diorite, Cobequid Highlands, Nova Scotia¹

I. Koukouvelas² and Georgia Pe-Piper³

Atlantic Geoscience Centre

Koukouvelas, I. and Pe-Piper, G., 1995: The role of granites in the evolution of the Folly Lake diorite, Cobequid Highlands, Nova Scotia; in Current Research 1995-D; Geological Survey of Canada, p. 33-38.

Abstract: The Folly Lake diorite is an earliest Carboniferous pluton in the Avalon terrane of northern Nova Scotia. It is bounded to the south by a major strike-slip fault zone, the Rockland Brook fault. Structural and petrological observations show that minor granite phases in the pluton decrease northwards from the fault and record a complex history of deformation. Strong mylonitic foliation in granite dykes hosted in undeformed diorite near the Rockland Brook fault indicate that granitic magma lubricated the deformation of the fault zone and the diorite pluton. The Rockland Brook fault is a positive flower structure similar to the Cobequid fault zone.

Résumé : La diorite de Folly Lake est un pluton du Carbonifère initial dans le terrane d'Avalon, dans le nord de la Nouvelle-Écosse. Elle est limitée au sud par une importante faille de décrochement, la faille de Rockland Brook. Des observations structurales et pétrologiques montrent que les phases accessoires de granite dans le pluton décroissent en direction nord à partir de la faille et témoignent d'une déformation complexe. Une forte foliation mylonitique dans les dykes de granite encaissés dans une diorite non déformée près de la faille de Rockland Brook indiquent qu'un magma granitique a lubrifié la déformation de la zone de faille et le pluton de diorite. La faille de Rockland Brook est une structure positive en forme de fleur, semblable à la zone de failles de Cobequid.

¹ Contribution to the Canada-Nova Scotia Cooperation Agreement on Mineral Development (1992-1995), a subsidiary agreement under the Canada-Nova Scotia Economic and Regional Development Agreement.

² Department of Geology, University of Patras, Patras, 26110 Greece

³ Department of Geology, Saint Mary's University, Halifax, Nova Scotia B3H 3C3

INTRODUCTION

In the Avalon Terrane of northern Nova Scotia, the Folly Lake diorite is a major latest Devonian-earliest Carboniferous pluton comprising diorite with minor granite bodies. It lies immediately north of the Rockland Brook fault (RBF), a major splay of the Cobequid fault zone. To the north and east of the Folly Lake diorite, the Hart Lake-Byers Lake granite pluton both cuts and is cut by the diorite. This paper examines the effect of granitic intrusion on the evolution of the diorite pluton. It is based principally on structural and petrological studies in a north-south cross section of the pluton west of the Trans Canada Highway.

Geological setting

The Avalon terrane in the Cobequid Highlands of Nova Scotia is bounded to the south by the Cobequid Fault and is cut by a series of subparallel strike slip faults, the most important of which is the Rockland Brook fault (Donohoe and Wallace, 1982, 1985). Much of the Cobequid Highlands is underlain by late Devonian to earliest Carboniferous diorite and granite plutons and associated volcanic rocks (Piper et al., 1993). The major faults are flower structures that controlled magma pathways and pluton emplacement (Pe-Piper and Koukouvelas, 1994; Koukouvelas et al., in prep.).

The Folly Lake diorite is the largest diorite pluton in the Cobequid Highlands (Fig. 1). It is bounded to the southeast by the Rockland Brook fault. To the north and east of the pluton is a major granitic pluton, the Hart Lake-Byers Lake pluton, which is also bounded to the south by the Rockland Brook fault.

The northern margin of the Hart Lake-Byers Lake pluton north of the Folly Lake pluton intrudes Silurian sedimentary rocks. Zircon U-Pb age determinations yielded an age of 363 ± 3 Ma for the Hart Lake-Byers Lake pluton (Doig et al., 1991). There are no geochronological determinations on the Folly Lake diorite, but the nearby and similar Wyvern pluton has yielded a K-Ar age of 357 ± 12 Ma (Pe-Piper et al., 1994).

Rockland Brook fault

The Rockland Brook fault (Miller et al., 1989) is an east-west-trending dextral strike-slip fault defined by mylonitic and cataclastic zones (Donohoe and Wallace, 1982, 1985). The typical width of the fault zone is about 1 km with a central plastic zone of ultramylonite a few tens of metres wide. Many kinematic indicators show dextral deformation, with predominant net strike-slip movement. The Rockland Brook fault extends to the southeast margin of the Pleasant Hills pluton, where it merges with the Cobequid fault zone. It appears to have been a pathway for magma to the Pleasant Hills Pluton (Koukouvelas et al., in prep.).

FIELD RELATIONSHIPS BETWEEN DIORITE AND GRANITE

The main phase of the Folly Lake diorite is a medium grained diorite, that is locally coarse grained. In places, the diorite contains small enclaves of fine grained diorite. The last diorite phase is a brecciated very coarse hornblende diorite in dykes a few centimetres wide (Fig. 3b).

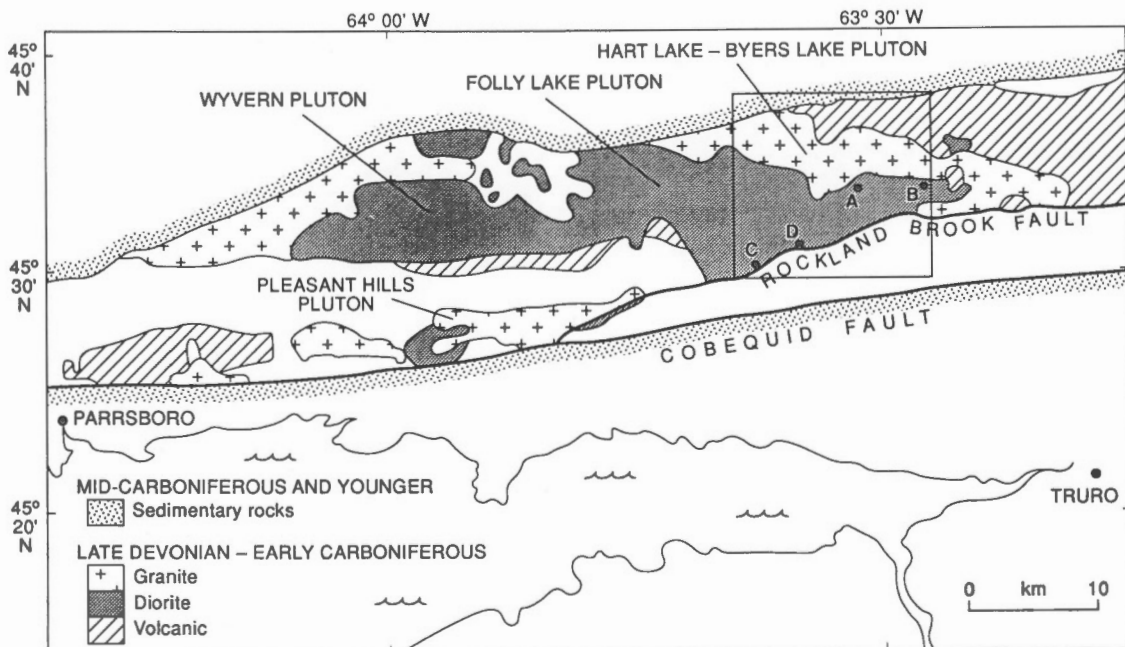


Figure 1. Map showing Folly Lake and Hart Lake-Byers Lake plutons and relationship to the Rockland Brook fault. Zone of detailed investigation indicated by box. A-E are locations of other figures. A = Permanent-Lafarge Quarry; B = Rory's Pond Road; C = East Branch Great Village River; D = Rockland Brook.

The main phase diorite is intruded by medium grained granite (Fig. 2), in places foliated, which makes up about 5 per cent of the pluton. Granite becomes progressively more abundant southward towards the Rockland Brook fault. Some granite occurs as bodies a few tens to a few hundred metres wide and up to a kilometre in length that appear to have been intruded northwards into the diorite (Fig. 3). On a smaller scale, granitic dykes from less than a centimetre to several metres wide cut the diorite (Fig. 4). Most wider dykes show irregular margins that are commonly lobate; narrower dykes are generally linear. Some granite bodies have a stopping relationship with the diorite, with linear (commonly orthogonal) contacts (Fig. 3a).

Both the diorite and medium grained granite are cut by rare medium diorite bodies and by common late-phase granite veins, rarely more than 10 cm wide, which are of variable grain size and in places are pegmatitic. The final igneous phase is represented by rare diabase dykes that cut all other lithologies: conjugate offsets in the dykes suggest that they are the result of east-west extension.

Some of the medium grained granite dykes are foliated and have parallel diorite enclaves (Fig. 5). Many granite dykes show a preferred orientation. The stoped angular margins of some bodies also suggest some tectonic control of the dyking. In places, the two margins of a dyke are offset to different amounts by strike-slip faults, which may also indicate syn-magmatic deformation.

Long-lived solid-state deformation is indicated by ductile folded granite dykes (Fig. 5) that include folded epidote veins and by more brittle folded dykes (Fig. 3c). Many such folded dykes indicate a top to north sense of ductile thrusting (Fig. 3d).

At the northern edge of the 1-km-wide Rockland Brook fault zone, where granite alternates with diorite and contains diorite enclaves, the granite is foliated and in places mylonitized

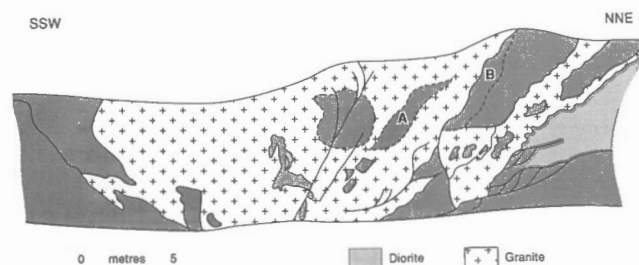


Figure 2. Sketch section of wall of Permanent-Lafarge Quarry north of Folly Lake (A in Fig. 1) showing a granite body intruded into diorite. At base of body (north-northeast) are 4-m-wide granite dykes including large diorite enclaves. This is separated by 4 m of diorite from the main granite body which is 14 m wide. At the base of this body are numerous small granite dykes intruding into diorite (B). The lower part of the main body includes a lens-shaped zone 6 m in length with abundant small diorite enclaves (A). In the upper part of the main body is a larger subcircular diorite enclave. The south-southwestern contact of the granite is irregular.

whereas the adjacent diorite (including enclaves) appears undeformed or only slightly foliated (Fig. 4D). Granitic mylonites become progressively more abundant towards the central plastic zone and the diorite also becomes progressively more deformed. Within 200 m of the central plastic zone, south-dipping dykes of granite are strongly foliated and plastically folded, indicating top-to-north ductile thrusting (Fig. 3e). South of the plastic zone, similar dykes show top-to-south movement (Fig. 3f).

In the northern part of the central plastic zone, both diorite and granite are characterized by numerous south-dipping thrust slices within an east-northeast-trending zone (clustering around the northwest sector of the net in Fig. 6). Individual thrust sheets may be composed of both diorite and granite components. These thrust surfaces, which are curved in cross-section, are characterized by vertical planes in the deeper parts that pass northward and upward into flat-lying movement planes. Ductile thrust-related fabrics are refolded on a metre to decametre scale by open to tight folds with axial surfaces with a moderate dip to the south-southeast. Folded granite dykes with similar style folds have a consistent Z-geometry with vergence patterns showing movement to the north-northwest. Their distribution is distinctly skewed, with the majority of hinges plunging east or east-southeast (Fig. 3e), clockwise from the earlier stretching lineations. This kind of skewed plunge and vergence distribution implies the presence of right-lateral differential shear during thrusting.

In the southern part of the main fault zone, smaller scale thrust slices are defined by thrust planes of similar geometry and ductile structural features show top-to-south movement (clustering around the southeast sector of the net in Fig. 6).

INTERPRETATION

Fold data analysis on both sides of the main fault shows that the intrusive granite dykes were deformed under ductile conditions while the stress field generating these folds was compatible with strike-slip movements. The style of movement in the vicinity of the Rockland Brook fault shows high-angle faults that are flattened to the north and south. This geometry implies a positive flower structure (Sylvester, 1988; Mandl, 1988) along the Rockland Brook strike-slip fault system.

Regionally, the Rockland Brook fault is the locus of dioritic magmatism (Donohoe and Wallace, 1982) and the fault zone is developed entirely in plutonic rocks. This suggests that the Rockland Brook fault is the pathway for voluminous magmatism in the eastern Cobequid Highlands, in much the same way as the Cobequid and Kirkhill faults were pathways in the western Cobequid Highlands (Piper et al., 1993). The abundance of granitic dykes and larger bodies near the Rockland Brook fault is further evidence that it controlled magma emplacement.

The plutons of the western Cobequid Highlands show that pluton emplacement was associated with strong northward thrusting (Waldron et al., 1989; Koukouvelas et al., in prep.). Similar evidence is found in the Folly Lake diorite on both a large (Fig. 2) and small scale (Fig. 3d).

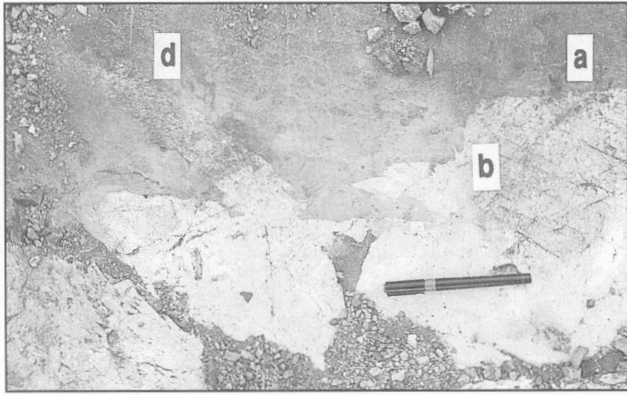


Figure 3a. Contact of granite with medium diorite showing dykes of granite (d) and contacts that are generally linear (a), but lobate (b) on a centimetre scale. Photo looking down [Fieldlog station no. 9410955] Rory's Pond Road (B in Fig. 1).



Figure 3d. Granite with ductilely deformed xenoliths of diorite in shear folds with top to north sense of movement. Photo looking down, up is north [9413015]. East Branch Great Village River (C in Fig. 1).

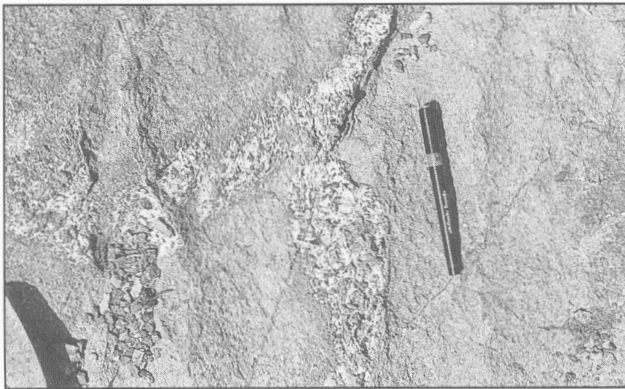


Figure 3b. Brecciated dyke of coarse hornblende diorite cutting main phase medium diorite. Photo looking down [9411082]. Rory's Pond Road.

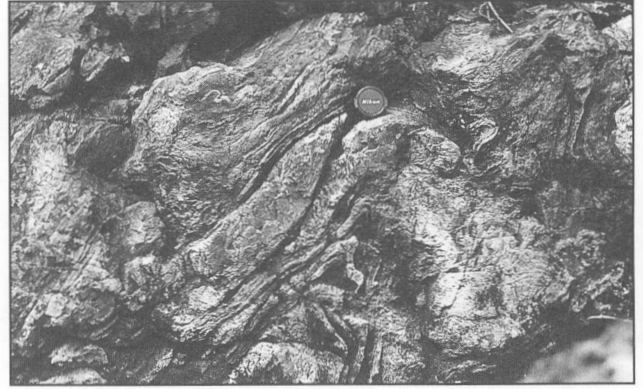


Figure 3e. Limb thrust in folded granitic dykes cutting medium diorite. Top to north plastic deformation in the Rockland Brook fault zone. Photo looking west [9412217]. Rockland Brook (D in Fig. 1).

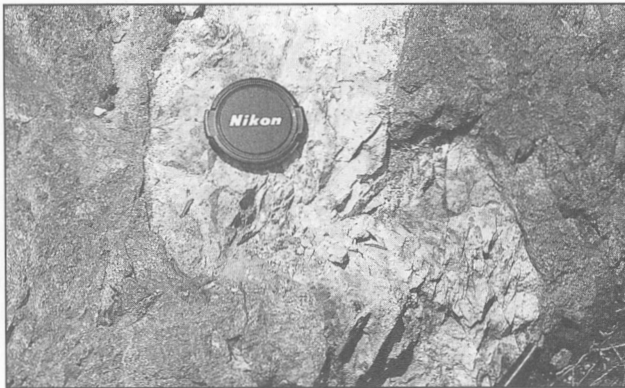


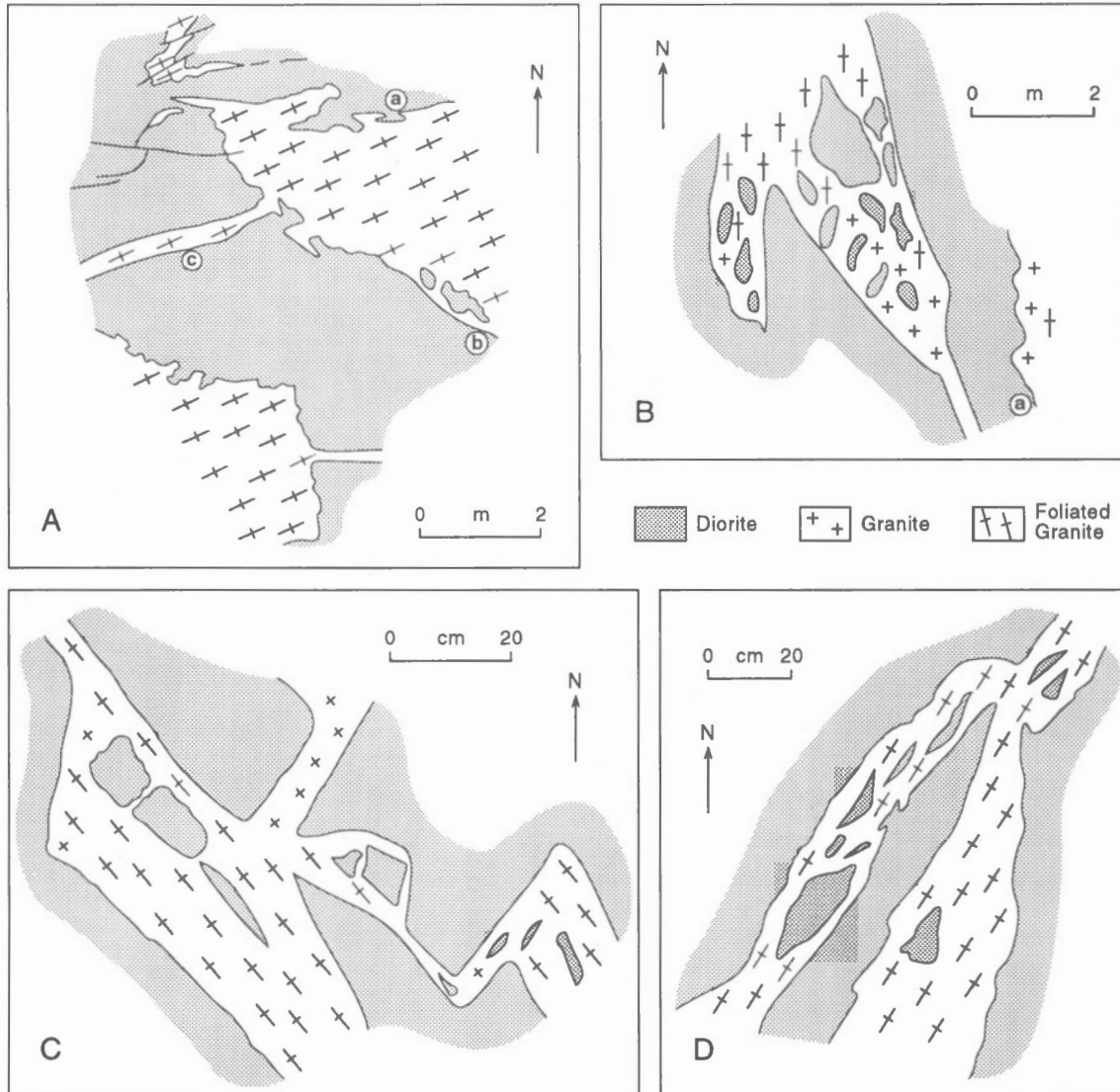
Figure 3c. Brittle-ductile folding of granite dyke in medium diorite. Photo looking northwest [9410955] Rory's Pond Road.



Figure 3f. Granite dykes in medium diorite showing top to south plastic deformation. Photo looking east, 1 m field of view [9412226]. Rockland Brook.

The presence of abundant strongly foliated granite in undeformed diorite at the northern edge of the Rockland Brook fault zone indicates that motion was taken up by granitic magmas or hot plastic granite. Similar relationships have been observed in Paleozoic shear zones in Newfoundland (Holdsworth, 1994) and from northern France (D'Lemos et al., 1992).

Farther north in the pluton, deformation is more inhomogeneous and there is less granite. Crosscutting relationships indicate that deformation persisted throughout the emplacement of the pluton. Much of the granite appears to have been emplaced into brittle-deformed diorite (Fig. 2a) that is largely of a strike-slip character.



- A)** Stopping relationships between granite and diorite, with both lobe-like contacts (a) and fault-related linear contacts (b). Note also dyking of granite into fine grained diorite (c). [9410955, Rory's Pond Road, looking down].
- B)** Northward widening of a granite dyke with linear margins that includes a swarm of poorly oriented diorite enclaves. Nearby, lobate contact between granite and diorite (a). [9412105, Higgins Mountain-Folly Mountain road, looking down].
- C)** Moderately foliated dykes of granite including oriented rectangular or lenticular diorite in concordance with syn-magmatic foliation of the granite. Note relationship of linear contacts of dyke to the foliation. [9412027, Higgins Mountain-Folly Mountain road, looking down].
- D)** Oriented enclaves of diorite in a strongly foliated granite vein. As the enclaves of diorite are undeformed, this suggests that the foliation in the granite is synmagmatic. [9412220, Rockland Brook].

Figure 4. Sketches of field relationships of dyke-like granite intrusions to diorite.

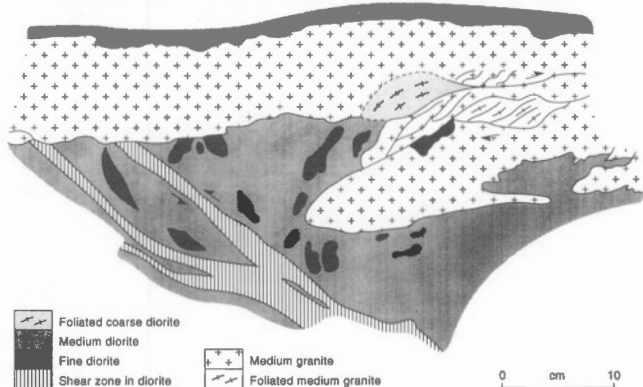
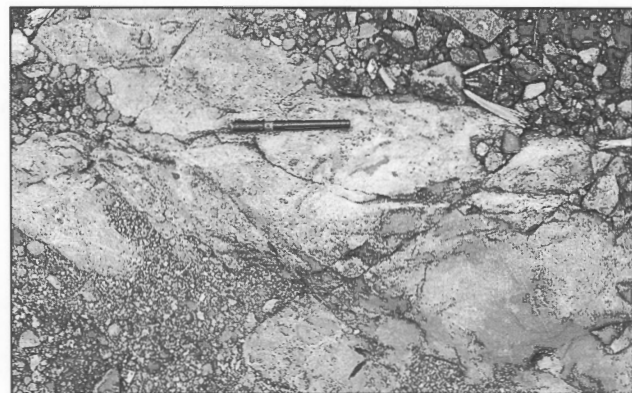


Figure 5. Photograph and sketch indicating granitic dyke truncating older shear zones in diorite. Granitic dyke was subsequently folded and cut by shear zone. Fine diorite enclaves in the main phase diorite are plastically folded with the granite. [9412010, Higgins Mountain - Folly Mountain Road]

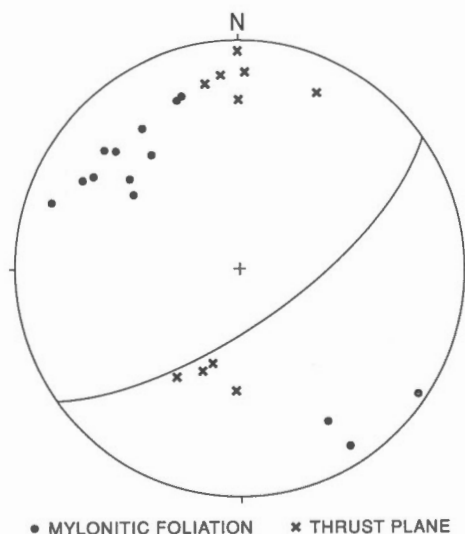


Figure 6. Lower hemisphere projection of structural observation across the Rockland Brook fault south of the Folly Lake pluton, showing poles to mylonitic foliations in granite (open rectangles) and poles to thrust planes affecting both granite and diorite (crosses). The great circle indicates the mappable trace of the Rockland Brook fault.

CONCLUSIONS

1. The Rockland Brook fault zone is a positive flower structure that acted as a pathway for dioritic and granitic magmas.
2. Much of the observed mylonitic deformation is concentrated in the earliest granite phase, indicating that the granite may have lubricated motion on the fault zone and northward thrusting of the diorite.
3. Granitic magmas that escaped from the fault zone show complex crosscutting relationships with diorite that indicate continued deformation throughout granitic magma emplacement.

REFERENCES

- D'Lemos, R.S., Brown, M., and Strachan, R.A.**
1992: Granite magma generation, ascent and emplacement within a transpression orogen; *Journal of the Geological Society of London*, v. 149, p. 487-490.
- Doig, R., Murphy, J.B., Nance, R.D., and Stokes, T.**
1991: Review of the geochronology of the Cobequid Highlands, Avalon composite terrane, Nova Scotia; in *Current Research, Part D*; Geological Survey of Canada, Paper 91-1D, p. 71-78.
- Donohoe, H.V. and Wallace, P.I.**
1982: Geological map of the Cobequid Highlands, Nova Scotia; Nova Scotia Department of Mines and Energy, scale 1:50 000.
- 1985: Repeated orogeny, faulting and stratigraphy of the Cobequid Highlands, Avalon Terrane of northern Nova Scotia; *Geological Association of Canada - Mineralogical Association of Canada Joint Annual Meeting, Guidebook 3*, Fredericton, New Brunswick, 77 p.
- Holdsworth, R.E.**
1994: Structural evolution of the Gander-Avalon terrane boundary: a reactivated transpression zone in the NE Newfoundland Appalachians; *Journal of the Geological Society of London*, v. 151, p. 629-646.
- Mandl, G.**
1988: *Mechanics of Tectonic Faulting: Models and Basic Concepts*; Elsevier; Amsterdam, New York, 407 p.
- Miller, B.V., Nance, R.D., and Murphy, J.B.**
1989: Preliminary kinematic analysis of the Rockland Brook Fault, Cobequid Highlands, Nova Scotia; in *Current Research, Part B*; Geological Survey of Canada, Paper 89-1B, p. 7-14.
- Pe-Piper, G. and Koukouvelas, I.**
1994: Earliest Carboniferous plutonism, western Cobequid Highlands, Nova Scotia; in *Current Research 1994-D*; Geological Survey of Canada, p. 103-107.
- Pe-Piper, G., Piper, D.J.W., Parlee, K., and Turner, D.S.**
1994: Geology of the headwaters of the River Philip, Cobequid Highlands; Geological Survey of Canada, Open File 2887.
- Piper, D.J.W., Pe-Piper, G., and Loncarevic, B.D.**
1993: Devonian - Carboniferous deformation and igneous intrusion in the Cobequid Highlands; *Atlantic Geology*, v. 29, p. 219-232.
- Sylvester, A.G.**
1988: Strike-slip faults; *Bulletin of the Geological Society of America*, v. 100, p. 1666-1703.
- Waldron, J.G.F., Piper, D.J.W., and Pe-Piper, G.**
1989: Deformation of the Cape Chignecto Pluton, Cobequid Highlands, Nova Scotia: thrusting at the Meguma-Avalon boundary; *Atlantic Geology*, v. 25, p. 51-62.

Geological Survey of Canada Project 920062

Halokinetic controls on the sedimentary architecture of the Inverness Formation, western Cape Breton Island, Nova Scotia¹

J.P.Brown²

Atlantic Geoscience Centre

Brown, J.P., 1995: Halokinetic controls on the sedimentary architecture of the Inverness Formation, western Cape Breton Island, Nova Scotia; in Current Research 1995-D; Geological Survey of Canada, p. 39-43.

Abstract: Braided fluvial sand bodies of the Inverness Formation consist of multiple stacked sand units (10-15 m thick) which combine to produce unusually thick sand bodies up to 200 m thick. Paleocurrent data from the fluvial sand bodies indicate frequent and radical changes of the sediment transport direction. The paleocurrent orientation shows changes of up to 180° between vertically adjacent sand units and has a range in excess of 90° within a single sand unit. Re-analysis of the Mabou 1978 Geophysical Survey, using seismic sequence stratigraphic and seismic facies analysis techniques, has revealed the presence of three salt diapirs originating from the Windsor Group. Progradational seismic sedimentological facies and incised, onlap, offlap and truncated seismic reflectors are used to reconstruct the sedimentary architecture of the Inverness Formation. It is evident from the spatial and temporal distribution of the salt diapirs and seismic facies that halokinesis had a dramatic effect upon the sedimentary architecture of the Inverness Formation.

Résumé : Les amas tressés de sable fluviatile de la Formation d'Inverness se composent de nombreuses unités sableuses superposées (de 10 à 15 m d'épaisseur) qui se sont combinées pour produire des amas exceptionnellement épais, pouvant atteindre 200 m. Les données sur les paléocourants révélées par les amas de sable fluviatile indiquent des changements radicaux et fréquents de la direction du transport sédimentaire. L'orientation des paléocourants montre des changements pouvant atteindre 180° entre des unités sableuses adjacentes sur le plan vertical, et elle présente un intervalle de plus de 90° au sein d'une seule unité sableuse. Une nouvelle analyse des données du levé géophysique de Mabou (1978) au moyen de techniques d'analyse des faciès et des séquences stratigraphiques sismiques, a fait ressortir la présence de trois diapirs salifères prenant leur source dans le Groupe de Windsor. Un faciès sédimentologique sismique de progradation et des réflecteurs sismiques découpés, d'aggradation, de progradation et tronqués sont utilisés pour reconstituer l'architecture sédimentaire de la Formation d'Inverness. D'après la distribution spatiale et temporelle des diapirs salifères et des faciès sismiques, il est évident que l'halocinèse a joué un rôle considérable dans l'architecture sédimentaire de la Formation d'Inverness.

¹ Contribution to Canada-Nova Scotia Cooperation Agreement on Mineral Development (1992-1995), a subsidiary agreement under the Canada-Nova Scotia Economic and Regional Development Agreement.

² Department of Earth Sciences, Dalhousie University, Halifax, Nova Scotia

INTRODUCTION

Fieldwork in the Port Hood-Inverness area commenced in the late summer of 1993 and data obtained from 1993 and 1994 fieldwork and subsequent analysis are presented here.

This report details the sedimentology of the Upper Carboniferous Inverness Formation and in particular the unusually thick fluvial sandbodies which contain evidence of frequent and radical changes of sediment transport direction.

Reinterpretation of the 1978 Mabou Geophysical Survey suggests that Windsor Group evaporites underwent halokinesis forming salt diapirs and that halokinesis may have controlled sediment dispersal patterns and thereby account for the dynamic nature of the fluvial system during the deposition of the Inverness Formation.

SEDIMENTOLOGY OF THE INVERNESS FORMATION

The sedimentology of the Inverness Formation can be subdivided into two distinct facies groups, the fluvial sandstone and the coal measure facies.

Trough cross-stratified sandstone facies

Lithology and geometry

This sandstone facies is dominated by a medium- to coarse-grained sandstone, with subordinate units of pebble conglomerate, siltstone, and grey shale. The sandstones are either trough cross-stratified (large amplitude, metre-scale troughs) or massively bedded with individual sandstone units ranging in thickness from 0.5 m to 2.0 m. The medium - coarse sandstone units form multistorey, stacked sandstone bodies, up to 10 m thick, consisting of two or more sandstone units. Individual sandstone units are not laterally continuous. Sandstone units typically have a concave upwards basal surface with a planar upper surface (where not removed by incision), forming lensoid sand bodies with an apparent aspect ratio of approximately 50:1.

Coarse channel lags containing coal (originally peat mats), lithic fragments (3 cm), and plant fragments define major incision surfaces at irregular intervals throughout the section. Mudstone intraclasts (30 cm) and coalified plant stems (1.0 m) are contained within the lower sections of some sandstone units, and are often associated with a coarse channel lag. Smaller mudstone intraclasts (3 cm) and coal debris are common throughout the section.

Vertical sequences within the fluvial facies

The sandstone, siltstone and shale components form fining upwards sequences up to 15 m thick. The bulk of each fining upwards sequence consists of a basal section of multistorey sandstone units, 5 - 10 m thick, as described above. These give way vertically to siltstone, interbedded siltstone and shales and finally a thick shale horizon. A single fining

upwards cycle is between 10-15 m thick, however, due to repeated incision and erosion by later sandstone units, this vertical sequence is hardly ever preserved in its entirety. A typical vertical sequence begins with a sandstone sequence, consisting of multistorey sandstone units, an attenuated (or absent) siltstone/shale sequence, followed by the basal sandstone unit of the next fining upwards sequence. This pattern of attenuated fining upwards, formed as a result of repeated incision, ultimately forms thick sandstone bodies e.g., Eagle (93 m) and Stack (63 m) Sandstone members (Dickie 1986), which are largely devoid of fine grained sediment.

Interpretation

The trough cross-stratified sandstone facies is interpreted as the deposit of a high energy, braided fluvial system. Vertical fining cycles represent channel incision, progressive channel filling by aggradation, channel abandonment and subsequent re-occupation, resulting in renewed channel incision. These cycles suggest rapid avulsion of the braided system within the paleovalley to re-occupy abandoned channel sites. The lack of paleosol development suggests either that avulsion was

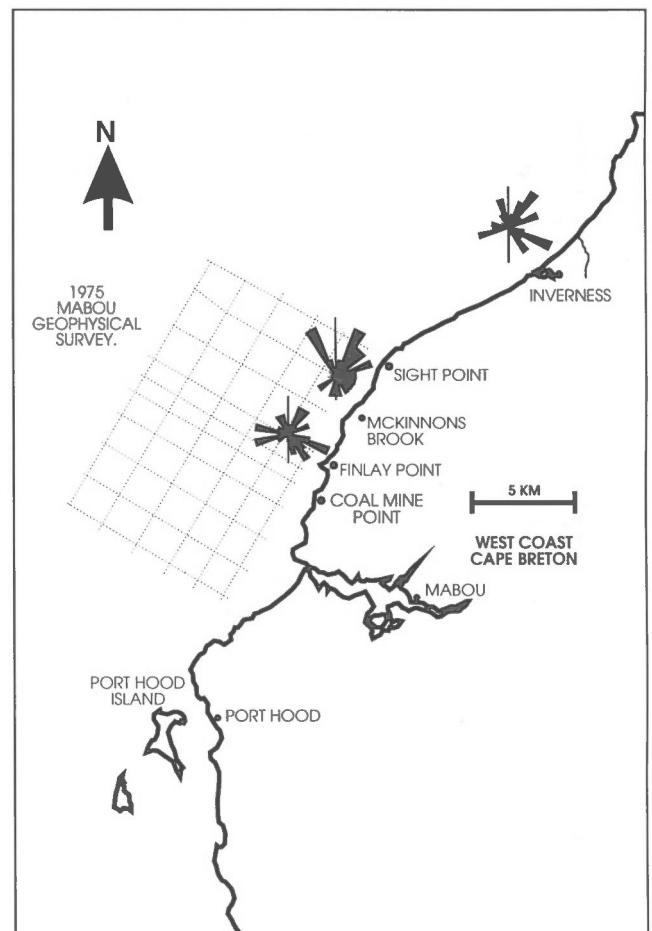


Figure 1. Location map and Mabou seismic coverage. Rose diagrams represent paleocurrent data.

frequent enough to inhibit pedogenesis, or that incision and erosion have removed paleosol horizons. Either scenario indicates a highly dynamic fluvial system.

The coarse channel lags are interpreted as flood discharge deposits. Flood discharge allowed transportation of coarse grained sediment and resulted in deep incision within the braided channel. The infrequent, but persistent occurrence of

the coarse channel lags within the sandbodies suggests that the fluvial system had both a high discharge range and a high temporal discharge variability.

On a smaller scale, the repeated incision of individual sandstone units into underlying strata indicates frequent switching of channels within the braided channel belt, resulting in scouring and reworking of bar and channel bodies within the braided channel.

Table 1. Paleocurrent data. M.S.=medium grained sandstone , F.S=fine grained sandstone, Trough=trough cross-stratified sandstone, ripple=ripple laminated sandstone, flute = flute cast.

Paleocurrent (Degrees)	Indicator	Lithology	Location	Paleocurrent (Degrees)	Indicator	Lithology	Location
48	Trough	M.S	Finlay Point	283	Trough	M.S	Inverness.
22	Trough	M.S	Finlay Point	168	Ripple	F.S	Inverness.
42	Trough	M.S	Finlay Point	330	Trough	M.S	Inverness.
145	Trough	M.S	Finlay Point	301	Trough	M.S	Inverness.
56	Trough	M.S	Finlay Point	130	Trough	M.S	Inverness.
40	Trough	M.S	Finlay Point	153	Trough	M.S	Inverness.
19	Trough	M.S	Finlay Point	145	Trough	M.S	Inverness.
19	Trough	M.S	Finlay Point	133	Trough	M.S	Inverness.
358	Trough	M.S	Finlay Point				
17	Trough	M.S	Finlay Point	123	Trough	M.S	McKinnons B.West
318	Trough	M.S	Finlay Point	143	Trough	M.S	McKinnons B.West
200	Trough	M.S	Finlay Point	193	Trough	M.S	McKinnons B.West
110	Trough	M.S	Finlay Point	50	Trough	M.S	McKinnons B.West
190	Trough	M.S	Finlay Point	342	Trough	M.S	McKinnons B.West
113	Trough	M.S	Finlay Point	230	Trough	M.S	McKinnons B.West
31	Trough	M.S	Finlay Point	336	Trough	M.S	McKinnons B.West
162	Trough	M.S	Finlay Point	27	Trough	M.S	McKinnons B.West
				23	Trough	M.S	McKinnons B.West
112	Trough	M.S	Inverness.	20	Trough	M.S	McKinnons B.West
115	Trough	M.S	Inverness.				
147	Trough	M.S	Inverness.	333	Trough	M.S	Port Hood
20	Trough	M.S	Inverness.	160	Trough	M.S	Port Hood
38	Trough	M.S	Inverness.	326	Ripple	F.S	Port Hood
100	Flute	Siltstone	Inverness.	65	Trough	M.S	Port Hood
129	Ripple	Siltstone	Inverness.	265	Ripple	F.S	Port Hood
33	Trough	M.S	Inverness.	253	Ripple	F.S	Port Hood
9	Trough	M.S	Inverness.	344	Trough	M.S	Port Hood
21	Trough	M.S	Inverness.	257	Trough	M.S	Port Hood
12	Trough	M.S	Inverness.	281	Trough	M.S	Port Hood
117	Trough	M.S	Inverness.	331	Trough	M.S	Port Hood
143	Trough	M.S	Inverness.				
44	Trough	M.S	Inverness.	65	Trough	M.S	McKinnons B.East
343	Trough	M.S	Inverness.	338	Trough	M.S	McKinnons B.East
36	Trough	M.S	Inverness.	60	Trough	M.S	McKinnons B.East
277	Trough	M.S	Inverness.	39	Trough	M.S	McKinnons B.East
62	Trough	M.S	Inverness.	330	Trough	M.S	McKinnons B.East
100	Trough	M.S	Inverness.	271	Trough	M.S	McKinnons B.East
97	Trough	M.S	Inverness.	17	Trough	M.S	McKinnons B.East
160	Trough	M.S	Inverness.	360	Trough	M.S	McKinnons B.East
174	Trough	M.S	Inverness.	43	Trough	M.S	McKinnons B.East
246	Trough	M.S	Inverness.	83	Trough	M.S	McKinnons B.East
111	Trough	M.S	Inverness.	147	Trough	M.S	McKinnons B.East
233	Trough	M.S	Inverness.	170	Trough	M.S	McKinnons B.East
50	Trough	M.S	Inverness.	47	Trough	M.S	McKinnons B.East
70	Trough	M.S	Inverness.	100	Trough	M.S	McKinnons B.East
26	Trough	M.S	Inverness.	36	Trough	M.S	McKinnons B.East
250	Trough	M.S	Inverness.				
285	Trough	M.S	Inverness.	36	Flute	F.S	Coal Mine Point
93	Ripple	F.S	Inverness.	54	Flute	F.S	Coal Mine Point

The lack of lateral accretion surfaces, and the multistorey nature of the sandstone units indicates that vertical aggradation was the dominant in-channel sedimentation process.

Coal measure facies

The thick fluvial sandbodies are intercalated with coal measure facies of a similar thickness, discussed by Gibling et al. (1994). Coal measure facies consist essentially of coal, shale and mudstone with subordinate sandstone units. The coal measure facies is therefore a finer grained facies than the fluvial sandbodies with a much lower sand:shale ratio and therefore represents a fundamentally different depositional environment.

Shale samples from the coal measure facies have undergone preliminary protozoan analysis. This analysis has identified several foraminifera genera including *Trochammina*, *Textularia* and *Ammotium*, which indicates that deposition took place within the upper tidal range, most likely within a vegetated (upper marsh) stillwater (Whiteman, pers. comm., 1993).

In offshore seismic sections and in coastal sections individual coal seams can be traced for several km. The 7'0" coal seam (Haites, 1952) in particular can be traced on seismic sections continuously from Inverness to Mabou Mines (Fig. 1). This indicates that deposition of the coal measure facies took place on a peneplained paleosurface which had no significant sedimentological barriers.

SEDIMENT TRANSPORT AND PALEOCURRENT DATA

The predominant paleocurrent recorded from the Upper Carboniferous (Inverness Formation) sediments within the field area is to the northeast. However, the fluvial sediments the field area show radical changes of paleocurrent direction (Table 1). Although the dominant paleocurrent orientation is northeast, the paleocurrent orientation has a 360° spread and changes of 180° were recorded between vertically adjacent sandbodies. Within individual sand bodies the paleocurrent orientation has some consistency, but still has a range in excess of 90°.

This wide spread of paleocurrents is inconsistent with braided fluvial systems from other areas of Nova Scotia. The South Bar Formation from the Sydney Basin which is of a similar age and sedimentology has a maximum paleocurrent spread of 90° (Gibling, pers. comm., 1994) which is more typical of braided fluvial systems in general.

SEISMIC DATABASE – THE 1978 MABOU GEOPHYSICAL SURVEY

Approximately 200 line-kilometres of multichannel seismic coverage was acquired in 1978 by McGregor Geoscience to assess nearshore mining potential and to identify major faults which may have endangered existing sub-sea mining operations (Fig. 1).

The seismic data have been reinterpreted using seismic sequence stratigraphic and seismic facies analysis principles. This approach aims to clarify what effect halokinesis had upon the sediment dispersal patterns and the development of sedimentary architecture of the Upper Carboniferous (Westphalian - Stephanian) sediments along the west coast of Cape Breton Island.

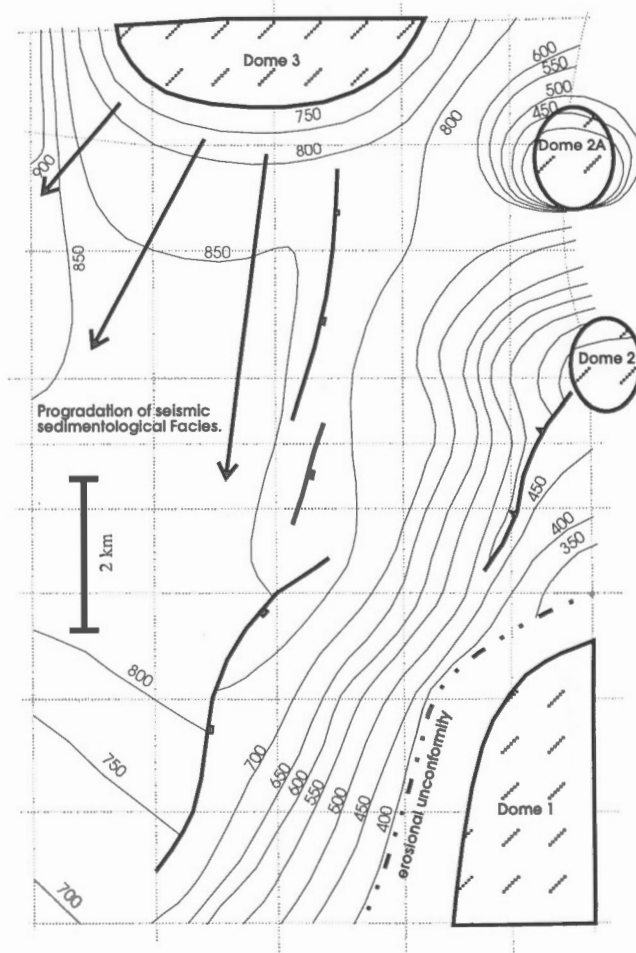


Figure 2. Structure and two way time contour map of the 7'0" coal seam. Diapiric salt structures, Domes 1 - 3, indicated by stippled pattern. Contour interval 50 ms.

The presence of salt structures in western Cape Breton is well documented (e.g., Howie, 1988; Haites, 1952). However no salt structures were originally interpreted from the Mabou seismic survey in the nearshore area.

Reinterpretation of the Mabou survey has revealed the existence of three salt structures (Dome 1-3) (Fig. 2), two of which are exposed in onshore beach sections at Coal Mine Point and Finlay Point.

The reproduction quality of the seismic data is poor; however, seismic sequences and seismic facies, interpreted as incised fluvial sand sheets, progradational, down lap and erosional truncation surfaces, have been tentatively defined. These seismic sedimentological features can be used to reconstruct sedimentary architecture and thereby propose sedimentological facies from packages of seismic reflectors. A second but vital use of the seismic sedimentological facies is to determine sediment transport direction and in particular sediment transport in relation to the position and geometry of the salt structures. In this way the role of the salt structures as sediment transport barriers and as sediment source areas can be evaluated. Preliminary geophysical interpretation indicates that the seismic sedimentological facies have a strong spatial and temporal relationship to the salt diapirs. Within seismic sections seismic sedimentological facies can be mapped which appear to be sourced from uplifted Carboniferous strata and which have a sediment transport direction orthogonal to the edge of the underlying diapir. In this way halokinesis may have had a fundamental control upon the sedimentation of Upper Carboniferous stratigraphy.

Future work will focus on the acquisition of new seismic data, reprocessing of the original data and synthetic modelling. This work will serve to clarify and validate this preliminary interpretation and allow a far more detailed seismic sedimentological description to be presented in future reports.

In conclusion it is proposed that nearshore and offshore halokinesis may have had a dramatic effect upon the sedimentary architecture and sediment transport direction of the Inverness Formation. Halokinetic effects included creation of local source areas due to the uplift of Carboniferous strata, creation of local depocentres as rim synclines, extensive modification of the regional subsidence rate due to salt withdrawal to feed embryonic diapirs and the formation of ephemeral sedimentological barriers due to diapiric uplift.

REFERENCES

- Dickie, J.R.**
1986: Upper Carboniferous fluvial sedimentation in the Gulf of St. Lawrence Coal Basin, Mabou Mines, Nova Scotia; BSc. Hons. thesis, Dalhousie University, Halifax, Nova Scotia, 118 p.
- Gibling, M.R., Marchioni, D.L., and Kalkreuth, W.D.**
1994: Detrital and organic facies of upper Carboniferous strata at Mabou Mines, western Cape Breton Island, Nova Scotia; in Current Research 1994-D; Geological Survey of Canada, p. 51-56.
- Haites, T.B.**
1952: Some geological aspects of the Inverness County Coalfield in comparison with those of the Sydney Coalfield; in Second Conference on the origin and Constitution of Coal, Crystal Cliffs, Nova Scotia, p. 112 - 134.
- Howie, R.D.**
1988: Upper Paleozoic Evaporites of Southeastern Canada; Geological Survey of Canada, Bulletin 380, 120 p.

Geological Survey of Canada Project 920062

Preliminary results from reprocessing of seismic reflection data in the Cumberland Basin, Nova Scotia¹

F. Marillier and P. Durling²

Atlantic Geoscience Centre, Dartmouth

Marillier, F. and Durling, P., 1995: Preliminary results from reprocessing of seismic reflection data in the Cumberland Basin, Nova Scotia; in Current Research 1995-D; Geological Survey of Canada, p. 45-52.

Abstract: Industry seismic reflection data collected in 1972 in the Late Devonian to Permian Cumberland Basin have been reprocessed using modern techniques. Major improvements in data quality were achieved and the range of recoverable data was extended from four to five seconds.

Several reprocessed seismic sections are shown. A section through the Malagash Anticline reveals its internal structure and suggests that salt flowage was associated with faulting. Another section indicates that the surface-defined Beckwith Fault extends to depth where it offsets near-base Windsor Group reflections by about one second. Finally, a section located near the Wallace Station No. 1 well links seismic data to the well, although it does not provide a rigorous tie. The section and synthetic seismograms suggest that, contrary to what was previously interpreted, the well did not reach Horton Group rocks, but rather bottomed above that unit in middle Windsor Group rocks.

Résumé : Des données industrielles de sismique-réflexion recueillies en 1972 dans le bassin de Cumberland (Dévonien tardif-Permien) ont été traitées de nouveau à l'aide de techniques modernes. On a pu ainsi améliorer considérablement la qualité des données et faire passer l'étendue des données récupérables de quatre à cinq secondes.

Les auteurs présentent plusieurs profils sismiques qui ont été traités de nouveau. Un profil à travers l'anticlinal de Malagash révèle la structure interne de l'anticlinal et porte à croire que le fluage du sel a été associé à la formation de failles. Un autre profil indique que la Faille de Beckwith, identifiée à la surface, se prolonge en profondeur, où elle provoque un décalage d'environ une seconde dans les échos produits près de la base du Groupe de Windsor. Enfin, un profil situé près du puits Wallace Station n° 1 relie les données sismiques au puits, bien qu'il ne fournisse pas de lien rigoureux. Ce profil et des sismogrammes synthétiques indiquent que, contrairement à une interprétation antérieure, le fond du puits n'a pas atteint les roches du Groupe de Horton, mais se trouve plutôt au-dessus de cette unité dans les roches du centre du Groupe de Windsor.

¹ Contribution to Canada-Nova Scotia Cooperation Agreement on Mineral Development (1992-1995), a subsidiary agreement under the Canada-Nova Scotia Economic and Regional Development Agreement.

² Durling Geophysics, 36 Beaufort Drive, Dartmouth, Nova Scotia B2W 5V4

INTRODUCTION

As part of a continuing study of the deep structure of offshore and onshore Carboniferous basins in the Gulf of St. Lawrence and in the surrounding land areas (Durling and Marillier, 1990, 1993; Durling et al., in press), we have recently started a compilation of seismic reflection profiles in the Cumberland Basin (Fig. 1). More than 1700 km of data exist in the basin. A large portion of the data was collected by industry in the early 1970s, but its quality reflects the lack of modern processing techniques. Reprocessing was needed to enhance data quality and to render old seismic sections comparable to more recent data in the basin. In this paper, we deal with some aspects of the reprocessing, and we illustrate results by interpreting a few reprocessed profiles.

GEOLOGICAL SETTING

The Cumberland Basin (Fig. 1), located in northern Nova Scotia, is part of the much larger Late Devonian to Permian Maritimes Basin (Roliff, 1962). It is the onshore, southwestern extension of the Magdalen Basin (Durling and Marillier, 1993) and is bounded to the south and west by the Cobequid

and Caledonia highlands, respectively (Fig. 1). It is separated from the Carboniferous Sackville Subbasin by a subsurface basement high known as the Hastings Uplift (Howie, 1986).

Geological mapping in the Cumberland Basin recently completed by Ryan and Boehner (1994) provides a detailed understanding of the stratigraphic and structural relationships expressed in the near surface. Ryan et al. (1991) subdivided strata within the basin into five stratigraphic groups; in order of descending age, they are the Horton, Windsor, Mabou, Cumberland, and Pictou groups. These units generally comprise coarse- to fine-grained, red to grey, continental clastic sediments. The exception is the Windsor Group, which consists of thick marine evaporites, including salt, and interbedded redbed clastic rocks. Faults and folds within the basin strike east to northeast and salt structures are indicated by Windsor Group outcrops and borehole data (Boehner, 1986).

REPROCESSING OF SEISMIC DATA

The reprocessed data are part of a survey shot throughout the Cumberland Basin in 1972 for Anschutz (Canada) Exploration Limited. Data were acquired with a vibroseis seismic source, a 48-trace recording system, a 67.06 m (220 ft) group interval,

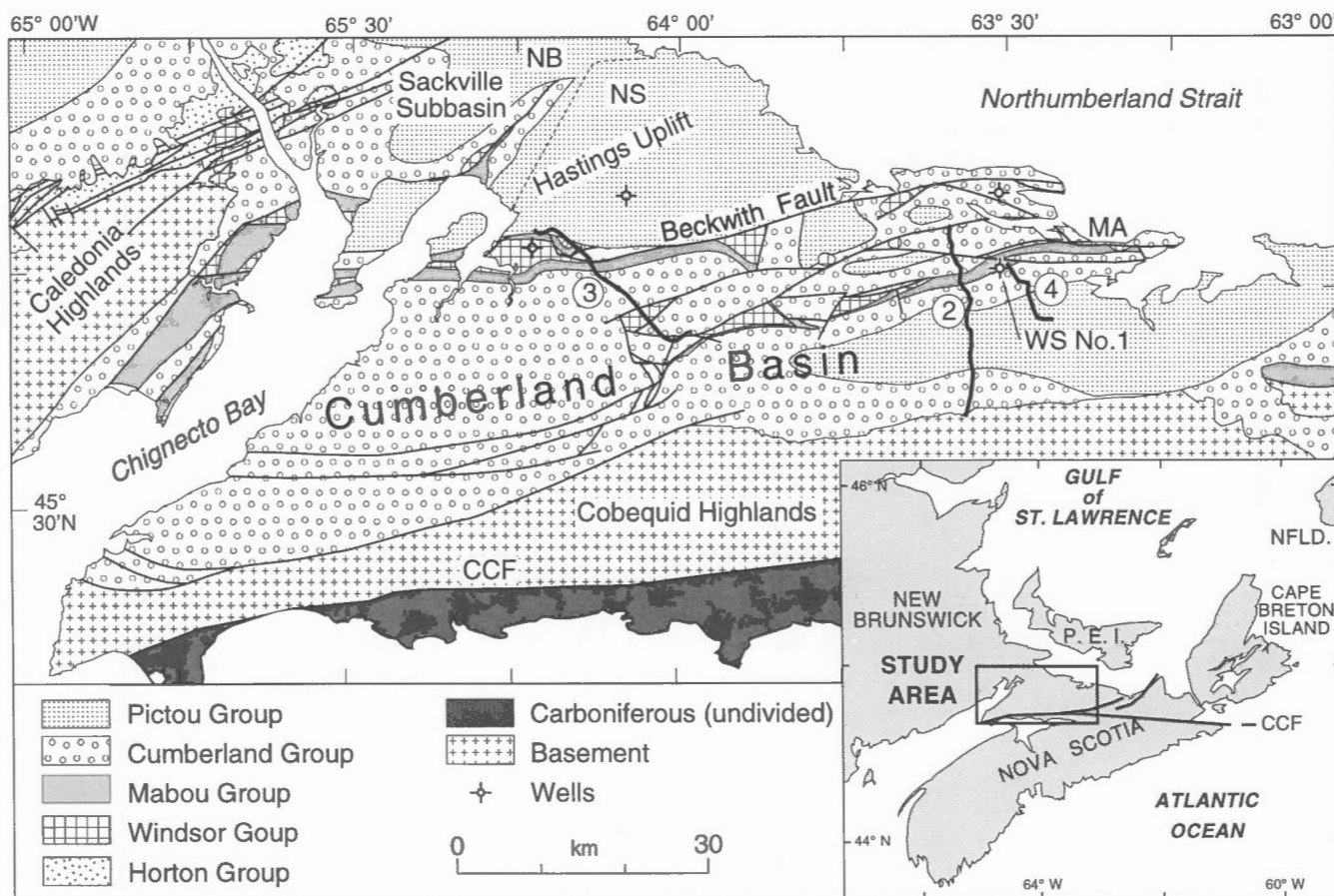


Figure 1. Location map of the Cumberland Basin with simplified geology (after Ryan and Boehner, 1994). Seismic profiles shown in this paper are indicated by their figure number (circled). Abbreviations: CCF - Cobequid-Chedabucto Fault, NB - New Brunswick, NS - Nova Scotia, MA - Malagash Anticline.

and a shot spacing of 201.17 m (660 ft) resulting in eight-fold coverage (see Table 1). Reprocessing was done under contract by Pulsonic Geophysical Limited (Calgary). A total of 204 km of data were reprocessed from the 483 km Anschutz survey. During the project we maintained close contact with the company to ensure that the specific objectives of the project were met. Test plots were received at the Atlantic Geoscience Centre for the main processing steps, and the ultimate decision on parameter choice remained with us. Processing steps are listed in Table 1.

The aim of the project was to enhance data quality in general, but more specific objectives included: 1) to obtain a clearer image of shallow parts of the seismic section in order to better tie with surface geological mapping; 2) to recover data beyond the original display limit of four seconds; 3) to ensure continuity of data quality from top to bottom of the section.

Field recording parameters and the availability of uncorrelated field tapes enabled us to reprocess up to six seconds of data. During the course of the work, it was found that seismic energy could not be recovered beyond five seconds, and this limit was adopted for final display. Many processing routines commonly used today such as binning, deconvolution, or noise reduction algorithms, were not available or rarely used at the time of original processing. Routines such

as deconvolution and migration that were not applied to the data in the original processing, can themselves bring major improvements to the data.

Before application of the various processing operators, thorough testing was carried out. Here, following the processor's report (Stevenson, 1994), we present a brief review of the main tests and processing steps in relation to data characteristics. Initial frequency filtering analysis indicated that the bulk of the seismic energy is between 15 and 55 Hz, which coincides with the source signal bandwidth. In the final display, all frequencies in that range were allowed. Frequency filtering also revealed some ringing at frequencies above 30 Hz in the lower part of the sections. This adverse energy, which was not affected by deconvolution, was removed by spectral balancing with a multiwindowed zero-phase filter. Deconvolution has the ability to compress a seismic signal distorted and broadened by the filtering effect of the earth. In this particular case, instead of processing each trace independently, surface-consistent designature deconvolution was applied that takes the average amplitude of the entire profile into account.

Irregular time delays or advances due to irregular thickness of the low-velocity weathered zone in the near surface can usually be corrected by measuring the seismic refraction velocity within this zone and applying the proper time correction. However, this technique proved ineffective in this project

Table 1. Acquisition and reprocessing parameters.

Field parameters:	
Source:	Vibroseis trucks, 7 second sweep, linear frequency 56 to 16 Hz
Recording length:	13 seconds
Sample rate:	4 milliseconds
No. of channels:	48
Group interval:	67.06 m
Source interval:	201.17 m
Fold:	800%
Reprocessing sequence:	
1. Demultiplex and correlation (6 second records)	13. Trace muting
2. Amplitude recovery	Offset (m): 800 800 3155
3. Geometry	Time (ms): 0 650 1400
4. Deconvolution (surface consistent designature deconvolution)	14. Automatic trim statics
5. Common depth point (CDP) gather	15. CDP stacking
6. Elevation correction (datum: sea level, replacement velocity: 3600 m/s)	16. Wave equation migration
7. Velocity analysis (semblance)	17. FX-deconvolution
8. Automatic surface consistent statics	18. Filter application
9. Velocity analysis (semblance)	Zero phase band pass:
10. Automatic surface consistent statics	10/15-55/65 Hz 0-1000 ms
11. Normal moveout (NMO) correction	5/10-55/65 Hz 1000-3000 ms
12. Spectral balance	5/10-50/60 Hz 3000-6000 ms
	19. Final display
	100 ms automatic gain control (AGC)
	combined with 1000 ms AGC

because first breaks were weak and distorted by reverberations. A weathered zone correction could not be applied, but data were corrected for elevation using an average velocity of 3600 m/s determined by averaging the velocity of the first breaks from several profiles. The removal of remaining irregular delays in the data was investigated with four different techniques. A two-pass surface consistent operator that maximizes the total power of the stacked data proved to be the most effective. It was followed by non-surface consistent

trim statics that tries to improve the seismic section trace by trace. However, this operator was not successful in all cases, and it was applied for a limited number of profiles only.

Several combinations of operators were tried to remove the large amount of incoherent noise and to migrate reflectors to their proper location. Combinations that included dip moveout and Radon transform were found unsuccessful. The best combination consisted of CDP stacking followed by

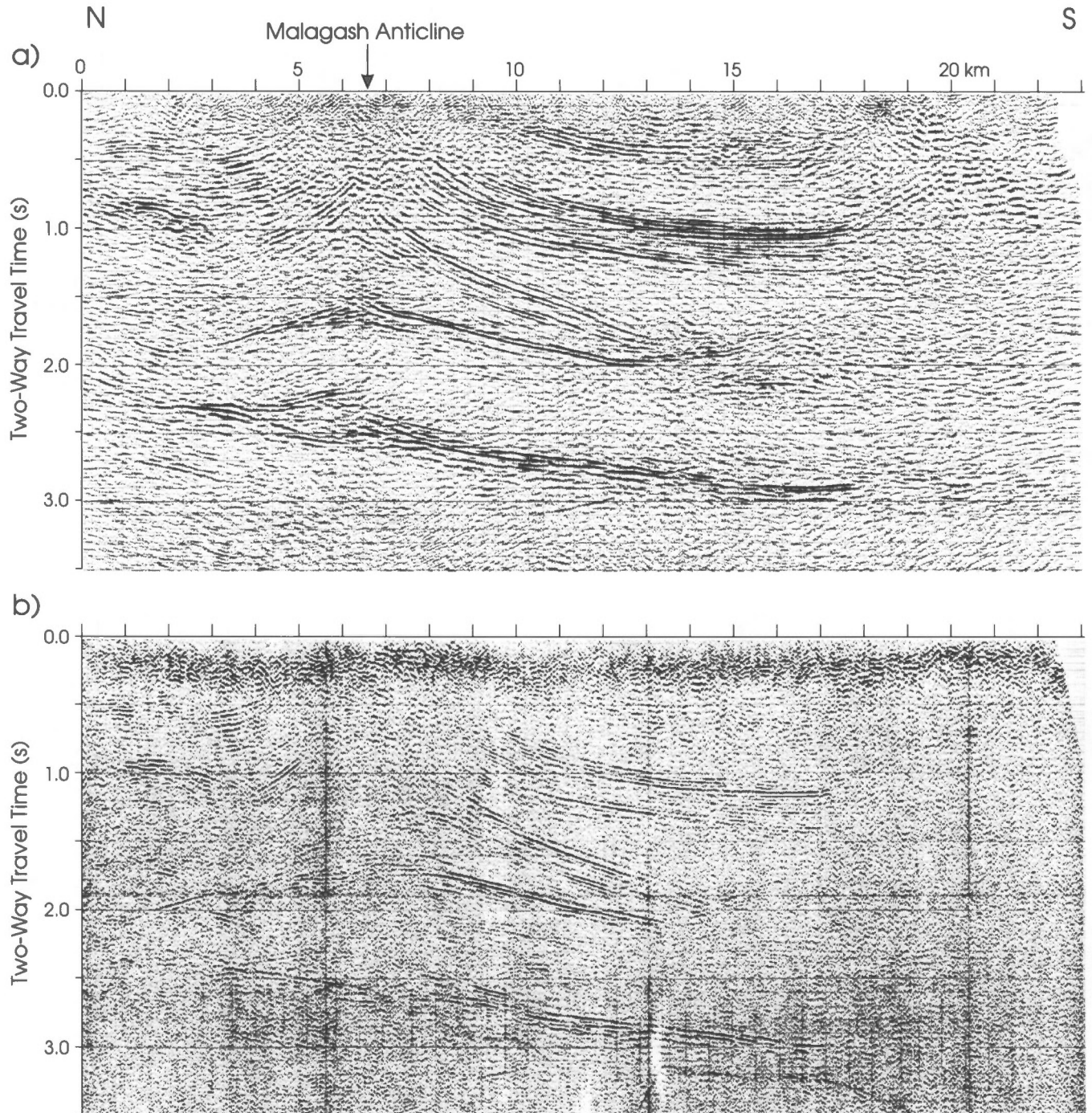


Figure 2. a) Reprocessed section of Line 2 after migration. b) Original unmigrated processing. Vertical to horizontal ratio is about 0.6 for an average velocity of 4 km/s. For location see Figure 1.

finite-difference migration and FX-deconvolution. FX-deconvolution involves transforming the data from the t-x (time-space) domain into the f-x (frequency-space) domain, designing deconvolution operators separately that are centred on different frequencies, and transforming the data back into t-x space.

Finally, a two-pass gain correction or AGC with 100 and 1000 ms windows was applied to the data before display. To tie the reprocessed data with the more recent Chevron Standard Limited survey, a time shift of -260 ms was applied.

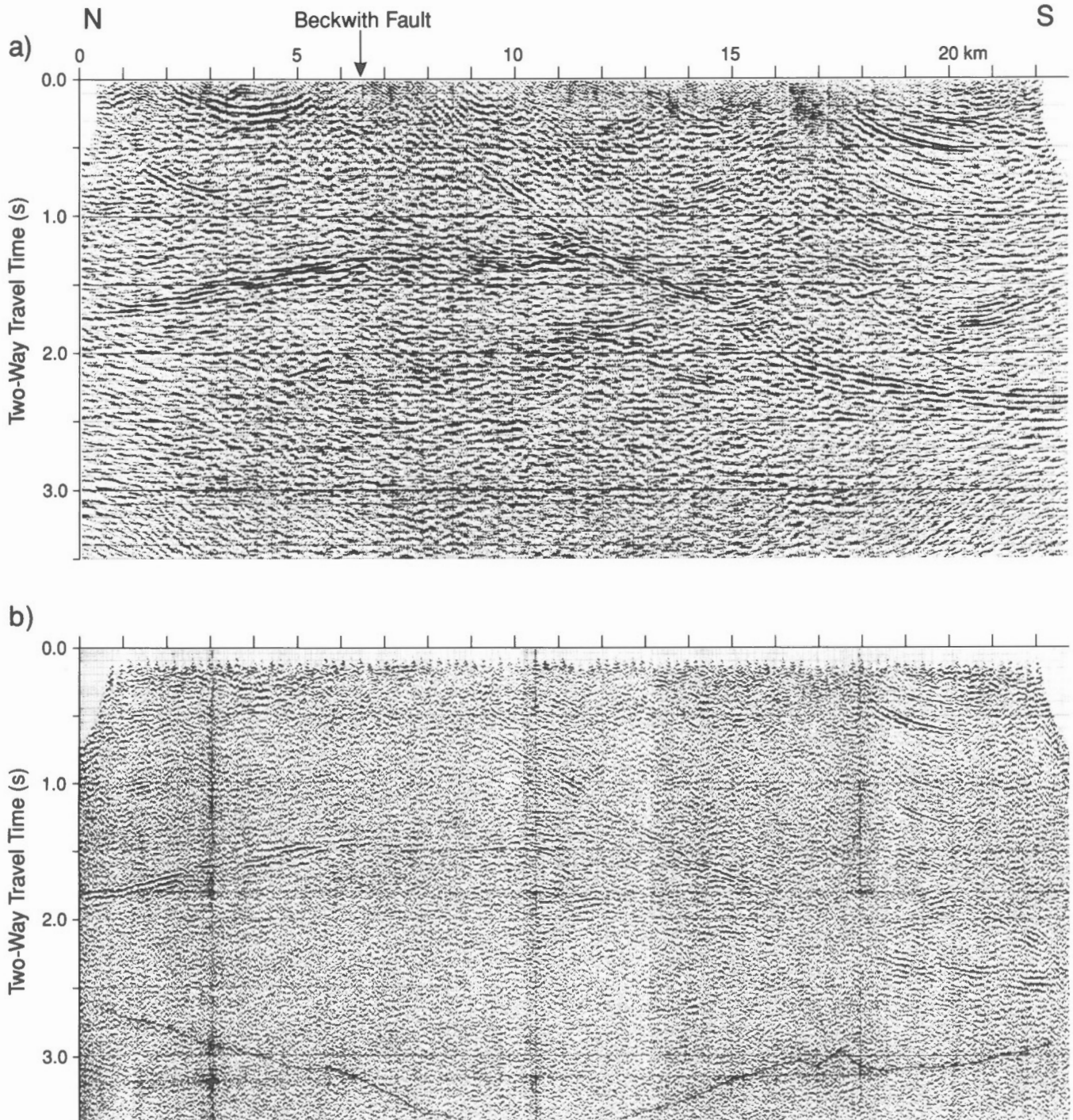


Figure 3. a) Reprocessed section of Line 6 after migration. b) Original unmigrated processing. Scale ratio is identical to that of Figure 2.

EXAMPLES OF REPROCESSED DATA

The section shown in Figure 2 crosses the Malagash anticline, an east-striking salt-cored structure (Ryan and Boehner, 1994). This section is a good example of how reprocessing enhanced the general quality of the section and also demonstrates how well the more specific reprocessing objectives were met. In general, the reprocessed section shows a much better signal-to-noise ratio, and reflections are more coherent and continuous. Reflections above 0.5 s two-way travel time (TWT) show higher amplitudes and greater continuity (see

for example between 10 and 15 km). Similarly, deep reflections at around 2.8 s near 2 km and at 3 s near 11 km are much clearer on the new section. These deep events indicate that high-amplitude and continuous reflections between 2.3 and 3.0 s do not coincide with the bottom of the basin. The high-amplitude reflections are tentatively correlated with the base of the Windsor Group, based on their similarity in appearance with base Windsor Group reflections in the Magdalen Basin (Durling and Marillier, 1993). In this particular section, migration has contributed considerably to clearing up the internal part of the Malagash Anticline. The

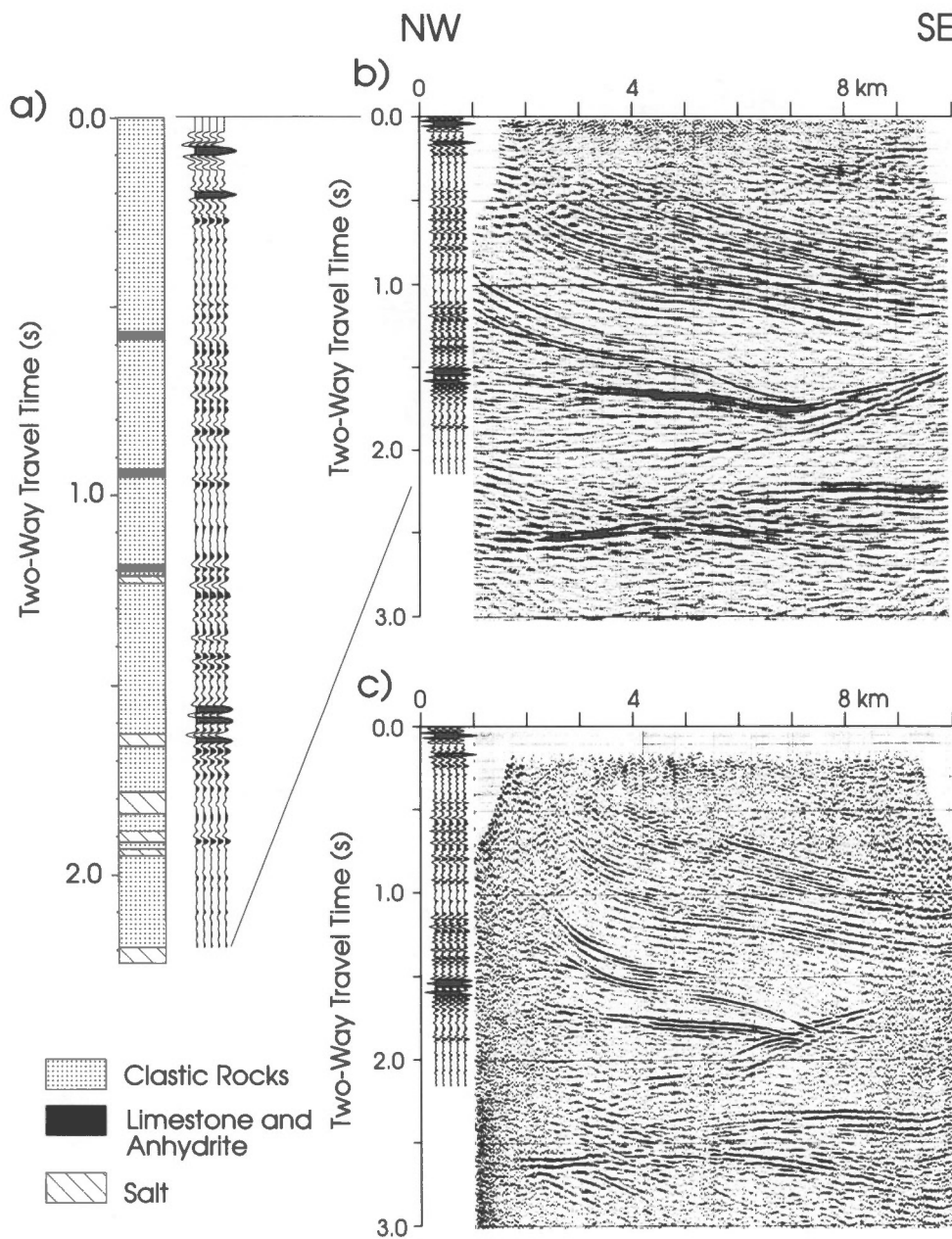


Figure 4. a) Well litholog with synthetic seismograms for the Wallace Station No. 1 well. b) Reprocessed section of Line 21 after migration. c) Original unmigrated processing. Scale ratio is identical to that of Figure 2.

presence of salt near the surface in the core of the anticline suggests that this feature is associated with salt tectonics. The elongate and narrow zone of disrupted reflections in the core of the structure suggests that salt tectonics was associated with faulting.

Line 6 (Fig. 3) runs across the Beckwith Fault (Fig. 1), which is mapped as an east-striking fault separating mainly Pictou Group rocks to the north from Windsor, Mabou, Cumberland, and Pictou Group rocks to the south. Reprocessing has significantly improved this section by rendering reflections more apparent at a variety of depths. This is particularly true for near-surface reflections that are now more clearly imaged along the entire length of the profile. Structural complexities in the shallow subsurface can now be inferred. A high-amplitude south-dipping reflection originating at 1.6 s near 15 km can be traced almost to the surface. This reflection is imaged on both the original and reprocessed sections, but its relationship to deeper reflections on the southern half of the line is clearer on the reprocessed section.

Line 6 crosses the mapped trace of the Beckwith Fault at about 6 km, where the surface projection of the south-dipping reflection occurs. This south-dipping event is interpreted as the extension at depth of the Beckwith Fault. The Hastings Uplift is indicated by the elevated basement between 5 and 15 km (at about 1.3 s at its shallowest location). The strong reflection at around 1.3 s near 10 km probably corresponds to a near-base Windsor Group event. It is offset across the fault in a normal displacement sense by 0.9 s TWT, or about 1800 m. However, latest movement on the fault appears to be reverse (Howie, 1986), suggesting at least two separate deformation episodes. Seismic data indicate that this fault represents a major structural boundary that separates the Cumberland Basin into two distinct domains: 1) horizontal strata north of the fault; and 2) folded and faulted strata associated with salt structures and lateral variations of sediment thickness south of the fault.

Correlation of seismic data to well data is of prime importance when interpreting seismic reflection profiles. However, well correlations to original Anschutz profiles were suspect because of their poor quality. The Wallace Station No. 1 well is about 750 m away from the northwest end of the seismic profile in Figure 4. Migration has greatly improved this section, and dipping reflections that do not reach the end of the original section (Fig. 4c) can now tentatively be tied with the well in the reprocessed section (Fig. 4b). Although the well is not located directly on the seismic profile and a rigorous tie is not possible, we feel that it is possible to establish a link because the well and the northwest end of the seismic section align along the strike of the Malagash Anticline (Fig. 1). The well was drilled to a total depth of 4537 m where, at the time of drilling, Horton Group rocks were interpreted (MacDonald, 1973). Ryan and Boehner (1994) suspected that drilling was completed in the Windsor Group, since typical basal Windsor Group lithologies were never encountered in the well (Fig. 4a). Synthetic seismograms based on sonic log and assumed densities correlate with the seismic section, especially at 1.5-1.6 s where high amplitudes are observed on both synthetic seismograms and seismic profiles. These reflections correspond to interbedded clastics and evaporites

of the Windsor Group (MacDonald, 1973). The seismically quiet zone from 1.9 s to total depth corresponds to a clastic sequence underlain by salt. This clastic sequence may be a lateral equivalent to the Tenneycape Formation (Giles, 1981). At greater depths, the strong seismic reflections observed at about 2.5 s on the northwest side of the section again resemble reflections observed near the base of the Windsor Group in the Magdalen Basin (Durling and Marillier, 1993). Basal Windsor Group reflections are laterally extensive in the Magdalen Basin and are usually the deepest high-amplitude continuous reflections in the basin. If the reflections at 2.5 s (Fig. 4) represent the base of the Windsor Group, which seems likely, then Horton Group rocks are probably not present at the bottom of the Wallace Station well. We therefore concur with Ryan and Boehner (1994) who argued that Horton Group rocks were not drilled at the bottom of the well, and we suggest that these rocks correlate with middle Windsor Group rocks (subzone 2 of Giles, 1981).

CONCLUSIONS

The modern processing techniques that have been applied to the Anschutz seismic data in the Cumberland Basin have significantly improved the quality of the data. Reprocessing has increased signal-to-noise ratio, improved coherency and continuity of reflections, migrated dipping reflections to their proper place, and increased the record length from 4.0 to 5.0 s. The reprocessed data offer a clearer picture of structural and stratigraphic relationships within the deep parts of the Cumberland Basin. Preliminary interpretation has already yielded some tantalizing results. It is expected that when the entire Anschutz dataset is reprocessed, an integrated three-dimensional view of the Cumberland Basin will be available that will contribute to a better understanding of the geology of this basin.

ACKNOWLEDGMENTS

We would like to thank Pembina Resources Limited (Calgary) for donating the Anschutz dataset to the Geological Survey of Canada. The data set is now part of the National Digital Seismic Database housed at the Atlantic Geoscience Centre, where it is accessible for non-business related purposes. Pulsonic Geophysical Limited and their main processor person, M. Stevenson, are thanked for facilitating our active participation in the choice of reprocessing parameters. Excellent quality data could thus be achieved. This paper benefited from the reviews of A. Grant and K. Coflin.

REFERENCES

- Boehner, R.C.
1986: Salt and potash resources in Nova Scotia; Nova Scotia Department of Mines and Energy, Bulletin 5, 346 p.
- Durling, P. and Marillier, F.
1990: Structural trends and basement rock subdivisions in the western Gulf of St. Lawrence, Northern Appalachians; *Atlantic Geology*, v. 26, p. 79-95.

Durling, P. and Marillier, F. (cont.)

1993: Structural elements of the Magdalen Basin, Gulf of St. Lawrence, from seismic reflection data; in Current Research, Part D; Geological Survey of Canada, Paper 93-1D, p. 147-154.

Durling, P., Howells, K., and Harvey, P.

in press: The geology of St. Georges Bay, Nova Scotia from shallow penetration marine seismic data; Canadian Journal of Earth Sciences.

Giles, P.S.

1981: Major transgressive-regressive cycles in the Middle to Late Viséan rocks of Nova Scotia; Nova Scotia Department of Mines and Energy, Paper 81-2, 27 p.

Howie, R.D.

1986: Windsor Group salt in the Cumberland Basin of Nova Scotia; Geological Survey of Canada, Paper 85-11, 12 p.

MacDonald, D.R.

1973: Geological wellsite report, Wallace Station No. 1, Nova Scotia, Canada; Nova Scotia Department of Natural Resources, Mines and Energy Branch, Assessment Report 11E/14B 39-E-47(01).

Roliff, R.A.

1962: The Maritimes Basin of Eastern Canada; Geological Association of Canada, Proceedings, v. 14, p. 21-41.

Ryan, R.J. and Boehner, R.C.

1994: Geology of the Cumberland Basin, Cumberland, Colchester and Pictou Counties, Nova Scotia; Nova Scotia Department of Natural Resources, Mines and Energy Branches, Memoir 10, 222 p.

Ryan, R.J., Boehner, R.C., and Calder, J.H.

1991: Lithostratigraphic revisions of the Upper Carboniferous to Lower Permian strata in the Cumberland Basin, Nova Scotia and the regional implications of the Maritimes Basin in Atlantic Canada; Bulletin of Canadian Petroleum Geology, v. 4, p. 289-314.

Stevenson, M.

1994: Atlantic Geoscience Centre, Northern Nova Scotia Prospect, 1994 seismic processing report; Internal report.

Geological Survey of Canada Project 880032

A preliminary microthermometric study of the Sugar Camp, Yankee Line, and MacPhails Brook Pb-Zn showings, Cape Breton Island, Nova Scotia¹

Guoxiang Chi and Martine M. Savard
Quebec Geoscience Centre, Sainte-Foy

Chi, G.-X. and Savard, M.M., 1995: A preliminary microthermometric study of the Sugar Camp, Yankee Line, and MacPhails Brook Pb-Zn showings, Cape Breton Island, Nova Scotia; in Current Research 1995-D; Geological Survey of Canada, p. 53-58.

Abstract: A number of small Pb-Zn occurrences are hosted by Carboniferous basal Windsor carbonates in addition to the Jubilee deposit on Cape Breton Island in Nova Scotia. This paper reports some preliminary microthermometric data on the Sugar Camp, Yankee Line, and MacPhails Brook showings, and compares them with data from the Jubilee and Gays River deposits.

Fluid inclusions from all the showings have first-melting temperatures lower than -55°C, indicating that the fluid composition may be modelled by the system H₂O-NaCl-CaCl₂. Bulk salinities are generally between 20 and 30 wt% NaCl equivalent, comparable to the Gays River deposit but statistically higher than the Jubilee deposit. Homogenization temperatures vary between 123-220°C, 79-110°C, and 66-118°C for the Sugar Camp, Yankee Line, and MacPhails Brook showings, respectively. The microthermometric attributes of the Sugar Camp showing have more affinities with those of the Gays River deposit than those of the Jubilee deposit.

Résumé : Plusieurs petits indices de Pb-Zn sont contenus dans les roches carbonatées de base du Groupe de Windsor en plus du gisement de Jubilee sur l'île du Cap-Breton en Nouvelle-Écosse. Le présent article documente quelques données microthermométriques préliminaires sur les indices de Sugar Camp, Yankee Line et MacPhails Brook, et les compare avec les données des gisements de Jubilee et Gays River.

Les inclusions fluides provenant de tous les indices ont des températures de première fonte inférieure à -55 °C, indiquant que la composition des fluides peut être modélisée par le système H₂O-NaCl-CaCl₂. La salinité varie généralement de 20 à 30 % au poids, en équivalent NaCl, ce qui est comparable au gisement de Gays River mais statistiquement plus élevé qu'au gisement de Jubilee. Les températures d'homogénéisation varient entre 123-220 °C, 79-110 °C et 66-118 °C, respectivement, pour les indices de Sugar Camp, de Yankee Line et de MacPhails Brook. Les attributs microthermométriques de l'indice de Sugar Camp s'apparentent mieux à ceux du gisement de Gays River qu'à ceux du gisement de Jubilee.

¹ Contribution to Canada-Nova Scotia Cooperation Agreement on Mineral Development (1992-1995), a subsidiary agreement under the Canada-Nova Scotia Economic and Regional Development Agreement.

INTRODUCTION

A number of Pb-Zn occurrences are hosted by Carboniferous basal Windsor carbonates along the southern margin of the Late Devonian-Permian Maritimes Basin. Besides economically significant deposits (e.g. the Gays River, Jubilee, Walton, Smithfield, Pembroke deposits), many showings have been discovered, and some are being prospected. Understanding the genetic link of ore occurrences (showings and deposits) requires an evaluation through geochemical and microthermometric investigations of not only the major deposits but also the minor showings.

Previous studies have used fluid inclusions to access the nature of ore-forming fluids and the physicochemical conditions during ore precipitation of the Gays River (Akande and Zentilli, 1984; Ravenhurst et al., 1989; Savard, 1992; Kontak, 1992; Chi and Savard, in prep.) and Jubilee (Hein et al., 1993; Chi et al., in prep.) deposits. This paper reports preliminary microthermometric data from the Sugar Camp, Yankee Line, and MacPhails Brook Pb-Zn showings on Cape Breton Island (Fig. 1). Results are compared with those of the Jubilee and Gays River deposits, and their implications on regional fluid flow patterns are briefly discussed.

LOCATION OF SAMPLES

The Sugar Camp showing is located about 9 km northeast of Port Hastings, 500 m to the southeast of MacGregors Lake (co-ordinates: 45°41.5'N, 61°18.7'W). Mineralization is hosted by the fine limestones of the Macumber Formation, which overlies clastic rocks of the Horton Group and is overlain by evaporites of the Carrols Corner Formation. Mineralization styles include minor and intense veining in the upper and lower parts and breccia cementation in the middle part of the Macumber Formation (Goodwin, 1988). The two samples used for microthermometric study come from the upper intense veining zone (Fig. 2A). Pyrite appears to be the first mineral to precipitate, followed by sphalerite and calcite, and then by calcite and barite. Calcite is either anhedral or fibrous, both postdating pyrite and being uniformly dull under cathodoluminescence.

The Yankee Line showing is near the intersection of Middle River and McDonald Brook (co-ordinates: 46°7.8'N, 60°55'W). Mineralization occurs as veinlets of galena-calcite-barite and as disseminations of galena in limestones of the Macumber Formation, which conformably overlies

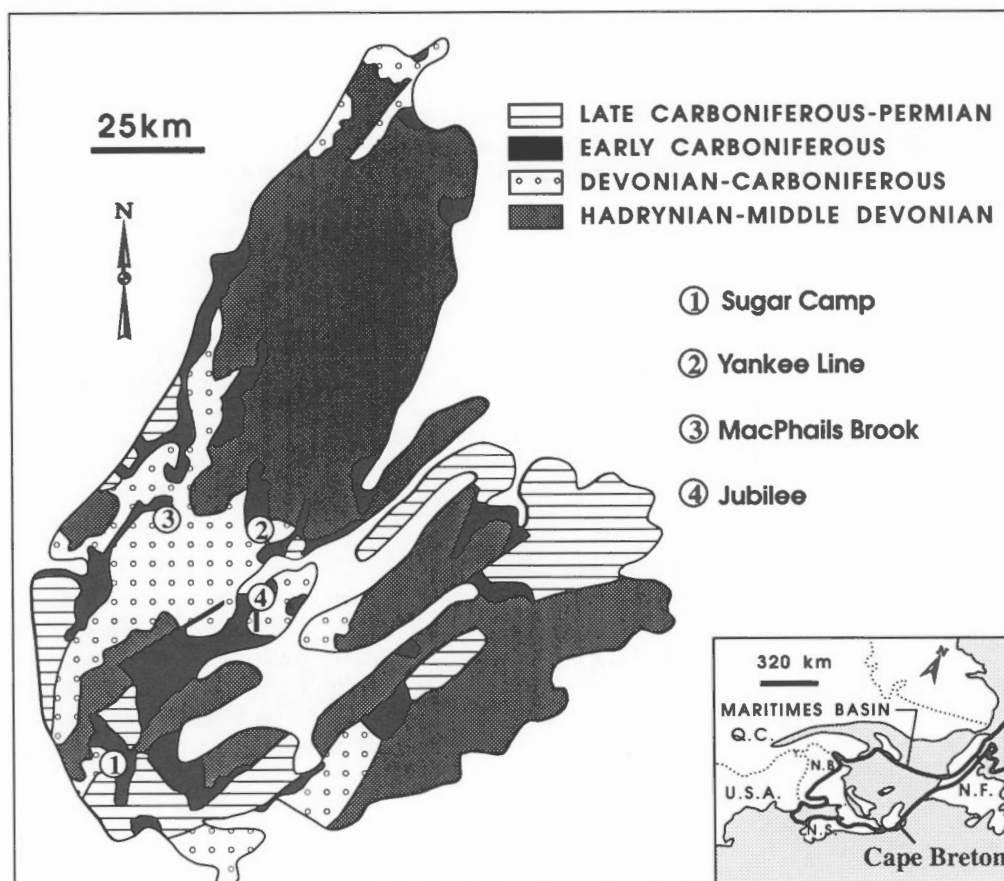


Figure 1. Regional geological map of Cape Breton Island (after Boehner et al., 1989) showing the location of the Sugar Camp, Yankee Line, and MacPhails Brook occurrences and the Jubilee deposit. The insert map shows the scope of the Maritimes Basin (after Howie and Barss, 1975).

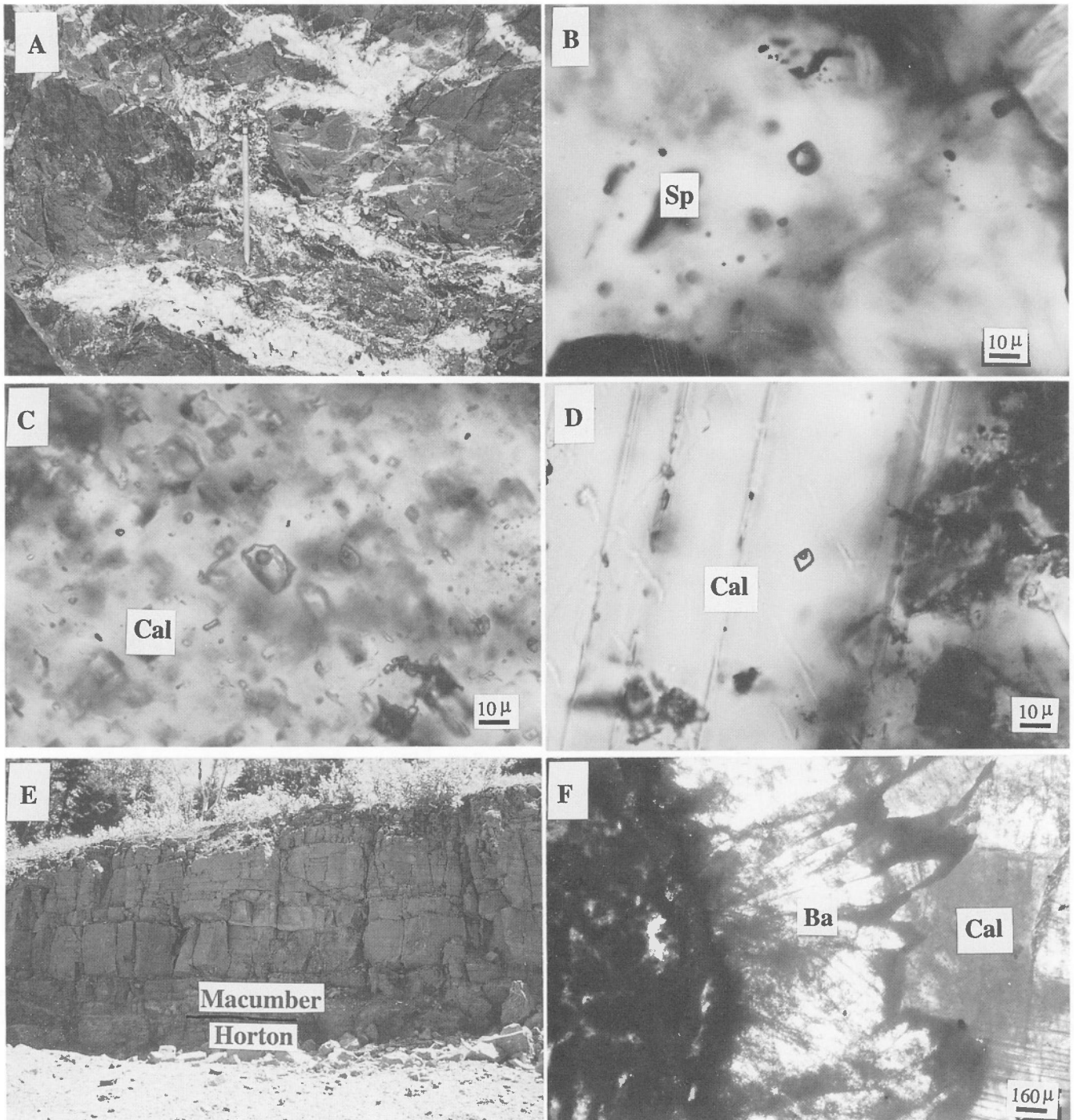


Figure 2. A) Calcite-pyrite-sphalerite-barite veins in carbonates of the Macumber Formation, Sugar Camp showing; B) cluster of fluid inclusions in sphalerite (Sp), Sugar Camp showing; C) randomly and densely distributed fluid inclusions in calcite (Cal), Sugar Camp showing; D) isolated fluid inclusion in calcite, Sugar Camp showing; E) laminated limestones of the Macumber Formation overlying clastic rocks of the Horton Group, Yankee Line showing; F) fibrous barite (Ba) cement followed by coarse anhedral calcite, Yankee Line showing.

Table 1. Fluid inclusion homogenization temperatures and salinities.

Locality	Host Mineral	Homogenization Temperature					Salinity (wt% NaCl equiv.)				
		No.	Min.	Max.	Mean	Std. Dev.	No.	Min.	Max.	Mean	Std. Dev.
Sugar Camp	Sphalerite	10	122,8	175,5	140,6	16,7	4	20,7	29,9	25,5	3,9
	Calcite	68	139,9	219,9	159,2	12,6	12	23,3	31,6	27,0	2,8
Yankee Line	Calcite	26	78,8	109,8	95,5	6,4	5	24,3	26,9	25,4	1,1
MacPhails Brook	Calcite	13	65,7	93,2	79,0	7,7					
	Fluorite	26	70,6	118,3	97,2	10,0	7	23,0	30,1	26,4	3,1
Jubilee	Sphalerite	36	40,6	228,1	91,4	38,3	18	14,3	24,9	17,8	3,7
	Calcite	53	66,2	224,4	100,4	37,2	31	11,1	25,6	15,1	4,0
Gays River	Sphalerite	41	92,2	197,8	137,2	19,3	27	18,9	28,1	24,5	1,5
	Calcite	89	56,4	212,4	121,2	35,8	14	13,6	33,4	22,5	4,3

Fluid inclusion homogenization temperatures and salinities obtained from sphalerite and syn- to post-ore calcite and fluorite from the Sugar Camp, Yankee Line, and MacPhails Brook showings, and data from the Jubilee and Gays River deposits for comparison. Many fluid inclusions in calcite from the Gays River deposit have very low salinities, i.e. less than 5 wt%; these inclusions are not used in the present comparison because their timing with respect to the mineralizing event is uncertain.

clastic rocks of the Horton Group (Fig. 2E). Barite is fibrous and appears to be the first cement, followed by precipitation of marcasite, and then by galena and calcite (Fig. 2F).

The MacPhails Brook showing is located on the east shore of Lake Ainslie, about 500 m east of the intersection of MacPhails Brook and the Route 395 (co-ordinates: 46°7.7'N, 61°7.9'W). Mineralization is hosted by carbonates of the Macumber Formation. One of the two samples used for microthermometric study comprises limestone breccia cemented by pyrite, followed by sphalerite, galena, and calcite. Some veinlets of galena postdate calcite. The other sample consists of barite and fluorite; their relationship with sulphides was not observed.

MICROTHERMOMETRIC RESULTS

Doubly polished thin sections of two samples from each of the showings were examined for fluid inclusions. The fluid inclusions were studied using the United States Geological Survey Heating/Freezing Stage to estimate the compositional system of the fluids, bulk salinities, and homogenization temperatures.

Sugar Camp

For the Sugar Camp showing, fluid inclusions were studied in sphalerite and coeval anhedral calcite. Barite contains numerous monophase (liquid) inclusions which were not studied. Fluid inclusions in sphalerite generally occur in clusters without obvious fracture control (Fig. 2B). Fluid inclusions in calcite are generally randomly and densely distributed (Fig. 2C), but are occasionally isolated (Fig. 2D). Randomly distributed and isolated fluid inclusions have similar microthermometric characteristics, and are possibly primary.

All fluid inclusions (from both sphalerite and calcite) comprise two phases (liquid + vapour bubble) at room temperature. They show fairly low first melting temperatures,

ranging from -80.2 to -55.6°C, indicating that the fluids may be modeled by the system H₂O-NaCl-CaCl₂. Salinities are estimated by using the H₂O-NaCl-CaCl₂ phase diagram (Williams-Jones and Samson, 1990) when both the second and last melting temperatures were observed, or by using the freezing point depression diagram of Crawford (1981) when only the last melting temperature was observed. Bulk salinities range from 20.7 to 29.9 wt% for fluid inclusions from sphalerite, and from 23.3 to 31.6 wt% for fluid inclusions from calcite (Table 1). Homogenization temperatures are 122.8-175.5°C for fluid inclusions from sphalerite, and 139.9-219.9°C for fluid inclusions from calcite (Table 1 and Fig. 3).

Yankee Line

For the Yankee Line showing, fluid inclusions were studied only in anhedral calcite, which is broadly contemporaneous with galena. The fibrous barite contains numerous monophase (liquid) inclusions which were not studied. A few tiny monophase (liquid) brown inclusions (possibly liquid hydrocarbons) were observed in the fibrous barite.

Fluid inclusions in calcite are generally randomly and densely distributed; some of them are relatively isolated. They comprise two phases (liquid + vapour bubble) at room temperature. First melting temperatures are between -68.2 and -63.7°C. Salinities are estimated in the same way as for the Sugar Camp showing, and range from 24.3 to 26.9 wt% (Table 1). Homogenization temperatures vary from 78.8 to 109.8°C (Table 1 and Fig. 3).

MacPhails Brook

For the MacPhails Brook showing, fluid inclusions were studied in anhedral calcite coeval with sphalerite and galena and in fluorite associated with barite. No fluid inclusions suitable for microthermometric study were found in sphalerite. Numerous brown monophase (liquid) petroleum inclusions occur along healed fractures crosscutting calcite.

Fluid inclusions in calcite are randomly distributed; some are relatively isolated. Fluid inclusions in fluorite generally occur in clusters without obvious fracture control. All fluid inclusions comprise two phases (liquid + vapour bubble) at room temperature. No freezing data have been obtained for fluid inclusions from calcite. First melting temperatures for fluid inclusions from fluorite are between -69.2 and -60.4°C ; salinities, estimated in the same way as for the Sugar Camp showing, range from 23.0 to 30.1 wt% (Table 1). Homogenization temperatures are 65.7 – 93.2°C for fluid inclusions from calcite, and 70.6 – 118.3°C for fluid inclusions from fluorite (Table 1 and Fig. 3).

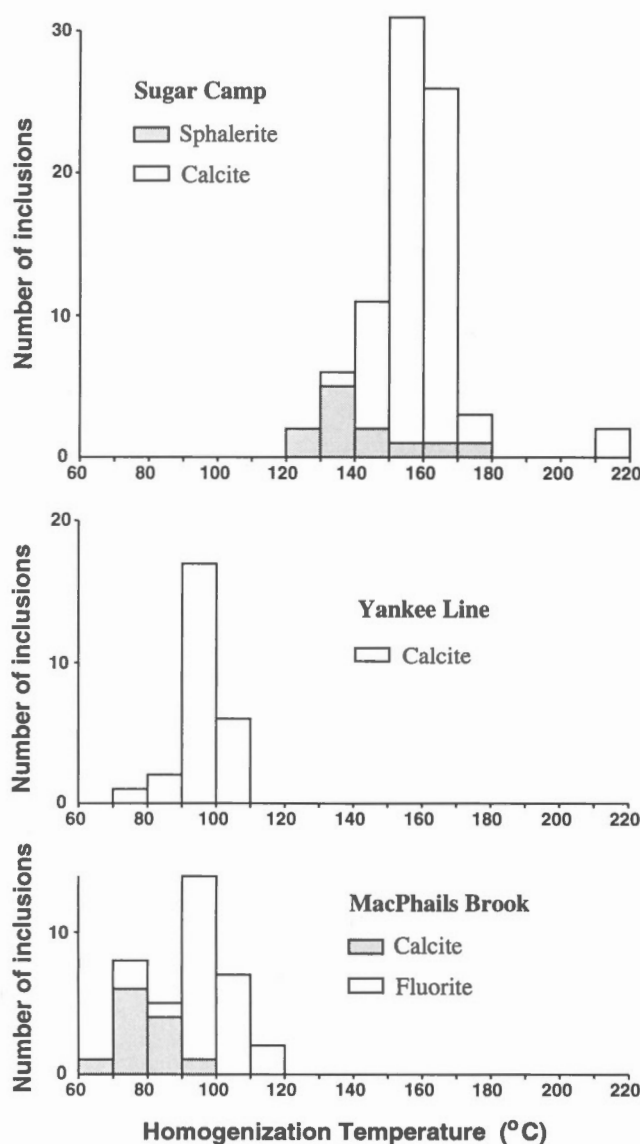


Figure 3. Histogram of homogenization temperatures of fluid inclusions from the Sugar Camp, Yankee Line, and MacPhails Brook showings.

COMPARISON WITH THE JUBILEE AND GAYS RIVER DEPOSITS

The microthermometric data documented above are compared with those from the Jubilee Zn-Pb deposit (Chi et al., in prep.) in the same region (see Fig. 1) and the Gays River Zn-Pb deposit (Chi and Savard, in prep.) about 200 km southwest of the region. The homogenization temperature and salinity data of the showings and deposits are summarized in Table 1. Some remarks may be made through this comparison.

Firstly, as indicated by the first melting temperatures of fluid inclusions, mineralizing fluids for the showings and deposits appear to have similar compositional system, i.e., $\text{H}_2\text{O}-\text{NaCl}-\text{CaCl}_2$, which is typical of basinal brines. Bulk salinities are broadly comparable among the showings and the Gays River deposit; the Jubilee deposit appears to have lower salinities, although high salinities (up to 25.6 wt%) are also recorded.

Secondly, with respect to homogenization temperatures, the Sugar Camp showing is similar to the Gays River deposit. The Yankee Line and MacPhails Brook showings are, in terms of statistics, similar to the Jubilee deposit when data from calcite coeval with ore precipitation are compared, but do not show the high homogenization temperatures (as based on a small number of inclusions) recorded in the Jubilee deposit.

SUMMARY

In summary, the present study indicates that the Sugar Camp, Yankee Line, and MacPhails Brook showings and the Jubilee deposit, although close in space and having similar geological setting, do not share the same microthermometric attributes. The relatively high homogenization temperatures recorded in the Sugar Camp showing, similar to the Gays River deposit, indicate that a major hydrothermal event has affected this part of the basin. The temperature difference between the Sugar Camp and Yankee Line + MacPhails Brook showings might be explained either by distinct mineralizing fluids with different temperatures or by equilibration of the same fluids to distinct local background temperatures. This ongoing study might have some implications for evaluation of ore potential of the Sugar Camp prospect and of the whole region.

ACKNOWLEDGMENTS

This study was financially supported by the Canada-Nova Scotia Cooperation Agreement on Mineral Development. We would like to thank Jean-Claude Bérubé for preparing the doubly polished thin sections, and Dr. Huan-Zhang Lu of l'Université du Québec in Chicoutimi for his careful review of the first draft of the manuscript.

REFERENCES

- Akande, S.O. and Zentilli, M.**
1984: Geologic, fluid inclusion, and stable isotope studies of the Gays River lead-zinc deposit, Nova Scotia; *Economic Geology*, v. 79, p. 1187-1211.
- Boehner, R.C., Giles, P.S., Murray, D.A., and Ryan, R.J.**
1989: Carbonate buildups of the Gays River Formation, Lower Carboniferous Windsor Group, Nova Scotia; in *Reefs, Canada and Adjacent Area*, (ed.) H.H.J. Geldstzer, N.P. James, and G.E. Tebbutt; Canadian Society of Petroleum Geologists, Memoir 13, p. 609-621.
- Crawford, M.L.**
1981: Phase equilibria in aqueous fluid inclusions; in *Fluid Inclusions: Applications to Petrology*, (ed.) L.S. Hollister and M.L. Crawford; Mineralogical Association of Canada, Short Course Handbook, v. 6, p. 75-100.
- Goodwin, T.A.**
1988: Exploration program, Sugar Camp Lake, Inverness County, Nova Scotia, for Seabright Explorations Incorporated; Nova Scotia Department of Mines and Energy, Assessment Report 11F/15C 27-Q-09 (05).
- Hein, F.J., Graves, M.C., and Ruffman, A.**
1993: The Jubilee Zn-Pb deposit, Nova Scotia: the role of synsedimentary faults; in *Mineral Deposit Studies in Nova Scotia*, v. 2, (ed.) A.L. Sangster; Geological Survey of Canada, Paper 91-9, p. 49-69.
- Howie, R.D. and Barss, M.S.**
1975: Upper Paleozoic rocks of the Atlantic Provinces, Gulf of St. Lawrence, and adjacent continental shelf; Geological Survey of Canada, Paper 74-30, p. 35-50.
- Kontak, D.J.**
1992: A preliminary report on geochemical, fluid inclusion and isotopic studies of the Gays River Zn-Pb deposit, Nova Scotia; Nova Scotia Department of Natural Resources Open File Report 92-014, 223 p.
- Ravenhurst, C.E., Reynolds, P.H., Zentilli, M., Krueger, H.W., and Blenkinsop, J.**
1989: Formation of Carboniferous Pb-Zn and barite mineralization from basin-derived fluids, Nova Scotia, Canada; *Economic Geology*, v. 84, p. 1471-1488.
- Savard, M.M.**
1992: Diagenèse pré- et post-minéralisation: implications pour le dépôt de Gays River, Nouvelle-Écosse; dans *Recherches en cours, Partie E*; Commission géologique du Canada, Étude 92-1E, p. 289-298.
- Williams-Jones, A.E. and Samson, I.M.**
1990: Theoretical estimation of halite solubility in the system NaCl-CaCl₂-H₂O: Application to fluid inclusions; *The Canadian Mineralogist*, v. 28, p. 299-304.

Geological Survey of Canada 920004BS

A further note on the occurrence of beryl associated with southern Nova Scotia plutons¹

K.L. Currie and J.B. Whalen
Continental Geoscience Division

Currie, K.L. and Whalen, J.B., 1995: A further note on the association of beryl with southern Nova Scotia plutons; in Current Research 1995-D; Geological Survey of Canada, p.59-64.

Abstract: Muscovite-tourmaline-garnet pegmatite associated with biotite-muscovite granodiorite to granite locally contains minor beryl. Biotite pegmatite associated with biotite tonalite does not contain beryl, but locally contains apatite prisms which resemble beryl. Host rocks exhibit complex compositional variation suggestive of magma mixing and hybridization. These complexities are reflected in changes in composition of associated pegmatites. Swarms of pegmatite sills and dykes occur along compositional discontinuities such as pluton-host rock contacts, internal compositional contacts, or contacts with mafic enclaves. This distribution, together with compositional variation of the pegmatites, and lack of evidence of a free hydrous phase, suggests formation by disequilibrium crystallisation of initially water-undersaturated magma.

Résumé : De la pegmatite à muscovite-tourmaline-grenat associée à une roche granodioritique à granitique à biotite-muscovite contiennent localement un peu de béryl. La pegmatite à biotite associée à une tonalite à biotite ne contient pas de béryl, mais contient localement des prismes d'apatite qui ressemblent au béryl. Les roches hôtes présentent une variation complexe de composition qui suggère un mélange de magma et une hybridation. Ces complexités se reflètent dans les changements de composition des pegmatites associées. Des essaims de sills et de dykes de pegmatite longent des discontinuités de composition telles que les contacts roches hôtes-pluton, les contacts internes de composition ou les contacts avec des enclaves mafiques. Cette distribution, de même que la variation de composition des pegmatites, et l'absence d'indices d'une phase hydratée libre, suggèrent la formation par cristallisation de déséquilibre de magma initialement sous-saturé d'eau.

¹ Contribution to Canada-Nova Scotia Cooperation Agreement on Mineral Development (1992-1995), a subsidiary agreement under the Canada-Nova Scotia Economic and Regional Development Agreement.

INTRODUCTION

About one third of the Meguma Zone of the Canadian Appalachians is underlain by granitoid plutons which fall into two groups, namely a northern group, dominated by the giant South Mountain Batholith, and a southern group, consisting of the Barrington Passage, Shelburne, and Port Mouton plutons (Fig. 1). Although both groups are peraluminous, they differ in petrography, chemistry, environment of emplacement, and possibly age. The northern plutons consist mainly of granodiorite and granite, including abundant Rb-rich 'specialized' granites such as the Davis Lake and New Ross plutons. They were emplaced into cool Cambro-Ordovician turbidites of the Meguma Group at relatively shallow levels, producing narrow hornfels aureoles. Although geochronological data are less complete and precise than desirable, the northern plutons appear to have been emplaced within a brief period at about 373-378 Ma (Hill, 1991). The southern plutons consist essentially of contrasting tonalite and granodiorite to granite (de Albuquerque, 1977) in varying proportions. They were emplaced into metamorphosed Meguma Group rocks which were at temperatures $>700^{\circ}\text{C}$ and pressures of <5 kbars (cordierite migmatite) around the Barrington Passage pluton (Raeside and Jamieson, 1992). Peak metamorphic conditions declined eastward to upper

greenschist grade around the Port Mouton pluton (Hope et al., 1988). The age of emplacement is essentially unknown. Ages ranging from mid-Ordovician (Rodgers, 1988) to late Carboniferous (Dallmeyer and Keppie, 1987; Reynolds et al., 1987) have been suggested on the basis of imprecise and disturbed Rb-Sr and Ar-Ar ages. A distinctive feature of the southern plutons is the presence of beryl-bearing pegmatites, which decrease in number from east to west. Although association of beryl with pegmatite is well established, the association of beryl with particular types of pegmatite and the localization of the beryl-bearing bodies are much less well understood. Since outcrop is generally very poor in this region, except along the sea coast, an easy, reliable guide to pegmatite locations, and the probability of beryl occurrence within particular pegmatites, would greatly facilitate prospecting. This contribution considers types of pegmatite, their localization, and their association with other rock types.

LITHOLOGICAL ASSOCIATIONS

The southern Nova Scotia plutons consist principally of biotite tonalite and biotite-muscovite granodiorite to granite. A volumetrically small, but genetically significant, amount of mafic rock (gabbro, diorite, lamprophyre) is present in all

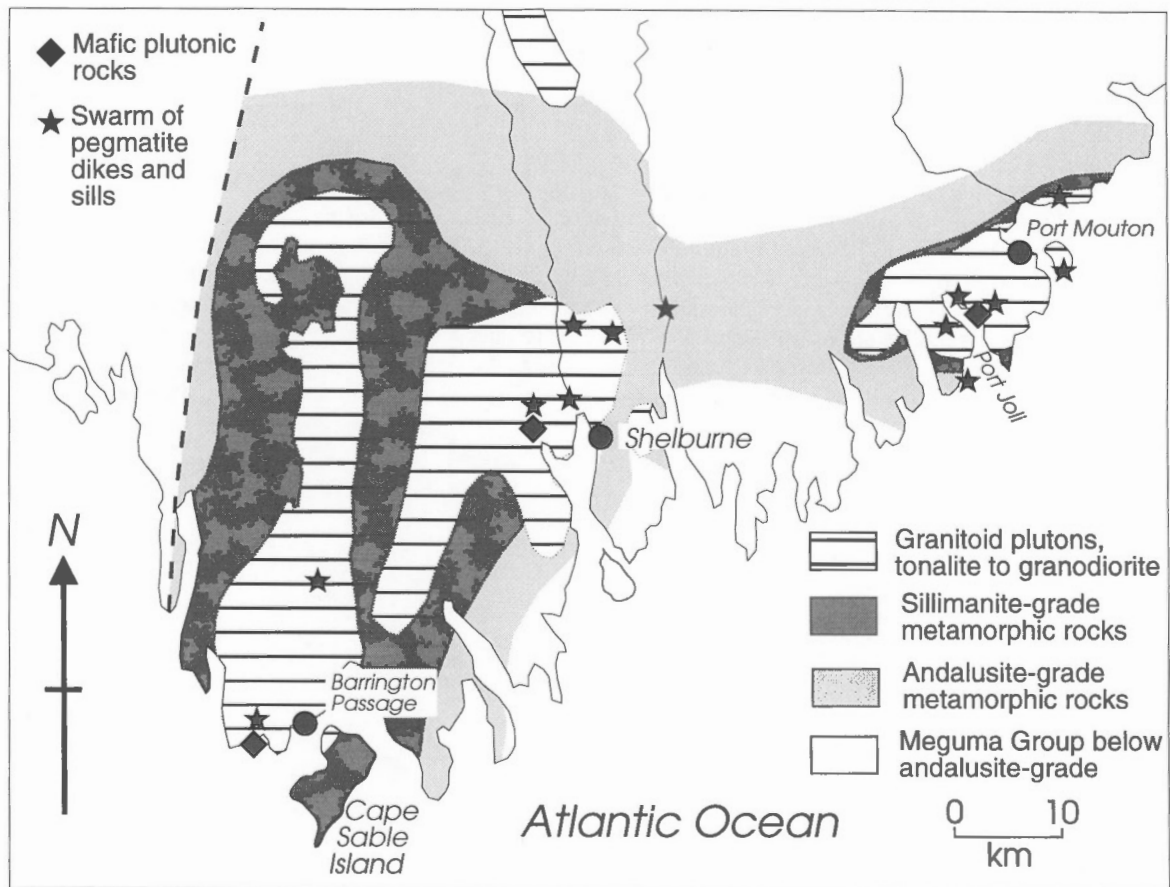


Figure 1. Geological sketch of the southern Nova Scotia plutons (modified after Raeside and Jamieson, 1992).

three plutons, most abundantly in the Barrington Passage pluton and least abundantly in the Port Mouton pluton. Conversely granodiorite and granite are most abundant in the Port Mouton pluton (about 80% by area) and least abundant in the Barrington Passage pluton (<5%). A significant proportion of the Port Mouton and Shelburne plutons consists of pegmatite (estimated at about 10% by area). Despite this simple petrography, the distribution of texturally diverse (but compositionally similar) phases is complex. Examples can be found of granodiorite intruding tonalite and vice versa (Fig. 2). More commonly lithologies are interlayered, or pass gradationally from one to another in outcrop. Attempts to map plutons by lithology have been unsuccessful (Douma, 1988; Rogers, 1988). Douma (1988) distinguished nine units in the Port Mouton pluton which she divided into three cycles. Her detailed maps of individual outcrops or areas show as many as six of these units occurring within a single outcrop or small area. Such an intimate mixture cannot be the result of ordinary

igneous fractionation. Evidence for complex mixing and hybridization processes is abundant around the small mafic enclaves. In a series of quarries in mafic rock near Shelburne (Fig. 1), a gabbroic rock forms bulbous 'pillows' in a tonalitic host (Fig. 3), exhibiting all the features typical of hybridization (compare Whalen, 1985). Similar complex physical mingling between tonalite and granodiorite can be observed along the northwest side of Port Joli in the Port Mouton pluton. In the Barrington Passage pluton, mafic rocks form a sheet-like mass extending 1 km along the seashore west of the village. This mass is surrounded by tonalite of hybrid appearance similar to that in the quarries near Shelburne. A large quarry near Barrington Passage contains numerous inclusions of mafic rocks with thin reaction rims surrounded by flow-textured tonalite (Fig. 4). Despite the local evidence for mixing and mingling, a number of distinct lithologies (including pegmatites) are common to all three plutons and most outcrops lack inclusions and appear superficially homogeneous.

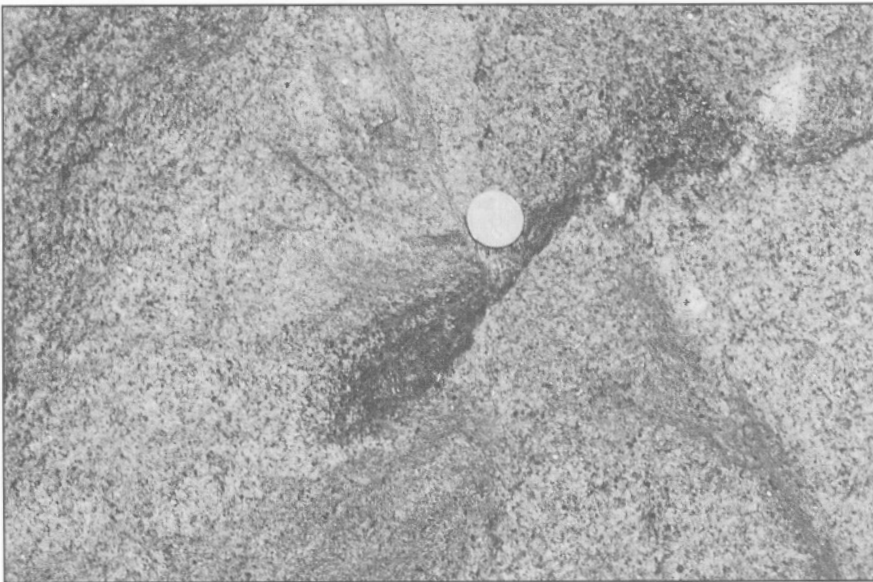
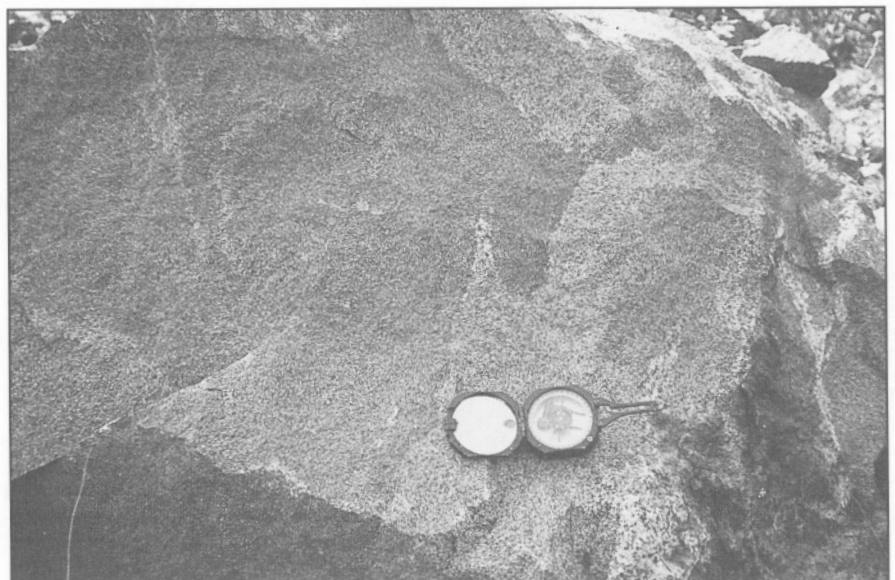


Figure 2.

Boudin-like inclusion of biotite-muscovite granodiorite in biotite tonalite. The granodiorite appears to have originally formed a 5 cm layer in the tonalite. Neither lithology shows a perceptible foliation. Outcrop at intersection of Highway 3 and Harts Point Road about 6 km southwest of Shelburne.

Figure 3.

Lobate, serrated, chilled contact of gabbro against tonalite. Rimmed xenocrysts can be seen in the hybrid tonalite. Quarry north of Highway 103, 4 km west of Shelburne.



Different lithologies contain distinct pegmatites. Tonalitic phases contain biotite-bearing pegmatites in which the biotite grows as elongate tabular crystals up to 10 cm in length, whereas granodioritic to granitic phases contain muscovite-bearing pegmatites lacking biotite and often interlayered with aplite (Fig. 5). Pegmatites of both varieties may form either sharply bounded, curvilinear masses (dykes or sills), or nebulous gradational patches (Fig. 6). The thickest sill observed was about 2.5 m thick. Nebulous patches tend to be less than 1 m across, and may be as little as 10 cm in largest dimension. Zoning of pegmatite is relatively rare and where present, tends to be imperfect and diffuse, with quartz cores and one or more feldspar-rich zones. Minor phases, such as garnet, tourmaline, and beryl, occur as erratic concentrations, commonly confined to one of the feldspar-rich zones. Like the major lithologies, pegmatites tend to grade from one type to another in complex fashion. The typical mineralogy of the biotite-bearing examples is biotite-K-feldspar-plagioclase-quartz,

but muscovite is common, either as overgrowths and replacements of biotite, or as independent books, often festooned around coarse quartz. Garnet and tourmaline occur in a biotite pegmatite cutting mafic rocks near Shelburne. Each occurs in a distinct zone, with a marginal tourmaline-rich zone outside a garnet-rich zone. Where garnet is present in biotite-bearing pegmatites, it invariably forms fine-grained intergrowths with quartz. The typical mineralogy of the muscovite-bearing examples is muscovite-K-feldspar-plagioclase-quartz. Garnet is commonly present as dodecahedra with few or no inclusions, while tourmaline is less commonly present, either as acicular crystals or as quartz-tourmaline intergrowths. Our observations suggest that beryl is found only in pegmatites containing primary muscovite, tourmaline, and garnet. In particular beryl and biotite appear not to coexist. We examined a number of reported occurrences of beryl in biotite-bearing pegmatites of the Shelburne pluton. In each case, the green hexagonal mineral proved to be apatite, as indicated initially

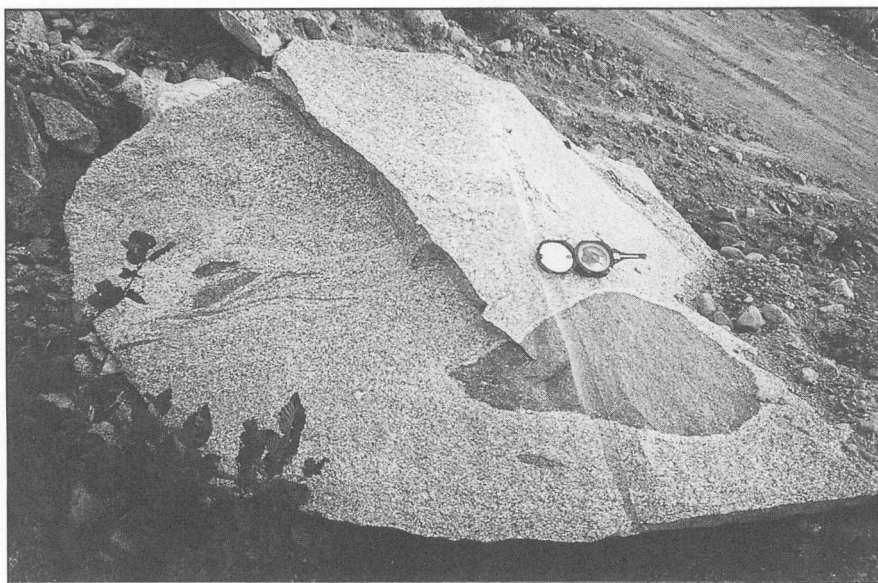
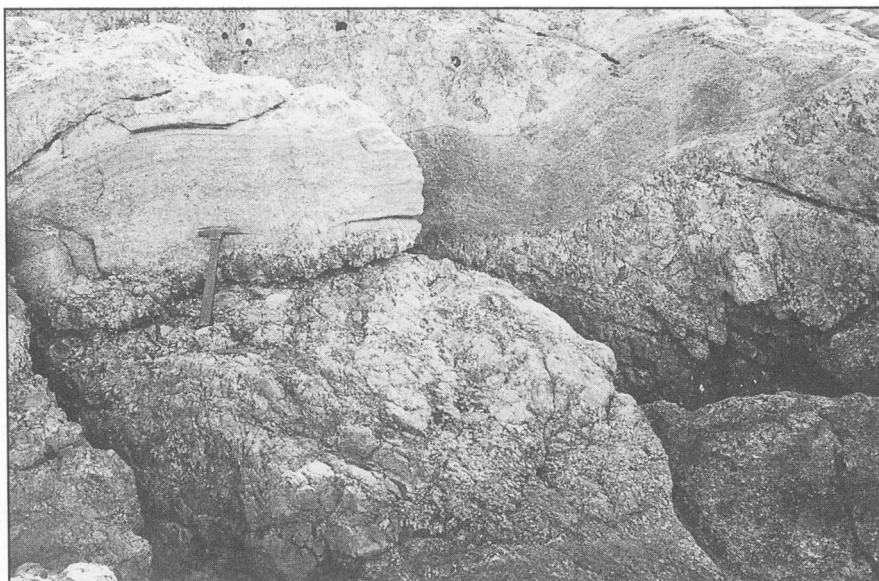


Figure 4.

Mafic inclusions in foliated tonalite from large quarry west of Barrington Passage. Note the flow lines around the inclusion, and the narrow leucocratic rim on the mafic inclusions.

Figure 5.

Muscovite-tourmaline pegmatite with internal finer grained, equigranular layer which is itself internally layered. Southwest Port Joli.



by scratching with a knife, and confirmed in two cases by X-ray diffraction. Muscovite-bearing pegmatites exhibit transitions toward greisen-like muscovite-quartz intergrowths. A large sill complex in southwest Port Joli contains numerous cone-shaped masses of radially aligned quartz and muscovite up to 10 cm in diameter and 3 cm high (Fig. 7) along the boundaries between aplitic and pegmatitic layers. Similar phenomena occur in the northeastern part of the Shelburne pluton.

Our observations show that pegmatite masses are not randomly distributed in the plutons, but are associated with compositional discontinuities such as the pluton-country rock boundary, internal boundaries between major phases, and margins of mafic inclusions, schlieren, and country rock inclusions. Some observations suggest that pegmatites were generated directly by mafic-felsic interactions. In mafic rocks near Shelburne, biotite pegmatite patches are found within

hybrid tonalite. In the Barrington Passage pluton, pegmatite dykes are exclusively associated with the contact of a sill-like mass of diorite or gabbro, whereas the surrounding tonalite is devoid of pegmatite.

DISCUSSION

Our observations strongly support the view that the origin of the southern plutons is complex. Presence of mafic rocks variably mixed and hybridized with more salic compositions suggests involvement of a mantle component, minor in amount at presently accessible parts of the pluton, but possibly of major importance at depth. Such a mantle component could act as a heat source, leading to melting of a compositionally heterogeneous crust. Extensive melting at crustal levels could explain both the dearth of mantle material at high levels in the

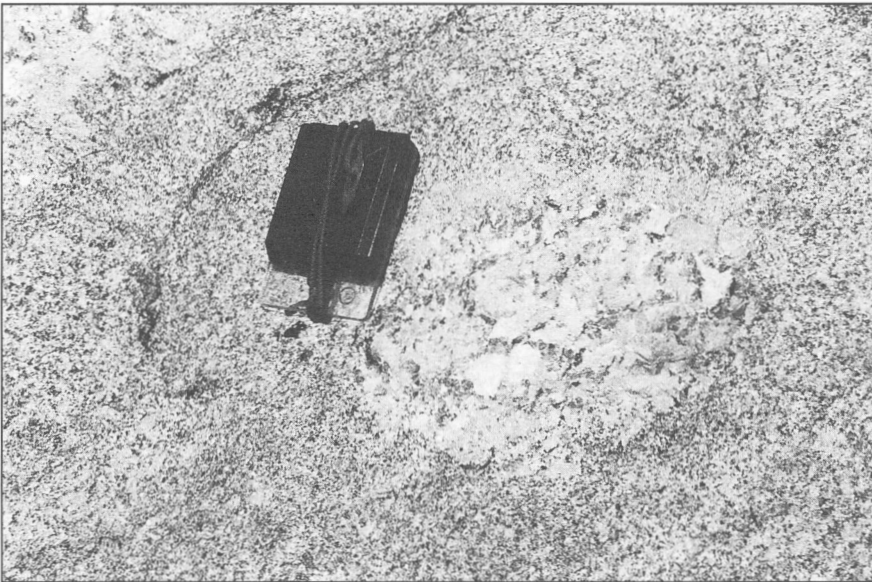
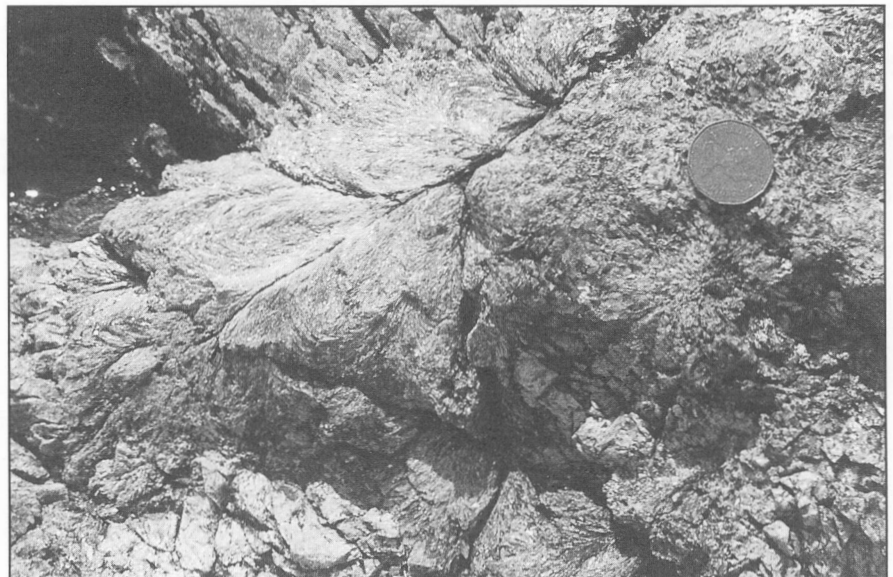


Figure 6.

Nebulous pegmatitic patch, Port Mouton.

Figure 7.

Cone-shaped radiating muscovite-quartz aggregates, Port Mouton.



crust, since a hot, light plastic lid cannot be readily intruded by denser mafic magma, and the presence of salic components which cannot be readily linked by fractional crystallization. We assume that the peraluminous tonalite component was derived by melting materials originally below the exposed Meguma Group. The source of the more potassic, salic, and peraluminous rocks could possibly have been the Meguma Group. We hope to better characterize these components by trace element geochemistry and isotopic analyses. At present we are uncertain whether other components are required, or whether mixing and mingling of three components is sufficient. A complex pattern of homogeneous units with well defined boundaries and hybrid mixed units appears to require separate magma sources, presumably at different levels, with each magma source cleansing itself of restite prior to mixing at higher levels. Our model is fairly close to that of Douma (1988) who also envisaged convective and turbulent mixing of magma from heterogeneous crustal sources, although her reasoning and lines of evidence diverged widely from ours.

Such models leave two crucial questions unresolved, namely (a) what was the cause of the very pronounced thermal high which caused a rise of the 600°C isotherms to depths of 12-15 km, and (b) what was the cause of pegmatite formation and mineralization. The rise of isotherms suggests shallow mafic magma emplacement whether due to delamination, extension or some other mechanism. However, this episode cannot be fitted into more regional models without more precise age data. Ages ranging from mid-Ordovician (Rodgers, 1988) to late Carboniferous (Dallmeyer and Keppie, 1987; Reynolds et al., 1987) have been suggested for plutonism and metamorphism. It has also been suggested that metamorphism is younger than plutonism (Dallmeyer and Keppie, 1987). Precise age data would have a major impact on understanding the development of the Meguma Zone. We plan to obtain such data so that models of origin and emplacement of the southern plutons can be placed on a more solid foundation.

Geologists very generally agree that pegmatites indicate crystallisation of hydrous magma. However, two diverse schools of thought have developed on genesis. One school, based on a now classic paper by Jahns and Burnham (1969), assumes equilibrium crystallization of water-saturated melt, implying a free hydrous phase throughout crystallization. This school emphasizes such features as quartz cores. The other school, typified by the review of London (1992), points out that experimental data do not support the Jahns/Burnham model, and instead emphasizes kinetic factors during non-equilibrium crystallization of initially water-undersaturated magma. There is no obvious evidence of a free hydrous phase, such as miarolitic cavities or hydrous alteration zones, in the southern Nova Scotia plutons. Some features such as the dendritic biotites of the pegmatites, the confinement of pegmatites to compositional boundaries, and the association of particular types of pegmatites with distinct lithologies are compatible with nonequilibrium crystallization of late differentiates. However, confident discrimination among various models requires precise temperatures and pressures

of formation, water fugacities, and some quantitative estimates of the nature of the hydrothermal phase, if any, which can be obtained from isotope and fluid inclusion data. The mineral assemblage (quartz-K-feldspar-plagioclase-biotite-muscovite-garnet) in many pegmatites is unusually favourable for P-T estimation, not only by thermodynamic means, but also for the application of isotopic geothermometry (Longstaffe, 1982). It should therefore be possible to fix the values of intensive variables with considerable precision. The relevant data are now being collected and analyzed.

REFERENCES

- de Albuquerque, C.A.R.**
1977: Geochemistry of the tonalitic and granitic rocks of the Nova Scotia southern plutons; *Geochimica et Cosmochimica Acta*, v. 41, p. 1-13.
- Dallmeyer, R.D. and Keppie, J.D.**
1987: Polyphase late Paleozoic tectonothermal evolution of the southwestern Meguma Terrane, Nova Scotia: evidence from $^{40}\text{Ar}/^{39}\text{Ar}$ mineral ages; *Canadian Journal of Earth Sciences*, v. 24, p. 1242-1254.
- Douma, S.**
1988: The mineralogy, petrology and geochemistry of the Port Mouton Pluton, Nova Scotia; MSc. thesis, Dalhousie University, Halifax, 324 p.
- Hill, J.D.**
1991: Petrology, tectonic setting, and economic potential of Devonian peraluminous granitoid plutons in the Canso and Forest Hill areas, eastern Meguma Terrane, Nova Scotia; *Geological Survey of Canada, Bulletin* 383, 95 p.
- Hope, T.L., Douma, S.L., and Raeside, R.P.**
1988: Geology of the Port Mouton - Lockeport area, southwestern Nova Scotia; *Geological Survey of Canada, Open File* 1768, 80 p.
- Jahns, R.H. and Burnham, C.W.**
1969: Experimental studies of pegmatite genesis. I. A model for the derivation and crystallisation of granitic pegmatites; *Economic Geology*, v. 64, p. 843-864.
- London, D.**
1992: The application of experimental petrology to the genesis and crystallisation of granitic pegmatites; *Canadian Mineralogist*, v. 30, p. 499-540.
- Longstaffe, F.J.**
1982: Stable isotopes in the study of granitic pegmatites and related rocks; *Mineralogical Association of Canada, Short Course Handbook* 8, p. 373-404.
- Raeside, R.P. and Jamieson, R.A.**
1992: Low-pressure metamorphism of the Meguma terrane, Nova Scotia; *Geological Association of Canada, Wolfville '92 Field Excursion C-5 Guidebook*, 25 p.
- Reynolds, P.H., Elias, P., Muecke, G.K., and Grist, A.M.**
1987: Thermal history of the southwestern Meguma Zone, Nova Scotia from a $^{40}\text{Ar}/^{39}\text{Ar}$ and fission track dating study of intrusive rocks; *Canadian Journal of Earth Sciences*, v. 24, p. 1952-1966.
- Rogers, H.D.**
1988: Field relations, petrography, and geochemistry of granitoid plutons in the Shelburne area, southern Nova Scotia; *Geological Survey of Canada, Open File* 1835, 128 p.
- Whalen, J.B.**
1985: The McGerrigle plutonic complex, Gaspé, Quebec: evidence of magma mixing and hybridization; in *Current Research, Part A*; *Geological Survey of Canada, Paper* 85-1A, p. 795-800.

Improving measurement accuracy of formation resistivity factor measurements for tight shales from the Scotian Shelf

T.J. Katsube, N. Scromeda, and M. Williamson¹
Mineral Resources Division

Katsube, T.J., Scromeda, N., and Williamson, M., 1995: Improving measurement accuracy of formation resistivity factor measurements for tight shales from the Scotian Shelf; in Current Research, 1995-D; Geological Survey of Canada, p. 65-71.

Abstract: Methods for improving measurement accuracy of formation resistivity factor (F) has been studied for nine shale samples from the Venture Gas Field, offshore Nova Scotia. F is one of the petrophysical parameters that provides information on shale seal quality for hydrocarbon exploration. It is determined by measuring electrical resistivity (ρ_m) for samples saturated with NaCl solutions with different resistivities (ρ_w) and inserting the values into the Patnode and Wyllie Equation:

$$1/\rho_m = 1/(F\rho_w) + 1/\rho_c,$$

where ρ_c is the pore surface resistivity. According to this equation, the relationship between $1/\rho_r$ and $1/\rho_w$ should be linear. Cases where deviation from linearity occur cause concern over measurement accuracy. A previous study suggested that the problem is eliminated by using NaCl solutions with high concentrations and long saturation times. Adopting this method solves the problem for six of the nine samples. The remaining three coincide with those that have minor amounts of kaolinite.

Résumé : Des méthodes pour améliorer l'exactitude des mesures du facteur de formation (F) ont été étudiées sur neuf échantillons de shale prélevés dans le champ gazéifère Venture au large de la Nouvelle-Écosse. F est l'un des paramètres pétrophysiques qui renseignent sur la qualité d'étanchéité des shales, donnée utile pour l'exploration des hydrocarbures. Il est déterminé en mesurant la résistivité électrique (ρ_m) d'échantillons saturés en solutions de NaCl à résistivité différente (ρ_w) et en insérant les valeurs dans l'équation de Patnode et Wyllie :

$$1/\rho_m = 1/(F\rho_w) + 1/\rho_c,$$

où ρ_c est la résistivité à la surface des pores. Selon cette équation, la relation entre $1/\rho_r$ et $1/\rho_w$ devrait être linéaire. Les cas où la linéarité n'est pas obtenue, l'exactitude des mesures est en cause. Une étude antérieure a indiqué que le problème est éliminé en utilisant des solutions de NaCl fortement concentrées et des temps de saturation prolongés. En adoptant cette méthode, le problème est résolu pour six des neuf échantillons. Les trois autres correspondent aux shales qui contiennent de faibles quantités de kaolinite.

¹ Atlantic Geoscience Centre, Dartmouth

INTRODUCTION

Information on the seal quality history of shale formations in sedimentary basins is required for modern hydrocarbon exploration (Williamson, 1992; Williamson and Smyth, 1992). Petrophysical characteristics of shale seals provide an important part of that information, and the formation resistivity factor, F , is one of the petrophysical parameters that provides that information. For this reason, various studies carried out at the GSC have included such data (e.g., Katsube et al., 1990; Katsube, 1993; Katsube and Williamson, 1994a,b).

We have previously published formation resistivity factor (F) data for 10 tight shale samples from the Venture Gas Field, offshore Nova Scotia (e.g., Katsube et al., 1990, 1991, 1992b). The measurement accuracy of the data obtained by using the measurement procedures applied at that time were estimated to be ± 50 per cent (Katsube, 1981). However, questions were raised about the reliability of this accuracy, thus resulting in studies (Katsube and Scromeda, 1993) being initiated to investigate this problem. The purpose of this paper is to document the results of an accuracy study carried out on nine of the previously studied ten tight shale samples. The results of a study performed for one of these ten samples has previously been published (Katsube and Scromeda, 1993).

The formation resistivity factor (F) is determined by measuring electrical resistivities (ρ_m) for a series of NaCl solutions with different values of pore fluid resistivity, ρ_w , and then inserting the results into the Patnode and Wyllie (1950) Equation:

$$1/\rho_m = 1/(F\rho_w) + 1/\rho_c \tag{1}$$

where ρ_c is the pore surface resistivity. According to this equation, the relationship between $1/\rho_m$ and $1/\rho_w$ should be linear, therefore allowing F and ρ_c to be determined from the slope and intersect of a regression line. However, systematic deviations from a strictly linear relationship are often large enough to make accurate estimates of F and ρ_c difficult. Usually five different NaCl concentrations from 0.02 to 0.5 N are used (Katsube, 1981) for the determination of F . According to a separate study (Katsube and Scromeda, 1993), the accuracy problem is significantly reduced by using NaCl concentrations greater than 0.02 N, and saturation times longer than 240 minutes. Therefore, while the usual combinations of NaCl concentrations are used in this study, but with longer saturation times, the elimination of measurement results for the lower concentrations will be considered as a method to improve the accuracy, whenever applicable.

Bulk electrical resistivity, ρ_r , represents the electrical resistivity of a sample when saturated with pore water having resistivities (ρ_w) resembling in-situ conditions. In this case, ρ_m is replaced by ρ_r in Equation (1). This equation indicates that ρ_r values should be smaller than those of ρ_c ($\rho_r < \rho_c$). However, actually this is not always the case (Katsube and Scromeda, 1993). Therefore, measurements that do not meet this criterion must be considered erroneous, and elimination of measurement results that are a cause of this error should also be considered as a method to improve accuracy.

METHOD OF INVESTIGATION

Samples

The nine shale samples have been obtained from depths of 4700-5600 m in three wells located in the Venture Gas Field, offshore Nova Scotia (Katsube et al., 1991). The lithological and petrofacies classification can be found in the literature (Katsube et al., 1991; Katsube and Williamson, 1994a,b). Cylindrical plugs with a diameter of 25.4 mm (1 inch) were cored in the vertical direction from 10.16 cm (4 inch) split core samples (Katsube et al., 1991). Such plugs were obtained from all nine samples, and subsequently cut into disc specimens.

Sample preparation

The disc-shaped specimens with diameters of 2.13-2.51 cm and thicknesses of 0.33-0.96 cm (Table 1) were cut out from the shale samples used in this study. First, the dimensions of the specimen were measured using a calliper. The results are used to determine the geometric factor, K_G , required for the electrical measurements, using the following equation:

$$K_G = r_D^2 \pi / l \tag{2}$$

where r_D is the diameter and l is the thickness of the specimen. These results are also listed in Table 1.

Subsequently, the specimens are placed under vacuum for 15 minutes and then immersed in a fluid (still under vacuum) for 15 more minutes. The specimen is then allowed to stand in the fluid (in covered beakers) for 24 hours under atmospheric pressure, before the electrical measurements are

Table 1. Dimensions of specimens cut out from the samples.

Samples	r_D (cm)	l (cm)	W (g)	K_G (m)	δ (g/cm ³)
V-1/V	2.474	0.543	7.0972	8.85	2.72
V-1/H	2.310	0.328	3.7366	12.78	2.72
V-2	2.499	0.690	9.0260	7.11	2.67
V-3*	2.494	0.568	7.3763	8.60	2.66
V-4	2.130	0.689	6.2174	5.17	2.53
V-5	2.482	0.584	7.7310	8.29	2.74
V-6	2.513	0.730	10.1055	6.79	2.79
V-7	2.508	0.556	7.1877	8.89	2.62
V-8/Q	2.500	0.619	7.8935	7.93	2.60
V-8/S	2.503	0.589	7.4728	8.35	2.58
V-9	2.511	0.955	12.9174	5.19	2.73
V-10	2.472	0.510	6.5492	9.41	2.68

r_D = Diameter.
 l = Thickness.
W = Weight.
 K_G = Geometric factor.
 δ = Bulk density.
V = Sample prepared for measurement in the vertical direction.
H = Sample prepared for measurement in the horizontal direction.
* = These data are included to complete the data for the original set of 10 shale samples (Katsube et al., 1990, 1991).

started. The fluid resistivities (ρ_w) are measured before saturating the specimen. The fluid is distilled water for the bulk electrical resistivity (ρ_r) measurements, and is a series of brines of various NaCl concentrations for the electrical resistivity (ρ_m) measurements which are used for formation resistivity factor (F) determinations. Under prolonged saturation times, the distilled water eventually changes to water with characteristics similar to that of the in-situ pore water (Katsube and Scromeda, 1993). The basic principles of this preparation follow those previously described (Katsube, 1981; Katsube and Walsh, 1987; Katsube and Salisbury, 1991).

Electrical measurements

The bulk electrical resistivity (ρ_r) measurements are carried out prior to the formation resistivity factor (F) determinations. The shale specimens are placed in a capacitance type sample-holder (Katsube and Collett, 1973) with graphite electrodes covering the two faces. The surfaces of the sides of the specimen are dried before measurement. The sample-holder is then placed in an enclosed space to reduce movement of air around it. This is a precautionary measure to minimize evaporation of fluid from the rock pores. The sample holder is connected to an automatic electrical impedance system which measures the in-phase and out-of-phase components of the impedance at frequencies of $1.0 - 10^6$ Hz, as described in Gauvreau and Katsube (1975).

The bulk electrical resistivity (ρ_r) is determined by techniques and procedures previously described (e.g., Katsube, 1981; Katsube and Walsh, 1987; Katsube et al., 1991; Katsube and Salisbury, 1991). First, the complex resistivity, ρ^* , is measured over a frequency range of $1.0-10^6$ Hz:

$$\rho^* = \rho_R + i\rho_I \tag{3}$$

where ρ_R is the real resistivity and ρ_I is the imaginary resistivity, obtained from impedance $Z(\theta)$ measurements:

$$\rho^* = K_G Z(\theta), \tag{4}$$

where θ is the phase angle.

Then the bulk electrical resistivity (ρ_r) is determined from the Cole-Cole plots of the complex resistivity (ρ^*) measurements, by the method described in Katsube (1975) and Katsube and Walsh (1987), or in more recent publications (e.g., Katsube et al., 1991; Katsube and Salisbury, 1991; Katsube and Scromeda, 1993). When electrical resistivity is measured over these frequencies, dielectric polarization, Warburg impedance and electrode polarization effects are reflected in the measurements (Katsube, 1975, 1977). A simple method applied to distinguish different mechanisms for improvement of the measurement accuracy is to use Cole-Cole plots where imaginary-resistivity (ρ_I) is plotted against real-resistivity (ρ_R) (Katsube and Walsh, 1987). Katsube (1975) considered plots consisting of three arcs (Fig. 1) and suggested that each arc includes the effect of different groups of electrical conduction mechanisms. It was proposed that the left-most arc reflects the effects of the dielectric constant, double layer, pore structure, and pore water chemistry. In accordance with this model, bulk electrical resistivity (ρ_r) is determined from the point where the left arc intersects the horizontal axis. These measurements are made at room temperature, with errors estimated to be generally in the ranges of 10-20 per cent.

Formation resistivity factor (F) determination

The electrical resistivity (ρ_m) is determined from the Cole-Cole plots of the complex resistivity (ρ^*) measurements, similarly to that of the bulk electrical resistivity (ρ_r), and is determined for a specimen saturated with brines made up of five different NaCl concentrations: 0.02 N, 0.05 N, 0.1 N, 0.2 N and 0.5 N. The saturation time is 210 minutes to 240 minutes prior to the electrical measurements. Saturation tests carried out on sample V-3 at the time of the porosity studies, described in Katsube et al. (1992a), indicated that the specimen was 95 per cent saturated at a saturation time of 120 minutes (Katsube et al., 1992a; Katsube and Scromeda, 1993) and 97 per cent saturated at 260 minutes, suggesting that a 210 minute saturation time represents more than a 95 per cent saturation. These electrical resistivity (ρ_m) measurements were made starting with the

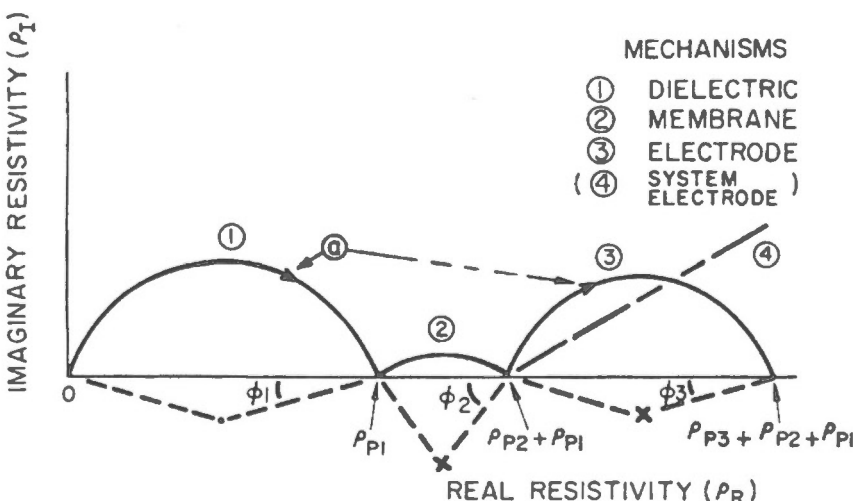


Figure 1. Description of method used to determine bulk electrical resistivity, ρ_r (ρ_{P1} in this figure), using Cole-Cole complex resistivity plots (Katsube, 1975; Katsube and Scromeda, 1993).

Table 2. Results of bulk electrical resistivity (ρ_r) measurements for the 10 shale samples from the Venture Gas Field.

Sample /Specimen	ρ_r (Ω -m)		Mean
	Mes. #1	Mes. #2	
V-1/V	112	127	120 \pm 8
V-1/H	37.5	47.0	42 \pm 5
V-2	584	688	636 \pm 52
V-3*	251	334	292 \pm 42
V-4	489	669	579 \pm 90
V-5	245	257	251 \pm 6
V-6	849	849	849 \pm 0
V-7	159	175	167 \pm 8
V-8/Q	359	408	384 \pm 25
V-8/S	172	199	186 \pm 14
V-9	702	789	746 \pm 44
V-10	233	194	214 \pm 20

ρ_r = Bulk electrical resistivity.
 Mes. (#1) = Measurement after 24-25 hours of saturation.
 Mes. (#2) = Measurement after 168-169 hours of saturation.
 * = These data are included to complete the data for the original set of 10 shale samples (Katsube et al., 1990, 1991).

lowest concentration of 0.02 N and proceeding in ascending order. Between measurements, the specimen is rinsed by immersing it overnight (12 hours) in distilled water, prior to the next measurement with a higher concentration. The formation resistivity factor (F) values were derived by the method described previously, using Equation (1).

EXPERIMENTAL RESULTS

The results of the bulk electrical resistivity (ρ_r) measurements are listed in Table 2. Measurements were made at 24 and 48 hours after saturation, to ensure that they represented ρ_r values stable with time. A variation within 20 per cent is considered to represent stability. The ρ_r values are in the range of 38-850 Ω -m, a slightly wider range compared to those of 120-580 Ω -m for the same samples previously reported (Katsube et al., 1990). No significant instability is observed in the measurements of this study (Table 2). The mean values for ρ_r are also listed in Table 4.

Table 3. Formation resistivity factor (F), surface resistivity (ρ_c) and electrical resistivities (ρ_m) for different NaCl solutions for the shale samples.

Sample	ρ_m ($\times 10^3 \Omega$ -m)					F \pm %	$\rho_c \pm$ % (Ω -m)	
	ρ_w (Ω -m)	5.00	1.86	1.03	0.61			0.29
		NaCl (N)	± 0.03	± 0.005	± 0.003			± 0.002
V-1/V	0.11	0.11	0.093	0.084	0.059	397 \pm 1 379 \pm 1	123 \pm 1 128 \pm 1	
V-1/H	0.051	0.044	0.033	0.030	0.022	127 \pm 2	51 \pm 1	
V-2	0.24	0.25	0.20	0.14	0.073	317 \pm 1 294 \pm 1 283 \pm 1	397 \pm 2 541 \pm 1 680 \pm 1	
V-4	0.24	0.22	0.20	0.089	0.045	167 \pm 2	781 \pm 11	
V-5	0.26	0.25	0.24	0.20	0.16	1289 \pm 1	278 \pm 1	
V-6	0.66	0.76	0.66	0.58	0.33	1859 \pm 5 1675 \pm 1	917 \pm 4 1034 \pm 1	
V-7	0.11	0.13	0.10	0.080	0.055	312 \pm 2 231 \pm 1	140 \pm 2 181 \pm 1	
V-8,Q	0.17	0.17	0.17	0.12	0.071	361 \pm 2 311 \pm 1	238 \pm 2 339 \pm 1	
V-8,S	0.098	0.10	0.10	0.080	0.056	364 \pm 4 304 \pm 1	121 \pm 2 148 \pm 1	
V-9U	0.33	0.39	0.41	0.37	0.25	2096 \pm 30 1570 \pm 1 1464 \pm 1	433 \pm 9 568 \pm 1 621 \pm 1	
V-10	0.095	0.093	0.085	0.068	0.044	254 \pm 1 227 \pm 1	114 \pm 1 133 \pm 1	

ρ_w = pore fluid resistivity
 ρ_m = electrical resistivity of the rock for solutions of different salinities
 F = formation resistivity factor
 ρ_c = surface resistivity
 X = data points used for formation resistivity factor determination

Results of the electrical resistivity measurements (ρ_m) used for formation factor (F) determination are listed in Table 3. The results for sample V-3 has been published previously (Katsube and Scromeda, 1993) and are not repeated here. The results of the F and ρ_c determinations using Equation (1) are listed in the last two columns of this table. The percentage errors, listed in these columns, are determined by taking the differences in the F and ρ_c values obtained by using the different regression lines: the reduced major axis (RMA) and the normal regression lines (NRL). Typical examples of the $1/\rho_m$ versus $1/\rho_w$ relationships observed when determining F and ρ_c are shown in Figure 2. The principles of the RMA are described in Davis (1986), and examples of related applications are found in Katsube and Agterberg (1990).

Figure 2a displays an example (sample V-5) where a good linear relationship exists between $1/\rho_m$ and $1/\rho_w$, and all 5 data points have been used to determine F and $1/\rho_c$. Figure 2b is an example (sample V-9) where there is a progressive deviation from linearity with decreasing NaCl concentrations (decreasing $1/\rho_w$ values), and only the three data points with the larger values

of $1/\rho_w$ have been used to determine F and ρ_c . Figure 2c displays an example (sample V-6) where two data points, which slightly deviate from the linear relationship between $1/\rho_m$ and $1/\rho_w$, have been eliminated to determine F and ρ_c .

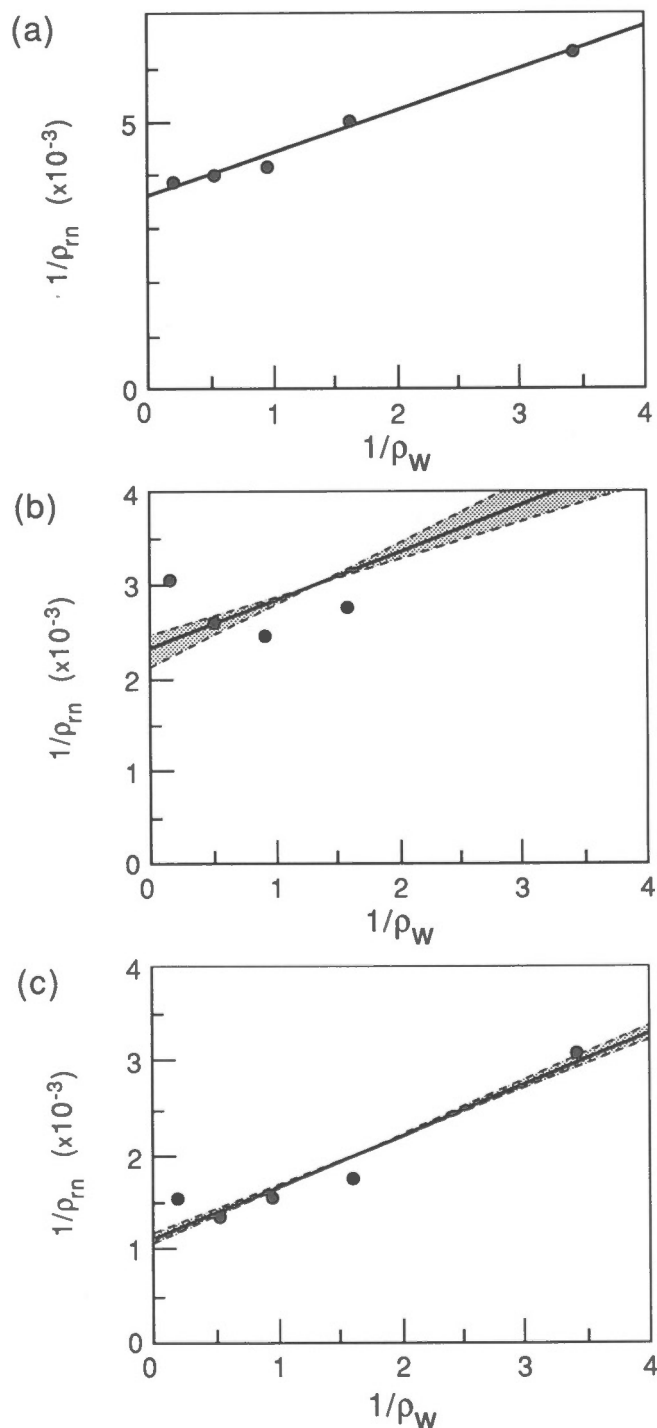
Bulk electrical resistivities (ρ_r) and pore surface resistivities (ρ_c) are listed in columns 3 and 4 of Table 4. Generally they show $\rho_r < \rho_c$, except for samples V-8, V-9, and V-10, thus raising concern about the accuracy of the formation factor (F) values for these three samples (4 specimens). Elimination of data points for low NaCl concentrations has not helped, as shown

Table 4. Final results for formation resistivity factor (F), surface resistivity (ρ_c) and bulk electrical resistivity (ρ_r) determinations, and a comparison with previous formation resistivity factor (F) values (Katsube et al., 1991).

Sample	F (1988)	ρ_r ($\Omega\text{-m}$) (1994)	ρ_c ($\Omega\text{-m}$) (1994)	F (1994)
V-1/V	541	120	128 \pm 5	379 \pm 18
V-1/H	140	42	51 \pm 1	127 \pm 5
V-2	236	636	680 \pm 280	283 \pm 34
V-3*	209*	292*	310 \pm 50*	162 \pm 11*
V-4	452	579	781 \pm 160	167 \pm 3
V-5	1030	251	278 \pm 3	1289 \pm 3
V-6	17600	849	1034 \pm 120	1675 \pm 180
V-7	433	167	181 \pm 41	231 \pm 81
V-8,Q	305	384	339 \pm 100	311 \pm 50
V-8,S	241	186	148 \pm 27	304 \pm 60
V-9	1630	746	621 \pm 190	1464 \pm 630
V-10	343	214	133 \pm 19	227 \pm 27

* = Values obtained from Katsube and Scromeda (1993).

Figure 2. Typical examples of $1/\rho_m$ as a function of $1/\rho_w$ (Equation 1), showing good and poor linear relationships: (a) Example (sample V-5) of a good linear relationship existing between $1/\rho_m$ and $1/\rho_w$, with all 5 data points used to determine F and ρ_c . (b) Example (sample V-9) of a case where progressive deviation from linearity is seen with decreasing NaCl concentrations (decreasing $1/\rho_w$ values), and only the three data points with the larger values of $1/\rho_w$ have been used to determine F and ρ_c . (c) Example (sample V-6) of a case where two data points which slightly deviate from the linear relationship between $1/\rho_m$ and $1/\rho_w$ have been eliminated to determine F and ρ_c .



in Table 3. For example, although progressive elimination of the low concentration values for sample V-9 has resulted in a progressive increase of ρ_c , it has not reached a level that can satisfy $\rho_r < \rho_c$. In the cases of samples V-6 and V-7, data points other than those of the lowest NaCl concentrations have been eliminated (Table 4) due to their deviation from linearity. These deviations have been interpreted to be due to measurement error, a possibility that always exists. Results of the final determinations for ρ_c and F are listed in columns 4 and 5 of Table 4. They are the values from Table 3 determined from the least number of data points (lower and higher ρ_c values) in each case. The error ranges in these columns have been determined from the range of ρ_c and F values displayed in Table 3. The results of previous determinations (Katsube et al., 1991) are also listed in Table 4 for comparison.

DISCUSSION AND CONCLUSIONS

This study indicates that it was necessary to progressively eliminate the data points for low NaCl concentrations for some of the shale samples in order to satisfy the requirement that bulk electrical resistivity (ρ_p) be smaller than pore surface resistivity (ρ_s); that is $\rho_r < \rho_c$. As a result, most of the samples satisfied that requirement, thus suggesting that most of the formation resistivity factor (F) and pore surface resistivity (ρ_s) values are accurate and reliable. However, this was not possible for three samples, thus leaving the concern that these have accuracy problems. This effect is less significant for formation resistivity factor (F) values, which only results in the possibility of error ranges being larger than those listed in Table 4. However, the pore surface resistivity (ρ_s) values for the three samples (4 specimens) that do not satisfy the requirement are considered to be unreliable. One interpretation offered is that they are actually slightly larger than the bulk electrical resistivity (ρ_p) values, for reasons not yet understood. It is interesting that, according to Katsube et al. (1991), these three shale samples are the only ones in this set that show the existence (minor amounts) of kaolinite. In addition to data points eliminated for reasons previously given, data points (samples V-6 and V-7) that were interpreted to deviate from linearity because of measurement error were also eliminated in the F and ρ_c determination process. However, such cases were relatively rare in this study.

The F and ρ_c values obtained by this study are in the range of 120-1700 and 50-1000 Ω -m, respectively. The F values are similar to those previously published (Katsube et al., 1990, 1991) for this set of samples, as shown Table 4, and resemble those of sedimentary rocks (Keller and Frischknecht, 1966; Keller, 1982). Only one previous F value (sample V-6) shows an F value that is about 10 times that obtained by this study.

ACKNOWLEDGMENTS

The authors express their appreciation to Q. Bristow (Geological Survey of Canada, Ottawa) for critically reviewing this paper and for his constructive comments that have benefitted this paper.

REFERENCES

- Davis, J.C.**
1986: Statistics and Data Analysis in Geology; John Wiley & Sons, p. 200-204.
- Gauvreau, C. and Katsube, T.J.**
1975: Automation in electrical rock property measurements; in Report of Activities, Part A; Geological Survey of Canada, Paper 75-1A, p. 83-86.
- Katsube, T.J.**
1975: The electrical polarization mechanism model for moist rocks; in Report of Activities, Part C; Geological Survey of Canada, Paper 75-1C, p. 353-360.
1977: Electrical properties of rocks; in Induced Polarization for Exploration Geologists and Geophysicists; Short Course Presented by the University of Arizona, Tucson, March 14-16, p. 15-44.
1981: Pore structure and pore parameters that control the radionuclide transport in crystalline rocks; Proceedings of the Technical Program, International Powder and Bulk Solids Handling and Processing, Rosemont, Illinois, 394-409. (Available from: CAHNERS Exposition Group, 222 West Adams Street, Chicago, Illinois 60606 U.S.A.).
1991: Petrophysical characteristics of granites, shales and gabbros, and their significance in nuclear fuel waste containment; in Proceedings, 1991 Joint International Waste Management Conference, Volume 2, Seoul, Korea, p. 313-320.
1993: Nano pore transport mechanism of tight shales from the Scotian Shelf; in Current Research, Part D; Geological Survey of Canada, Paper 93-1D, p. 121-127.
- Katsube, T.J. and Agterberg, F.P.**
1990: Use of statistical methods to extract significant information from scattered data in petrophysics; in Statistical Applications in the Earth Sciences, (ed.) F.P. Agterberg and G.F. Bonham-Carter; Geological Survey of Canada, Paper 89-9, p. 263-270.
- Katsube, T.J. and Collett, L.S.**
1973: Measuring techniques for rocks with high permittivity and high loss; Geophysics, v. 38, p. 92-105.
- Katsube, T.J. and Salisbury, M.**
1991: Petrophysical characteristics of surface core samples from the Sudbury structure; in Current Research, Part E; Geological Survey of Canada, Paper 91-1E, p. 265-271.
- Katsube, T.J. and Scromeda, N.**
1993: Formation factor determination procedure for shale sample V-3; in Current Research, Part E; Geological Survey of Canada, Paper 93-1E, p. 321-330.
- Katsube, T.J. and Williamson, M.A.**
1994a: Shale petrophysics and basin charge modelling; in Current Research, Part D; Geological Survey of Canada, Paper 94-1D, p. 179-188.
1994b: Effects of diagenesis on shale nano-pore structure and implications for sealing capacity; in Clay Minerals (Proceedings of the Conference on Diagenesis, Overpressuring and Reservoir Quality), 25-26 March, 1993, Cambridge, England.
- Katsube, T.J. and Walsh, J.B.**
1987: Effective aperture for fluid flow in microcracks; International Journal of Rock Mechanics and Mining Sciences and Geomechanics Abstracts, v. 24, p. 175-183.
- Katsube, T.J., Best, M.E., and Mudford, B.S.**
1991: Petrophysical characteristics of shales from the Scotian shelf; Geophysics, v. 56, p. 1681-1689.
- Katsube, T.J., Murphy, T.B., Best, M.E., and Mudford, B.S.**
1990: Pore structure characteristics of low permeability shales from deep formations; in Proceedings of the 1990 Society of Core Analysts (SCA) 4th Annual Technical Conference, August 1990, Dallas, Texas, Paper SCA-9010, p.1-21.
- Katsube, T.J., Scromeda, N., and Williamson, M.**
1992a: Effective porosity of tight shales from the Venture Gas Field, offshore Nova Scotia; in Current Research, Part D; Geological Survey of Canada, Paper 92-1D, p. 111-119.
- Katsube, T.J., Williamson, M., and Best, M.E.**
1992b: Shale pore structure evolution and its effect on permeability; in Symposium Volume III of the Thirty-Third Annual Symposium of the Society of Professional Well Log Analysts (SPWLA), The Society of Core Analysts Preprints, Oklahoma City, Oklahoma, June 15-17, 1992, Paper SCA-9214, p. 1-22.

Keller, G.V.

1982: Electrical properties of rocks and minerals; in Handbook of Physical Properties of Rocks, Volume I (ed.) R.S. Carmichael; CRC Press, Inc., Florida, p. 217-293.

Keller, G.V. and Frischknecht, F.C.

1966: Electrical Methods in Geophysical Prospecting; Pergamon Press, New York, 517 p.

Patnode, H.W. and Wyllie, M.R.J.

1950: The presence of conductive solids in reservoir rocks as a factor in electric log interpretation; Transactions of the American Institute of Mining, Metallurgical and Petroleum Engineers, v. 189, p. 47-52.

Williamson, M.A.

1992: The subsidence, compaction, thermal and maturation history of the Egret Member source rock, Jeanne D'Arc Basin, offshore Newfoundland; Bulletin of Canadian Petroleum Geology, v. 40, no. 2, p. 136-150.

Williamson, M.A. and Smyth, C.

1992: Timing of gas and overpressure generation in the Sable Basin offshore Nova Scotia; Bulletin of Canadian Petroleum Geology, v. 40, no. 2, p. 151-169.

A tale of shale - stratigraphic problems in the Gander River map area, Newfoundland

K.L. Currie

Continental Geoscience Division

Currie, K.L., 1995: A tale of shale - stratigraphic problems in the Gander River map area, Newfoundland; in Current Research 1995-D; Geological Survey of Canada, p. 73-80.

Abstract: The ophiolitic Gander River Complex is imbricated with sedimentary cover of diverse derivations (Davidsville Group, Weirs Pond Formation) to record major shortening in post-Caradoc to pre-Llandovery time, contemporaneous to thrusting of the Hamilton Sound Group (volcanics plus Caradoc black shale and chert) over Davidsville Group. The Davidsville Group forms a turbiditic, fining-upward sequence without volcanic component emplaced on a continental slope or rise. The Indian Islands Group, a marine shelf assemblage unconformably overlying the Hamilton Sound and Davidsville groups, spans much of Silurian time. The Duder Complex, basement to the region between the Reach Fault and Dog Bay Line, forms an accretionary prism of early Silurian age in which blocks cannot be readily correlated with surrounding units. Redbeds of the Ludlow or younger Ten Mile Lake Formation postdate the Botwood Group, which is absent east of the Reach Fault.

Résumé : Le complexe ophiolitique de Gander River est imbriqué à une couverture sédimentaire de diverses origines (Groupe de Davidsville, Formation de Weirs Pond) indiquant un important raccourcissement du post-Caradocien au pré-Llandovérien, contemporain du chevauchement du Groupe de Hamilton Sound (volcanites, ainsi que schiste noir et chert caradociens) au-dessus du Groupe de Davidsville. Le Groupe de Davidsville forme une séquence turbiditique, à granodécroissance vers le haut, sans composante volcanique, déposée sur un talus ou glacis continental. Le Groupe d'Indian Islands, assemblage de plate-forme marine reposant en discordance sur les groupes de Hamilton Sound et de Davidsville, remonte pour la majeure partie au Silurien. Le Complexe de Duder, formant le socle de la région entre la faille de Reach et la ligne de Dog Bay, constitue un prisme d'accrétion du Silurien précoce dans lequel on ne peut établir une corrélation, à prime abord, entre les blocs et les unités avoisinantes. Les couches rouges de la Formation de Ten Mile Lake du Ludlowien ou d'une époque plus récente sont postérieures au Groupe de Botwood, qui est absent à l'est de la faille de Reach.

INTRODUCTION

A seminal geological map of Botwood map-area (NTS 2E) published by Williams (1964) established a stratigraphic framework for central Newfoundland still in use today. According to this synthesis, sedimentary strata faced west, away from the early Ordovician Gander River Ultramafic Belt (GRUB; now Gander River Complex) toward the Silurian rocks of central Newfoundland. As interpreted by subsequent workers (Kennedy and McGonigal, 1972; Blackwood, 1982), this implied that all Ordovician sedimentary strata above the Gander River Complex belonged to a single unit (Davidsville Group) conformably overlain by a single Silurian unit. A flaw in this scheme, little noted at the time, was the presence of two diverse Silurian sections, a marine shelf sequence (Indian Islands Group), and a red sandstone-terrestrial volcanic sequence (Botwood Group). Williams et al. (1993) pointed out that this relationship required a Silurian terrane boundary (Dog Bay Line), and that correlations of Ordovician strata across this line needed to be reconsidered. Strata of the Davidsville Group cannot all face west since isoclinal folding

is ubiquitous (Currie et al., 1979; Blackwood, 1982; Evans et al., 1992). The stratigraphy of the Davidsville Group may therefore be more complex than previously thought. This contribution reconsiders the stratigraphy of a key area of the Botwood map sheet, namely the Gander River map area (NTS 2E/2, Fig.1) in light of new data from a network of forest access roads which have uncovered numerous large, clean glaciated exposures.

Shales proved to be particularly difficult to correlate because evidence of facing rarely survives the intense cleavage ubiquitous in shales in this region and several shale units lithologically resemble each other. Interlayered shale and sandstone or siltstone also occur in several units. Remapping indicates that diverse shale and shale-containing units have been confused in the past. Stratigraphic nomenclature follows Williams et al. (1993) and Currie (in prep.). In general terms the units considered are the Davidsville Group (sedimentary cover to the ophiolitic Gander River Complex), the Hamilton Sound Group (a mafic volcanic-black shale and chert assemblage thrust eastward over the Davidsville Group in late Caradoc or Ashgill time), the Indian Islands Group a Silurian

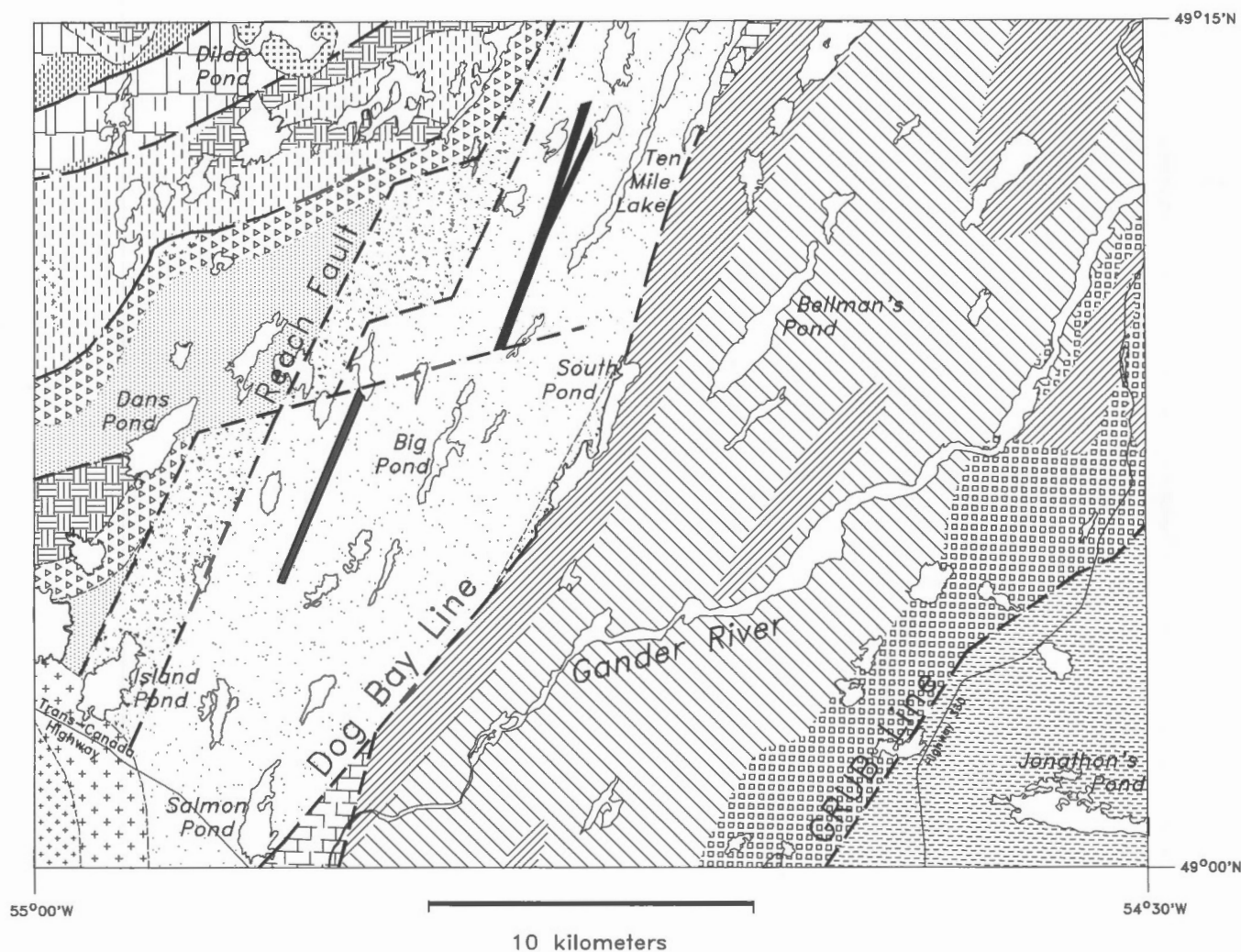


Figure 1. Simplified geological map of the Gander River map area (2E/2), Newfoundland.

marine shelf assemblage unconformably overlying the Hamilton Sound and Davidsville groups, the Exploits Group (a turbidite-mafic volcanic-chert-black shale assemblage), the Botwood Group (a continental to shallow marine volcanic-red sandstone association), and the Duder Complex (tectonites which separate the Botwood and Indian Island groups along the Dog Bay Line).

DESCRIPTIONS OF UNITS

Davidsville Group

The Davidsville Group comprises clastic sedimentary rocks whose base rests directly on the Gander River Complex, an ophiolitic allochthon emplaced in early Arenig time (Colman-Sadd et al., 1992). The stratigraphy of the

LEGEND FOR GANDER RIVER MAP-AREA

JURASSIC



pegmatitic hornblende-biotite gabbro

LATE SILURIAN
AND DEVONIAN

MOUNT PEYTON IGNEOUS COMPLEX



granite, granodiorite, granophyre



gabbro, diorite



mafic dikes

SILURIAN
Ludlow



TEN MILE LAKE FORMATION; red shale, cross-bedded sandstone and siltstone

West of Dog Bay Line

East of Dog Bay Line

Llandovery-
Wenlock



WIGWAM FORMATION; grey-green to buff micaceous sandstone and siltstone



INDIAN ISLANDS GROUP; limestone breccia, limy siltstone, gray to red shale



LAWRENCETON FORMATION; basalt, interflow red siltstone; ignimbrite

Ashgill?



DUDER COMPLEX; intensely fissile shale and siltstone with sparse large blocks of volcanic, plutonic and sedimentary rocks

BADGER GROUP



turbiditic conglomerate and pebbly greywacke



turbiditic greywacke and sandstone

EXPLOITS GROUP

Caradoc



BAYTONA FORMATION; graphitic black Mn-shale and chert; multicoloured chert

Llanvirn
-Llandeilo



LOON HARBOUR VOLCANICS; basalt breccia and agglomerate; tuff, greywacke

DAVIDSVILLE GROUP



HUNTS COVE FORMATION; gray and green shale, siltstone-shale rhythmites



OUTFLOW FORMATION; turbiditic sandstone and conglomerate; (includes undifferentiated BARRYS PONDS FORMATION)

Arenig

Tremadoc



GANDER RIVER COMPLEX; ultramafic rocks, mafic volcanics, trondhjemite, plagioclase porphyry



GANDER GROUP; grey-green feldspathic sandstone; minor dark shale toward the top (west)

— fault

--- geological contact ---

Davidsville Group has been a problem since its original (unsatisfactory) definition by Kennedy and McGonigal (1972) because it consists largely of homogeneous, dark grey shale whose intense cleavage masks isoclinal folding and fault imbrication, both of which are known to be present from favourable exposures. Pickerill et al. (1979) divided the group into six mappable units, but were unable to propose a stratigraphy. O'Neill and Blackwood (1989) informally divided the group into a basal Weirs Pond Formation, a medial Hunts Cove Formation of shale rhythmites and an upper Outflow Formation with sandstone and pebble conglomerate interlayered with shale rhythmites. Currie (1992, in prep.) pointed out that "Weirs Pond Formation" as used by O'Neill and Blackwood (1989) includes two diverse units, namely a calcareous quartz sandstone, limestone and limy shale unit accumulated on a stable marine shelf, and turbiditic conglomerate ranging from basal brecciated Gander River Complex with minor sedimentary infilling to upper pebbly or granule sandstone interbedded with greenish shales. The name Weirs Pond Formation is here restricted to the marine shelf sequence which forms an exotic fragment (Currie, 1992, in prep.) and the name Barrys Ponds formation (Currie, 1992) is used for the breccia and conglomerate. The Outflow Formation of O'Neill and Blackwood (1989) overlies the Barrys Ponds formation, but underlies the Hunts Cove Formation. This relation can be observed at numerous localities, but is strikingly well exposed at the type locality of the Outflow Formation on the east side of The Outflow of Gander Lake (gridref 561239, NTS 2D/15), on the Trans-Canada Highway (gridref 598252, 2D/15), on Highway 330 (gridref 843537, 2E/1) and on a woods road near South Pond (gridref 619381). The stratigraphy of the Davidsville Group used in this report is therefore, from the bottom up, Barrys Ponds formation (informal), Outflow Formation, Hunts Cove Formation.

The Barrys Ponds formation outcrops sporadically along and within the western margin of the Gander River Complex from Barrys Ponds (gridref 915584, 2E/1 and 2E/8) as far as Gander Lake, and consists of brecciated Gander River Complex with sedimentary infilling (sand, pebble conglomerate) grading into coarse clast to matrix-supported conglomerate with clasts of Gander River Complex in a serpentine and chromite-bearing matrix. The thickness of the formation varies rapidly due to both depositional factors and tectonic excision. Relations can be examined along Highway 330 north of Gander where the formation is folded into (and with) the Gander River Complex (gridref 817482), fault imbricated with the complex (828506) and (gradationally) above the complex (842531). The observed thickness varies from 0 to 260 m.

The Outflow Formation overlies the Barrys Ponds formation above an abruptly gradational contact, although this contact is nowhere well exposed. The best relations are observed along Highway 330 near gridrefs 842531 and 817482. The lower part of the Outflow Formation comprises thick bedded (30-100 cm) pebble to cobble conglomerate grading upward to sandstone. Serpentine pebbles are characteristic of this lower part, but the bulk of the debris is everywhere felsic, mainly blue quartz, porphyry, and grey feldspathic psammite clasts. Bed thickness and grain size decrease upward. Much of the formation has bed thicknesses

of 5-10 cm, with graded pebble to granule sandstone in the lower part and parallel-laminated sandstone grading to grey-green siltstone-shale laminae in the upper part. Thick (to 1.5 m) beds of graded or massive sandstone occur rarely in the upper part of the formation. There is complete gradation from Outflow Formation to Hunts Cove Formation by thinning of beds and increase in proportion of siltstone-shale rhythmites. I have arbitrarily defined a boundary at 25 per cent sandstone, which corresponds to an average bed thickness of about 3 cm. This criterion permits confident assignment of even reasonably small outcrops. The apparent thickness of the Outflow Formation varies from a minimum of about 60 m along Highway 330 (where the base of the formation is faulted off), to almost 500 m on the west shore of Gander Bay (where small folds are present in the section). Based on measured sections and map patterns, the best estimate for the thickness of the formation is 200-300 m.

According to O'Neil and Blackwood (1989), the Hunts Cove Formation includes the "shale" portion of the Davidsville Group. This covers a considerable variety of lithologies ranging from siltstone and mudstone rhythmites through mudstone-shale rhythmites to several varieties of shale. The formation could possibly be formally subdivided but this is not attempted here. The base of the Hunts Cove Formation can be examined along the Trans-Canada Highway, Highway 330 and on various woods roads north and south of Bellmans Pond. Close to the Gander River Complex the basal facies is a pale green mudstone bedded on a centimetre scale which contains sporadic pale purple intervals up to a metre thick. West of Gander River the basal facies is pale grey mudstone-shale rhythmites with centimetre-scale beds grading from basal mudstone to darker grey shale. Both facies contain within them occasional massive sandstone beds 2 to 65 cm thick. The upper part of the formation consists of homogeneous dark grey shale, commonly intensely cleaved. Rare exposures in fold cores preserve cleavage-bedding relations, showing that beds were 5 to 20 cm thick. The distribution of the Outflow Formation, combined with cleavage-bedding relations from favourably oriented roadcuts, gives the gross fold structure. Dividing the width of synclines in shale by two suggests the thickness of the Hunts Cove Formation does not exceed 1000 m. It could be less because of undetected folds, but it could also be greater because the top of the formation has nowhere been observed. Assuming a thickness of 1000 m, the total thickness of the Davidsville Group is about 1300 to 1400 m.

The age of the Davidsville Group is not directly known since it is unfossiliferous. (All fossil localities formerly attributed to the "Davidsville Group" in fact date the Weirs Pond Formation or the Main Point Formation of the Hamilton Sound Group.) However its age is constrained between the Arenig obduction of the Gander River Complex (Colman-Sadd et al., 1992) and the Llandovery age of the overlying Indian Islands Group. The late Arenig-Llanvirn ages of fossils from the Weirs Pond Formation probably also date the Davidsville Group, because both both form a sedimentary cover on the Gander River Complex. An upper age limit is established by the late Caradoc or Ashgill arrival of the Hamilton Sound Group.

The Davidsville Group forms a simple fining-upward turbiditic sequence with no volcanic component, not even such distal precursors as chert or coticles. There are no mass slumping deposits such as olistostromes. Pickerill et al. (1979) suggested that the fine rhythmites of the Hunts Cove Formation are contourites. The Davidsville Group is interpreted to have accumulated on a relatively stable continental slope or rise environment far from volcanic activity. Most of the Davidsville Group exhibits a single period of tight to isoclinal, upright folds plunging gently either to north or south. Asymmetric folds up to 2 m in amplitude plunge down the dip within a few hundred metres of major faults. Such folds are interpreted to show the sense of transcurrent motion on the faults. Complex folding (involving downward-facing folds and at least four periods of folding (Piasecki, 1992)) immediately south of the Hamilton Sound Group is presumed caused by emplacement of the allochthonous Hamilton Sound Group.

Hamilton Sound Group

The Hamilton Sound Group comprises an assemblage of graphitic, manganiferous pyrite-rich black graptolitic shale and chert (Main Point Formation), basaltic pillows, agglomerate, tuff and conglomerate (Noggin Cove Formation) and black and white centimetre-scale siltstone rhythmites rich in vermicular coticles (Woody Island Formation). The correct ordering of these units is not known from field observations because of complex internal faulting and folding of the units (Johnston, 1992), and the obscuring of most contacts by igneous intrusion. The general assemblage however is identical to parts of the Exploits Group to the west, and the Main Point Formation has yielded a mid-Caradocian *D. clingani* zone assemblage identical to the black shale capping the Exploits Group (Williams, 1972).

Rocks of the Hamilton Sound Group were originally lumped with the Davidsville Group (Williams, 1964; Kennedy and McGonigal, 1972; Currie et al., 1980; O'Neill and Blackwood, 1989) on the basis that the shales and siltstones are similar. However the overall character of the rocks is quite different, since the Hamilton Sound Group is rich in volcanically derived material. The Davidsville Group lacks chert and the coal-black graphitic, sulphidic shale typical of the Main Point Formation. Coticles are unknown in the Davidsville Group. The structure of the Hamilton Sound Group is also substantially more complex than that of the Davidsville Group. Johnston (1992) and Piasecki (1992) have identified four periods of folding in these rocks, and fault imbrication is clearly significant, although identification of particular faults is difficult because of poor inland exposure and the high proportion of intrusive rocks in this region.

The Hamilton Sound Group is fringed by the Carmanville Mélange consisting of decametre-scale blocks of volcanic rocks of the Noggin Cove Formation and ultramafic rocks of the Gander River Complex, as well as various other lithologies of uncertain derivation, all in a matrix largely derived from the Main Point Formation. The Hamilton Sound Group is presently interpreted as broadly correlative to the Exploits

Group, emplaced by east or southeast thrusting in post-Main Point pre-Indian Island time (late Caradoc-Ashgill) by sliding on a film of Carmanville Mélange (Currie, in prep.).

Another similar allochthon is well exposed in a quarry near Glenwood (gridref 561269, 2D/15) where the Outflow Formation is faulted over bedded black chert and shale (Main Point Formation). The north-trending bounding fault can be traced north for 8 km to the Dog Bay Line. On the east side of the Gander River at the Trans Canada Highway it separates granule sandstone of the Outflow Formation from siltstone of the Indian Islands Group (Fig.2). A west-southwest-trending fault separating black chert from Hunts Cove Formation is exposed on the west shore of The Outflow near 557254. Mélange has not been observed associated with this allochthon, but the southern boundary fault has an unusually broad zone of breccia (>50 m) which may represent remains of a tectonic melange. Strikes within the allochthon are roughly east-west, perpendicular to the strike of the Outflow Formation.

Indian Islands Group

The Indian Islands Group forms a Silurian marine shelf assemblage found as isolated fragments along the east side of the Dog Bay Line (Williams et al., 1993). The group rests unconformably on the Hamilton Sound Group (Williams et al., 1993), but contact with the Davidsville Group has only been observed along high-angle east-over-west faults.

The Indian Islands Group consists of discontinuous basal limestone or limestone breccia (Seal Island Formation) grading up into calcareous siltstone (Charles Cove Formation) and eventually into shale (Horwood Formation). The basal limestone may be reduced to jumbled metre-scale slabs, as at Seal Island (gridref 844788 2E/8) or form a coherent, distinctively vuggy buff limestone and limy shale horizon as at Salmon River (gridref 539293). In either case the formation is thin, not more than 10 m thick, and may be absent. Where present it is richly fossiliferous with a Llandovery coral (*Halysites*) and brachiopod fauna. The Seal Island Formation is conformably overlain by the Charles Cove Formation, greenish grey, hard calcareous siltstone bedded on a scale of 5 to 10 cm with a low tenor of limestone lenses 1 to 5 cm thick and up to 50 cm long. Outcrops of this formation have in the past been incorrectly assigned both to the Botwood Group and to the Outflow Formation. The limestone lenses are distinctive where present. The formation is distinguished from the Outflow Formation by lack of grading, and uniform silty composition, and from (most of) the Wigwam Formation by lack of mica. A Wenlock fossil was recovered from the Charles Cove Formation by Wu (1979) north of the mapped area. The thickness of the Charles Cove Formation is uncertain because folding is difficult to detect. An apparent thickness of 1200 m on the Salmon River appears to represent a single fold, suggesting a minimum thickness of about 600 m. The upper unit of the Indian Islands Group, the Horwood Formation comprises grey shale with distinctive millimetre-scale buff siltstone beds. This unit occurs near Horwood (grid ref 768768), and near Glenwood (gridref 528270). The formation is thin, about 20-50 m, grading upward into red shale and

siltstone of the Ten Mile Lake Formation which oversteps the Dog Bay Line (Fig. 2, see also Currie, 1993). The Indian Islands Group exhibits a single period of close upright folding identical in style to the Davidsville Group.

Miscellaneous sedimentary relicts in the Gander River Complex

As noted above, the Weirs Pond Formation comprises fossiliferous limestone, limy shale, and orthoquartzite of late Arenig to Llanvirn-Llandeil age (compare Blackwood, 1982; O'Neill, 1991) occurring as a series of fault slivers within the Gander River Complex and stretching from Gander Lake more than 100 km to the northeast. None of the slivers is more than a few tens of metres thick, and the longest is about 2 km. Unconformable contacts on the Gander River Complex are exposed at Weirs Pond (O'Neill, 1991) and Cuff Pond (Currie et al., 1979), but these occurrences are bounded on both sides by the Gander River Complex. In general the Weirs Pond Formation is notably less cleaved and deformed than nearby Davidsville Group strata.

In addition to the Weirs Pond Formation, black shale and siltstone, possibly of several ages, are found within the Gander River Complex. Graptolitic Caradoc black shale occurs on Weirs Pond (O'Neill, 1991). Black shale and siltstone of unknown affinity occur along Highway 330 (gridref 689451), and at several locations on woods roads. None of these occurrences is more than a few metres thick or a few tens of metres in length. Like the Weirs Pond Formation, they are bounded on both sides by the Gander River Complex. Similar enclaves of Barrys Ponds and Outflow formations occur within the Gander River Complex

Duder Complex

The Duder Complex (Currie, 1993), which may underlie all of the area between the Dog Bay Line and the Reach Fault, comprises a variably tectonized shale and siltstone matrix with tectonic inclusions of sedimentary and igneous rocks ranging from centimetre size to mappable blocks tens or hundreds of metres across, all oriented with strike roughly parallel to cleavage. The matrix of the Duder Complex ranges from pale grey-green homogenous mudstone, whose strong cleavage is not apparent on glaciated surface, to intensely

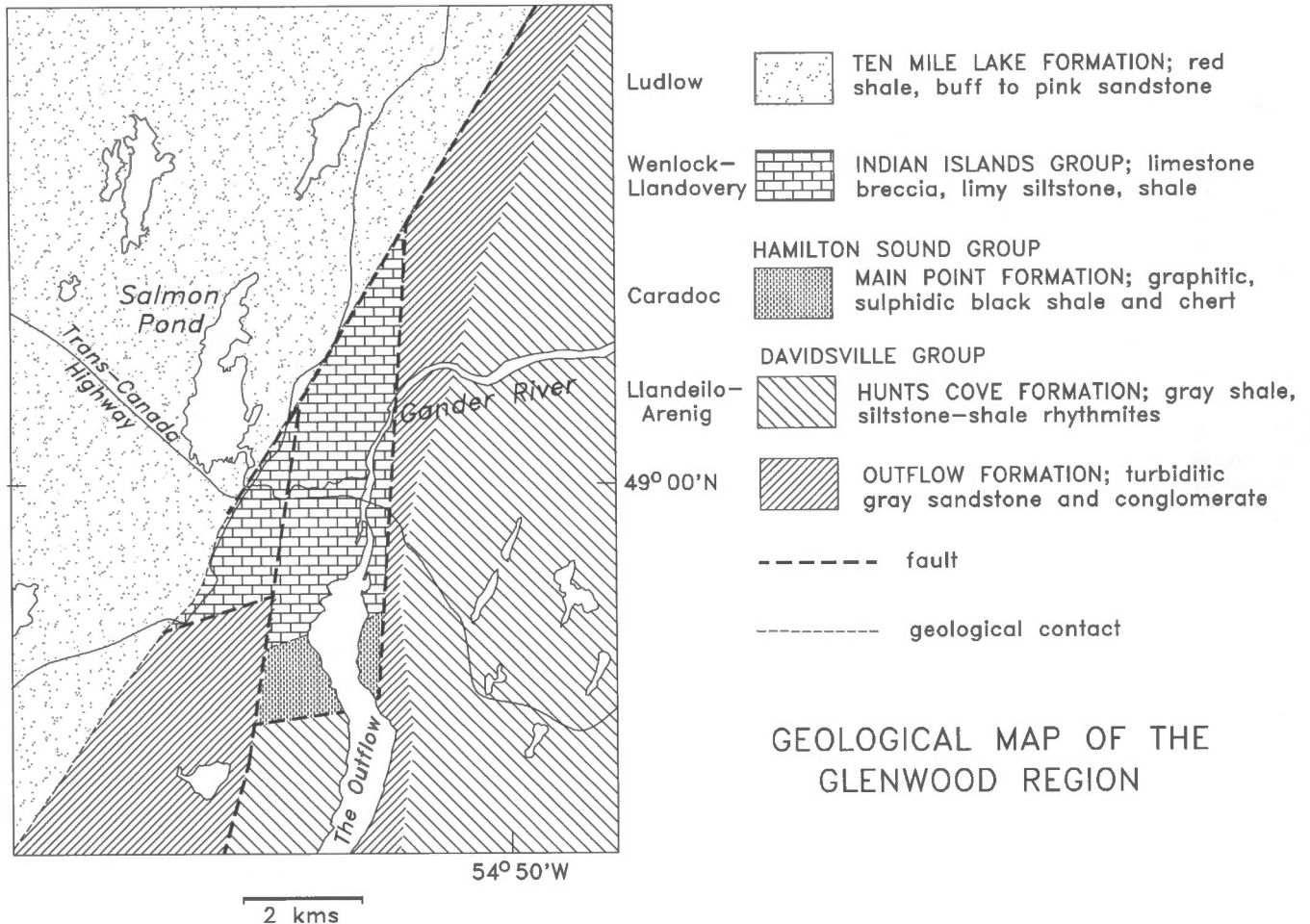


Figure 2. Geological map of the Glenwood region, central Newfoundland. The town of Glenwood lies on the west side of the Gander River south of the Trans-Canada Highway.

cleaved dark grey to black shale and siltstone which typically exhibits manganese mirror or pyrolusite dusting on cleavage surfaces. Igneous blocks include gabbro, pillow lava (at 535444 and 556454) and salic volcanics (615403), while sedimentary blocks include turbiditic siltstone and sandstone with olistostrome beds, coarse conglomerate with granodiorite boulders and thin limestone. The derivation of these blocks is uncertain. Preliminary chemical analyses of the igneous rocks (unpublished data) do not resemble igneous rocks of the Exploits or Botwood groups, but are more closely comparable to analyses of older arc volcanics published by Swinden et al. (1990). Some sedimentary blocks resemble parts of the New Bay Formation of the Exploits Group. A few conglomerates could derive from the Badger Group.

The matrix of the Duder Complex was in the past identified with the Botwood Group (compare Fig. 1 with Evans et al., 1992), while the larger blocks were identified as dykes, or correlated with various units of the Exploits Group. The matrix can be distinguished from the Botwood Group by intense cleavage and total lack of sedimentary features. The presence of inclusions is an unmistakable, but relatively rare identifier.

The Duder Complex is a major tectonic complex bounded by a terrane boundary on one side (Dog Bay Line) and by a fault (Reach Fault) on the other. Williams et al. (1993) and Currie (in press) gave reasons for assuming significant west-directed late Ordovician and Silurian subduction along the Dog Bay Line. Accepting this model strongly implies that the Duder Complex forms an accretionary wedge prism on the hanging wall of this subduction zone.

Botwood Group and Ten Mile Lake Formation

According to the standard stratigraphy (Williams, 1972), the lower Silurian Botwood Group comprises basal volcanics (Lawrenceton Formation) overlain by micaceous sandstone with subordinate shale and siltstone (Wigwam Formation). The volcanics are unmistakable where well exposed. Basalt flows display amygdaloidal bases and slaggy red tops with red interflow siltstone. Ignimbritic rhyolite occurs to the west and north of the map area. The Wigwam Formation, olive-green to buff, fine grained micaceous sandstone, commonly weathering a pale rusty shade, and minor greenish shale, is poorly exposed in the map area.

Between the Reach Fault and the Dog Bay Line a sequence of bright red to purple shale and siltstone with subordinate sandstone has traditionally been assigned to the Botwood Group (Evans et al., 1992). However the Lawrenceton Formation does not occur in this area and the lithology of the redbeds is atypical of the Wigwam Formation. Both north and south of the map area (near gridrefs 717667 and 533277 respectively) the redbeds can be traced across the Dog Bay Line where they conformably overlie middle to late Silurian strata (Boyce and Ash, 1994) of the Indian Islands Group. Because of these anomalies Currie (1993) assigned the redbeds to the Ten Mile Lake Formation of presumed Ludlow or Pridoli age. Commonly the redbeds exhibit only open folding, but strong cleavage and deformation occurs near the Reach Fault.

Evans et al. (1992) noted a region of grey, homogeneous sandstone near Island Pond, and depicted a north-northeast-trending gradational contact within the Botwood Group separating redbeds from grey beds. Additional mapping suggests this boundary is sharp, presumably faulted, separating grey micaceous sandstone and pebbly sandstone from a red shale-dominated sequence (Ten Mile Lake Formation). The sandstone somewhat resembles Wigwam Formation, but volcanics (Lawrenceton Formation) are absent, and the sandstone does not weather to the usual buff shade. At least two metre-scale volcanic blocks occur within it, indicating that it forms part of the Duder Complex.

DISCUSSION

The major stratigraphic observations and conclusions resulting from this restudy of the Gander River map area may be stated in point form as follows.

1. The Gander River Complex is extensively imbricated with sedimentary cover of Davidsville Group and Weirs Pond Formation derivation, units which were deposited far apart, and hence records major shortening in post-Caradoc to pre-Llandovery time.
2. The Davidsville Group forms a continentally derived, turbiditic, fining-upward sequence without volcanic component emplaced on a relatively stable continental slope or rise.
3. The Hamilton Sound Group and correlative strata to the south form allochthons thrust over the Davidsville Group in post-Caradoc to pre-Llandovery time. The stratigraphy of these slices suggests that they were derived from the Exploits Group or correlative strata.
4. The Indian Islands Group forms a marine shelf assemblage unconformably overlying the Hamilton Sound and Davidsville groups, and spanning much of Silurian time.
5. The Duder Complex forms basement to the region between the Reach Fault and Dog Bay Line. The position and character of the complex suggest that it is an accretionary prism of early Silurian age. Blocks in this mélange cannot be readily correlated with surrounding units.
6. Redbeds of the Ludlow or younger Ten Mile Lake Formation are younger than the Llandovery Botwood Group. Typical Botwood Group (volcanics plus micaceous sandstone) is not present east of the Reach Fault in Gander River map area. Micaceous sandstones in the southwest corner of the area form part of the Duder Complex.

The stratigraphy outlined above has been used (Currie, in prep.), to support a model in which the Gander River Complex represents a relict of the eastern part of the Lower Paleozoic Iapetus Ocean obducted eastward onto the Avalonian margin in lower Arenig time (Colman-Sadd et al., 1992). After a polarity flip, eastward subduction of Iapetus built a volcanic arc west of the area now considered (Swinden et al., 1990) while the Davidsville Group began accumulating between the arc and the continent to the east. In late Arenig time the

volcanic arc rifted (Swinden et al, 1990) leading to formation of the Dunnage Mélange (Williams, 1994) and Exploits Group (O'Brien, 1993). By late Caradoc to Ashgill time development of the rift basin ceased, and tectonic inversion commenced, as evidenced by deposition of coarse and coarsening-upward clastics (Badger Group, Williams et al., 1993) presumably due to arrival of Laurentia, or some fragment of it at the subduction zone. The eastern part of the Exploits Basin was thrust eastward over the Davidsville Group to form the Hamilton Sound Group, and the Davidsville Group and Gander River Complex were imbricated. During Llandovery-Wenlock time the floor of the basin in which the Exploits Group had accumulated was consumed by westward subduction on the Dog Bay Line creating the Duder Group as an accretory prism while the Indian Islands Group accumulated on the eastern passive margin and the Botwood Group on the active western margin. Continent-continent collision occurred in Wenlock or Ludlow time. Following a hiatus in Ludlow time, during which the Ten Mile Lake Formation sedimented across the Dog Bay Line, all rocks were deformed, metamorphosed and intruded during climactic Late Silurian- Devonian events.

REFERENCES

- Blackwood, R.F.**
1982: Geology of the Gander Lake (2D/15) and Gander River (2E/2) area, Newfoundland; Newfoundland Mineral Development Division, Report 82-4, 56 p.
- Boyce, W.D. and Ash, J.S.**
1994: New Silurian-Devonian(?) faunas from the Gander (NTS 2D/15) and Botwood (2E/3) map areas; Newfoundland Department of Mines and Energy, Geological Surveys Branch, Report 94-1, p. 53-64.
- Colman-Sadd, S.P., Dunning, G.R., and Dec, T.**
1992: Dunnage-Gander relationships and Ordovician orogeny in central Newfoundland; a sediment provenance and U/Pb age study; *American Journal of Science*, v. 292, p.317-355.
- Currie, K.L.**
1992: A new look at Gander-Dunnage relations in Carmanville map-area, Newfoundland; *in* Current Research, Part D; Geological Survey of Canada, Paper 92-1D, p. 27-33.
1993: Ordovician-Silurian stratigraphy between Gander Bay and Birchy Bay, Newfoundland; *in* Current Research, Part D; Geological Survey of Canada, Paper 93-1D, p. 11-18.
- Currie, K.L., Pajari, G.E., and Pickerill, R.K.**
1980: Carmanville map-area, Newfoundland (2E/8); Geological Survey of Canada, Open File 776.
- Currie, K.L., Pickerill, R.E., and Pajari, G.E.**
1979: Tectono-stratigraphic problems in the Carmanville area, northeastern Newfoundland; *in* Current Research, Part A; Geological Survey of Canada, Paper 79-1A, p. 71- 76.
- Evans, D.T.W., Hayes, J.P., and Blackwood, R.F.**
1992: Gander River; Newfoundland Geological Surveys Branch, Map 92-21.
- Johnston, D.**
1992: The Noggin Cove Formation, Carmanville area, northeastern Newfoundland: a back-arc volcanic complex; *in* Current Research, Part E; Geological Survey of Canada, Paper 92-1E, p. 249-257.
- Kennedy, M.J. and McGonigal, M.H.**
1972: The Gander and Davidsville groups of northeastern Newfoundland; new data and geotectonic implications; *Canadian Journal of Earth Sciences*, v. 9, p. 452-459.
- O'Brien, B.H.**
1993: A mappers guide to Notre Dame Bay's folded thrust faults: evolution and regional development; Newfoundland Department of Mines and Energy, Geological Surveys Branch, Report 93-1, p. 279-291.
- O'Neill, P.P.**
1991: Geology of the Weirs Pond area, Newfoundland (NTS 2E/1); Newfoundland Department of Mines and Energy, Geological Surveys Branch, Report 91-3, 144 p.
- O'Neill, P.P. and Blackwood, R.F.**
1989: A proposal for revised stratigraphic nomenclature of the Gander and Davidsville groups and the Gander River ultrabasic belt of northeastern Newfoundland; Newfoundland Department of Mines and Energy, Mineral Development Division, Report 89-1, p. 127-130.
- Piasecki, M.A.J.**
1992: Tectonics across the Gander-Dunnage boundary in northeastern Newfoundland; *in* Current Research, Part E; Geological Survey of Canada, Paper 92-1E, p. 259-268.
- Pickerill, R.K., Pajari, G.E., and Currie, K.L.**
1979: The nature, origin and significance of the Carmanville ophiolitic melange, northeastern Newfoundland; *Canadian Journal of Earth Sciences*, v. 16, p. 1439-1451.
- Swinden, H.S., Jenner, G.A., Fryer, B.J., Hertogen, J., and Roddick, J.C.**
1990: Petrogenesis and paleo-tectonic history of the Wild Bight Group, an Ordovician rifted island arc in central Newfoundland; *Contributions to Mineralogy and Petrology*, v. 105, p. 219-241.
- Williams, H.**
1964: Botwood, Newfoundland (2E); Geological Survey of Canada, Map 60-1963.
1972: Stratigraphy of Botwood map-area, northeastern Newfoundland; Geological Survey of Canada, Open File 113, 103 p.
1994: The Dunnage Melange, Newfoundland, revisited; *in* Current Research 1994-D; Geological Survey of Canada, p. 23-32.
- Williams, H., Currie, K.L., and Piasecki, M.A.J.**
1993: The Dog Bay Line : a major Silurian tectonic boundary in northeast Newfoundland; *Canadian Journal of Earth Sciences*, v. 29, p. 2481-2494.
- Wu, T.W.**
1979: Structural, stratigraphic and geochemical studies in the Horwood Peninsula-Gander Bay area, northeastern Newfoundland; MSc. thesis, Brock University, Saint Catherines, Ontario, 183 p.

Geological Survey of Canada Project 730044

The Plage-Charron, Quebec, landslide of August 5, 1994

J.M. Aylsworth, D.E. Lawrence, and J.A. Traynor
Terrain Sciences Division

Aylsworth, J.M., Lawrence, D.E., and Traynor, J.A., 1995: The Plage-Charron, Quebec, landslide of August 5, 1994; in Current Research 1995-D; Geological Survey of Canada, p. 81-86.

Abstract: On August 5, 1994, a landslide involving approximately 5000 m³ of Leda clay occurred along the Ottawa River at Plage-Charron, south of Eardley, Quebec. The failure followed an extreme precipitation event in a year when precipitation was well above normal values. It is the most recent in a series of relatively small landslides that occur at a frequency of about one per year along an arcuate, 1.6 km long bluff in Champlain Sea clays. The landslide is described, a history of regular slope failure along the bluff is documented, and factors of safety are estimated for the slope.

Résumé : Le 5 août 1994, un glissement de terrain a entraîné environ 5 000 m³ d'argile à Leda le long de la rivière des Outaouais à Plage-Charron, au sud d'Eardley (Québec). La rupture a eu lieu après un période de précipitations extrêmes alors que les précipitations de l'année étaient déjà au-dessus des valeurs normales. Il s'agit du plus récent d'une série de glissements de terrain relativement petits qui se sont produits à une fréquence d'environ un par année le long d'une longue falaise arquée de 1,6 km dans des argiles de la Mer de Champlain. Le glissement de terrain est décrit, l'historique des ruptures de pente survenues le long de la falaise est documenté et des facteurs de sécurité sont estimés pour la pente.

INTRODUCTION

In the first few hours of August 5, 1994, a landslide occurred on the north shore of the Ottawa River, about 2 km south of the village of Eardley, Quebec, at Plage-Charron (Lat. 45°32'N; Long. 76°06'W) (Fig. 1).

The landslide, about 70 m long and 35 m wide at its widest point, involved approximately 5000 m³ of material. It took place on a 12 m high slope in Champlain Sea clay. Its full extent could not be accurately determined as the debris extended into the Ottawa River.

No one observed the event; however, a local cottage resident, living less than 50 m from the slide, reported that her dog was barking around midnight on August 4th or early August 5th. She investigated on several occasions but failed to determine what was upsetting the animal. The landslide was discovered later the same day.

There were no injuries or damaged buildings as a result of the landslide, however the slide scarp comes within 15 m of a summer cottage on an adjacent property. This building has been declared unfit for human habitation by the local municipal authority because of the risk of further slope movement, effectively destroying the value of the property.

SITE

The landslide occurred on a steep bank at the head of a large oval embayment in the north shore of the Ottawa River (Fig. 1). A 10-12 m high clay bluff, scalloped by scars of numerous small landslides, begins 0.25 km west of the recent failure and extends 1.6 km eastward along the shore of the bay. Above the bluff, flat farmland extends 1.5 km back from the river.

Although most of the area adjacent to the bluff consists of agricultural fields, three cottages are located immediately west of the landslide and approximately 15 m back from the edge of the bluff. A slightly elevated (0.3-1 m) gravel lane, 35 m behind the bluff, parallels the back of the cottage properties. The lane and a shallow ditch, dug parallel to the

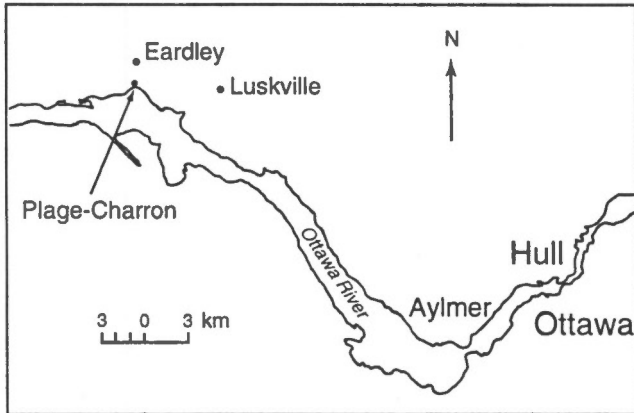


Figure 1. Location map.

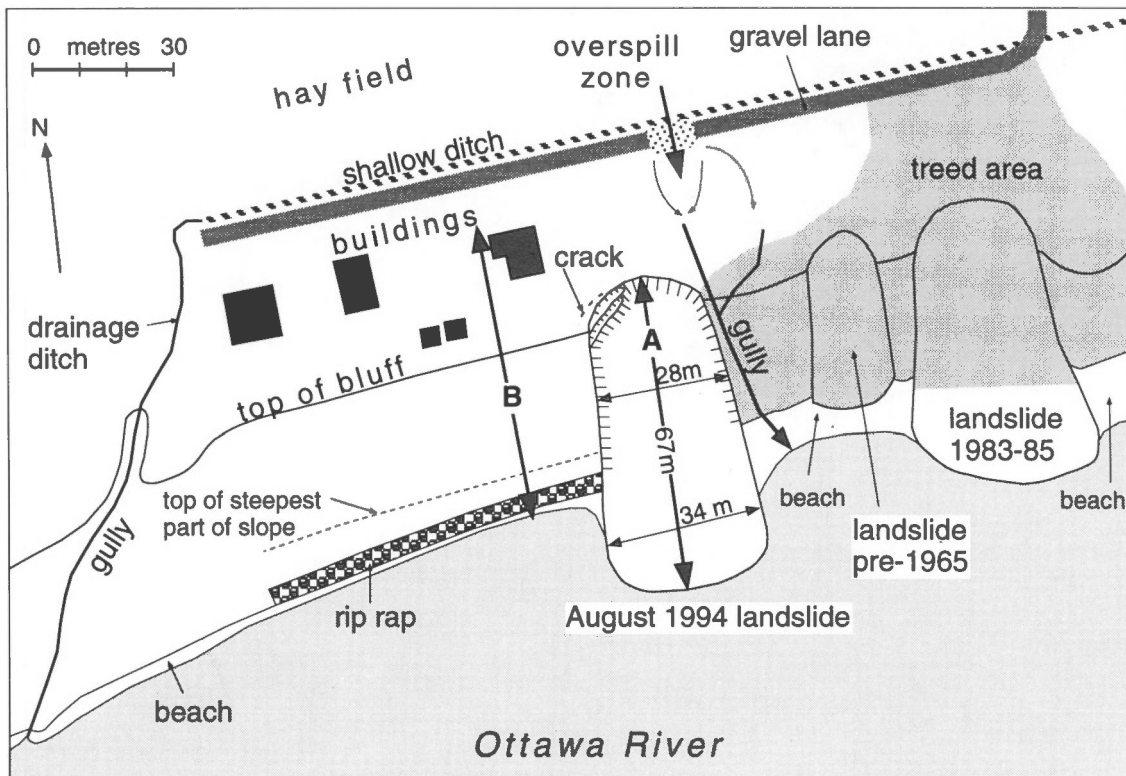


Figure 2. Site map. Profiles shown in Figure 6 are located at 'A' (landslide profile) and 'B' (undisturbed slope profile).

lane on the north side, intercept drainage from the fields behind (Fig. 2). Opposite the eastern side of the recent landslide scarp, a low zone in the lane directed overflow from the field towards the bluff and into a small gully 1-3 m east of the failure. A larger gully to the west of the cottages has been extended back to the lane by a shallow ditch in an effort to direct drainage from the field away from the cottages.

Riprap was placed at the base of the bluff below the cottage properties in 1987 in an effort to stabilize the bank, in which small slumps had occurred in the 1980s. The recent failure lies just beyond the eastern end of the riprap and approximately 2 m from the property line of the most easterly of the cottages.

SURFICIAL GEOLOGY

Surficial sediments present in the region consist of deep-water deposits of the Champlain Sea — clay, silt, and silty clay — generally overlain by a veneer of silt or silty clay deposited in abandoned river channels following withdrawal of the sea (Richard et al., 1977). A major terrace scarp lying 1.5 to 2.0 km back from the river is lined with ancient landslide scars and deposits similar to those of the present scarp. Offshore, the shallow waters of the bay are underlain by acoustically layered clay (W.W. Shilts, pers. comm.). The mouth of the bay is marked by a sharp escarpment down to a deep channel scoured by drainage from Glacial Lake Agassiz and other glacial lakes (W.W. Shilts, pers. comm.).

The silty veneer is absent in the immediate vicinity of the landslide. Marine clay consists of red and blue-grey rhythmites. On the landslide scarp 10-15 cm of red clay layers alternate with 20-25 cm of grey clay layers, and the colour

change is gradational. The surface clay is very stiff and tends to fracture into blocks. Irregularly shaped, hard calcareous clay concretions are common.

Champlain Sea clays are commonly referred to as 'Leda clay' and are known to be particularly susceptible to flow failures. The term 'clay' refers not to clay mineralogy but solely to particle size. These sediments are derived from rock flour produced by glacial abrasion. They commonly exhibit high sensitivity related to high water content within the clay, the flocculated fabric of the clay particles, low electrical attraction between the particles, low overburden pressures during deposition of the clays, and postdepositional leaching of salts from the clays (Carson and Bovis, 1989). Upon disturbance, Leda clay loses most of its shear strength and a rapid earthflow may occur. Numerous landslides in the Ottawa Valley-St. Lawrence Lowlands have occurred within Leda clay sediments. Unlike some sensitive clay failures which completely remobilize, flowing great distances (i.e. 1993 Lemieux flow; Brooks et al., 1994), the flows near Plage-Charron are stiffer, forming a hummocky toe not far from the base of the slope.

LOCAL LANDSLIDE HISTORY

Regular airphoto coverage (1965, 1968, 1975, 1978, 1981, 1983, 1985, 1987, and 1990), much of it at a scale of 1:15 000, as well as verbal accounts by some cottage owners and observations by the authors, have facilitated reconstruction of the slope failure history since 1965 (Fig. 3). The 1965 photos reveal a bank scalloped by numerous landslide scars, four of which seem to have occurred a few years prior to 1965. Twenty-four failures of various sizes have occurred between 1965 and 1987, on average one per year. Small failures on the 1983 photos had either continued to retrogress or were reactivated into larger failures

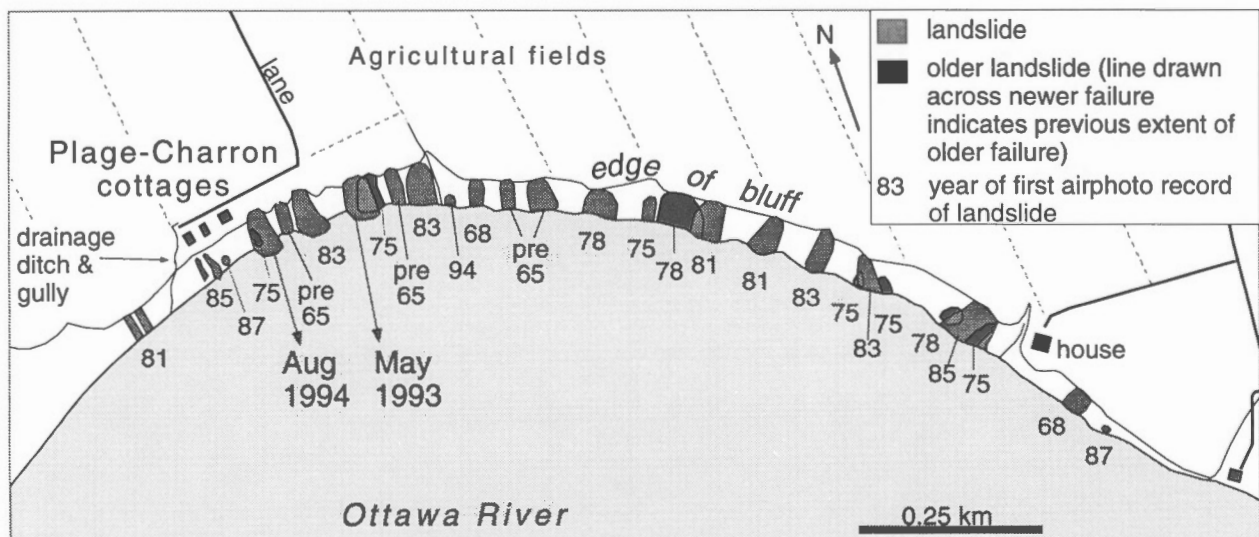


Figure 3. Map of slope failures, 1965 to 1994, along a 1.6 km length of bluff east of Plage-Charron. Date of failure refers to date the failure is first recorded on an airphoto; therefore, failure may have occurred anytime after the previous airphoto coverage. Many landslide scars are visible on the 1965 airphoto; only those estimated to have occurred not long before 1965 are shown on the map.

by the time of the 1985 photos. It is not uncommon to find older failures, even those that have been revegetated and seem stable, incorporated within newer failures some two to twenty years later. No new failures were visible on the 1990 airphotos, the last of the series. A visual evaluation of the bank near the August 1994 failure shows a few very small recent slumps and two recent larger movements. One occurred in May 1993 and the other is the August 1994 landslide. Large slope failures are less common on the extreme east and west ends of the bluff. Most landslides seem to extend approximately the same distance back into the bank. The recent failure is representative of the size and form of most of the larger landslides.

In the case of all the larger failures, movement occurred as an earthflow with the classic bimodal profile of steep headwall area and low profile toe extending out from the shoreline. Cracking behind the head scarp is noticeable on several scars, including the August 1994 landslide. Landslide toes are usually eroded within a few years of failure. Some small failures, and perhaps the initial failure of larger ones, occur near the base of the slope as simple slumps of an oversteepened part of the slope.

Landslides are an important factor in shoreline retreat. The pattern of shoreline retreat in this region seems to be a cycle of steepened slope, landslide, toe erosion, steepened slope, and landslide again. Probably this pattern has been repeating since the river assumed its present level.

Airphotos reveal that, prior to 1968, the bluff in front of the three cottages was gullied and sometime shortly before May 1975, these gullies were eliminated and the slope angle

was reduced by the owners. Two small fresh looking flows appear on the 1985 photo, and another very small failure lies beside them on the 1987 photo. The riprap was placed to protect the slope following this failure.

In early to mid May, 1993, a large landslide occurred 150 m east of the recent failure (A. Bouchard, pers. comm.). This feature incorporated, in part, a large area that had failed prior to May 1975 (Fig. 3). Groundwater and drainage conditions probably contributed to this failure. Above-normal snowfall in 1993, with heavy snowfall in March and early April, combined with a rapid spring melt and heavy spring rainfall would have caused the water table to lie near or at the ground surface. Considering the nature of the clay soil, large amounts of water likely stood on the fields behind the bluffs.

The landslide of August 5, 1994, located just east of the cottage properties, incorporated the area of a previous smaller flow. The recent landslide is also associated with heavy rainfall conditions and poor drainage.

THE PLAGÉ-CHARRON LANDSLIDE OF AUGUST 5, 1994

As in 1993, the region experienced above-normal precipitation in the first half of 1994 and heavy rain immediately preceding the failure. At Ottawa International Airport, June 1994 was the second wettest month on record (R. Bryant, pers. comm.), with 165.4 mm precipitation, 225 per cent above normal; precipitation in July totaled 114.6 mm, 133 per cent above normal. During the week of July 31-August 6, a total of 76.1 mm of rain fell at

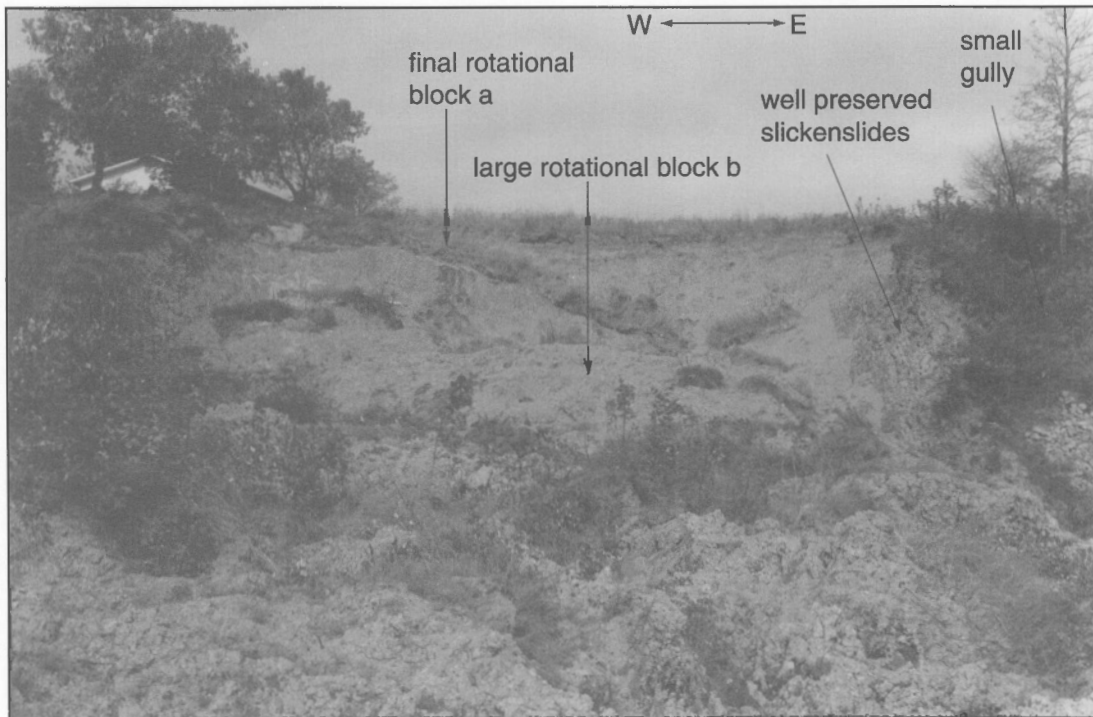


Figure 4. View of landslide looking towards the head scarp from a position midway down the foot. Note proximity to cottage.

Luskville, Quebec, 6.5 km east of Plage-Charron. At Luskville, on August 4, prior to the landslide, 50.8 mm of rain fell between 10:00 am and 8:00 pm in a storm associated with a tornado which passed through Aylmer, Quebec.

Local residents observed a small failure at the base of the slope in early spring. Jason Kyritzopoulos and André Bouchard reported extensive standing water on the field behind their properties. At the low spot on the lane, the water overspilled and drained towards the bluff. These groundwater and runoff conditions likely played a key role in the failure.

The failure was rotational in several retrogressive segments. Remoulded debris moved as an earthflow and extended out into the river. The scar extends 10 m back into the flat land above the bluff, and the floor of the crater lies 7 m below the original profile. Two narrow slices of bank have subsided along the headwall on the west side (block a; Fig. 4), and another incipient failure, a crack, approximately 10 cm wide and up to 50 cm deep, lies about 2 m behind the scarp on the west side (see Fig. 2). A large rounded hump of sediment (block b; Fig. 4) occupies the crater 10 to 25 m away from the head scarp. The first two metres, the back of the hump, is a fragmented and back-tilted slab of turf. This further indicates rotational failure. Slickensides are well preserved on the flanks of the crater.

In contrast to the rounded hump within the crater, the debris forming the 40 m long foot of the landslide has a more irregular surface – hummocky and fractured (Fig. 5). Large fractures trending across the foot produce a ridged effect in the upper two thirds of the foot. Fractures parallel to the long axis occur near the toe. The foot extends 25 m out from the shoreline before disappearing beneath the water. The river is now eroding the toe.

When observed 11 days after the failure, the surface of the debris was desiccated. The surface of all material in the crater, including the crater walls, is characterized by blocky clay fragments of various sizes. Even fresh exposures tend to

fragment into blocks as they dry. In contrast to this, on October 4, water was observed in the low areas at the base of the headwall and on the foot, and low areas in the toe of the landslide were more viscous, deforming readily underfoot.

A large boulder, known to mark the eastern limit of the riprap, is still in its original position (André Bouchard, pers. comm.), although it is in contact with landslide debris. Little or none of the area protected by riprap was involved in the failure.

The bank is composed of alternating layers of red and grey clay. The index properties of the clays are summarized in Table 1.

Preliminary slope profiles were measured at two locations; ‘A’, through the axis of the slide, and ‘B’, on the adjacent unfailed slope approximately 20 m to the west (Fig. 6). As no subsurface geotechnical test results are currently available for the site, the input values for the slope stability analysis are based on those used by Mitchell (1970) in his analysis of the Breckenridge slide of April 1963 (internal angle of friction, ϕ , of 23° and cohesion, c , of 8.8 kPa). This slide is located about 13 km southeast of the Plage-Charron slide and occurred in similar materials. It was also assumed that the piezometric surface was at the ground surface and that the entire slope was a uniform clay.

Slope analysis was carried out using “SLOPE/W” software, a product of Geo-Slope International of Calgary. Factors of safety (F.S.) computed by Bishop’s Simplified Method indicated a F.S. in the range of 1.05 to 1.09. Janbu’s Simplified Method indicated a factor of safety in the range of 0.95 to 1.13.

Note: Factor of safety is the ratio of the available shear strength to the shear strength required for stability. A factor of safety of 1.25 indicates that the forces holding up the slope exceed the critical state (1) by 25 per cent. A F.S. ≤ 1 indicates that the slope is unstable. Small changes to critical geotechnical parameters, i.e. strength parameters, slope geometry,

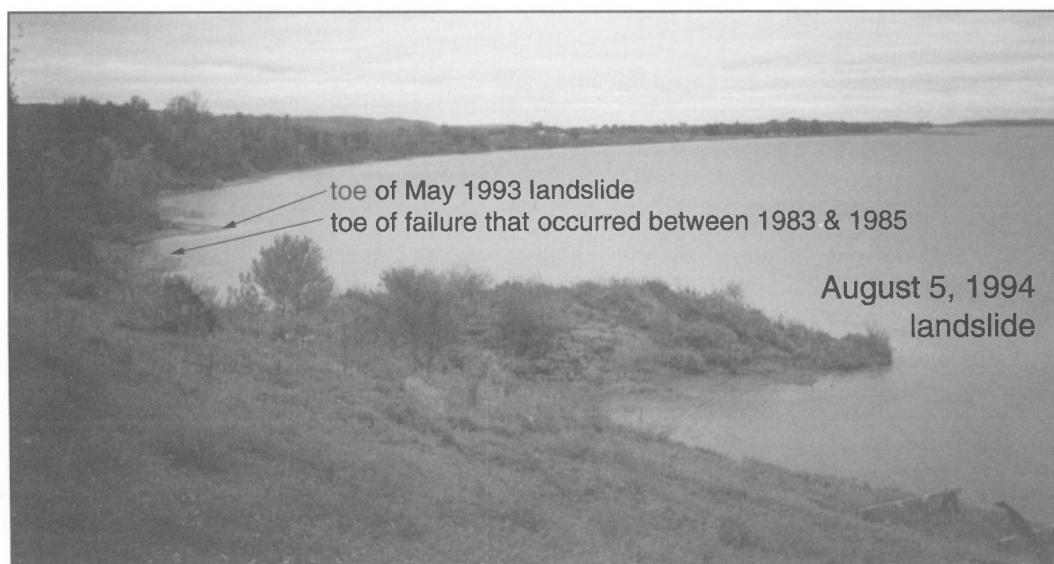


Figure 5. View of landslide foot from top of bluff in front of cottages. Cusped shoreline beyond foot represents toes of two earlier landslides.

Table 1. Summary of soil properties

Clay	γ kN/m ³	W %	W _p %	W _L %	I _p	I _L	undrained strength Cu (kPa)*		Sensitivity S _t
							natural	remoulded	
grey		62	26	75	49	0.73			
red		57	26	73	47	0.65			
undefined	16						35.4-74.5	9.0-21.7	3.5-11

*field vane shear tests

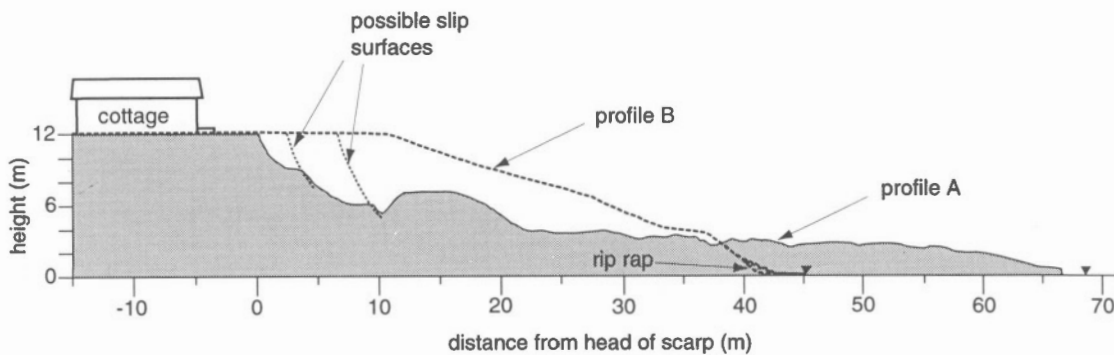


Figure 6. Slope profiles. 'A' through landslide and 'B' 20 m west of the landslide. Locations of slope profiles are shown on Figure 2.

and groundwater pressures, may have a profound effect on the stability of natural slopes in Leda clays where the factor of safety is less than 1.25.

SUMMARY

This landslide at Plage-Charron is the most recent in a series of relatively small landslides that have been documented along an arcuate 1.6 km long clay bluff. Examination of a series of airphotos which span approximately 30 years indicates that, on average, landslides occur at a rate of approximately one per year. It is estimated that almost all of the bluff has been subjected to slope failure over the last 60 to 100 years. Slope failure along this bluff must be considered an ongoing and continuous geomorphic process rather than a series of isolated incidents.

Preliminary slope stability analysis in the vicinity of the most recent slide indicates that the factor of safety is about unity. With only minor changes to local groundwater or soils conditions, the slope could fail. Oversteepening of the slope profile by natural or artificial changes could induce failure.

Most of the bluff is bordered by agricultural land; however, at the western end of the bluff there are three cottages and at the eastern end a new home has been built within the past six years. Should there be further pressure to develop this reach of the Ottawa River, it would be wise for local authorities to develop setback regulations. Development should only be undertaken

with full knowledge of potential slope instability problems, and no building construction should take place adjacent to the bluff prior to consultation with a geotechnical engineer.

ACKNOWLEDGMENTS

The authors wish to thank Xian-Qin Hu for carrying out the slope stability analysis and Brent Ward who critically reviewed the manuscript.

REFERENCES

- Brooks, G.R., Aylsworth, J.M., Evans, S.G., and Lawrence, D.E.
1994: The Lemieux landslide of June 20, 1993, south Nation Valley, southeastern Ontario – a photographic record; Geological Survey of Canada, Miscellaneous Report 56, 18 p.
- Carson, M.A. and Bovis, M.J.
1989: Slope processes; in Chapter 9 of Quaternary Geology of Canada and Greenland, (ed.) R.J. Fulton; Geological Survey of Canada, Geology of Canada, no. 1 (also Geological Society of America, The Geology of North America, v. K-1), p. 583-594.
- Mitchell, R.J.
1970: Landslides at Breckenridge, Pineview Golf Club and Rockcliff; National Research Council, Division of Building Research, Technical Paper No. 322.
- Richard, S.H., Gadd, N.R., and Vincent, J.S.
1977: Surficial materials and terrain features, Ottawa-Hull, Ontario-Québec; Geological Survey of Canada, Map 1425A, scale 1:125 000.

Particle size analysis of fine grained Champlain Sea sediments from a borehole near Ottawa, Ontario

J.A. Traynor

Terrain Sciences Division

Traynor, J.A., 1995: Particle size analysis of fine grained Champlain Sea sediments from a borehole near Ottawa, Ontario; in Current Research 1995-D; Geological Survey of Canada, p. 87-90.

Abstract: Grain size distributions of postglacial sediments from a continuously sampled borehole in the Mer Bleu bog, east of Ottawa, were determined using the Brinkman particle size analyzer of the Mineral Tracing and Sedimentology Laboratory, Terrain Sciences Division. Forty of fifty samples were thought to be deposited in a marine environment. Clay-sized material (<0.002 mm) ranged from 13 per cent to 49 per cent and averaged 30 per cent, and a fining-upward trend was noted. The relatively small amount of clay in the samples is consistent with emerging delta front and delta top environments of deposition described by others, but the regional significance of the fining-upward trend is unknown. The similarity in grain-size distribution of sediment in samples from a more distal part of the basin to the Mer Bleu samples suggests that proximity to the basin centre is not the only factor influencing the clay-sized content of marine sediments.

Résumé : Les répartitions granulométriques des sédiments post-glaciaires provenant d'un trou de sondage dans la tourbière Mer bleue, à l'est d'Ottawa, où l'échantillonnage a été continu, ont été déterminées au moyen de l'analyseur de la taille de particules Brinkman du laboratoire de sédimentologie de la Division de la science des terrains. On suppose que quarante des cinquante échantillons ont été déposés dans un environnement marin. La fraction argileuse (<0,002 mm) variait entre 13 % et 49 %, pour une moyenne de 30 %. Une granodécroissance vers le haut a été observée. La quantité relativement petite d'argile dans les échantillons est compatible avec des milieux de sédimentation émergents sur front et sommet deltaïques décrits par d'autres chercheurs, mais la signification régionale de la tendance à la granodécroissance vers le haut n'a pas été établie. La similitude des répartitions granulométriques entre les échantillons provenant d'une partie plus distale du bassin et les échantillons de la Mer bleue laisse suggérer que la proximité du centre du bassin n'est pas le seul facteur influant sur la fraction argileuse des sédiments marins.

INTRODUCTION

In March 1993 the Terrain Dynamics Subdivision of Terrain Sciences Division coordinated the drilling and continuous sampling of a 62.5 m borehole (GSC93-GEOMAG) to demonstrate geophysical equipment (Douma and Nixon, 1993) (Fig. 1). The hole was drilled east of Ottawa on a sand-capped ridge surrounded by the Mer Bleu bog. The ridge was an island in a channel of the Ottawa River formed during regression of the Champlain Sea and abandoned about 7650 years ago (Gadd, 1987).

The core provided an opportunity to determine grain-size distribution over a sequence of postglacial deposits dominated by marine sediments. Marine clay is one of the most widespread surface or near-surface deposits in the Ottawa-St. Lawrence Lowlands and has contributed to many landslides in the region. Determination of grain-size characteristics of these deposits may be significant for identifying areas potentially sensitive to landslides, as a relationship between soil sensitivity and soil texture has been noted (Penner, 1965; Quigley, 1980). Fifty subsamples of the core were analyzed using a Brinkman particle size analyzer and the results are presented here.

PREVIOUS WORK

There has been no systematic regional survey of grain size characteristics of Champlain Sea sediments in the Ottawa area. Previous work shows that these sediments range in size from bouldery gravel and sands associated with subaqueous fans and beaches to fine grained sediments, including varved or massive clay and silt deposited in deep water (Fransham and Gadd, 1977; Rust, 1977; Gadd, 1986). Generally, more fine grained sediments were deposited near the centre of the former Champlain basin and coarser materials, near the margins (Karrow, 1961). Leroueil et al. (1983) found that grain size varied from site to site but that sediments were coarser (20 to 60% <0.002 mm) at the margins of the Champlain Basin and finer (60 to 85% <0.002 mm) in low-lying areas near the basin centre.

Douma and Nixon (1993) described sediments in GSC93-GEOMAG (Fig. 2) and correlated the major units with lithofacies described by Gadd (1986) and those in a nearby borehole (CRF-21A). The soft varved clay overlying till was correlated with Gadd's glaciomarine rhythmite unit. The overlying stiff grey to olive-grey clay was correlated with a sequence of sediments associated with marine prodelta, delta front, and delta top environments of deposition, consecutively. The uppermost clay and sand units were interpreted as fluvial terrace deposits.

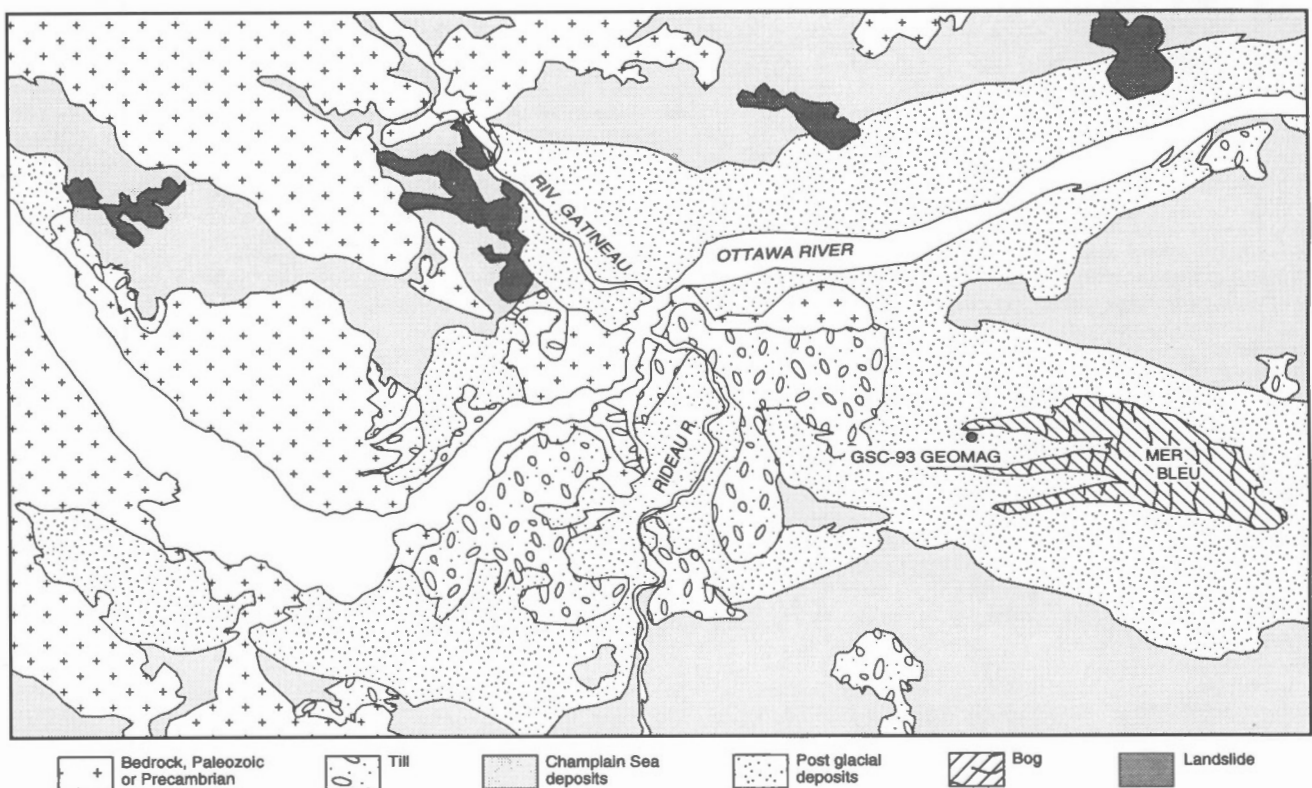


Figure 1. Generalized surficial geology of the Ottawa area showing the location of borehole GSC93-GEOMAG near Mer Bleu bog (modified from Fransham et al., 1976).

METHODS

The core, collected with Shelby tubes, was processed and logged at the Geotechnical Laboratory of Carleton University. Fifty samples were collected, forty of which were from the marine sediment portion of the core. The boundaries between lithological units were usually estimated by inspecting the sediments exposed at the ends of the Shelby tubes during coring.

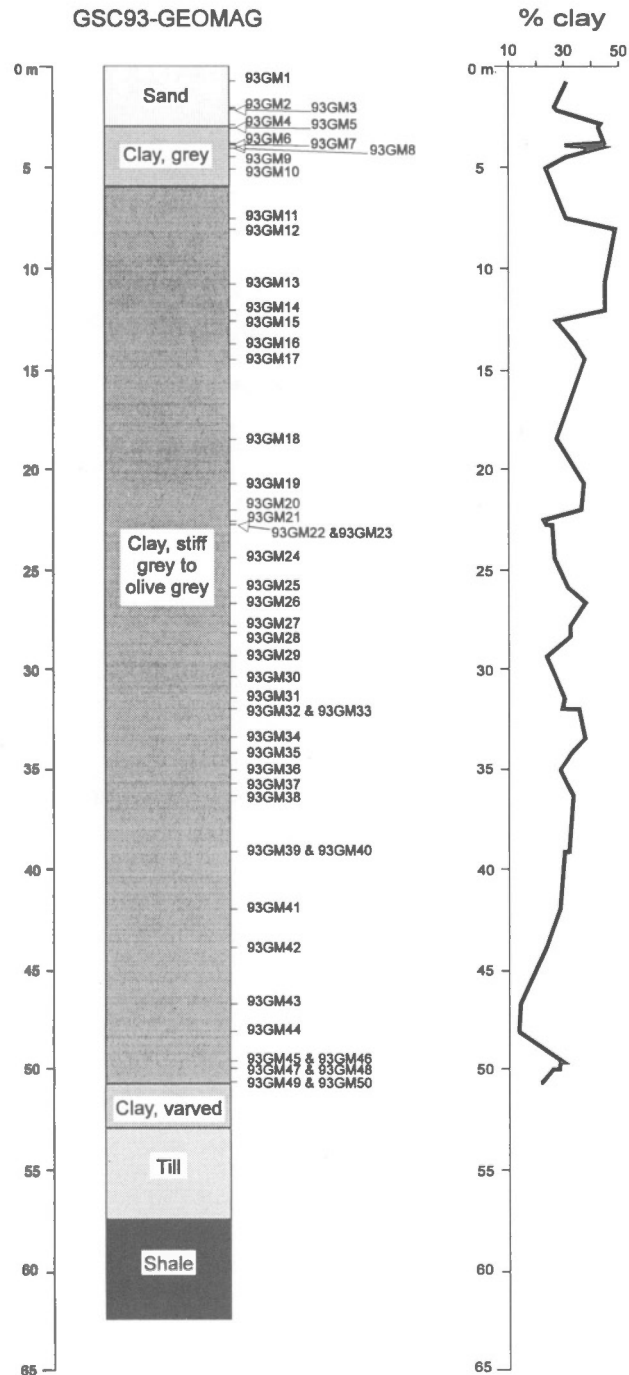


Figure 2. Description of GSC93-GEOMAG core (after Douma and Nixon, 1993). Also shown is per cent of clay-sized material (<0.002 mm) in the <0.063 mm fraction.

At the Mineral Tracing and Sedimentology Laboratory of Terrain Sciences Division, the samples were passed through a <0.063 mm sieve and disaggregated using a dispersant. Grain-size distribution in the <0.063 mm fraction was determined using a Brinkman particle size analyzer and results were compiled in tables and graphs. All 50 samples were analyzed in two days.

RESULTS AND DISCUSSION

The samples submitted for this study were composed entirely of silt- and clay-sized material (<0.063 mm). Only two of the samples contained coarse silt (0.063 to 0.031 mm); the remainder were composed of particles finer than 0.031 mm. The content of clay-sized (<0.002 mm) material varies with depth in GSC93-GEOMAG and is shown in Figure 2. The clay content of 40 marine sediment samples (93GM11-93GM50) ranges between 13 and 49 per cent with the average being 30 per cent. Generally, clay content increases upwards in the core.

Marine sediments in this borehole are coarser than those described by Gadd (1986) as deep-water prodelta deposits but are similar in texture to those deposited in emerging delta front and delta top environments. Earlier studies showed that clay-sized contents in samples from deep-water and prodelta deposits were 62 per cent and 72 per cent, respectively, and in delta front and delta top deposits, 50 per cent and 14 per cent, respectively (Fransham and Gadd, 1977; Gadd, 1986). The relatively minor amount of clay-sized material suggests that the prodelta unit is missing at this site.

The fining-upward trend in marine sediments (Fig. 2) is not consistent with Gadd's (1986) interpretation of Champlain Sea depositional environments, and its regional significance is not known. The increase in energy associated with a prograding delta would likely result in a coarsening of sediment over time. Cyclic changes in the per cent clay content with depth may represent changes in water depth associated with ice front fluctuations.

Results of this and earlier studies show that the texture of fine marine sediments in the Ottawa area is variable. Clay-sized contents from samples from three adjacent sites immediately northwest of Mer Bleu range between 67 and 89 per cent (Penner, 1965). Grain-size distribution of sediments sampled at the site of the 1993 Lemieux landslide, which lies closer to the centre of the Champlain Sea basin, are similar to the sediments from this study (Fig. 3). The texture of the Lemieux samples is generally coarser than that of samples collected east of Ottawa by Penner (1965), despite being much further from the Champlain Sea limit. Thus, it seems that some factor other than proximity to the basin centre has a strong influence on the clay content of marine sediments.

Determination of grain-size distribution using a Brinkman particle size analyzer proved a very rapid method for analysis of fine grained samples, compared to the traditional pipette method. In addition, it is efficient and requires only small amounts of material. When a group of samples was analyzed using both techniques, slightly lower values in the clay-sized

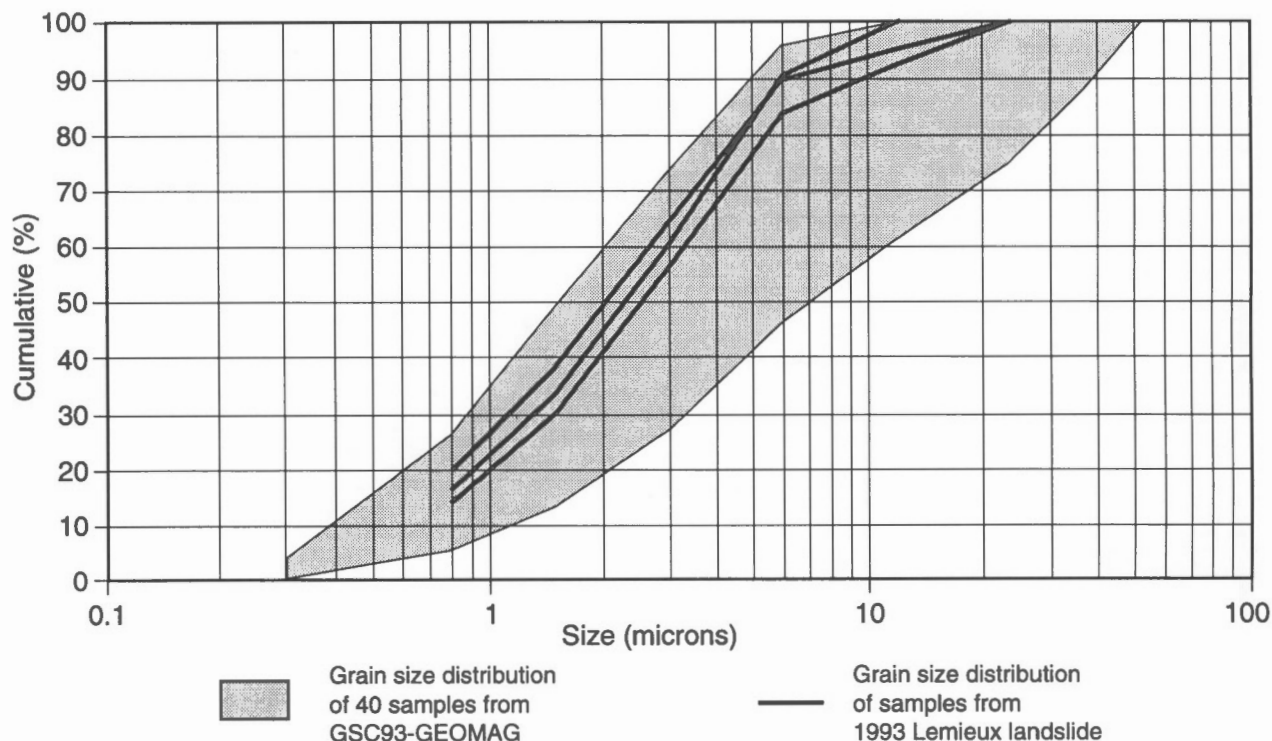


Figure 3. Grain-size distribution in the <0.063 mm fraction of forty marine sediment samples from GSC93-GEOMAG, and three samples collected from the 1993 Lemieux landslide site.

range and slightly higher values for the silt-sized range were obtained using the Brinkman method (Wilson, unpub. data). These analytical discrepancies may account for the small difference in mean clay contents of samples from proximal Champlain Sea lithofacies collected from GSC93-GEOMAG and from cores collected by Fransham and Gadd (1977). As differences are very small (averaging 6.4 per cent and 4.2 per cent for silt and clay, respectively), it does not preclude comparing data obtained using this method with data from earlier studies.

REFERENCES

- Douma, M. and Nixon, F.M.**
1993: Geophysical characterization of glacial and postglacial sediments in a continuously cored borehole near Ottawa, Ontario; in *Current Research, Part E*; Geological Survey of Canada, Paper 93-1E, p. 275-279.
- Fransham, P. and Gadd, N.R.**
1977: Geological and geomorphological controls of landslides in Ottawa valley; *Canadian Geotechnical Journal*, v. 14, p. 531-539.
- Fransham, P.B., Gadd, N.R., and Carr, P.A.**
1976: Sensitive clay deposits and associated landslides in Ottawa Valley; Geological Survey of Canada, Open File 352.
- Gadd, N.R.**
1986: Lithofacies of Leda Clay in the Ottawa basin of the Champlain Sea; Geological Survey of Canada, Paper 85-21.
1987: Quaternary evolution of the Ottawa area; in *Quaternary of the Ottawa Region and Guides for Day Excursions*, (ed.) R.J. Fulton; International Union for Quaternary Research, XIIth International Congress, p. 75-80.
- Karrow, P.F.**
1961: The Champlain Sea and its sediments; in *Soils in Canada*, (ed.) R.F. Legget; Royal Society of Canada, Special Publication No. 3, Toronto, 229 p.
- Leroueil, S., Tavenas, F. et LeBihan, J-P.**
1983: Propriétés caractéristiques des argiles de l'est du Canada; *Canadian Geotechnical Journal*, v. 20, p. 681-705.
- Penner, E.**
1965: A study of sensitivity in Leda clay; *Canadian Journal of Earth Sciences*, v. 2, p. 425-441.
- Quigley, R.M.**
1980: Geology, mineralogy, and geochemistry of Canadian soft soils: a geotechnical perspective; *Canadian Geotechnical Journal*, v. 17, no. 2, p. 261-285.
- Rust, B.R.**
1977: Mass flow deposits in a Quaternary succession near Ottawa, Canada: diagnostic criteria for subaqueous outwash; *Canadian Journal of Earth Sciences*, v. 14, p. 175-184.

Geological Survey of Canada Project 830016JA

Northeastern North American earthquake potential – new challenges for seismic hazard mapping

John Adams, Peter W. Basham, and Stephen Halchuk
Geophysics Division

Adams, J., Basham, P.W., and Halchuk, S., 1995: Northeastern North American earthquake potential – new challenges for seismic hazard mapping; in Current Research 1995-D; Geological Survey of Canada, p. 91-99.

Abstract: Most previous seismic hazard maps for eastern Canada and the United States were essentially based on a model that assumes a continuation of the historical pattern and rate of seismicity. New evidence from global studies of earthquakes in stable continental regions has shown that most of the larger earthquakes occur through reactivation of relatively young (<500 Ma) rift faults that break the integrity of the continental crust. Thus, current seismicity associated with those structures suggests that future large earthquakes in northeastern North America may occur elsewhere on the same structures, even on the historically-quiet portions. The impact of such geological associations on the hazard estimates depends critically on the sizes of the zones, and the relative weights that are given to "geological" and "historical" earthquake source zones in the hazard model. We suggest here a "robust" approach, using the highest hazard from several plausible models, and argue that its non-probabilistic basis represents an acceptable compromise.

Résumé : La plupart des cartes antérieures figurant les zones de risque sismique dans l'est du Canada et des États-Unis se fondaient essentiellement sur un modèle supposant une continuité des tendances historiques et du taux de sismicité. De nouveaux indices tirés d'études globales des tremblements de terre dans des régions continentales stables indiquent que la plupart des grands séismes sont causés par la réactivation de failles de rift relativement jeunes (<500 Ma) qui brisent l'intégrité de la croûte continentale. Ainsi, la sismicité actuelle associée à ces structures laisse supposer que les futurs grands séismes dans le nord-est de l'Amérique du Nord pourraient se produire ailleurs dans les mêmes structures, même dans les portions antérieurement calmes. Les répercussions de telles associations géologiques sur les évaluations des risques dépendent grandement des dimensions de ces zones, ainsi que des poids relatifs attribués aux zones d'origine des séismes, «géologiques» et «historiques», dans le modèle des risques. Nous suggérons ici une approche «robuste», en utilisant les risques les plus élevés tirés de plusieurs modèles plausibles, et soutenons que sa base non probabiliste représente un compromis acceptable.

INTRODUCTION

A few statistics will illustrate the earthquake magnitude scale and put the earthquake occurrence of eastern North America in perspective. There are about 7500 earthquakes greater than magnitude (M) 4 around the world each year, and about 1100 of $M \geq 5$, 100 of $M \geq 6$, and 9 of $M \geq 7$. In eastern North America (east of the Rockies, see Fig. 1) the United States Geological Survey (USGS) and Geological Survey of Canada (GSC) typically locate 90 earthquakes greater than $M3$ each year; perhaps half of these are felt. Within this area, an average year will see a dozen $M \geq 4$ and one or two $M \geq 5$; an average decade will see perhaps two $M \geq 6$; and the average century, two $M \geq 7$. For comparison, in the last decade (1982-1992) eastern Canada alone had sixteen $M \geq 5$ and six $M \geq 6$. In the northeastern United States, there were only two $M \geq 5$ earthquakes, $M5.2$ in the Adirondacks in 1983 and $M5.0$ in Ohio in 1986.

The seismicity map (Fig. 1) contains the basic information on the spatial distribution of seismic hazards. One does not need to have any earth science understanding to see that the

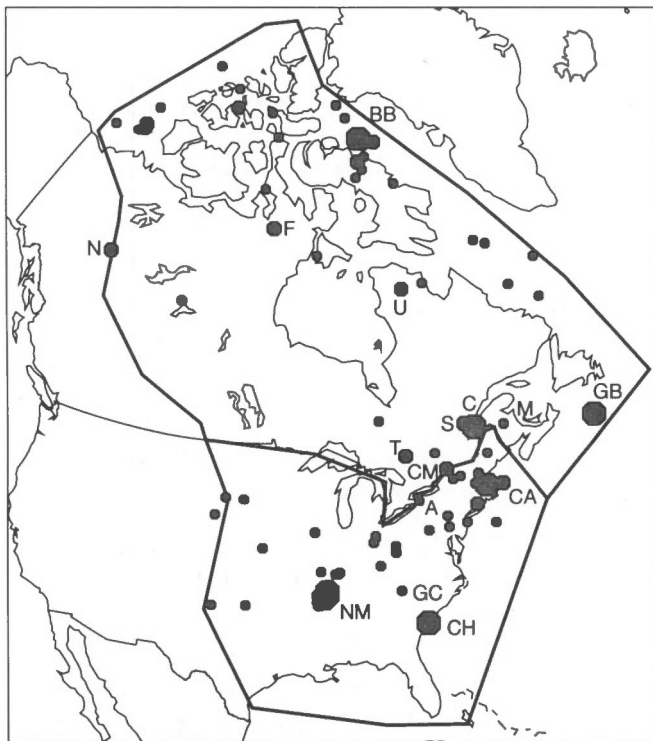


Figure 1. Map of historical earthquakes for magnitude (M) 6 and greater (all known) and $M \geq 5$ (since 1920) for eastern North America. Small, medium, and large dots represent $M \geq 5$, 6, and 7, respectively. Note that the earthquake record in the Arctic is incomplete for $M \geq 5$ before 1964, for $M \geq 6$ before 1930, and for $M \geq 7$ before 1920. Earthquakes discussed in the text are identified by letter codes as follows: BB, Baffin Bay; F, Franklin Lake; N, Nahanni; U, Ungava; C, Charlevoix; S, Saguenay; T, Timiskaming; CM, Cornwall/Massena; A, Attica; M, Miramichi; GB, Grand Banks; CA, Cape Ann; GC, Giles County; NM, New Madrid; CH, Charleston.

earthquakes form a halo around a less-active region in the centre of the continent (a halo that is even more evident when the hundreds of $M > 3$ earthquakes are plotted), and that the hazard should be similarly distributed.

Previous seismic hazard maps (e.g., Basham et al., 1985 for Canada; Algermissen et al., 1982 for northeastern U.S.) included available geological information where appropriate, but of necessity were based chiefly on what was known from the historical seismicity record. The subsequent decade of seismicity has not proved this approach wrong in the U.S., as the Adirondacks and Ohio earthquakes were moderate earthquakes that occurred in areas of recognized hazard. The approach proved less satisfactory in Canada, where the decade 1982-1992 produced a number of significant earthquakes remarkable for their size, location, or effects, including:

- 1985 Nahanni, Northwest Territories, $M6.9$ and $M6.6$, 1988 $M6.0$ (perhaps just inside the North America stable craton; exceeded the largest historical event by nearly two magnitude units).
- 1988 Saguenay, Quebec, $M5.9$ (earthquake very deep in the crust, area of extremely low previous seismicity, enhanced high frequency radiation equivalent to $M6.5$).
- 1989 Ungava, Quebec, $M6.3$ (very shallow, produced the first historical surface faulting in eastern North America).

Thus, the current hazard maps underestimated the hazard, fortunately in mainly unpopulated regions, even during the decade since their adoption. On the other hand, some other recent earthquakes have occurred in areas recognized for their low-level seismicity, and have confirmed the historical pattern: 1982 Miramichi, New Brunswick ($M5.7$ and $M5.4$), 1990 Mont-Laurier, Quebec ($M5.0$), and 1992 Franklin Lake, Northwest Territories ($M6.0$).

This paper updates the overview of Basham (1989), which discussed seven of the earthquake sources of large events in North America and summarized twelve possible causal relations for the earthquakes less than $M6$. In contrast to that paper, which discussed the larger earthquakes on an individual basis, we begin with a geological overview, and discuss how the historical earthquakes can be fitted into a conceptual framework, and then how future earthquakes, occurring within that framework, will affect our views on the distribution of seismic hazard.

CAUSES OF LARGE EARTHQUAKES IN THE "STABLE" CONTINENT

Earthquakes greater than magnitude 7 (this century: 1929 Grand Banks and 1933 Baffin Bay), and greater than $M8$ (at New Madrid, central U.S., in 1811/12) have happened in the middle of the North American plate distant from any plate boundary. These large earthquakes dominate any assessment of hazard, and in computing seismic hazard maps we are faced with three questions: what is the likely rate of occurrence of the larger earthquakes? how big can such intraplate earthquakes be? and can they occur just anywhere in the plate interior?

The seismicity map (Fig. 1) shows that the distribution of the historical seismicity is non-random, and so geologists and seismologists have sought to rationalize the earthquake locations. In our own early work (Basham et al., 1983; Basham and Adams, 1989) we considered that the entire Atlantic passive margin should be treated as a source zone, and effectively defined a geological source zone centred on the rift-margin faults formed during the opening of the Atlantic. Thus we concluded that the continental shelf and slope off the eastern United States - only 200-250 km from either Boston or New York - might experience earthquakes as large as the 1929 Grand Banks earthquake off the east coast of Canada.

The best current hypothesis, championed by Arch Johnston of Memphis State and a team that worked for Electric Power Research Institute (EPRI), is that most stable continental earthquakes occur through the reactivation of relatively young (<500 Ma) rift faults that break the integrity of the continental crust. Coppersmith et al. (1987) and Johnston (1989) reached this conclusion from a study of worldwide analogs for the North American continent, and showed that 71 per cent of the seismicity of stable continental regions was associated with extinct intra-continental rifts or continental passive margins (one-sided rifts). Further, all of the 17 earthquakes of magnitude 7 and greater in their compilation are closely associated with the imbedded rifts or passive margins. Many of these earthquakes appear to be occurring through reactivation of the rift faults (formed in an extensional environment) as thrust or strike-slip events in the current compressive stress field.

Though the EPRI team were concerned primarily with maximum magnitudes in the eastern U.S., their 'reactivated rift' hypothesis provides a good explanation for the location of most large eastern earthquakes. Two one-sided rifts are important for earthquakes in the northeastern U.S. and southeastern Canada: the Atlantic margin, which was formed by the opening of the Atlantic Ocean in Triassic to Cretaceous times (the modern 'passive margin'), and the Iapetan paleo-

margin along the ancient edge of the Grenville-aged continent formed by the opening of the Iapetus (Proto-Atlantic) Ocean about 600-550 Ma ago. That ancient rifting left a thinned and weakened continental margin, which during the closing of the Iapetus Ocean about 440-310 Ma ago was overthrust by the Appalachian mountain range. A schematic section (Fig. 2) shows the relationships of the tectonic units.

GEOLOGICAL SOURCE ZONES FOR EASTERN CANADA AND THE ADJACENT UNITED STATES

A philosophy of geological source zones for seismic hazard estimation has been refined by Rus Wheeler of the USGS (Wheeler, 1991; Wheeler and Johnston, 1992). Briefly, a geological source zone is a region with a common geological history that distinguishes it from neighbouring areas. It is normally large (with respect to the size of typical seismicity clusters) because there is usually insufficient information to justify a finer division. It must have faults of the same age and type, a seismicity style that is consistent between seismicity clusters, and be in a single stress province. Then faults of the same age and type are presumed to be potentially seismogenic throughout the zone.

We show in Figure 3 approximate geographical limits for a set of geological source zones (GSZ) relevant to Canada. Because this study was done for Canada, the zone boundaries were extended only far enough into the U.S. to ensure the correct computed hazard in Canada. Relative to Wheeler (1991) and Wheeler and Johnston (1992), we distinguish more source zones, as we briefly describe below (refer also to Fig. 2):

Atlantic Rifted Margin (ARM) zone represents the rifted edge of the North American continent that was thinned by listric normal faulting during the early stages of the opening of the Atlantic Ocean. The zone extends offshore from the

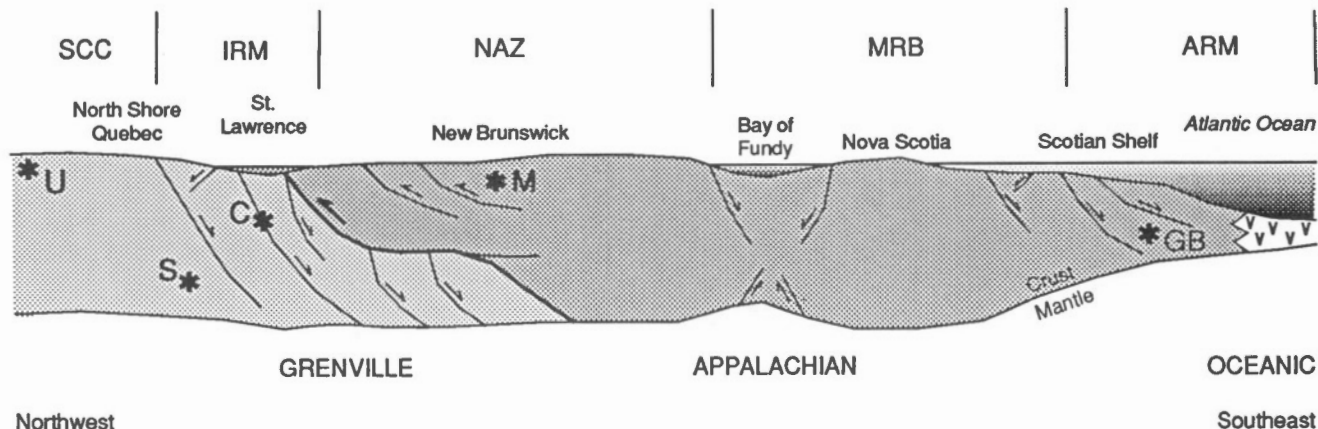


Figure 2. Cartoon cross-section across the eastern margin of North America (based in part on a figure by Wheeler, 1991). Line of profile is located in Figure 3. Stipple distinguishes the main orogenic belts. Stars with letters show representative positions of some Canadian earthquakes. Three-letter codes above the section indicate geological source zones described in the text. Arrows represent block movement during the formation of the faults, not their present motion.

landward limit of significant extension to the edge of the continental crust. Magnitude 7 earthquakes in 1929 and 1933 occurred on the Canadian part of the margin; on the U.S. part one or two earthquakes may have occurred off Boston in the 1700s, and in 1992 a M4.8 earthquake occurred off New Jersey. Large ($M > 6.5$) earthquakes in this zone may be tsunamigenic if they disturb unstable sediment accumulations on the continental slope, as did the Grand Banks earthquake.

Mesozoic Rifted Basins (MRB) zone extends from the landward limit of significant extension on the Atlantic margin – the "hinge" zone – to the landward edge of limited Mesozoic extension. Other than the amount of extension involved, the other key difference from Atlantic Rifted Margin zone is that the Mesozoic Rifted Basins zone lacks the large thickness contrast between continental (25-35 km) and oceanic (5-10 km) crust that occurs in the former. That contrast may amplify the stresses acting and cause a higher rate of seismicity in the Atlantic Rifted Margin than within the Mesozoic Rifted Basins. The Mesozoic

Rifted Basins zone encloses the Triassic basins that exist mostly offshore in the Bay of Fundy and Gulf of Maine, and onshore basins such as the Hartford and Newark basins. Similar basins exist in Virginia and are inferred to exist in the southern Appalachians in Georgia. The crust in this zone underwent only limited extension, but the reactivation of the Appalachian thrust faults and the creation of the rift-bounding faults makes them good candidates for reactivation in the present stress field (though the basins themselves have low seismicity, Seeber and Armbruster, 1988). Although convincing evidence does not yet exist, we postulate that the 1886 Charleston earthquake could be due to the reactivation of faults that were formed or reactivated during the Mesozoic rifting episode.

Northern Appalachians (NAZ) zone extends from the landward limit of Mesozoic extensional faulting to the seaward limit of thinned Grenville crust of the Iapetan passive margin. It comprises much of the Appalachian

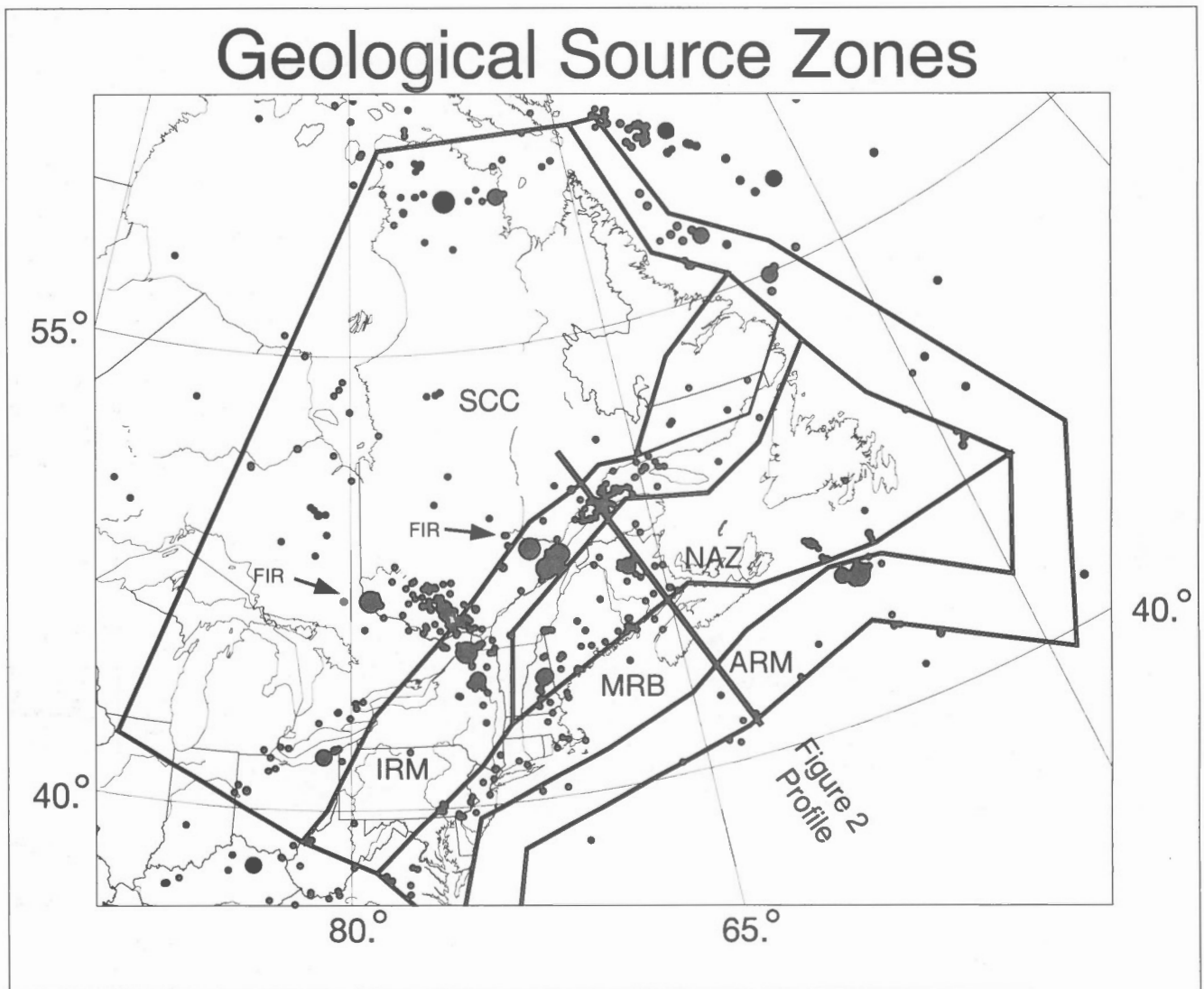


Figure 3. Geological source zones for southeastern Canada and the adjacent U.S. with representative seismicity. The failed Iapetan rifts (FIR) along the Ottawa River and Saguenay Fiord are indicated by arrows.

Orogen (comprises sedimentary and metamorphic rocks and rootless plutons) that over-rode the passive margin. All earthquakes with known depth are relatively shallow, less than 10 km, the paradigm example being the Miramichi earthquake sequence of 1982 (Wetmiller et al., 1984).

Iapetan Rifted Margin (IRM) covers the faulted edge of the Grenville continental crust that was rifted and thinned during the initial opening of the Iapetus Ocean. This zone is substantially as defined by Wheeler (1991). Paleozoic sedimentary rocks laid down along the ancient continental margin were subsequently faulted in the Late Ordovician, apparently by normal faults. Under the current stress regime these ancient normal faults are being reactivated as chiefly thrust faults in Canada and as strike-slip faults in the U.S. The paradigm earthquake is Charlevoix 1925, for which the moment magnitude has been revised significantly downwards (to 6.2) by Bent (1992). The great depth extent of seismicity - from the surface to 30+ km deep at Charlevoix - and the length of the faults suggest much larger earthquakes are possible.

Iapetan Rifted Margin as drawn includes all examples of extension entirely within the stable, Grenville-aged continental crust, even those representing only minor extension, as at Attica, New York and in southern Labrador. In fact, most of the extension (and perhaps therefore most of the large faults capable of being reactivated) lies along the ancient continental margin in a narrow zone which goes along the St. Lawrence Valley from the Strait of Belle Isle (between Newfoundland and Labrador) to Lake Champlain, east of the Adirondacks. Grenville-aged crust to the southeast of this has been thinned much more than the relatively-intact crust to the northwest. If we were to redefine the source zone to contain only the former margin faults, the remaining region of normal faulting within the continent would be analogous to the limited extension in the onshore Mesozoic basins (MRB zone) inboard of the Atlantic passive margin. By analogy, therefore, we term these 'Iapetan rift basins', although as we know, some of their faults have moved in extension in post-Iapetan times. We discuss the possible future significance of this redefinition later.

Failed Iapetan Rifts (FIR) represent zones of normal faults, without much total extension, which have caused partial weakness of the craton. In Canada, failed arms extend up the Saguenay Fiord and the Ottawa River (Saguenay and Ottawa-Bonnechere grabens); in the U.S. the Reelfoot Rift (site of the New Madrid earthquakes) and southern Oklahoma aulacogen (site of a prehistoric M7+ earthquake) are similar. Paradigmatic earthquakes are Timiskaming 1935 M6.2 and Saguenay 1988 in Canada and New Madrid 1811/12 in the U.S. Fault dimensions and earthquake depths are likely to be similar to the Iapetan Rifted Margin. The seismicity in western Quebec, adjacent to the Ottawa-Bonnechere Graben, is included in the Failed Iapetan Rifts rate statistics, even though it is thought to be occurring through reactivation of faults formed by the passage of North America over a hotspot (Adams and Basham, 1991).

Stable Craton Core (SCC) represents the part of the continent least affected by Phanerozoic extensional faulting. This zone and its earthquakes are significant to issues such as disposal of nuclear fuel waste, but space does not allow a discussion of this subject here.

SOME PROBLEMS WITH USING THE GEOLOGICAL SOURCE ZONES

Spatial issues

From a cursory view of Figure 3 it is evident that though the geological zones divide the continent into seismically active and less active zones, each Geological Source Zone contains both seismic and relatively aseismic parts. This is despite having defined the zones to include the same sort of geological features, of presumed similar potential for activity. To take the Iapetan Rifted Margins as an example, the zone comprises a seismically active central third and seismically less-active eastern and western thirds. The rate of activity in the centre is twenty times that of the ends. A redefinition of Iapetan Rifted Margins to exclude the 'Iapetan rifted basins' would remove much of the aseismic regions in southern Labrador (a thin line on Fig. 3 shows the suggested boundary here), and in western New York and western Pennsylvania. However, such a finer subdivision may exceed our current level of knowledge, and, in any case, aseismic regions would still remain along the ancient margin proper.

Within the central third of Iapetan Rifted Margins, the seismicity is not evenly distributed, being concentrated in a number of well-known seismicity clusters (Lower St. Lawrence, Charlevoix, Montreal) separated by aseismic regions. We have argued (Adams and Basham, 1991) that such aseismic regions are likely a temporal artifact of our short human timescale - in the immediate future one or more large earthquakes might fill in part of these regions, and if we were to wait for five or ten thousand years we might well not be able to distinguish the current seismic from the aseismic regions. Hence, either the future activity in eastern Pennsylvania would be similar to that in the present St. Lawrence valley, or we are missing some fundamental understanding that would allow us to predict the spatial distribution of earthquakes better.

Dealing with the spatial variability within the geological zones poses challenges. At the moment we prefer a model for the Iapetan seismicity that incorporates the appropriate seismicity clusters (Fig. 4a; high-seismicity clusters are TIM, MNT, CHV and BSL; low-seismicity clusters are PEM, TRR, SAG, TAD, CHA) into a single large zone (Fig. 4b, IRX zone) which does not, however, cover the same large geographic area as the geological source zone Iapetan Rifted Margin. That is, we do not have confidence that our understanding of which geological structures are seismogenic is sufficiently complete, for geology to completely dominate historical experience.

Temporal issues

For the purposes of earthquake-resistant design we are interested in the exposure of a structure to ground motions during its lifetime, a lifetime that is usually considerably less than the length of the historical record. It could be argued that geological processes operate very slowly within continents,

and so the chance of an aseismic part of a Geological Source Zone becoming seismically active in the near future is low. For the next 50 years, it might therefore be rational to expect a continuation of what has happened in the immediate past at about the same level (i.e. seismicity will re-occur in historically active clusters).

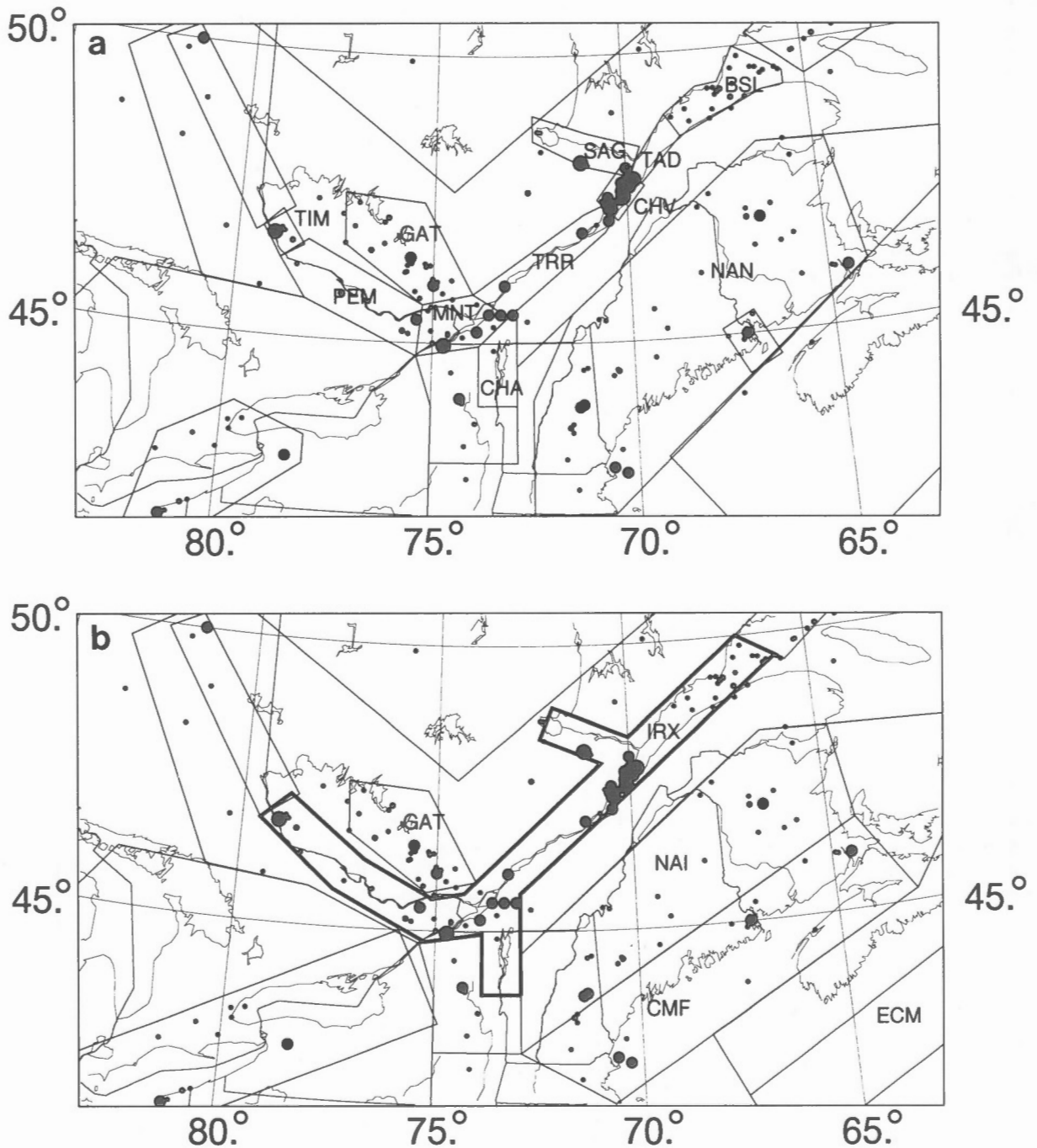


Figure 4. Seismic source zones for southeastern Canada developed under a) the "historical" and b) the "geological" model. The IRX zone (outlined in heavy line) incorporates the important contributions from the Iapetan rifted margin (IRM) and the failed Iapetan rift arms (FIR) geological source zones. Note how the seismicity is clustered and the historical source zones are defined around each cluster. Note how the NAZ, MRB and part of ARM geological source zones (Fig. 3) have been implemented as NAI, CMF and ECM in Figure 4b.

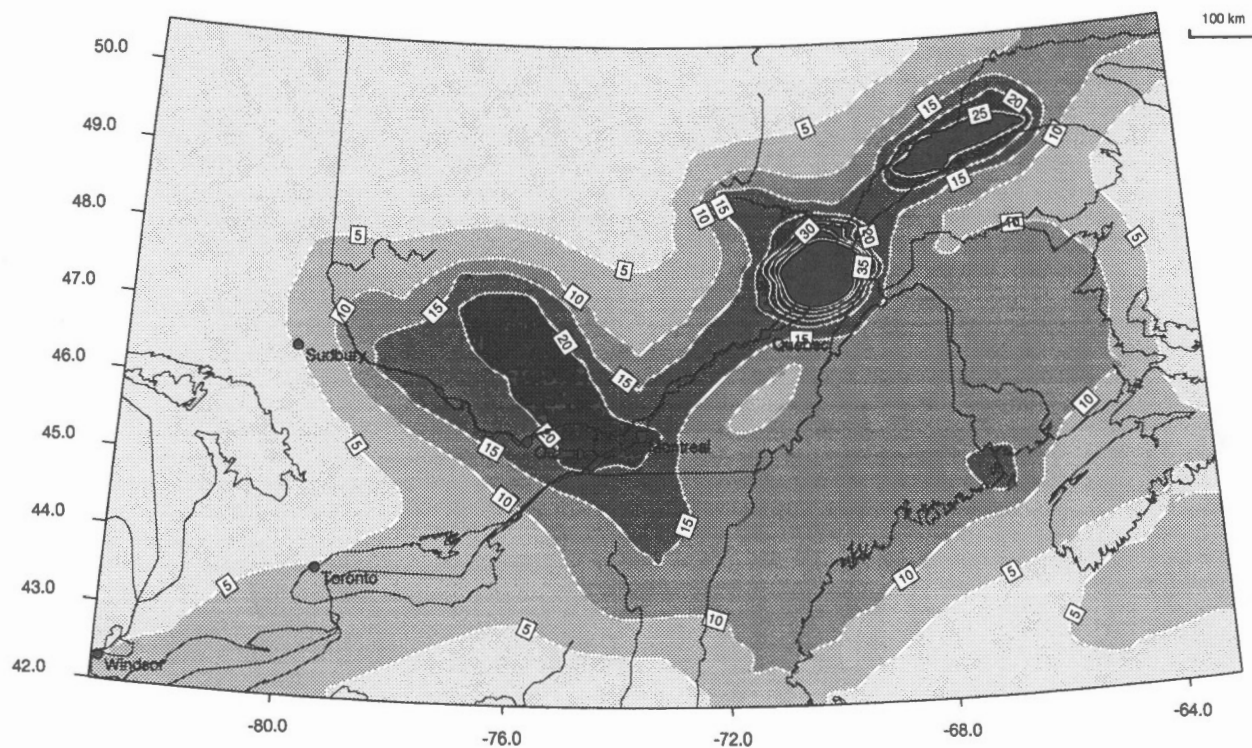
Nevertheless, our past earthquake history, and the geological understanding implied in the Geological Source Zone model, indicate this is not the entire story. Only at Charlevoix have large historical earthquakes repeated; all other historical $M > 5.5$ earthquakes (such as Timiskaming, 1935 and Saguenay, 1988) have been the first of their size at their locality. Under this hypothesis we might consider the clusters of low-level seismicity - such as occur today near the 1935 epicentre - as long-delayed aftershocks to large earthquakes that occur randomly in time and irregularly in space within a Geological Source Zone. We have not explored this avenue further because the implication that the historical seismicity clusters in fact represent single isolated earthquakes and their aftershocks makes the description of their activity by a Poissonian process suspect.

Recent work in the field of paleoseismology, which seeks to use the geological record to extend the historical record of large earthquakes, has suggested that some large earthquakes (Charleston, New Madrid, Timiskaming) may have been preceded by prehistorical earthquakes in the past hundreds to thousands of years. However the results are still too patchy to be incorporated fully into hazard analysis. The field also needs to be viewed in the context that most researchers have

been funded to search for paleo-earthquakes in the vicinity of historical events; if the same effort were expended throughout the eastern U.S., we suspect that many new earthquake sources would be found, such as the vicinity of the Wabash valley paleo-earthquake (Obermeier et al., 1991).

ON HAZARD COMPUTED BY COMBINING ALTERNATIVE SOURCE ZONE MODELS

An immediate consequence of using more geological concepts is a much lower hazard estimate for places of high historical seismicity, but only slightly higher hazard in aseismic places. For trial use, we have suggested that a simple combination of the geological-biased and the historical-seismicity-biased models will suffice for future probabilistic maps. For example, weighting the two models by a simple fraction (such as $1/2:1/2$) preserves the seismicity budget and yet allows for the possibility of large earthquakes in hitherto aseismic regions. The fractionally-combined models produce markedly lower hazard in historically active regions (e.g., Charlevoix), somewhat higher hazard in areas without large



Southeastern Canada "Robust" model - Peak Ground Acceleration
EPRI attenuation; 50th %ile; 0.0021 p.a.; sigma = 0.7

Figure 5. Trial seismic hazard map of southeastern Canada using the "robust" approach for combining results from a seismicity-biased and a geological-biased source model. Parameter contoured is the highest of the two median values of peak horizontal ground acceleration (%g) from the models, computed for a probability of 10 per cent in 50 years using the EPRI (McGuire et al. 1988) strong ground motion relation.

historical earthquakes (e.g., Trois Rivières), and substantially unchanged hazard in some places (e.g., Montreal) where the hazard is insensitive to the model used.

This results in a classic dilemma. By attempting to accommodate large earthquakes in geologically likely regions that have not yet had earthquakes we have reduced protection in regions with a history of damaging earthquakes! This is a consequence of assuming a constant "seismicity budget" (representing the expected seismic energy release rate) and is a necessary condition for preserving the probabilistic basis of seismic hazard maps.

We wish to produce robust hazard estimates that preserve the protection level required by the historical earthquakes yet provide additional protection required by the regional geological information and the unresolved spatial and temporal issues we have discussed. In our view the "robust" estimate should: i) include all reasonable explanations of the seismicity, and by doing so attempt to quantify our ignorance; ii) be unlikely to change significantly because of the occurrence of a single earthquake, even if that earthquake significantly exceeds design levels near the epicentre; iii) be relatively insensitive to future conceptual breakthroughs in seismotectonic understanding; and iv) be insensitive to the whim of the day.

Therefore, for discussion purposes, we suggest the following solution. We first compute the probabilistic hazard for a 100 per cent Historical-biased and for a 100 per cent Geological-biased model using the same grid of points, and then choose the higher value for each grid point to be contoured for the "robust" map (Fig. 5). While two models are clearly the minimum, we doubt that more than a few more would be either needed or appropriate. The mapped "robust" estimates are "probabilistic" at any one place, in that for each site and every ground motion parameter being computed there is an identifiable probabilistic hazard calculation made using a particular source-zone model. Hence for design purposes (for a building or a city) the map provides a suitable probabilistic hazard value, though from a regional perspective the map as a whole is not probabilistic, because the model used differs from site to site.

The chief advantage of the "robust" approach is that it preserves protection in areas of high seismicity but also provides increased protection in currently aseismic areas that are geologically likely to have future large earthquakes. A further advantage is that the approach is computationally simple, and it is easy to explain what was done. The main disadvantage is that the map is not a probabilistic map because each of the alternative models are weighted 100 per cent. Hence, some earthquakes are "counted twice". For example, the five $M > 6$ historical earthquakes at Charlevoix are used in the Historical-biased model to produce a high-hazard "bullseye" near Charlevoix, but also used in the Geological-biased model to produce a moderate level of seismic hazard near Trois Rivières. By using different source zones each weighted 100 per cent and choosing the highest value to be contoured, the implied annual seismic moment (= earthquake energy) release is higher than the historical rate. This violates a key

premise of probabilistic seismic hazard mapping, that the historical rate of earthquakes provides the correct "seismicity budget", which is considered inviolate.

An attempt was made to determine the amount of "extra" seismic moment release that would have to be added to the historical model in order for it to match the seismic hazard levels of the "robust" map for the populated region of the Ottawa and St. Lawrence valleys. Regions of the historical model that produced lower hazard values than the "robust" map were identified, and the seismicity rates of the corresponding seismicity source zones were then augmented until their computed hazard matched the "robust" hazard levels. Five zones required a seismicity increase, and as expected all of them were relatively aseismic in the historical model. Although the increases in these zones were by factors of 2.5 to 4, the total "augmented" annual seismic moment release was only 30 per cent larger than the total for the historical model. A 30 per cent augmentation of the average annual moment release is equivalent to a magnitude 6.6 earthquake happening next year, or an uncounted magnitude 7 earthquake having occurred shortly before the Europeans arrived in North America. Therefore we consider that a "robust" hazard map, based on a limited range of plausible models, may be acceptable in the interests of preserving safety in high seismicity areas and promoting safety in potentially active regions.

Thus given the uncertainty in the correct seismic moment release rate, we consider augmenting the seismicity budget by 30 per cent is a justifiable conservatism for the level of engineering protection it will provide, relative to the assumed level of safety at 10 per cent in 50 years. Perhaps as our knowledge increases over the next decades, both to constrain the parameter estimates and to understand how, why, and where earthquakes can happen, we will be able to refine the values and reduce the seismicity budget augmentation and its explicit conservatism.

CONCLUSIONS

It is clear from the above discussion that there are still many parts of the seismic hazard mapping process that are uncertain. For a structural engineer, expecting variations of strength of a few per cent in a stock steel order, the uncertainties may seem daunting. Though some of the uncertainty in seismic hazard estimation is irreducible, due to random fluctuations in the processes and vagaries in the earth, other uncertainties can be reduced as our understanding improves. The geological basis for earthquake distribution and the "robust" approach to combining source models presented here are a step forward, even though it may seem that we are claiming less certainty than before. By incorporating geological understanding and quantifying the uncertainty there should be less surprise in the location of the next $M > 6$ earthquake in the east; though as have past earthquakes, it will doubtless provide a considerable impetus for further improvement in the hazard estimates.

ACKNOWLEDGMENTS

We acknowledge an extremely fruitful exchange of ideas with Rus Wheeler, Arch Johnston, Dieter Weichert, and many other North American colleagues. Stephanie Hiscock assembled the geological information and computed the initial hazard consequences of the Geological Source Zone model for a student work report supervised by Adams in 1991. Reviews of an earlier version of this paper by Rus Wheeler and Maurice Lamontagne have substantially focussed our message.

REFERENCES

- Adams, J. and Basham, P.W.**
1991: The seismicity and seismotectonics of eastern Canada; Chapter 14 in *Neotectonics of North America*, (ed.) D.B. Slemmons, E.R. Engdahl, M.D. Zoback, and D.D. Blackwell; Geological Society of America, Decade Map Volume 1: p. 261-276.
- Algermissen, S.T., Perkins, D.M., Thenhaus, P.C., Hanson, S.L., and Bender, B.L.**
1982: Probabilistic estimates of maximum acceleration and velocity in rock in the contiguous United States; United States Geological Survey, Open-File Report 82-1033, 99 p.
- Basham, P.W.**
1989: A Paleozoic-Mesozoic rift framework for seismic hazard assessment in eastern North America; in *Current Research, Part F*; Geological Survey of Canada, Paper 89-1F, p. 45-50.
- Basham, P.W. and Adams, J.**
1989: Problems of seismic hazard estimation in regions with few large earthquakes: examples from eastern Canada; *Tectonophysics*, v. 167, p. 187-199.
- Basham, P. W., Adams, J., and Anglin, F.M.**
1983: Earthquake source models for estimating seismic risk on the eastern Canadian continental margin; *Proceedings 4th Canadian Conference on Earthquake Engineering*, Vancouver, Canada, June 1983, p. 495-508.
- Basham, P. W., Weichert, D.H., Anglin, F.M., and Berry, M.J.**
1985: New probabilistic strong seismic ground motion maps of Canada; *Bulletin of the Seismological Society of America*, v. 75, p. 563-595.
- Bent, A.L.**
1992: A re-examination of the 1925 Charlevoix, Quebec earthquake; *Bulletin of the Seismological Society of America*, v. 82, p. 2097-2113.
- Coppersmith, K. J., Johnston, A.C., and Arabasz, W.J.**
1987: Methods for assessing maximum earthquakes in the central and eastern United States; Working Report, Electric Power Research Institute, Palo Alto, California, EPRI Research Project 2556-12.
- Engdahl, E.R. and Rinehart, W.A.**
1988: Seismicity Map of North America; Geological Society of America, Centennial Special Map CSM-4, scale 1:5 000 000.
- Johnston, A.C.**
1989: The seismicity of 'Stable Continental Interiors'; in *Earthquakes at North Atlantic Passive Margins: Neotectonics and Postglacial Rebound*, (ed.) S. Gregersen, and P.W. Basham; Kluwer Academic Publishers Dordrecht, p. 299-327.
- McGuire, R.K., Toro, G., and Silva, W.**
1988: Engineering Model of Earthquake Ground Motion for Eastern North America; report NP-6074, Electric Power Research Institute, Palo Alto, California, EPRI, Research Project 2556-16.
- Obermeier, S.F., Bleuer, N.R., Munson, C.A., Munson, P.J., Martin, W.S., McWilliams, K.M., Tabaczynski, D.A., Odum, J.K., Rubin, M., and Eggert, D.L.**
1991: Evidence of strong earthquake shaking in the Lower Wabash Valley from prehistoric liquefaction features; *Science*, v. 251, p. 1061-1063.
- Seeber, L. and Armbruster, J.G.**
1988: Seismicity along the Atlantic seaboard of the U.S.: intraplate neotectonics and earthquake hazard; in *The Atlantic Continental Margin: U.S.*, (ed.) R.E. Sheridan, and J.A. Grow; Geological Society of America, *The Geology of North America*, v. I-2: p. 565-582.
- Wetmiller, R.J., Adams, J., Anglin, F.M., Hasegawa, H.S., and Stevens, A.E.**
1984: Aftershock sequences of the 1982 Miramichi, New Brunswick, earthquakes; *Bulletin of the Seismological Society of America*, v. 74, p. 621-653.
- Wheeler, R.L.**
1991: Earthquakes and the Iapetan passive margin in eastern North America; in *Proceedings, Geological Survey of Canada workshop on eastern Seismicity Source Zones for the 1995 Seismic Hazard Maps*, (comp.) J. Adams; Geological Survey of Canada, Open File 2437, p. 73-85 and 272-283.
- Wheeler, R.L. and Johnston, A.C.**
1992: Geologic implications of earthquake source parameters in central and eastern North America; *Seismological Research Letters*, v. 63, p. 491-514.

Geological Survey of Canada Project 890047

Aeromagnetic survey program of the Geological Survey of Canada, 1994-1995^{1, 2, 3, 4}

R. Dumont, F. Kiss, P.E. Stone, K. Anderson, D.J. Teskey, R.A. Gibb,
and G. Palacky⁵

Geophysics Division

Dumont, R., Kiss, F., Stone, P.E., Anderson, K., Teskey, D.J., Gibb, R.A., and Palacky, G., 1995: Aeromagnetic survey program of the Geological Survey of Canada, 1994-1995; in Current Research 1995-D; Geological Survey of Canada, p. 101-104.

Abstract: In 1994, high resolution aeromagnetic surveys totalling 103 446 line km were flown in three areas of Manitoba and Saskatchewan. These surveys were partially funded by industry and (for the Saskatchewan portion) by the Canada-Saskatchewan Partnership Agreement on Mineral Development (1990-1995). A detailed gradiometer survey totalling 12 573 line km was flown in Nova Scotia and funded by the Canada-Nova Scotia Cooperation Agreement on Mineral Development (1992-1995). An airborne electromagnetic/magnetic survey totalling 13 730 line km was flown in the Chibougamau greenstone belt of Quebec funded under the Special Assistance Program for the Mining Sector of the Chapais-Chibougamau Region (1992-1995). The program to level the Canadian aeromagnetic profile dataset to eliminate the effect of survey boundaries was completed for the Northwest Territories and eastern Alberta. Drape computation and levelling of the British Columbia surveys is in progress. Six thousand line kilometres of high-resolution aeromagnetic data have been flown west of Banks Island by the Institute for Aerospace Research, National Research Council, as part of the Polar Margin Aeromagnetic Program.

Résumé : En 1994, des levés aéromagnétiques à haute résolution totalisant 103 346 km linéaires ont été effectués dans trois régions du Manitoba et de la Saskatchewan. Les fonds nécessaires provenaient en partie de l'industrie privée et pour la portion des travaux située en Saskatchewan, de l'Entente de partenariat Canada-Saskatchewan sur l'exploitation minérale (1990-1995). Un levé détaillé au gradiomètre vertical de 12 573 km linéaires a été effectué en Nouvelle-Écosse, dans le cadre de l'Entente de coopération Canada-Nouvelle-Écosse sur l'exploitation minérale (1992-1995). Un levé aéromagnétique et électromagnétique totalisant 13 730 km linéaires a été effectué dans la ceinture de roches vertes de Chibougamau sous l'égide du Programme de soutien du secteur minier de la région de Chapais-Chibougamau (1992-1995). Les travaux entrepris dans le cadre du programme pancanadien de nivellement des données aéromagnétiques en profils pour éliminer l'effet des limites des levés ont été complétés dans les Territoires du Nord Ouest et l'est de l'Alberta. Le calcul à hauteur constante et le nivellement des levés de la Colombie-Britannique se poursuivent. Un levé aéromagnétique de 6 000 km linéaires a été effectué à l'ouest de l'île Banks par l'Institut de recherche aérospatiale dans le cadre du Programme aéromagnétique de la marge polaire.

¹ Contribution to Canada-British Columbia Agreement on Mineral Development (1991-1995), a subsidiary agreement under the Canada-British Columbia Economic and Regional Development Agreement.

² Contribution to Canada-Saskatchewan Partnership Agreement on Mineral Development (1990-1995), a subsidiary agreement under the Canada-Saskatchewan Economic and Regional Development Agreement.

³ Contribution to Canada-Nova Scotia Cooperation Agreement on Mineral Development (1992-1995), a subsidiary agreement under the Canada-Nova Scotia Economic and Regional Development Agreement.

⁴ Contribution to Special Assistance Program for the Mining Sector of the Chapais-Chibougamau Region (1992-1995), under the Canada-Quebec Subsidiary Agreement on the Economic Development of the Regions of Quebec.

⁵ Mineral Resources Division

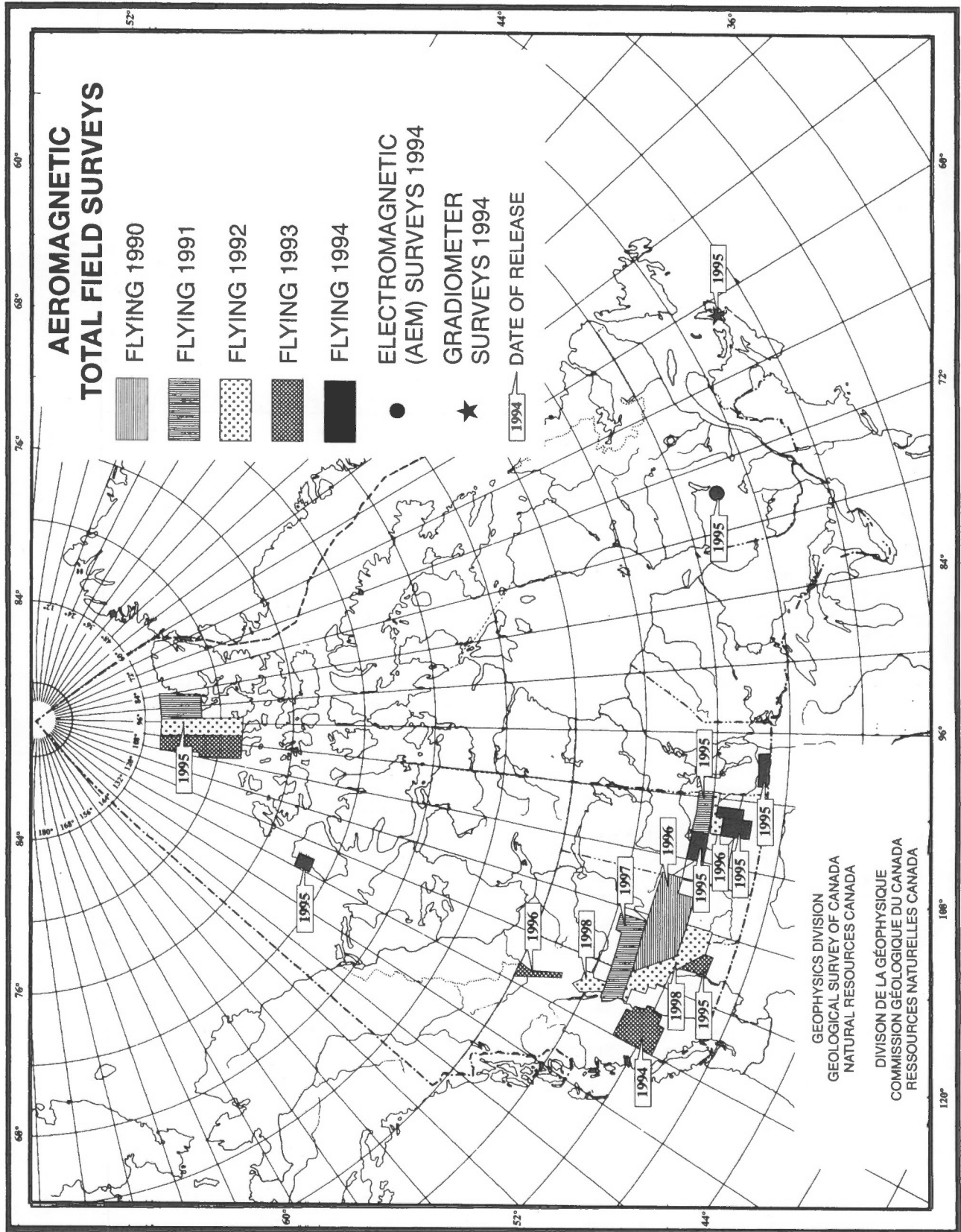


Figure 1. Aeromagnetic surveys in progress, 1994-1995.

INTRODUCTION

The aeromagnetic survey program of the GSC continued in 1994-95 with activity in four on-going projects in British Columbia, Saskatchewan and Manitoba, Quebec, and the Arctic Ocean west of Banks Island. One new project was commenced in Nova Scotia. Survey activity for 1994 is shown in Figure 1 and summarized in Table 1.

BRITISH COLUMBIA

Compilation of the 110 000 line km survey (Fig. 1), which was initiated last year, continued in 1994. The Interior Plateau survey (82 700 line km) was partially funded under the Canada-British Columbia Agreement on Mineral Development (1991-1995), and the data were released as an open file (Geological Survey of Canada, 1994) in November 1994. These data will support detailed geological mapping and future mineral exploration programs. Data for the southeast and northeast blocks will be released to the public in 1995 and 1996 respectively. Two industry partners participated in a cost-sharing agreement with the GSC to survey these areas.

SASKATCHEWAN AND MANITOBA

The fourth phase of a multiyear program to complete regional aeromagnetic coverage of southern Saskatchewan and Manitoba was carried out in 1994. This year's program in Saskatchewan (44 387 line km) was funded by the GSC, three industry partners, the Province of Saskatchewan, and the

Canada-Saskatchewan Partnership Agreement on Mineral Development (1990-1995). In Manitoba, a 36 225 line km survey was funded by the GSC and two industry partners. A second survey in Saskatchewan (22 834 line km) funded by the GSC was also carried out (Fig. 1, Table 1). These surveys meet the dual objectives of mapping the Precambrian basement beneath the Phanerozoic cover, and of providing a fundamental tool for kimberlite exploration.

QUEBEC

The second and third phases of the three year Special Assistance Program for the Mining Sector of the Chapais-Chibougamau Region were combined to perform a systematic multicoil, multifrequency helicopter-borne electromagnetic and magnetic survey of a greenstone belt in the Chapais-Chibougamau region of Quebec. The Quebec Ministère des Ressources naturelles (MRNQ) and the Geological Survey of Canada are cooperating to provide new digital survey data and geophysical maps resulting from these airborne electromagnetic/magnetic surveys, which are designed to stimulate mineral exploration in this area.

The latest data totalling 13 730 line km will be published as an open file by MRNQ in the winter of 1995.

NOVA SCOTIA

A helicopter-borne gradiometer survey was carried out in western Cape Breton Island (12 573 line km) to assist detailed geological mapping in areas of specific interest for mineral

Table 1. Aeromagnetic survey activity in 1994-1995.

SURVEY	TYPE	LINE KM	LINE SPACING	ALTITUDE	YEAR OF PUBLICATION
British Columbia 1993-94	Aeromagnetic Total Field	3 600	1.6 km	1 370 m ASL	1996
		4 800	1.6 km	1 830 m ASL	1996
		82 700	0.8 km	305 m MTC	1994
		19 100	0.8 km	305 m MTC	1995
Saskatchewan Phase IV 1994 (Regina area)	Aeromagnetic Total Field	44 387	800 m	150 m MTC	1995
Saskatchewan 1994 (Saskatoon)	Aeromagnetic Total Field	22 834	800 m	150 m MTC	1995
Manitoba 1994 (Virden)	Aeromagnetic Total Field	36 225	800 m	150 m MTC	1995
Nova Scotia 1994 (Western Cape Breton)	Aeromagnetic Gradiometer/VLF-EM	12 573	300 m	150 m MTC	1995
Quebec 1993-94 Lac des Vents area	Aeromagnetic Frequency Domain EM	13 730	100 m	30 m MTC	1995
Banks Island	Aeromagnetic Total Field	6 000	4 km	305 m MTC	1995

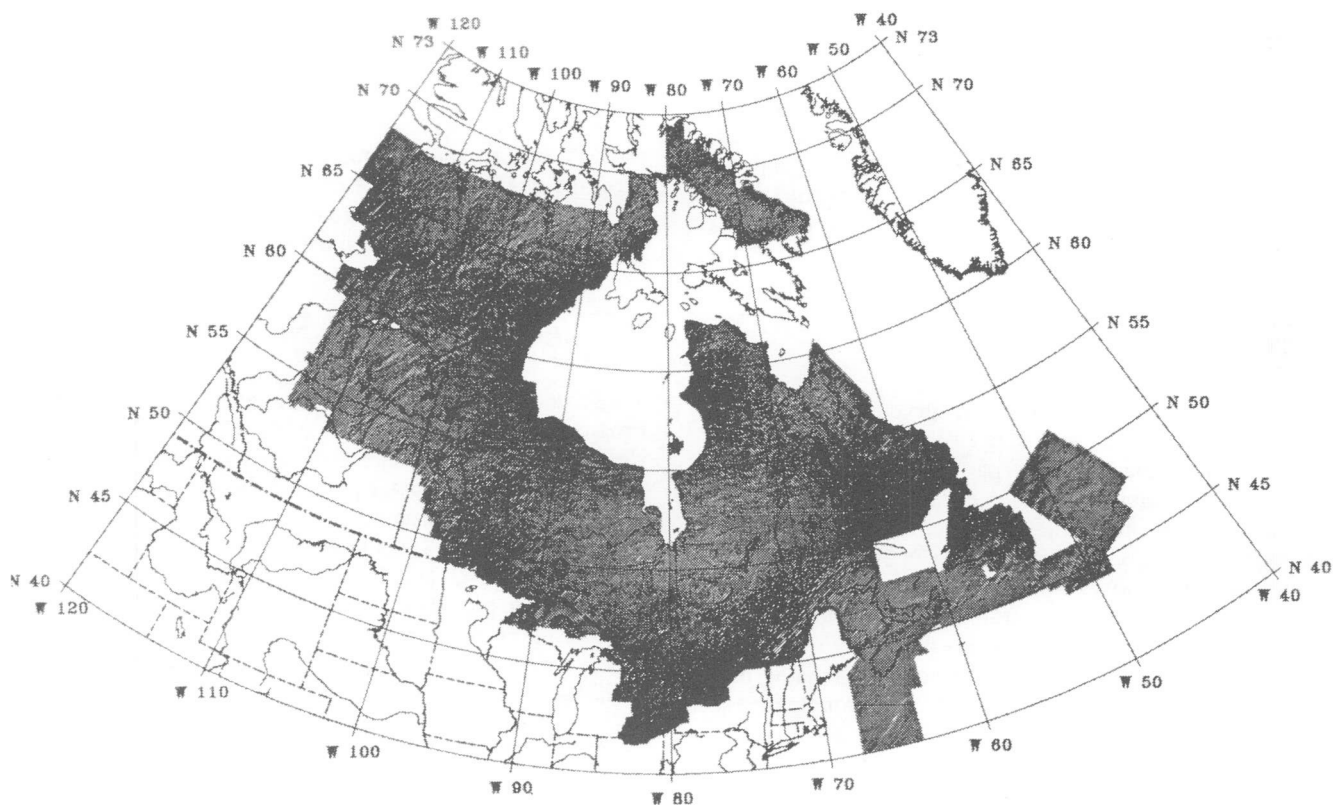


Figure 2. Levelled aeromagnetic profile data.

exploration. Funding was provided by the Canada-Nova Scotia Cooperation Agreement on Mineral Development. The data will be released to the public in the spring of 1995.

NORTHWEST TERRITORIES, ALBERTA, BRITISH COLUMBIA

The editing and levelling of previously flown aeromagnetic profile data for all of Canada has been undertaken by the Geological Survey of Canada to achieve a homogeneous levelled dataset free from survey boundary effects. With this process, seamless and finer magnetic grids can be generated more economically and more efficiently by government, industry, and university clients. In 1994, the GSC processed and levelled the aeromagnetic dataset for the Northwest Territories including Baffin Island, the eastern half of Alberta, and part of British Columbia (Fig. 2). Draping (computing magnetic data to a draped surface) of the constant altitude surveys over the Rockies was initiated in order to bridge the surrounding drape-flown surveys in Alberta and western British Columbia.

ARCTIC OCEAN WEST OF BANKS ISLAND

A total field survey totalling 6000 line km was flown over the Arctic Ocean west of Banks Island under the Polar Margin Aeromagnetic Program (PMAP) by the Institute for Aerospace Research, National Research Council. Digital data and associated aeromagnetic maps of this survey merged with oil company data to the east which were acquired from the National Energy Board, will be released as an open file publication in 1995.

REFERENCES

Geological Survey of Canada

1994: High resolution aeromagnetic survey of the Interior Plateau, British Columbia; Geological Survey of Canada, Open File 2785.

Geological Survey of Canada Projects 900033, 910028, 910029, 920024, 920027, 930002

National gravity survey program of the Geological Survey of Canada, 1994-1995

D.B. Hearty and R.A. Gibb

Geophysics Division

Hearty, D.B. and Gibb, R.A., 1995: National gravity survey program of the Geological Survey of Canada, 1994-1995; in Current Research 1995-D; Geological Survey of Canada, p. 105-107.

Abstract: Seven gravity surveys were completed under the national gravity survey program in 1994: two were reconnaissance surveys located in Coronation Gulf and Dease Strait in the Arctic and west of the Queen Charlotte Islands; three were detail gravity surveys near Bolton, Ontario, near New Glasgow, Nova Scotia, and in the St Lawrence River near La Malbaie, Quebec; and two were gravity control network surveys in Nova Scotia and on Ellesmere Island and Greenland in the high Arctic. Approximately 2123 new gravity stations and 5100 line kilometres of dynamic gravity observations were collected on these surveys. These data will be added to the National Gravity Database. In addition, Canada participated in the fourth International Comparison of Absolute Gravimeters in Sèvres, France and made absolute gravity measurements at one site in Manitoba and eleven sites in British Columbia in support of the GSC's crustal dynamics program.

Résumé : Sept levés gravimétriques ont été complétés en 1994 dans le cadre du programme national de levés gravimétriques; deux de ces levés ont été des levés de reconnaissance dans le golfe Coronation et le détroit de Dease, dans l'Arctique et l'ouest des îles de la Reine-Charlotte; trois ont été des levés gravimétriques détaillés près de Bolton (Ontario), près de New Glasgow (Nouvelle-Écosse) et dans le fleuve Saint-Laurent, près de La Malbaie (Québec); et deux ont été des levés gravimétriques aux fins du canevas de contrôle en Nouvelle-Écosse ainsi que dans l'île d'Ellesmere et au Groenland, dans le Haut Arctique. Des observations gravimétriques dynamiques ont été faites à partir d'environ 2 123 nouvelles stations gravimétriques et le long de 5 100 kilomètres linéaires au cours de ces levés. Ces données seront ajoutées à la Base de données gravimétriques nationale. De plus, le Canada a participé à la quatrième Comparaison internationale des gravimètres absolus, à Sèvres, en France, et a effectué des mesures gravimétriques absolues à un site au Manitoba et à 11 sites en Colombie-Britannique, en appui au programme de la CGC sur la dynamique crustale.

INTRODUCTION

In 1994-1995, the national gravity mapping program comprised two reconnaissance surveys, three local surveys over geological targets and two network inspection surveys, one in support of the Canadian Gravity Standardization Network and, the other to establish the infrastructure for a major reconnaissance survey on Ellesmere Island, in Nares Strait and on northwestern Greenland planned for 1995-1996. A regional ice survey in the Arctic contributed to the mapping of the Arctic channels and a dynamic gravity survey supported studies being conducted by the Pacific Geoscience Centre over the Explorer Plate west of the Queen Charlotte Islands. Local target surveys were conducted in various parts of Canada in support of research projects of the Continental Geoscience Division, the Terrain Science Division, the Geophysics Division and two universities in Nova Scotia, and contributed to the rationalization and reprocessing of older gravity data by the Nova Scotia Research Foundation.

Details of these surveys and highlights from the gravity standards program and gravity map production are given below.

ARCTIC CHANNELS

Between February 24 and April 18, 1994, a gravity and bathymetry survey was completed on the ice surface in Coronation Gulf and Dease Strait between Richardson Island and Cambridge Bay. The survey, part of the national gravity mapping program, was carried out by the Geophysics Division in co-operation with the Canadian Hydrographic Service (CHS) and the Polar Continental Shelf Project (PCSP). A total of 542 gravity stations with corresponding bathymetry was established at a spacing of 6 km. Horizontal positioning was obtained by real-time differential GPS using Magnavox MX300 GPS receivers in the helicopters linked to a master station by two remote transmitters. The bathymetry survey was year two of a four year project to complete the reconnaissance bathymetry mapping for a major tanker route through the Arctic islands. Spot soundings on the ice were used to validate the Through The Ice Bathymetry System (TIBS) which was slung from a helicopter at 10 to 15 m above the ice surface to acquire detailed bathymetry in shallow water areas.

EXPLORER PLATE

In June 1994, the Geophysics Division, in collaboration with the Pacific Geoscience Centre (PGC), conducted a joint seismic and gravity survey west of the Queen Charlotte Islands between latitudes 48° and 54°N and between longitudes 128° and 137°W in support of research studies of the Explorer Plate. A total of 4100 line kilometres of continuous gravity data was collected along the seismic lines aboard the *CSS Tully*.

Gravity measurements were obtained using the GSC's LaCoste and Romberg dynamic linear gravimeter, SL1. Horizontal positioning was provided using a single Trimble NavTrac XL receiver. The data are currently being processed and will be added to the National Gravity Database in early 1995.

ST LAWRENCE RIVER

At the request of the Seismology and Geomagnetic Subdivision, Geophysics Division, a dynamic gravity and bathymetry survey was conducted in the St Lawrence River between Quebec and the Saguenay River during a two week period in August 1994. The survey was carried out by the Geophysics Division in collaboration with CHS (Quebec region) using the GSC's dynamic linear gravimeter, SL1, in a 12 m launch. Approximately 1000 kilometres of continuous gravity and bathymetry data were collected along profiles at 1 km line spacing. Horizontal positioning was established using differential GPS with Turbo Rogue receivers and bathymetry was obtained using an onboard digital sounder. The processed data will supplement existing geological, geophysical and seismic data in the area and will contribute to the understanding of the seismically active Charlevoix area. In addition, this survey provided an initial opportunity to evaluate improvements to the gyro-stabilized platform controller and data acquisition system for the GSC's dynamic linear gravimeter and to demonstrate its capability in a small launch instead of a much larger vessel. The data will be added to the National Gravity Database and made available through the Geophysical Data Centre.

OAK RIDGES MORAINÉ, BOLTON, ONTARIO

In response to a request from the Terrain Sciences Division, the Geophysics Division supervised a detail gravity survey in the Bolton area north of Toronto in support of the Oak Ridges Hydrogeology Project. More than 1400 gravity stations were established at 500 m intervals along seismic lines and existing parallel roads running southwest to northeast covering parts of three 1:50 000 NTS map sheets. Gravity observations were conducted using a Scintrex CG-3 AUTOGRAV gravimeter, horizontal positions were scaled from 1:50 000 maps and vertical positions were derived from altimeter measurements with datum control supplied by the abundance of provincial and federal bench marks. The objective of the survey was to evaluate the use of gravity data as a cost effective means of mapping the bedrock surface beneath the moraine and to delineate subsurface stratigraphy and bedrock topography. Initial interpretation of the gravity measurements along two profiles where shallow seismic reflection surveys have already been interpreted has produced favourable and encouraging results.

ST MARY'S AND STELLARTON BASINS, NEW GLASGOW, NOVA SCOTIA

In response to a request from the Continental Geoscience Division (CGD), the Geophysics Division conducted a detail gravity survey in the New Glasgow area of Nova Scotia during two weeks in September 1994. The survey was conducted in collaboration with F. Chandler (CGD), J. Waldren (St. Mary's University), B. Murphy (St Francis Xavier University), and K. Howells (Nova Scotia Research Foundation). Approximately 95 gravity observations were made at 200 m intervals along two profiles over the western end of the St Mary's Basin along Highway 289 between Lansdowne and Eastville and along a logging road to Dickey Lake and 171 observations were made at approximately 300 m intervals along several other shorter profiles corresponding to older data in the New Glasgow area and west of Pictou. Gravity measurements were made using a Scintrex CG-3 AUTOGRAV gravimeter at all stations and using a LaCoste and Romberg gravimeter at every tenth station. Horizontal positions were derived from single receiver GPS measurements using a Trimble Basic unit or scaled from 1:10 000 photomosaic maps for the area where the GPS was deemed to be unsatisfactory and vertical positions were derived from altimetry using provincial bench marks for datum control. Gravity data in the St Mary's Basin will be used in studies to map the boundary between the Meguma and the Avalon composite terranes and profiles in the New Glasgow/Pictou area will assist in the reprocessing and evaluation of older data in the files of the Nova Scotia Research Foundation and will contribute to the studies of the Stellarton Basin.

GRAVITY STANDARDS

Approximately 120 of the more than 1550 active reference sites of the Canadian Gravity Standardization Net (CGSN) were inspected as part of the annual program to ensure the integrity of this network which provides datum for all relative gravity surveys completed under the National Gravity Mapping Program and for geophysical exploration industry surveys. Stations in Nova Scotia and the high Arctic were inspected and categorized according to national standards, photographs were taken, corresponding databases were updated and descriptions will be recompiled. Three LaCoste and Romberg gravity meters and one Scintrex gravity meter were calibrated over the Ottawa to Inuvik calibration line and

the dynamic gravimeter, SL1, was calibrated over the British Columbia calibration line from Manning Park to Hudson's Hope. These surveys provided updated scale factors for the respective gravity meters and an evaluation of their performance over the gravity range in which they are normally deployed.

Canada successfully participated in the Fourth International Comparison of Absolute Gravimeters (ICAG) in Sèvres, France with seven other countries (Austria, Finland, France, Germany, Italy, Japan, and U.S.A.). Although the data are still in the processing stage, preliminary comparison with the results from 1990 agree to within the published error limits. The final results of experiments performed during the campaign will be published in a special issue of *Metrologia* in early 1995.

Absolute measurements were conducted at 12 sites in Manitoba and British Columbia in support of studies on the movement of tectonic plates in the Cascadia Subduction Zone and secular change studies related to crustal dynamics. New sites were established in Pinawa, Manitoba, and Bamfield, Pelham View and Hankin, British Columbia, and repeat measurements were conducted at Albert Head (2), Nanoose, Little Qualicum Falls, Ucluelet, Vaseux Lake and Penticton (2) in British Columbia.

GRAVITY DATABASE AND MAP PRODUCTION

The National Gravity Database contains more than 700 000 data points corresponding to a variety of land, ice and offshore measurements for the Canadian landmass, lakes and adjacent offshore areas. This year approximately 9600 new data points from regional or site specific surveys conducted by the Geophysics Division will be added to the digital holdings. These data, along with all previously collected data, are available through the Geophysical Data Centre in digital, gridded, profile or map form.

One Open File Bouguer gravity map corresponding to the regional survey conducted in the Canadian Cordillera in 1993 was produced at a scale of 1:2 000 000 (GSC Open File 2930, Bouguer gravity anomaly map of northern British Columbia, Yukon and Northwest Territories).

Geological Survey of Canada Projects 930029, 930030, 930031

AUTHOR INDEX

Adams, J.	91	Lavoie, D.	1
Anderson, K.	101	Lawrence, D.E.	81
Aylsworth, J.M.	81	Marillier, F.	45
Basham, P.W.	91	Murphy, J.B.	11
Brown, J.P.	39	Naylor, R.D.	19
Chandler, F.W.	19	Palacky, G.	101
Chi, G.-X.	53	Pe-Piper, G.	27, 33
Currie, K.L.	59, 73	Piper, D.J.W.	27
Dumont, R.	101	Rice, R.J.	11
Durling, P.	45	Sangster, D.F.	1
Gibb, R.A.	101, 105	Savard, M.M.	53
Gillis, K.S.	19	Scromeda, N.	65
Halchuk, S.	91	Stokes, T.R.	11
Hearty, D.B.	105	Stone, P.E.	101
Katsube, T.J.	65	Teskey, D.J.	101
Keppie, D.F.	11	Traynor, J.A.	81, 87
Kiss, F.	101	Waldron, J.W.F.	19
Koukouvelas, I.	27, 33	Whalen, J.B.	59
		Williamson, M.	65

NOTE TO CONTRIBUTORS

Submissions to the Discussion section of Current Research are welcome from both the staff of the Geological Survey of Canada and from the public. Discussions are limited to 6 double-spaced typewritten pages (about 1500 words) and are subject to review by the Chief Scientific Editor. Discussions are restricted to the scientific content of Geological Survey reports. General discussions concerning sector or government policy will not be accepted. All manuscripts must be computer word-processed on an IBM compatible system and must be submitted with a diskette using WordPerfect. Illustrations will be accepted only if, in the opinion of the editor, they are considered essential. In any case no redrafting will be undertaken and reproducible copy must accompany the original submissions. Discussion is limited to recent reports (not more than 2 years old) and may be in either English or French. Every effort is made to include both Discussion and Reply in the same issue. Current Research is published in January and July. Submissions should be sent to the Chief Scientific Editor, Geological Survey of Canada, 601 Booth Street, Ottawa, Canada, K1A 0E8.

AVIS AUX AUTEURS D'ARTICLES

Nous encourageons tant le personnel de la Commission géologique que le grand public à nous faire parvenir des articles destinés à la section discussion de la publication Recherches en cours. Le texte doit comprendre au plus six pages dactylographiées à double interligne (environ 1500 mots), texte qui peut faire l'objet d'un réexamen par le rédacteur scientifique en chef. Les discussions doivent se limiter au contenu scientifique des rapports de la Commission géologique. Les discussions générales sur le Secteur ou les politiques gouvernementales ne seront pas acceptées. Le texte doit être soumis à un traitement de texte informatisé par un système IBM compatible et enregistré sur disquette WordPerfect. Les illustrations ne seront acceptées que dans la mesure où, selon l'opinion du rédacteur, elles seront considérées comme essentielles. Aucune retouche ne sera faite au texte et dans tous les cas, une copie qui puisse être reproduite doit accompagner le texte original. Les discussions en français ou en anglais doivent se limiter aux rapports récents (au plus de 2 ans). On s'efforcera de faire coïncider les articles destinés aux rubriques discussions et réponses dans le même numéro. La publication Recherches en cours paraît en janvier et en juillet. Les articles doivent être envoyés au rédacteur en chef scientifique, Commission géologique du Canada, 601, rue Booth, Ottawa, Canada, K1A 0E8.

Geological Survey of Canada Current Research, is released twice a year, in January and July. The four parts published in January 1995 (Current Research 1995- A to D) are listed below and can be purchased separately.

Recherches en cours, une publication de la Commission géologique du Canada, est publiée deux fois par année, en janvier et en juillet. Les quatre parties publiées en janvier 1995 (Recherches en cours 1995-A à D) sont énumérées ci-dessous et sont vendues séparément.

Part A: Cordillera and Pacific Margin
Partie A : Cordillère et marge du Pacifique

Part B: Interior Plains and Arctic Canada
Partie B : Plaines intérieures et région arctique du Canada

Part C: Canadian Shield
Partie C : Bouclier canadien

Part D: Eastern Canada and national and general programs
Partie D : Est du Canada et programmes nationaux et généraux